Hemp Fibre Reinforced Sheet Moulding Compounds

Harish Patel

School of Engineering and Materials Science

Queen Mary University of London

A thesis submitted for the degree of

Doctor of Philosophy

April 2012

I would like to dedicate this thesis to my loving parents Narmada
and Shantilal Patel

Acknowledgements

First and foremost, I would like to thank my supervisor Prof Ton Peijs for his always insightful suggestions and expert guidance. His unwavering commitment to his students and constant demand for excellence really helped me bring this work to fruition. It has been a privilege and memorable experience to work with Ton.

Secondly, I would like to express my sincere appreciation to Prof. Paul Hogg and Dr Guogang Ren for their support and guidance and initiating this inter-disciplinary project.

I would like to express my gratitude to Building Research Establishment (BRE) and Engineering and Physical Sciences Research Council (EPSRC) for funding that made this research possible. Thanks also to Dr. Mizi Fan (BRE) for his help and assistance. I am also grateful to Menzolit Lt. (Lancashire, UK) for allowing us to use the SMC equipment and providing the raw materials. The help and assistance in the preparation of the composites, as well as stimulating discussions with Mr Steve Crowther are also gratefully acknowledged. I acknowledge Mr John Hobson, Hemcore Ltd (Halesworth, UK) for providing the hemp fibre mats used in the present study.

I am thankful to Queen Mary University of London (QMUL), UK, for providing all the facilities and a friendly environment, which helped me to work with all the colleagues peacefully and enthusiastically. I appreciate QMUL for organising presentations, poster sessions and other activities, which showed active involvement of QMUL towards the completion of the project.

I would like to express my sincere appreciation to the staff and technicians at QMUL for helping full-heartedly during the project. I am

also grateful to all the graduate students and colleagues who helped me during the project. Some of them are Dhanushka Hapuarachchi, Vimalan Balasubramaniam, Anjum Malhotra and Dawei Hu. I would like to thank workshop staff in the School of Engineering and Materials Science for helping and designing some of the apparatus used for the study.

Words cannot express my gratitude towards my parents (Mr. Shantilal Patel and Mrs. Narmada Patel), wife (Neha Patel), brother and sister-in-law (Kishor and Manisha Patel), sister and brother-in-law (Pushpa and Jignesh Patel), nieces (Krishi and Nancy) for their love, moral support and encouragement during this study. Finally, I would like to acknowledge all my teachers who taught me directly or indirectly.

Harish Kumar Patel

Abstract

Glass fibres are by far the most extensively used fibre reinforcement in thermosetting composites because of their excellent cost-performance ratio. However, glass fibres have some disadvantages such as non-renewability and problems with ultimate disposal at the end of a materials lifetime since they cannot be completely thermally incinerated. The possibility of replacing E-glass fibres with hemp fibres as reinforcement in sheet moulding compounds (SMC) is examined in this thesis. The composites are manufactured with existing SMC processing techniques and similar resin formulation as used in the commercial industry. An attempt is made to enhance/optimise the mechanical properties of hemp/polyester composites. For this the fibre-matrix interface is modified via chemical modifications with alkaline and silane treatments.

Influence of hemp fibre volume fraction, calcium carbonate ($CaCO_3$) filler content and fibre-matrix interface modification on the mechanical properties of hemp fibre-mat-reinforced sheet moulding compounds (H-SMC) is studied. The results of H-SMC composites are compared to E-glass fibre-reinforced sheet moulding compounds (G-SMC). In order to get a better insight in the importance of these different parameters for the optimisation of composite performance, the experimental results are compared with theoretical predictions made using modified micromechanical models such as Cox-Krenchel and Kelly-Tyson for random short-fibre-reinforced composites. These models are supplemented with parameters of composite porosity to improve the prediction of natural fibre composite tensile properties.

The influence of impact damage on the residual flexural strength of the H-SMC composites is investigated to improve the understanding

of impact response of natural fibre reinforced composites. The result of penetration and absorbed energies during non-penetrating impact of H-SMC composites are investigated and compared to values for G-SMC. A simple mechanistic model has been developed for H-SMC composites and is used to get an insight into the impact behaviour of these composite as well as to provide a guideline to compare the experimental results with theoretically calculated data.

The fracture toughness properties in terms of the critical-stress-intensity factor K_{Ic}, and critical strain energy release rate, G_{Ic}, of H-SMC and G-SMC composites are studied using the compact tension (CT) method. It was shown that fracture toughness of H-SMC composites is significantly lower than that of glass fibre reinforced composites (G-SMC). However, results show that with an optimum combination of fibre volume fraction, ($CaCO_3$) filler and surface treatment of the hemp fibres can result in H-SMC composites that have fracture toughness properties that can be exploited for low to medium range engineering applications. It is recommended that to further improve the fracture toughness properties of these natural fibre reinforced composites more research needs to be devoted to the optimization of the fibre-matrix interface properties and ways of reducing porosity content in these composites.

Finally, environmental impact of H-SMC composite with conventional G-SMC composite for automotive and non-automotive applications was compared. The composites were assumed to be made in a traditional SMC manufacturing method. Two different types of performance requirements; i.e. stiffness and strength were investigated for both the non-automotive and automotive parts. Two different disposal scenarios: landfill and incineration of the SMC product at the end of life was considered. The LCA results demonstrate that the environmental impact of H-SMC composites is low than the reference G-SMC composites. G-SMC composites have a significantly higher environmental impact on climate change, acidification and fossil fuels

than H-SMC composites. Where as H-SMC composites have a much higher impact on land use and ecotoxicity than G-SMC composites.

Contents

List of Figures

List of Tables

Chapter 1

Introduction

Generally speaking, a composite is considered to be any multiphase material that exhibits a significant proportion of the properties of both constituent phases such that a better combination of properties is realised [Callister, 2003]. In addition, the constituent phases must be chemically dissimilar and separated by a distinct interface. Many composite materials are composed of just two phases; one is termed the matrix, which is continuous and surrounds the other phase, often called the dispersed phase or reinforcement. Figure 1.1 shows a simple classification scheme of composite materials. In engineering, the most important composites are those in which the dispersed phase is in the form of a fibre or filler. Fillers are usually added to the matrix phase to improve both the mechanical properties and reduce the overall cost of the composite. In fibre-reinforced composites the fibres have very high strength and modulus with small diameter in the range 7-15 μm [Hull & Clyne, 1981] while the matrix is ductile or brittle with usually considerable resistance to chemical environments. By combining fibre and matrix a composite material is produced with high strength and stiffness that is also considerably chemical resistant. The matrix phase of fibre composites may be a metal, polymer or ceramic. Polymers are most widely used as matrix materials because of their ductile and low density properties. There are two main types of polymers with both thermosets and thermoplastics used as matrix in composite materials. Figure 1.2 shows the most commonly used thermoplastic and thermosetting resins.

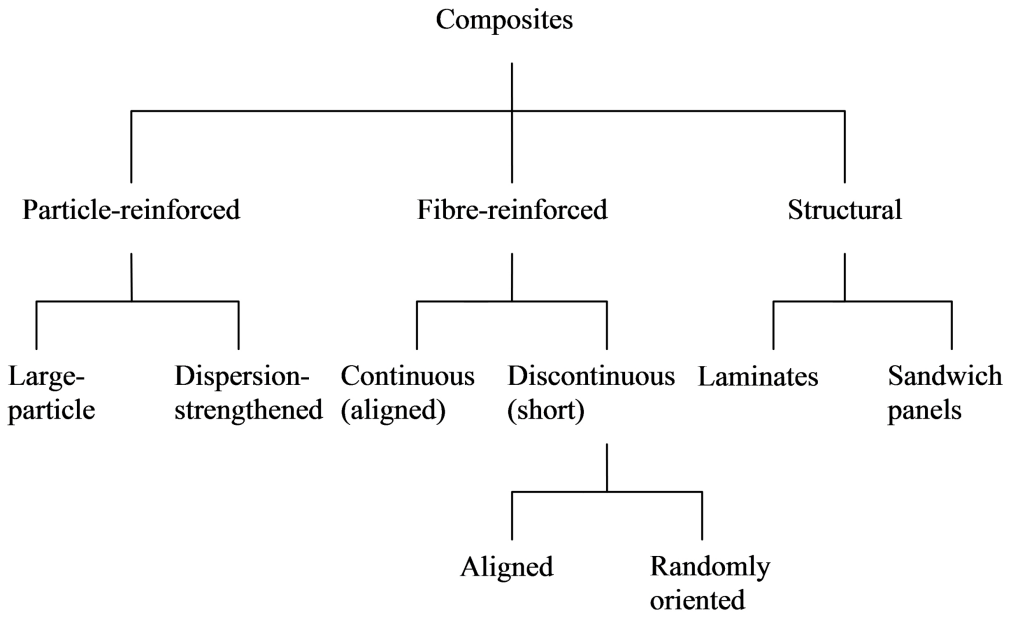

Figure 1.1: Characterisation of composite materials.

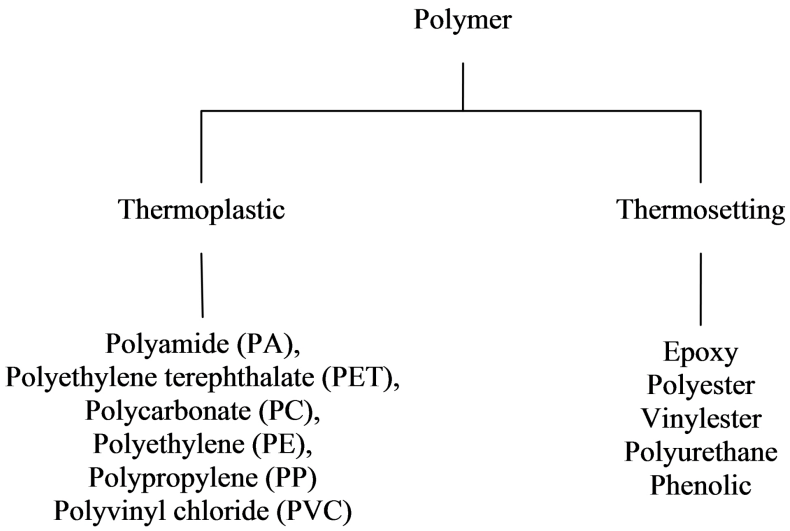

Figure 1.2: Characterisation of polymeric materials.

In thermosets, the liquid resin is converted into a hard brittle solid by a cross-linking process which leads to the formation of a tightly bound three-dimensional network of polymer chains. The mechanical properties depend on the molecular units making up the network and on the length and density of the cross-links. Epoxy and polyester resins are the most commonly used thermosetting polymer resins in the composite industry due to the range of physical and mechanical properties that they impart.

In thermoplastic, the liquid resin can be repeatedly softened by heating and hardened by cooling. Unlike thermosets, the molecular chains in thermoplastic resins do not form cross-links. The most commonly used contemporary thermoplastic resins are polyethylene and polypropylene.

The composite material developed in this study is based on thermosetting resin and therefore the literature onwards will mainly be focused on thermosetting resins and more specifically on polyester resin.

1.1 Thermosetting composites

Thermosetting resins have been used in composites as early as 1909 in the form of phenolics. However, it was not until the 1940s that growth of the structural composite industry saw thermosetting resin used in significant quantities [Holloway, 1994]. As matrix materials for composites, thermosetting resins offer a wide range of advantages over thermoplastics, including low viscosity, higher strength, better wetting and impregnation of the fibres, lower temperature and low pressure for processing, and hence less expensive product tooling. In the current research an unsaturated polyester resin is used to improve the cost-performance of the thermosetting composite. Polyester resins offer a number of advantages for high volume composites applications such as low price and good wear properties. Moreover, polyester resins have good chemical and water resistance and can be easily processed.

Polyester is formed from a reaction between a dicarboxylic acid and a dialcohol. The polymer is linked by ester functional groups and the resulting polymer is called polyester. The chemical reaction to form polyester is shown in Figure 1.3.

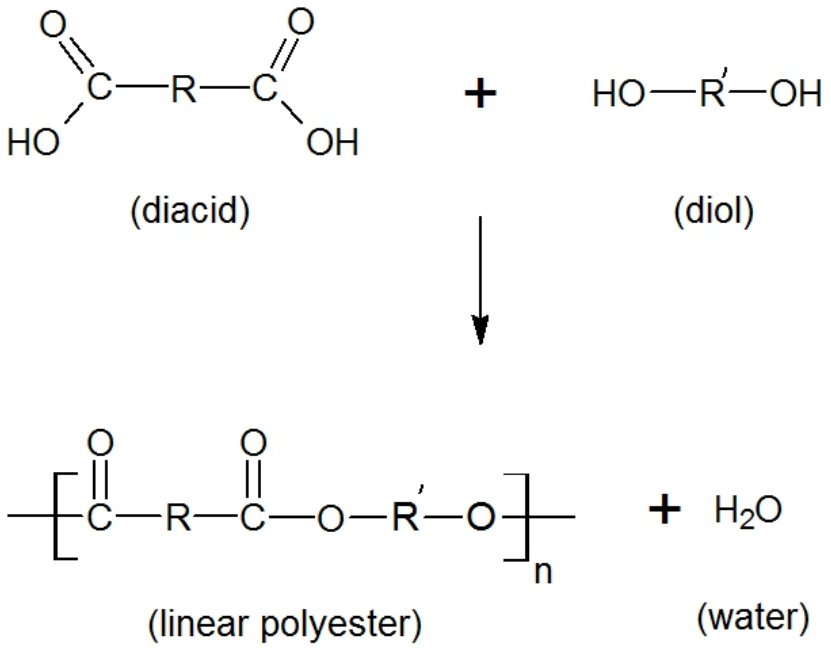

Figure 1.3: Schematic of the chemical reaction to form polyester.

Polyester is a thermosetting resin that contains two or more double bonds between the carbon atoms and is therefore referred to as unsaturated. There are two principal types of polyester resins used as standard laminating systems in the composites industry. Orthophthalic polyester resin is the standard economic resin used for many applications. Isophthalic polyester resin is now becoming the preferred material in industries such as marine where its superior water resistance is desirable.

Polyester thermosetting resins are produced by polymerising a linear polyester resin with a low molecular weight co-reactant. The most popular co-reactant is styrene because it is low cost, copolymerises readily with polyester aliphatic unsaturated groups and makes the resin easier to handle by reducing its viscosity. The styrene content of polyester resins ranges from 15 to 50 wt.%. A molar ratio of at least 2, of styrene unsaturated groups over polyester unsaturated groups, is usually required to achieve decent curing kinetics. Catalysts are added to the resin system shortly before use to initiate the polymerisation reaction. The catalyst does not take part in the chemical reaction but simply activates the process. An

accelerator is added to the catalysed resin to enable the reaction to proceed at workshop temperature and/or at a greater rate.

The molecular chains of the polyester can be represented as shown in Figure 1.4, where 'R' indicates the reactive sites in the molecule. With the addition of styrene, and in the presence of a catalyst, the styrene cross-links the polymer chains at each of the reactive sites to form a highly complex three-dimensional network.

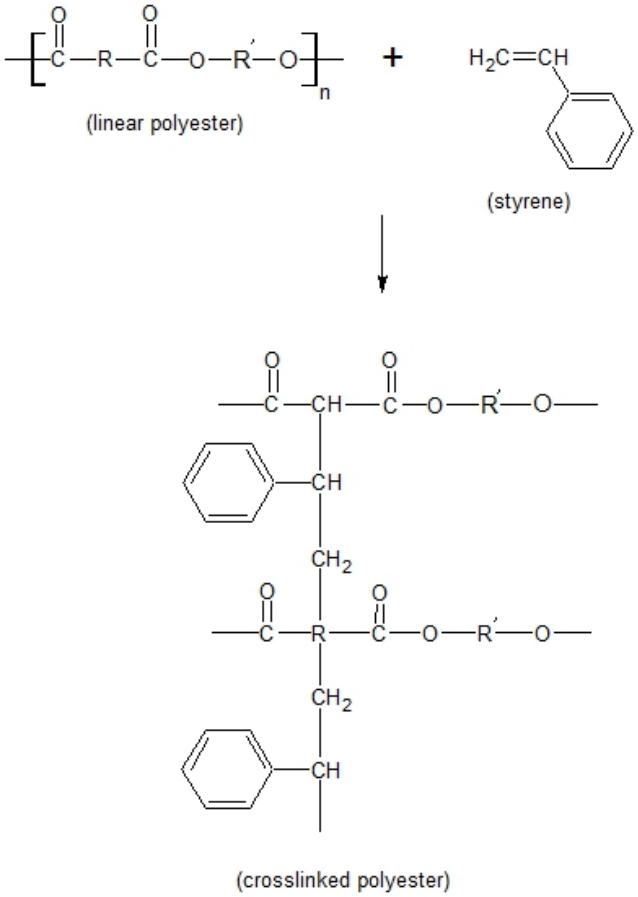

Figure 1.4: Schematic showing the polymerising of a linear polyester resin to form a complex three-dimensional structure of a thermoset polyester resin.

The polyester resin is then said to be 'cured' and is now a hard solid. The cross-linking or curing process is called 'polymerisation'. It is a non-reversible reaction. Polyester resins are used in a variety of processing methods, including in-

jection moulding, pultrusion, filament winding, compression moulding, and resin transfer moulding. Many polyester formulations contain thickening agents that make them suitable for sheet moulding compounds (SMC) or bulk moulding compounds (BMC). Polyester composite products range from furniture, playground equipment, bowling balls to boats, automotive body panels, and chemical storage tanks. Polyester resins when unmodified are transparent, are also commonly used as coating materials, for example, as gel coats on boat hulls, combining the good mechanical and chemical resistance of these materials.

1.2 Processing of thermosetting composites

One of the principal processing methods for the production of short glass fibre reinforced thermosetting composites is sheet moulding compound (SMC). In a SMC process the fibre reinforced composite is produced in sheet form. SMCs are one of the most widely used type of thermoset composites due to their good mechanical and aesthetical properties. They are used in many applications in the production of industrial components, for a variety of different sectors ranging from sport to automotive and marine fields, just to mention a few (Figure 1.5).

Figure 1.5: Rear boot of a car made of sheet moulding compounds with carbon fibre as the reinforcing agent.

SMC composites are usually made with glass fibres, chopped into small segments and distributed in random orientation in a resin system. The resin system is made by mixing other ingredients with polyester resin, such as:

(i) catalyst

(ii) filler

(iii) release agent

(iv) stretching agent

(v) thickening agent

(vi) thermoplastic additives and

(vii) pigment

The function of the catalyst is to reduce the reaction activation energy between the unsaturated resin chains and the styrene which acts as a bridge between the resin chains in order to give the required reticulation. The choice of the catalyst depends on the polymerisation temperature of the compound, which normally varies between 140 and 160°C. The catalyst makes up only 0.3-1.5% of the resin system. The most commonly used catalysts are peroxides due to their low cost. However, these catalysts are unstable and therefore are controlled through the addition of inhitors such as benzoquinone. The filler is used to reduce the cost of the product, decrease shrinkage of the resin, and improve the surface finish. Furthermore, fillers enhance the dimensional stability of the product; also improve the wettability of the material and its filling capacity inside the mould. The most commonly used filler in SMC composites is calcium carbonate $CaCO_3$. The function of the release agent is to create a resin incompatible oily film thereby enabling detachment of the piece from the mould. Normally Ca and Zn stearate are used as release agents making up 1-2% of the resin system. Stretching agents such as polyurethane are used to increase the elastic modulus of the component and to provide shock resistance. They are also used to fill the mould better as they have low-shrinkage. The function of the thickening agent is to increase the

viscosity of the resin system therefore making it easier to reproduce the resin system with the same properties. The thickening agent makes up 1-3% of the resin system. The most widely used agent is magnesium hydroxide ($MgOH_2$) due to its low cost. Ionic links are formed between magnesium and the carboxylate group (-COOH) on the resin chains, which causes the viscosity to increase. The role of thermoplastic additives is to reduce the shrinkage of the SMC material. They act by inserting themselves between two polymer chains and forcing the styrene to be attached in the most expanded possible way. For this purpose vinyl acetate and polystyrene are used as thickening agents. Pigments are added to the SMC to impart colour to the component. They are usually added in powder form in quantities ranging from 1-5%. Figure 1.6 shows a diagrammatic picture of a SMC manufacturing machine.

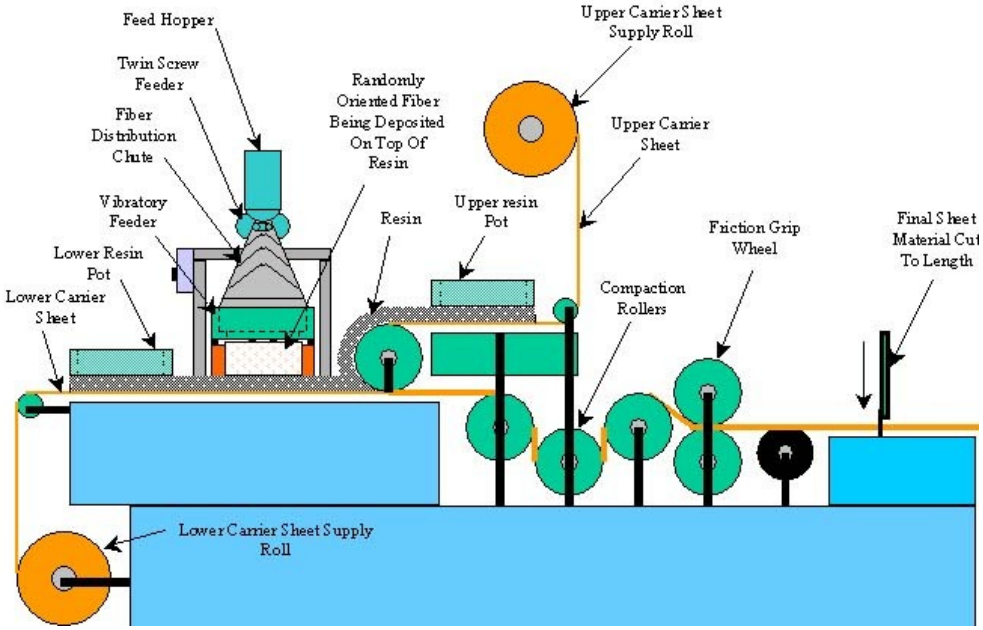

Figure 1.6: The production process for SMC sheets.

The process of manufacturing glass fibre reinforced SMC begins when continuous strands of glass fibre (roving) are chopped into required lengths (usually less than 50 mm). The chopped strands are deposited onto a bottom layer of paste made from resin and filler. The paste and chopped glass fibre strands travel

through the processing machine, on a carrier film. A top layer of resin and filler paste sandwiches the fibres to the bottom layer of paste, and is covered by a top layer of carrier film. The "fibre and paste sandwich" is then compacted by a series of rollers to make a continuous sheet of moulding compound. Figure 1.7 shows examples of sheets of moulding compound.

Figure 1.7: Picture of glass fibre SMC prepregs.

The sheets are then stored for a few days before moulding to allow the prepreg to thicken to a mouldable viscosity. The aged SMC is then weighed, and placed into a heated compression mould (120-180°C) which under pressure (500-2500 bar) forms a composite part (Figure 1.8). Typical compression moulding cycle times of 30 seconds to several minutes are possible with thicker parts requiring more dwell/curing time.

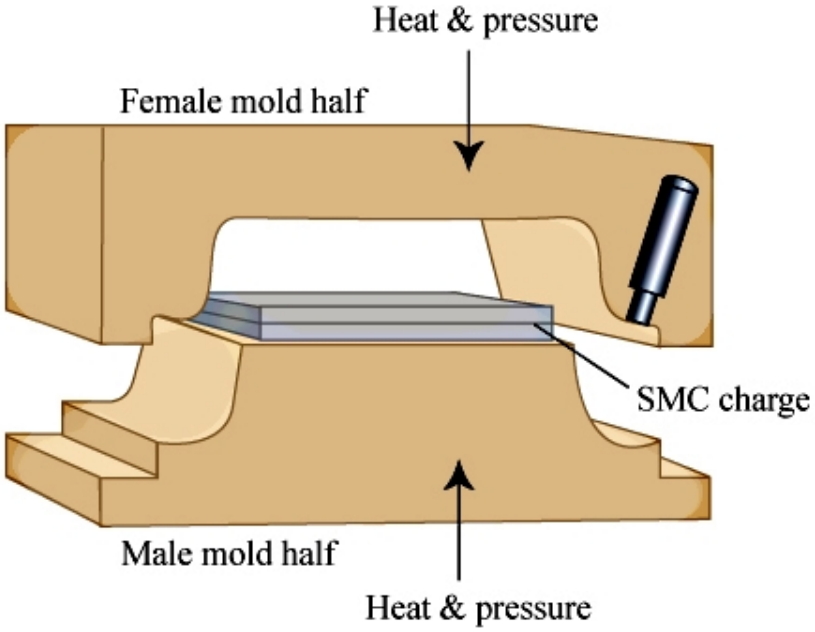

Figure 1.8: Schematic of SMC prepreg loading into a compression press.

1.3 Thermosetting composite reinforcements

Glass fibres are by far the most extensively used reinforcements in thermosetting composites because of their excellent cost-performance ratio. However, glass fibres have some disadvantages; like problems associated with the disposal of glass fibre filled composites at the end of the materials lifetime since they cannot be thermally incinerated/recycled and they leave behind a residue that can damage the incineration furnace. Additionally these fibres are very abrasive which leads to increased tool wear therefore increasing overall maintenance cost. Furthermore, glass fibres pose some health and safety problems, like skin irritations during handling of the products and glass fibres are (although still not scientifically proven) suspected to affect the lungs both during production and use.

In recent years the interest in natural materials has increased considerably due to the increased awareness of environmental and recyclability issues. Environmental legislation as well as ethical consumerism is putting pressure on manufacturers of material and end-products to consider the environmental impact of

their products at all stages of their life-cycle.

In light of all these environmental concerns, composite manufacturers are turning their attention to more environmental friendly reinforcements such as plant fibres like flax, hemp, jute, kenaf and sisal. There are many research papers available reviewing the properties, performance and applications of natural fibres and their composites [Hassan *et al.*, 2010; John & Thomas, 2008; Mantia & Morreale, 2011; Mukherjee & Kao, 2011; Summerscales *et al.*, 2010a,b; Thiruchitrambalam *et al.*, 2010; Zini & Scandola, 2011].

Plant fibres have some advantages which make them suitable for reinforcement in composites materials:

- They are a renewable and abundant resource [Wu, 2009], while the amount of energy necessary for its "production" is lower than that of glass,
- They can be incinerated for energy recovery since they possess a good calorific value with no residue left in the combustion furnaces [George *et al.*, 2001],
- The amount of CO_2 uptake during its growth and the efforts necessary to grow and harvest the fibre is matched with the CO_2 which is released during the rotting or burning process. Natural fibres are therefore favoured for the overall CO_2 balance,
- The result in less abrasive wear of processing equipment: Natural fibres do less mechanical damage to processing equipment and tooling during processing (e.g. mould shear edges), recycling (e.g. extruders), etc, thus lowering overall maintenance costs compared to glass [de Bruijn, 2000],
- They possess a low specific weight which results in a higher specific stiffness and possibly strength than glass fibre [Peijs, 2000; Singleton *et al.*, 2003],
- They can be produced with low investment cost, particular for non-wovens [Joseph *et al.*, 2000],
- Due to their natural origin, natural fibres do not cause skin irritation during handling and when these fibres are applied in thermoplastic products, no sharp fibres or sharp splintering occurs during collision,

- They possess good thermal and acoustic insulating properties
- They are biodegradable leading to fully biodegradable composites when added to a biodegradable resin
- Natural fibres generally have a significantly lower density (about 40% less) compared to glass, which gives better fuel efficiency (or maximum load capacity) when their parts are applied in transportation applications [de Bruijn, 2000].

Natural fibres are abundantly available in developing countries like Bangladesh and India, therefore it is in the economic interests of these countries to research new applications areas like composite reinforcement. Another positive outcome of using natural fibres is that workers in developing countries will benefit directly from the economical possibilities of natural fibre composite. With the upgrading of indigenous technology, enterprising workers will both increase their ability to generate income and will finally receive the recognition they lack in developing countries [Rijswijk *et al.*, 2003].

1.4 Natural fibre composites: an introduction

The concept of using natural fibres as reinforcement in composite materials is not a new idea. Man has been using natural fibres, as construction materials for buildings for centuries. The first composite materials known in history were reinforced with natural fibres. In ancient Egypt some 3,000 years ago; bricks were made from a mixture of straw and loam, dried in the sun. Additionally the first polymer matrix composites developed in the early 20th century were reinforced with natural fibres. Large quantities of sheet, tubes and pipes for electronic purposes were reinforced with paper or cotton. In the 1950s for example, the body of the East German car 'Trabant' was made of natural fibres (cotton) embedded in a polyester matrix. However with the advent of metals and the steadily rising performance of technical and standard plastics and the development of synthetic fibres with better performance, the use of natural fibres for reinforcing purposes declined. Since then, the use of natural fibres was limited to the production

of rope, string, clothing, carpets and other decorative products. The rise of composite materials began during the 1960s when glass fibres in combination with tough rigid resins could be produced on a large scale.

In recent years much of the research has been focused on natural-fibre-reinforced composites based on either thermosetting matrices like polyester and epoxy [Aziz *et al.*, 2005; Dhakal *et al.*, 2007b; George *et al.*, 1999; Hepworth *et al.*, 2000; Satyanarayana *et al.*, 1986; Towo & Ansell, 2008] or thermoplastics matrices, such as polypropylene (PP) or polyethylene (PE), together with various types of plant and crop fibres [Adedelmouleh *et al.*, 2007; Bledzki *et al.*, 2004; Bos *et al.*, 2006; Facca *et al.*, 2007; Garkhail *et al.*, 2000; Georgopoulos *et al.*, 2006; Liu & Dai, 2008; Panthapulakkal & Sain, 2007; Zampaloni *et al.*, 2007]. The principal advantage of polyester resin as matrix material for natural fibre composites is their low cost. Moreover, polyester resins offer a balance of properties (including mechanical, chemical and electrical) dimensional stability. Also, polyester resins offer other advantages like ease of handling and processing.

1.5 Natural fibre composites: present & future applications

Presently, natural fibres are used as reinforcements for technical applications in the automobile and packaging industries (e.g. egg boxes). Flax and hemp are the two most common fibres used in the automobile industry for door panels, seat backs, headliners, package trays, dashboards, and trunk/boot liners. Most of the developmental work for natural fibre composites in interior trim was focused on polypropylene (PP) based composites produced by compression moulding, thermoforming extruded sheet or commingled mats of PP and plant fibres. Figure 1.9 shows sections of a Mercedes car made of flax fibre reinforced thermoplastic resin.

Figure 1.9: Various car components that are made of flax fibre reinforced polypropylene for a Mercedes car (Photo courtesy of Daimler Chrysler AG).

Natural fibres are also used to produce door upholstery and furniture (Figure 1.10). Another large-scale application of natural fibre is to use them as building materials. An important advantage of thermosets over thermoplastics in building applications is that they offer better wetting of the fibres due to lower viscosity and hence superior mechanical properties. Composites are emerging with an increasing role in building materials to replace timber, steel, aluminium, concrete etc. In contrary to India where natural fibre reinforced materials have been used for building and similar applications for many years, application in the western world started in the mid-nineties in Japan and in the US followed more recently by Europe. With the scarcity of natural wood, the application of wood and plant fibre filled materials is set to increase. The market for wood plastic composites (WPC) has recorded growth rates of 100% between 1995 and 2000 in the USA [Bledzki *et al.*, 2002].

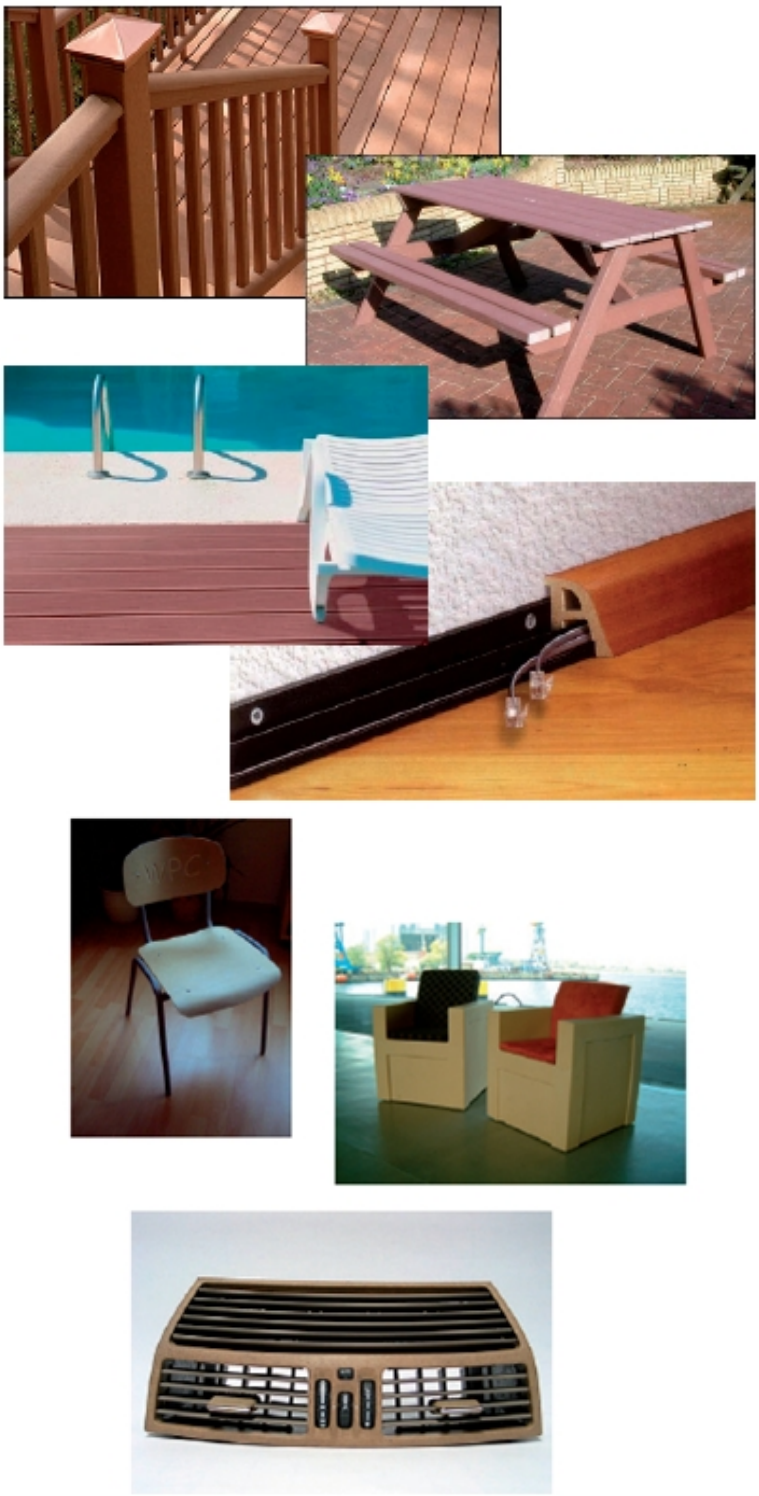

Figure 1.10: Some example of natural fibre composite applications.

The applications of natural fibres are also increasing and products that were once made of natural wood, metals and glass fibre reinforced composites are being replaced by natural fibre materials. The next step for natural fibres is to be used for advanced composite applications such as aerospace and as load bearing structures. There has to be much research carried out on fibre properties, interface properties and fibre quality to develop such advanced composites based on natural reinforcements. However, due to advantages of weight, mechanical stability and price, interest in the application of natural fibre composites is growing in the aerospace industry in both the US and Europe [Bledzki *et al.*, 2002].

Pandey *et al.* [2010] have analysed the recent advancement in the application of cellulose based materials in different sectors including: building and construction industry, adhesives and cellulose-based nanocomposites and have given a future perspective of natural fibres and their composites.

1.6 Natural fibre composites: barriers & challenges

For a successful application of natural-fibre-reinforced thermosetting composites in engineering applications some barriers have to be overcome:

1. Natural fibres are hydrophilic where most polymeric resins are generally hydrophobic, meaning there is poor interaction between the fibre and matrix leading to a weak interface, resulting in inferior mechanical performance [Wambua *et al.*, 2003a] and increased water absorption [Arbelaiz *et al.*, 2005a].

2. Natural fibres have a high rate of moisture absorption that can affect the durability of the composite in outdoor applications as well as its susceptibility to poor dimensional stability and rotting [Peijs *et al.*, 1998]. Microcracking of the composite resulting from fibre swelling [Hill & Hughes, 2010] can result in degradation of mechanical properties.

3. Natural fibre composites tend to have low impact strength. The reason for this is not yet all that well understood but it maybe due to either the poor

fibre-matrix adhesion resulting in extensive fibre pull-out without much energy being absorbed or a too strong interface leading to brittle fracture without any fibre pull-out.

4. The processing temperature of composites has to be relatively low in order to not degrade the natural fibres

5. The quality of the fibres is variable because it depends on unpredictable influences such weather and soil content. Also the use of fertilisers, herbicides and other chemicals to grow the plant can have hazardous impact on the bio-sphere. This tends to off-set the advantages gained at end-of-use such as CO_2 neutral and incineration for energy recovery.

6. The growing of these fibres would occupy land which could be used to grow food.

1.7 Research partners

The work described in this thesis has been performed at QMUL (Queen Mary University of London) from roughly 2004 to 2008. This work has been performed in conjunction with:

- Funding by Technology Strategy Board (TSB): the Engineering and Physical Sciences Research Council (EPSRC),
- The Building Research Establishment (BRE): which is a world leading research, consultancy, training, testing and certification organisation,
- Menzolit Ltd : one of the largest producers of SMC and DMC composites in the world
- Hemptechnology Ltd: non-woven hemp mats were purchased from Hemptechnology Ltd.

Hemp fibre was selected for the study because of its availability in the UK. This study was initiated because of the sustainable nature of hemp fibres along with the economical benefits foreseen from hemp fibres.

1.8 Aims & Objectives

The overall objective of the present project was to examine the possibility of replacing E-glass fibres with natural fibres as reinforcement in sheet moulding compounds (SMC). The main application area for these composites was for building materials such as false walls and ceiling panels.

The specific aims of the study were:

1. To optimise the mechanical performance of the H-SMC composites in terms of fibre volume fraction and CO_2 filler content.

2. To enhance the mechanical properties of these H-SMC composites by modifying the fibre-matrix interface via chemical modifications with alkaline and silane treatments.

3. To compare the experimentally obtained tensile strength and modulus of H-SMC composites with theoretical predictions made using micromechanical models of tensile strength and modulus.

4. To study the influence of impact damage on the residual flexural strength of these H-SMC composites.

5. To develop a simple mechanical model to better understand the impact behaviour of the H-SMC composites.

6. To investigate the fracture toughness properties of these H-SMC composites in terms of the critical-stress-intensity factor K_{Ic} and critical strain energy release rate G_{Ic}.

7. To compare the environmental impact of H-SMC composites with conventional glass fibre reinforced (G-SMC) composites.

1.9 Structure of this thesis

In keeping with the layout of a traditional thesis the present report is organised into sub-sections in the following way:

Chapter 2: A literature review on natural fibres in general and hemp fibres is reported. A brief history on natural fibres and their physical and chemical structures are given. Additionally details of how hemp fibres are extracted from the hemp plant is presented as well as the mechanical properties of various natural fibres in comparison with traditional fibres.

Chapter 3: This chapter involves chopped random hemp fibre mat reinforced composites. The results on the optimisation of the mechanical properties of hemp/polyester composites manufactured through a sheet moulding process (SMC) followed by compression moulding of these hemp fibre mats impregnated with thermoset unsaturated polyester resin are reported and discussed. The effects of hemp fibre content, $CaCO_3$ filler content and fibre-matrix interfacial adhesion on the macromechanical properties of composites are reported and discussed. To provide a better understanding of the mechanical behaviour of the composites the experimental results are compared to theoretically calculated mechanical results generated from modified micromechanical models for random fibre composites, which take into account the effect of composite porosity on the composite properties.

Chapter 4: As discussed above, natural fibre reinforced composites have often poor properties in impact. In this chapter the impact behaviour of hemp fibre composites are tested using the falling weight impact method and are presented and discussed. Again the effect of hemp fibre content, $CaCO_3$ filler content and fibre-matrix interfacial adhesion on the penetration and absorbed energies of the composites are reported and discussed. A simple mechanistic model has been developed for this hemp fibre composite and is used to get a better insight into the impact behaviour of these composites as well as to provide a guideline to compare the experimental results with theoretically calculated data.

Chapter 5: In this chapter the residual flexural properties after low velocity non-penetrating impact of hemp fibre composite are compared to glass fibre composites and presented here. The effect of incident impact energy and fibre volume fraction on the damage tolerance and residual properties of H-SMC is discussed.

Chapter 6: The fracture toughness properties in terms of the critical-stress-intensity factor K_{Ic}, and critical strain energy release rate, G_{Ic}, of H-SMC are studied using compact tension (CT) method and presented in this chapter. The

influence of hemp fibre content and $CaCO_3$ filler content on the fracture toughness rate is reported. Also the influence of fibre surface treatments on fracture toughness is studied and discussed.

Chapter 7: Here a study is presented on the environmental impact of the various types of hemp fibre reinforced materials using a life cycle assessment (LCA) technique.

Chapter 8: Finally, some general conclusions and recommendation for future work are given.

Chapter 2

Natural fibres

The cell is one of the most basic units of life. All living organisms from plants to animals are built up of cells. However, there is one factor that distinguishes plant cells from animal cells. Plant cells have a rigid *cell wall* whereas animal cells do not. The plant cell walls are usually enlarged and this makes these cells responsible for the good structural integrity of the plants. The cell walls are elongated in shape with a high aspect ratio (length/diameter ratio) and hence they are often called *fibres*. A single cell of the plant is often termed elementary fibre. The fact that natural fibres come from natural origin means that the dimensions of each fibre is different even if the fibres are from the same plant. The dimensions of some of the most commonly used natural fibres as reinforcement in composite materials are given in Table 2.1. The major part of this research has been done on hemp fibres. However, where results and theories were not available for hemp, information based on other bast and wood fibres has been presented. It is assumed that the observations made on these fibres can be applied to lignocellulose fibres from other plants as well.

2.1 Classification of natural fibres

Natural fibres can be derived from either plant or animal sources. The majority of useful natural textile fibres are plant based with the notable exceptions of wool and silk.The classification according to natural and plant origin is shown in

Table 2.1: Dimensions of selected natural fibres. Data from [Lilholt & Lawther, 2000].

Fibre type	Elementary fibre length, mm	Elementary fibre width, μm
Flax	33 (9-70)	19 (5-37)
Hemp	25 (5-55)	25 (10-50)
Jute	2 (2-5)	20 (10-25)
Sisal	3 (1-8)	20 (8-41)
Cotton	18 (10-40)	20 (12-38)
Softwood	3.3	33
Hardwood	1.0	20

Figure 2.1 which is based on the most commonly used fibres. There are at least 1000 types of plants that bear fibres which can be used as reinforcement in composite materials. The plant-based fibres are extracted from different parts of the plant such as stems, leaves and seed hairs. The most widely used plant fibres as composite reinforcement are the bast fibres including flax, hemp, kenaf, sisal and jute. These fibres are abundantly available throughout the world, particularly in developing countries like China, India and Brazil and they come from renewable resources. Other large sources of natural fibres are recycled waste paper and wood, also agricultural residues such as rice and coffee husks, bagasse, and many more.

2.2 Natural fibre composition

Although there are considerable differences in the physical features of the various vegetable fibres, there is also a great similarity among all these fibres. In general, natural fibres are composed principally of four chemical groups: cellulose, hemicellulose, lignin, and a miscellaneous group which includes pectinaceous materials, inorganic compounds, etc. It is these components that determine the mechanical properties of the fibre and therefore of the plant. The molecular structure and composition of these polymers is very different. Furthermore the content of these polymers is highly variable between plants fibres and is influenced by climatic conditions, age and the digestion process (Table 2.2).

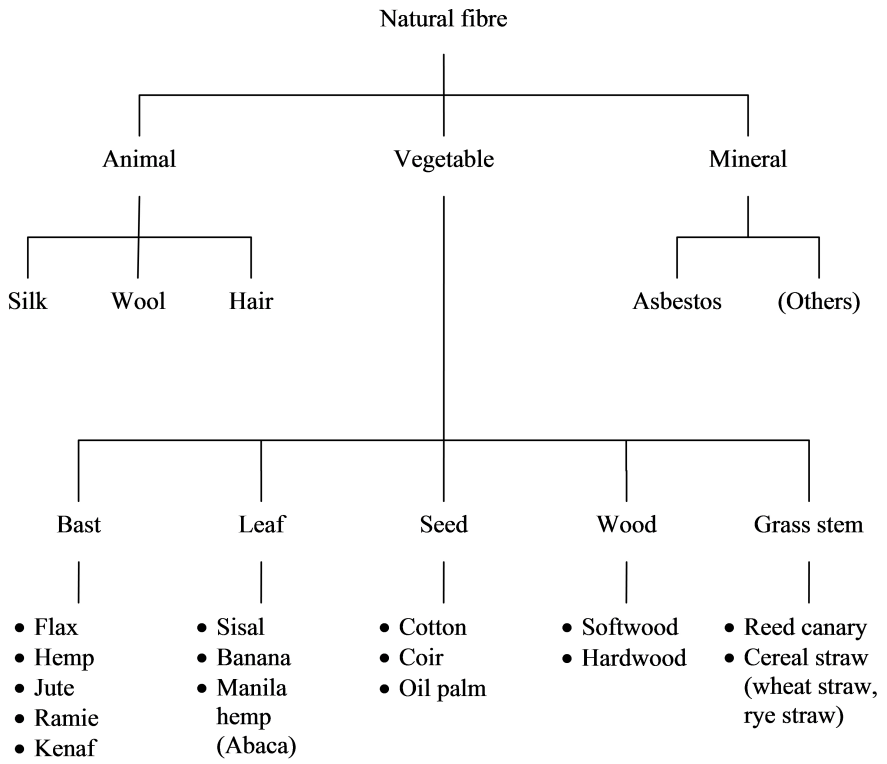

Figure 2.1: Classifications of fibre according to origin.

Table 2.2: Chemical composition and structural parameters of selected natural fibres [Mohanty *et al.*, 2000]

Fibre	Cellulose wt.%	Lignin wt.%	Hemicellulose wt.%	Pectin wt.%	Wax wt.%	Microfibril angle (°)
Hemp	70.2-74.4	3.7-5.7	17.9-22.4	0.9	0.8	6.2
Flax	71	2.2	18.6-20.6	2.3	1.7	10.0
Jute	61-71.5	12-13	13.6-20.4	0.2	0.5	0.8
Sisal	67-78	8-11	10.0-14.2	10.0	2.0	20.0
Cotton	82.7	-	5.7	-	0.6	-
Softwood	40-44	25-31	25-29	-	-	-
Hardwood	43-47	16-24	25-35	-	-	-

Cellulose, the major constituent is a long-chain polymeric poly-saccharide carbohydrate, of beta glucose. The cellulose monomers are linked together through beta-1,4 glycosidic carbon bonds by condensation (Figure 2.2). The repeating unit in a cellulose chain consists of two glucose units, which are orientated 180° to each other. Cellulose is a flat and ribbon-like linear chain polymer. The degree of polymerisation (DP) is the number of glucose units in the chain. On average DP of wood is 10,000 [Siau, 1995], for hemp fibre it is 7000 [Thygesen *et al.*, 2002]. Cellulose fibres usually consist of over 500,000 cellulose molecules with 2.5 billion hydrogen bonds. It is the large number of hydrogen bonds, which is the basis of high tensile strength of cellulose, with a theoretical strength of about 15 GPa in the chain direction [Lilholt & Lawther, 2000].

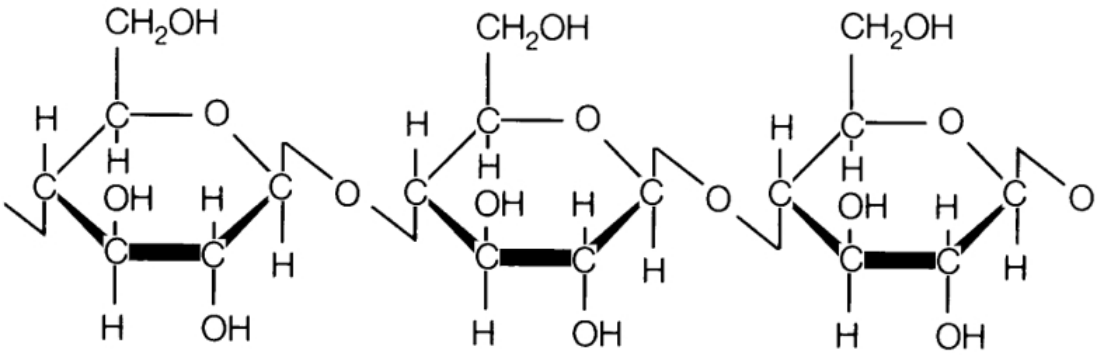

Figure 2.2: Structured formula of cellulose [Lu *et al.*, 1999].

Cellulose is synthesised in the cell wall of the plant. The glucose monomers in cellulose form hydrogen bonds within its own chain producing an elementary fibrillar unit, called a *micellar strand*. When hydrogen bonds are formed between chains they produce a large *microfibril*. The number of cellulose chains in a microfibril varies depending on the type of plant. The cellulose chain is divided into two distinct regions: regions of high order, i.e. *crystalline region*, and regions of low order, i.e. *amorphous regions*. It is generally agreed that these regions are not well defined but, rather, the transition is gradual from crystalline to amorphous, i.e., there are various degrees of lateral order. The degree of crystallinity varies depending on the fibre; for wood fibres it between 60 and 70% [Siau, 1995] and for cotton fibres it is between 40 and 45%. With a few exceptions, natural

cellulosic fibres have a cellulose I crystal lattice structure.

Hemicellulose is a polysaccharide composed of a variety of carbohydrates including glucose, xylose, arabinose, galactose and mannose (Figure 2.3). Compared to cellulose, hemicellulose molecules are more branched, non-linear and have lower molecular mass with a degree of polymerisation (DP) between 50 and 200. The most prevalent hemicellulose polymer chains are xylans and glucomannans. Hemicellulose forms covalent bonds to lignin by attaching ferulic acid and p-coumaric residues [Bjerre *et al.*, 1997]. Hydrogen bonds are formed between xylan and cellulose. The degradation of the bonds in hemicellulose leads to the disintegration of the fibres into cellulose microfibrils resulting in lower fibre bundle strength.

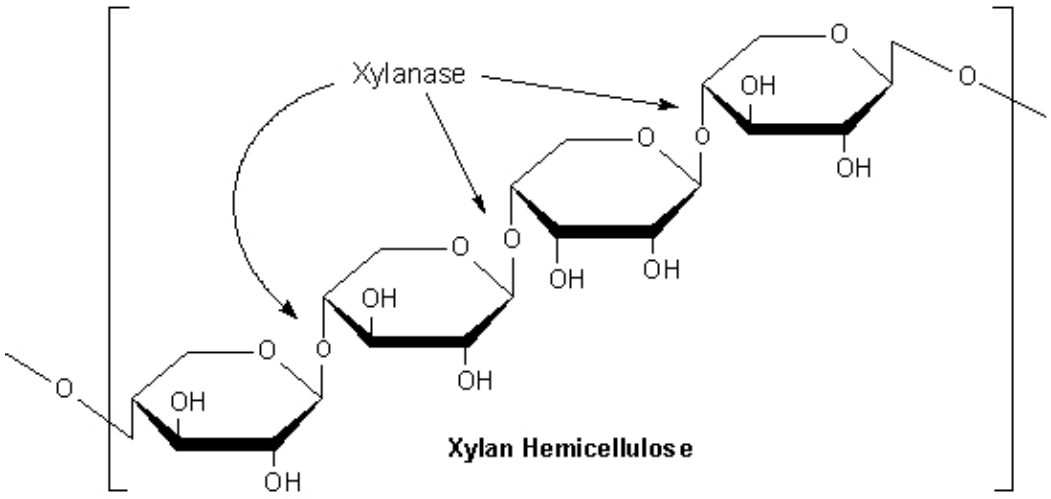

Figure 2.3: Structural formula of hemicellulose (courtesy Sigma-Aldrich).

Lignin is a complex polymer of phenylpropane units, which are cross-linked to each other with a variety of different chemical bonds (Figure 2.4). Lignin is a highly branched molecule which consists of various types of substructures which repeat in random manner. The mechanical property of lignin is about 4 GPa (Young's modulus), much lower than that of cellulose [Bledzki & Gassan, 1999].

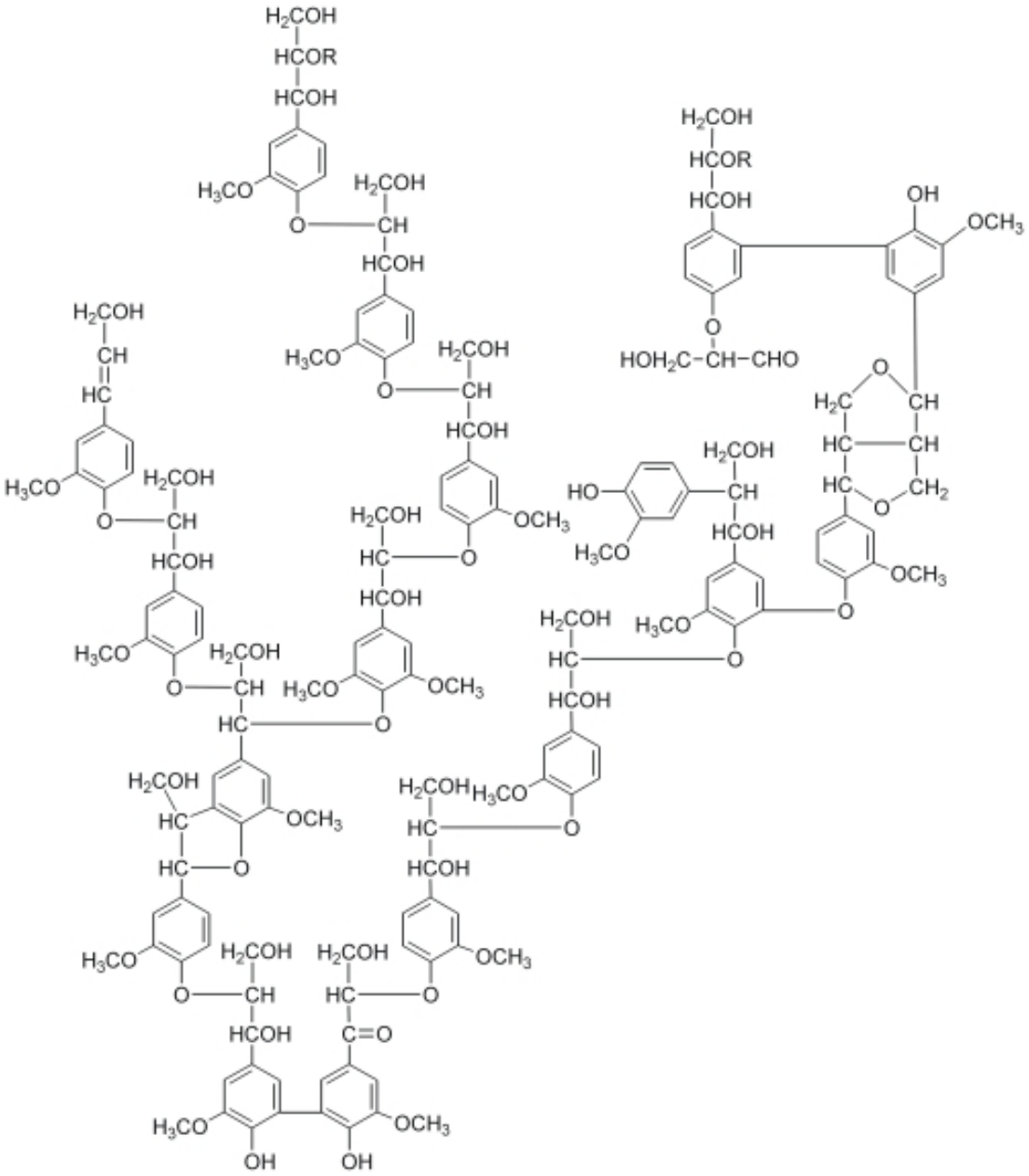

Figure 2.4: Structural formula of lignin [Adler, 1977].

2.3 Structure of a single natural fibre

The wall of a plant cell is composed of three major layers: the middle lamella, a primary wall and a second wall (Figure 2.5). The *middle lamella*, composed mainly of lignin and pectin, serves as the glue bonding adjacent cells together. The wall itself is made up of a *primary wall* and a three-layered secondary wall. The cellulose microfibrils in the primary and secondary walls are aligned in a certain way, and it is the angle that the microfibrils are to the axis of the cell wall that is defined as the *microfibril angle*. The microfibril angle generally determines the mechanical properties of cellulose based fibres. Table 2.2 gives the microfibril angle of some common natural fibres and wood. In the primary wall the microfibrils form a loose, irregular net-like orientation. The outer layer of the secondary wall is called the transition layer because its structure is intermediate between the structure of the primary wall and the secondary wall. In the outer layer, the microfibrils are more precisely oriented, but are nearly perpendicular to the long axis of the cell at an angle of about 50° to the fibre axis. In the middle layer of the secondary wall, the microfibrils run almost parallel to each other in a tight helix structure around the cell, forming an angle of 10 to 20°. This layer is the thickest, forming between 60 to 80% of the cell wall [Siau, 1995] and therefore the microfibril angle in this layer has the greatest effect on the overall properties of the fibre. The smaller the angle the microfibrils make with the long direction of the cell, the stronger the cell is. It is stated that lower microfibril angles in the middle layer results in fibre bundles with high tensile strength, about 1200-1500 MPa for hemp fibre [Garkhail, 2001]. In the inner layer of the cell wall, the microfibrils are once again oriented almost at right angles to the cell's long axis. Several studies of fibre composition and morphology have found that the microfibril angle tends to control the mechanical properties of cellulosic fibres. It was reported that a lower microfibril angle resulted in higher work of fracture in impact testing [Pavithran *et al.*, 1987].

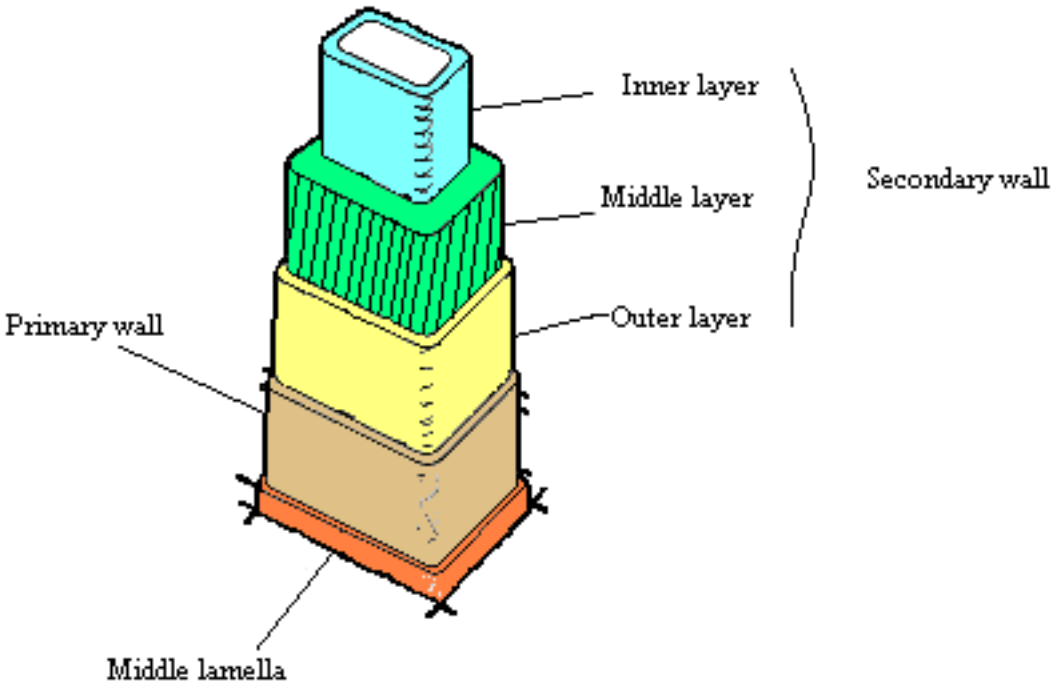

Figure 2.5: Cross-section of a hemp fibre (Courtesy of DoITPoMS Teaching and Learning Packages, University of Cambridge).

2.4 Physical & mechanical properties

The mechanical and physical properties of different natural fibres are given in Table 2.3 and 2.4. The specific strength and stiffness of natural fibres are comparable to those of E-glass fibres. However, due to their natural origin they show much higher variability of the various parameters than synthetic fibres [Virk *et al.*, 2010]. The properties of the natural fibres are influenced by several factors such as:

Table 2.3: Mechanical properties of natural fibres compared to conventional fibres [Li *et al.*, 2005]

Fibre	Density (g/cm^3)	Elongation (%)	Tensile strength (MPa)	Young's modulus (GPa)
Hemp	-	1.6	690	-
Flax	1.5	2.7-3.2	345-1035	40-70
Jute	1.3	1.5-1.8	393-773	26.5
Sisal	1.5	2.0-2.5	511-635	9.4-22.0
Cotton	1.5-1.6	7.0-8.0	287-597	5.5-12.6
Softwood Kraft	1.5	-	1000	40.0
E-glass	2.5	2.5	2000-3500	70.0
Carbon (standard)	1.4	1.4-1.8	3000	230

Table 2.4: Physical characteristics of plant fibres [Garkhail, 2001]

Fibre	Specific gravity (g/cm^3)	Moisture regain (%)	Absorption (%)	Volume swelling (%)
Cotton	1.52	7-8.5	7-8	-
Flax	1.40	12	7	30
Jute	1.46	14	12	45
Hemp	1.48	12	8	-
Sisal	1.20-1.45	-	11	40

- All natural fibres contain *defects and imperfections*, which reduce the strength. The extent of these cracks is dependent on the anisotropy of the fibre structure, and for high anisotropy the stress concentration of transverse cracks is low and thus not a decisive factor for fibre strength. The origin of defects in natural fibres and how, ultimately, they affect the properties of composite materials reinforced with such fibres has been reviewed by [Hughes, 2012].

- *Fibre length*: the strength of all fibres is dependent on the test length. However, the strength of natural fibres is significantly more dependent on the length of the fibre than for the case of glass fibres [Mieck *et al.*, 2003] because strength at fibre lengths exceeding the cell length is controlled by the bonding between cells rather than the intrinsic strength of the elementary cells or fibres.

- The *fibre diameter* and cross-sectional shape also influences the tensile strength [Mukherjee & Satyanarayana, 1986] and modulus [Summerscales *et al.*, 2011] of the fibre, with smaller diameter fibres having higher tensile strength and modulus.

- The *degree of cellulose crystallinity*. Natural fibres consist of regions which are less ordered i.e. amorphous regions which are potential weak points due to the lower number of chains per cross-sectional area resulting in low local strength.

- The tilt angle of the cellulose microfibrils to the longitudinal axis of the fibre, i.e the microfibril angle greatly influences the tensile strength and stiffness of the fibre. High fibre strength is obtained by a lower microfibril angle i.e. about $\pm 5°$, the microfibril angle for hemp is one of the lowest at $6.2°$ and for flax it is $10°$ [Bledzki & Gassan, 1999]. The microfibril angle for wood fibres varies greatly from $5°$ to $60°$.

- The *degree of polymerisation* of the highly orientated cellulose microfibres affects the strength of the fibre, in general the strength is inversely proportional to the degree of polymerization for fibres with ideal structure.

- The *cellulose content* of the fibres also influences the fibre strength, fibres having higher cellulose content results in high tensile strength. The cellulose content and the microfibril angle are presented in Table 2.2, it can be seen that the cellulose content of hemp and flax fibres is 78% and 71% by weight respectively.

Many of these factors work together to reduce the strength of the fibre, e.g., high orientation leads to anisotropy, which reduces the severeness of cracks and

the amorphous region, effecting the degree of polymerisation. Moreover, properties depend on *growing (climate)*, *harvesting conditions* and *processing methods*. This poses two problems: quality characterisation of fibres and difficulties in application of traditional composite theories.

Single fibre tensile (SFT) tests are the most common methods to measure modulus and tensile strength of natural fibres. It is important to mention that elementary fibres (10-20 μm in diameter) have considerably higher strength then technical fibres (50-100 μm in diameter) [Bos *et al.*, 2002]. A schematic picture of a technical and elementary (fibre cell) flax fibre is shown in Figure 2.6.

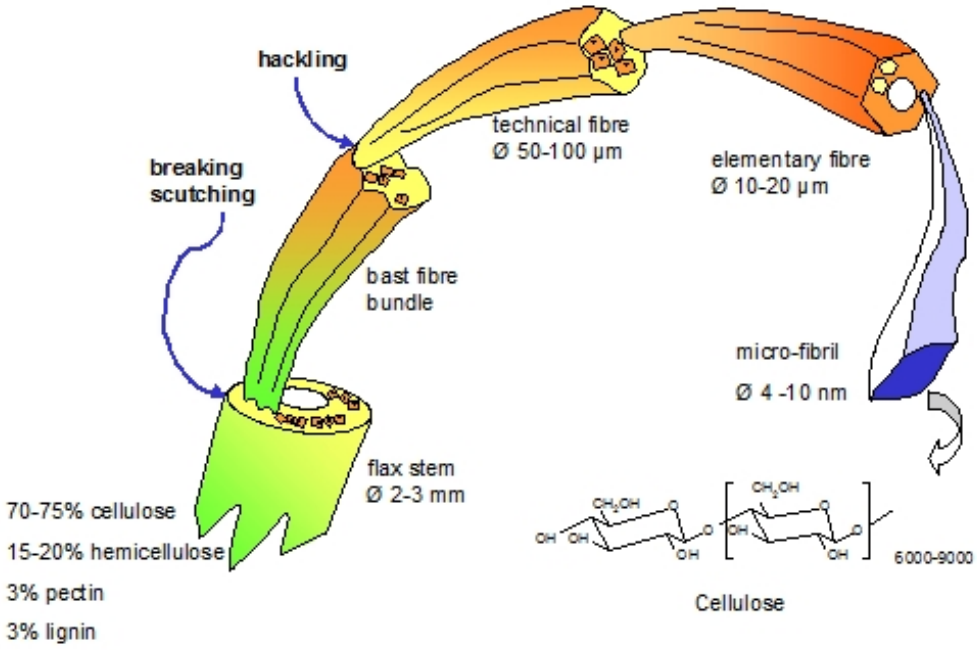

Figure 2.6: Schematic picture of a technical and elementary (fibre cell) flax fibre [van den Oever *et al.*, 2000].

Elementary fibres of flax [Baley, 2002; Bos *et al.*, 2002; Davies & Bruce, 1998; Joffe *et al.*, 2003] nettle [Davies & Bruce, 1998] and wheat straw [Hornsby *et al.*, 1997] are tested at single gauge length. In many studies Weibull distribution is used to approximate strength distribution of natural fibres [Bos *et al.*, 2002; Davies & Bruce, 1998; Joffe *et al.*, 2003]. Nonlinearity of stress-strain response

(strain-hardening) is reported [Baley, 2002; Hornsby *et al.*, 1997]. The increase of the Young's modulus with strain is explained with a reorganisation of the cellulose fibrils in the direction of the fibre (loading) axis. From fatigue tests it is established that this effect is irreversible [Baley, 2002].

Another method used to measure fibre strength is the loop test. Using this method it is possible to determine the compressive strength of fibres. Analysing fibre failure qualitatively by ESEM [Bos & Donald, 1999] and quantitatively [Bos *et al.*, 2002] it was reported that the compressive strength of flax fibres is about 80% that of tensile strength.

2.5 History of hemp

Hemp (*Cannabis sativa*) is among the oldest textile fibres on the planet. For centuries, its fibres have been used to make ropes, sails and clothing. The history of hemp provides a fascinating story going back more than 10,000 years to the beginnings of pottery. The Columbia History of the World states that the oldest relic of human industry is a bit of hemp fabric dating back to approximately 8,000 BC. China has an unbroken history of hemp textile production dating from 4,500 BC with the spread to rest of Asia around 1,000 BC and reaching Europe around 800 BC. It became an important crop of enormous economic and social value supplying much of the world's need for food and bast fibre. Sailing ships became dependent on canvas (from the word cannabis), hemp rope and oakum due to it being 3 times stronger than cotton and rot resistant to salt water. In 1175 hemp was taxed and in 1535 Henry VIII passed an act compelling all landowners to sow 1/4 of an acre, or be fined. During this period hemp was a major crop and up to the 1920's 80% of clothing was made from hemp textiles.

In 1930s cannabis was banned in North America because its leaves and flowers contain a hallucinogenic drug know as delta-9 tetrahydrocannabinol (THC). Figure 2.7 shows the different cross-sectional stem structure between industrial hemp and marijuana. In 1942, the government lifted the ban and encouraged farmers to cultivate hemp to help with the war effort, widely distributing a film called "Hemp for Victory" produced by the USDA. This relaxation of the laws against hemp was terminated by 1957, and the ban continues today under the

1972 Controlled Substances Act. It was banned internationally in 1961 under the United Nations' Single Convention on Narcotic Drugs. In the UK ban on hemp was lifted in 1993 when Hemcore Ltd were granted the first license for trial plots. There are now approximately 80 hemp farms growing a total of 2,500 hectares in the UK. To put this into perspective, in 1992 600,000 hectares of land were put to set-aside. This area of hemp would give a yield of over 6 million tons of biomass and 120,000 tons of fibre.

Hemp is said historically to have over 25,000 diverse uses ranging from paints, printing inks, varnishes, paper, bibles, government documents, bank notes (UK included), food, textiles (the original 'Levi's' jeans were made from Hemp cloth), canvas (artists canvases were used by the great masters) and building materials. With modern technical developments uses have increased to composite boards, motor vehicle brake and clutch pads, plastics, fuels, bio-diesel and Eco-solid fuel. In fact, anything that can be made from a hydrocarbon (fossil fuel) can be made from a carbohydrate (William Hayle, 1930).

Figure 2.7: Cross-section of industrial hemp (left) and marijuana (right).

2.6 Advantages of hemp

Hemp is one of the most environmentally friendly crops to be found, as it actually improves soil condition. Hemp grows tall and thick, shading and mulching the ground, while its deep taproots break up and aerate the soil. This contributes to healthy microbial life and nutrient content in the soil, and the shading eliminates competing weeds. Other advantages include:

- Hemp is naturally resistant to most insects, moulds, and other pests. Hemp requires little fertiliser and few if any pesticides, which means it is cheap and requires minimal effort to grow. It also means the environment is not contaminated.
- Hemp fibres are longer, stronger, more absorbent and more mildew-resistant than cotton.
- Hemp can be made into a variety of fabrics, and fabrics of at least 50 per cent hemp are more effective than other fabrics at blocking the sun's ultraviolet rays.
- Hemp can be made into fine quality paper. The long fibres in hemp allow such paper to be recycled several times more than wood-based paper and produce more pulp for paper-making.
- With a low lignin content, hemp can be pulped using fewer chemicals than when pulping wood.
- Hemp can displace wood fibre and save forests for watershed, wildlife habitat and recreation as well as for oxygen production and carbon sequestration which reduces global warming.

2.7 Hemp structure: from plant to fibre

In botany plant from which the hemp fibre is produced is called *Cannabis sativa*, it is an annual plant that belongs to the bast fibre plant (Figure 2.8). The average hemp plant grows to between 2 - 4 meters in height in about 12 - 14 weeks growth,

producing 5 - 9 tons of biomass per hectare. Approximately 20% of the plant is fibre resulting in approximately 1 to 2 tonnes of fibre depending on the variety of the plant and the processing conditions. Hemp plants have no branches and few leaves, which are concentrated at the top of the plant.

Figure 2.8: Pictures of a hemp plant and leaf grown for hemp fibre.

The plant fibre is a very complex structure; the fibre is basically a composite by itself. A schematic of the structure of a flax fibre with a similar structure as hemp from its stem to the microscopically fine elementary fibre is shown in Figure 2.6. The plant stem is about 0.15-0.3 cm in diameter [George *et al.*, 2001] and consist of 15 to 40 bast fibre bundles which contains one meter long technical bast fibres which are bonded together in part by a pectin and lignin interphase to form bast fibre bundles. The technical fibres are composed of 40 or more cells or so-called elementary fibres which are 20 to 50 mm in length and between 10 and 25 μm in diameter [Singleton *et al.*, 2003]. The elementary fibres overlap over considerable length and are bonded together by a pectin interphase [van den Oever *et al.*, 2000]. The elementary fibres consist of a microfibrillar cellulose phase and a matrix phase, which is mainly composed of hemicellulose and lignin. These microfibrils are 10 nm in diameter and therefore infact nanofibres and are made up of 30 to 100 cellulose molecules in extended chain conformation [Stamboulis *et al.*, 2000]. As discussed above the orientation angle of the microfibrils and the cellulose content primarily determine the mechanical properties of the fibre.

A schematic cross-section of the hemp plant stem with different layers is shown

in Figure 2.9. Generally, most bast fibres have a similar stem structure. The interior of the hemp stem is made up of short, woody fibres (hurds) and the outer portion of the stem contains the longer bast fibres. The outside of the stem is covered with bark, also called the epidermis, which provides a thin protective layer for the plant cells. Inside the epidermis is the cortex, a thin layer of walled cells that has no fibre, but does contain chlorophyll. The next layer is the phloem or parenchyma which contains short cells that have chlorophyll and long cells that are bast fibres. The bast fibres are bound and arranged in bundles.

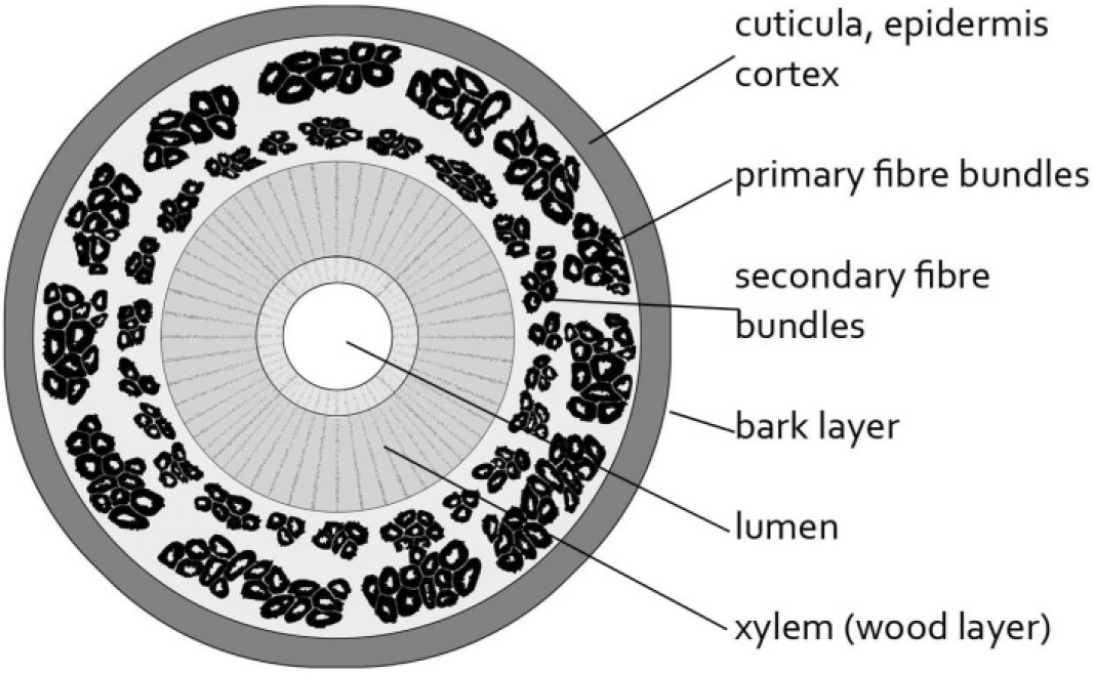

Figure 2.9: Schmatic cross-section of hemp stem [Pakarinen, 2012].

Figure 2.10 shows the location of bast fibres in an optical microscope picture of flax fibre stem. The cambium layer separates the bast from the pith (woody core). It is the growth area, which produces hurds on the inside and bast and bark on the outside. Although this is the differentiation layer, it is also an abscission layer where fibre and hurds separate during the retting/breaking process. Pith or hurd is composed of thick, woody tissue used to support the plant. This area makes up 60-75% of the total mass of the stem. At the center there is a hollow

core (lumen) which runs from top to bottom of the stem. Each plant is made up of approximately 30% bast fibre, 60% hurd, and 10% dust and waste. The bast fibres are 10 to 100 times longer than the woody fibres in the pith. Their diameter are approximately the same; however the cell walls of the bast fibres are 5 to 10 times thicker than those of woody fibres. The fibre content is given in relation to the weight of the whole stem. In hemp 20-35% w/w of the stem is fibres.

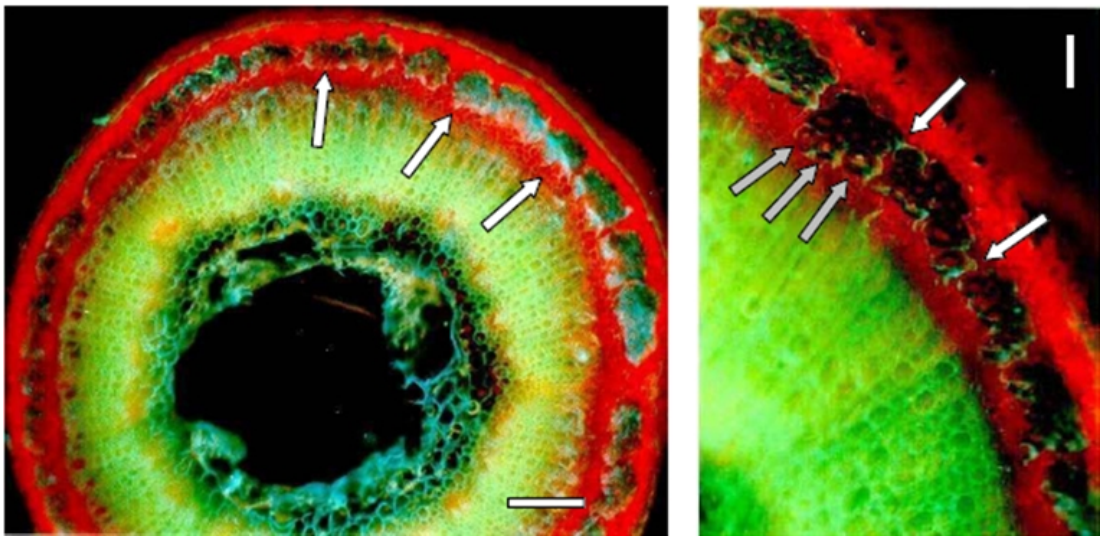

Figure 2.10: Photographs of a cross-section of a flax stem. (left) The white arrows show the bast fibres. The scale bar represents 0.1 mm. (right) The white arrows show spots where the interfibre bonding within the bundle is virtually absent, the grey arrows show the individual elementary fibre. The scale bar represents 50 μm [Bos, 2004].

2.8 Hemp fibre processing

The processing of hemp from the plant to the fibre mat is a long and established process in the textile industry involving cultivation, harvesting, retting, drying, scutching and hackling. Figure 2.11 outlines the processes involved in obtaining hemp fibres from the plant.

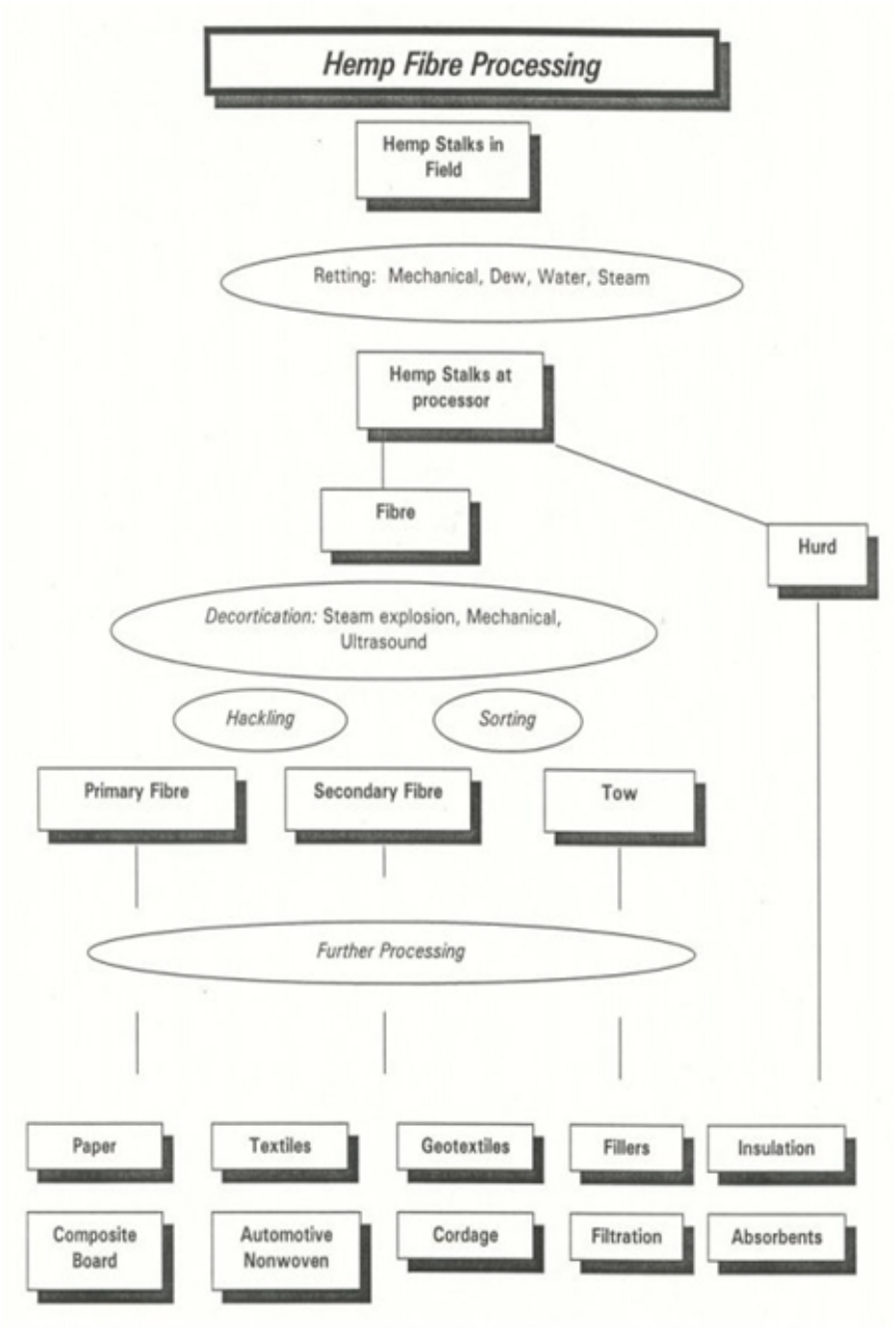

Figure 2.11: Flowchart showing the processing steps involved in obtaining various forms of hemp fibre materials from the plant.

2.8.1 Cultivation & harvesting

Hemp requires limited pesticides because it grows so quickly and attracts few pests. The plant is a prolific and sustainable environmental crop growing at any latitude from Norway to the Equator in northern latitudes; hemp is usually planted between early March and late May. Hemp grows successfully at a density of at least 150 plants per square meter.

The hemp plants are harvested either manually or mechanically (Figure 2.12). Afterwards they are spread out in the field to dry. The equipment used for harvesting and the timing of the harvest affects the quality and the potential applications of hemp fibre. Fibre hemp is ready to harvest about the time the plant is finished producing pollen and the first seeds start to develop. However, this does vary with the variety and maturity of the fibre desired. If left beyond this stage, the fibre becomes too coarse. Fibre from the male plant dies soon after pollination. It is coarse and good for fibreboard and other products since it is stronger than younger fibre. Because hemp is sensitive to light, early planting will produce taller crops and thus more fibre.

Figure 2.12: Picture of harvesting of hemp fibre using a combine harvester (Photo courtesy of Manitoba Agriculture-Food and Rural, Manitoba, Canada).

2.8.2 Retting

Once the hemp is harvested, it must go through a process called retting in order to separate the fibre from the rest of the plant. This is not an easy process and can be accomplished through several methods where moisture, micro-organisms, or chemistry break down the bark tissue that binds the fibre and non-fibre portions, making them easier to separate:

- Dew retting occurs when the stalks are left in the field so that rain, dew, or irrigation is used to keep the stems moist. This may take up to 5 weeks and produces a coarse fibre with a light brown colour. A picture of dew retting process is shown in Figure 2.13.
- Water retting occurs when stems are bundled and then submerged in water so that bacteria break down the pectin. This takes 7-10 days and produces a better quality fibre.
- Warm water retting occurs when bundles are soaked for 24 hours after which the water is replaced. Heat is then applied to warm the batch for the next two or three days. This gives a very uniform, clean fibre.
- Green retting is an all mechanical process that separates the components and is used when the fibre is needed for textiles, paper, or fibreboard products.
- Chemical retting occurs when chemicals are used to dissolve the pectin, allowing the components to be separated. This shortens the time to as little as 48 hours when the next process can then be instigated. This produces a very high quality product.

The most common retting used is the dew retting and water retting. Water retting produces a more uniform and higher quality fibre but the process is time consuming and costly and can pollute the body of water being used for the process.

Figure 2.13: Picture showing dew retting of hemp in the field (Photo courtesy of Henfaes Research Centre, University of Bangor).

2.8.3 Breaking & scutching

Once the stalks are retted, dried, and baled, they are brought to central location for processing. Here the fibres are separated from the hurds (woody core) in a process known as decortication. There are many decorticating methods but the most common ones are the mechanical and steam explosion. Once the stalks are retted, dried, and baled, they are brought to a central location for processing. With mechanical separation, in a process called breaking, stalks are passed between fluted rollers to crush and break the woody core into short pieces (called hurds), separating some of it from the bast fibre (see Figure 2.14).

Figure 2.14: Example of breaking machine, the hemp stems are fed between the rollers.

The remaining hurds and fibre are separated in a process called scutching. Fibre bundles are gripped between rubber belts or chains and carried past revolving drums with projecting bars that beat the fibre bundles, separating the hurds and broken or short fibres (called tow) from the remaining long fibre (called line fibre) (see Figure 2.15). Mechanical decortication may be carried out on either fresh green stems or dry stems. Dry decortication is said to be quicker and not to be confined to the harvesting season. However, decortication of fresh stems produces a fibre of better quality. Recently, alternative fibre separation processes have been developed, using technologies such as ultrasound and steam explosion, which is much less labour intensive. In the steam explosion method, steam, and additives when neccessary, under pressure and with increased temperature, penetrates the space between fibres of the bast fibre bundle. In this way, the middle lamella and the fibre adherent substances are elementarised "softly" and made water soluble. These can be then removed by subsequent washing and rinsing. According to the desired quality of the elementarised fibres, the pressure of the steam can also be reduced suddenly to atmospheric, and blown out along with the substrate, to a settling chamber. The combination of chemical and mechanical treatment produces an effective loosening of the rigid bast fibre structure and thereby a further splitting into single fibres.

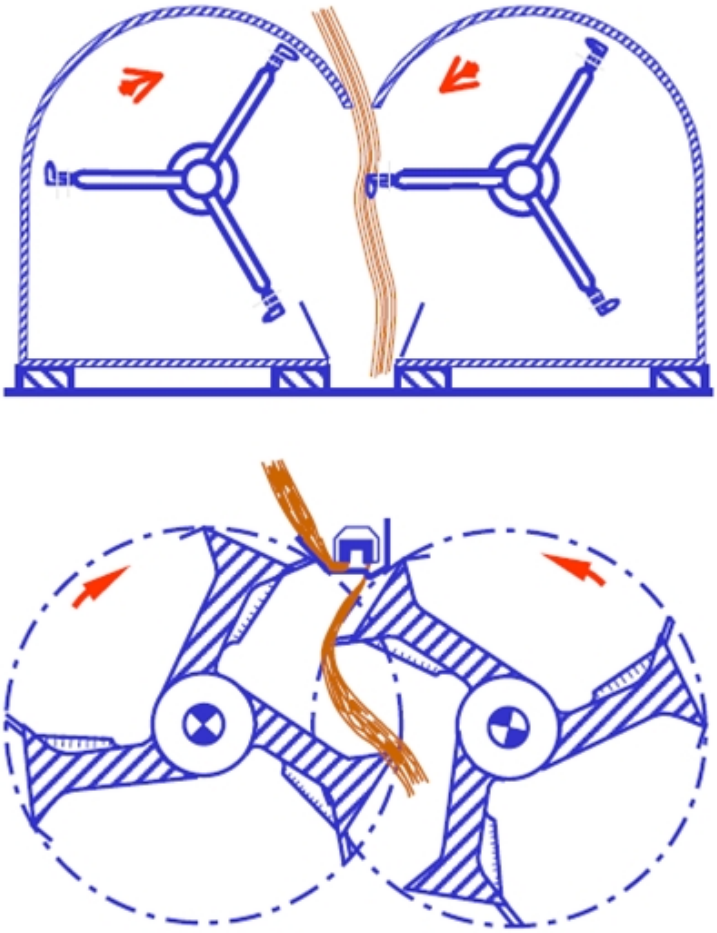

Figure 2.15: Example of scutching turbines [Bos, 2004].

2.8.4 Hackling

In this process the fibre is pulled through various different sized heckling combs or heckles. A heckle is a bed of “nails” - sharp, long-tapered, tempered, polished steel pins driven into wooden blocks at regular spacing. A good progression is from 4 pins per square inch, to 12, to 25 to 48 to 80. The first three will remove the straw, and the last two will split and polish the fibres. Some of the finer stuff that comes off in the last hackles is called ”tow” and can be carded like wool and spun. It will produce a coarser yarn than the fibres pulled through the heckles

because it will still have some straw in it. In Figure 2.16 an overview is given of the fibre yield obtained at each stage of the processing of flax fibre.

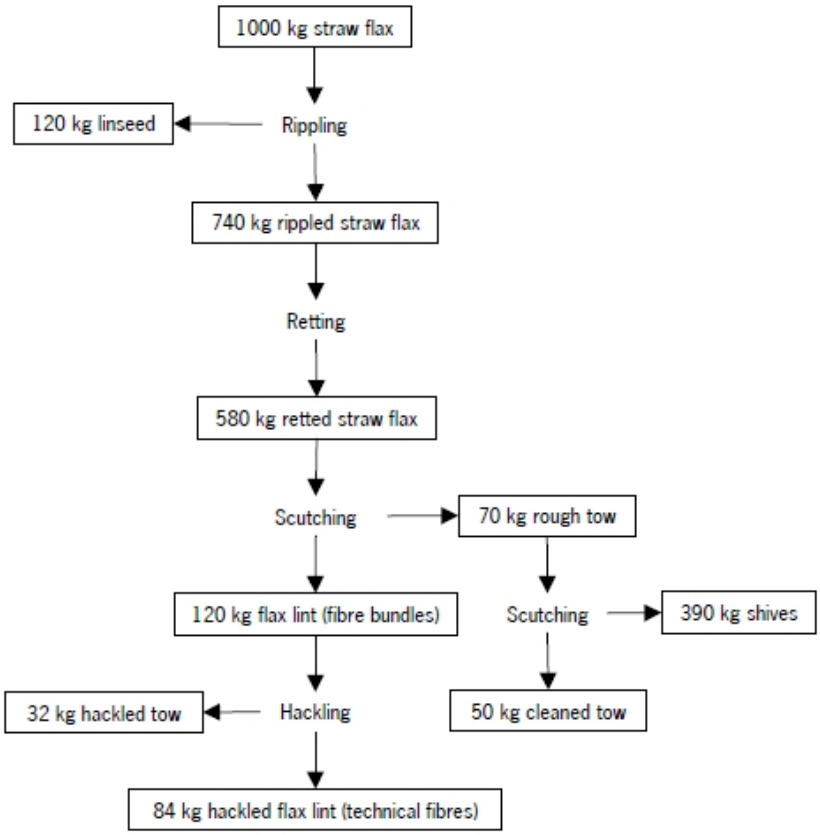

Figure 2.16: Traditional flax fibre isolation methods and their respective products [Bos, 2004], side products of the rippling process are chaff and ripple waste (240 kg), the weight loss during retting is due to the loss of water soluble components, the rest of the weight loss is due to the loss of dust.

2.9 Processing of non-woven natural fibre mat

The needle punch process is illustrated in Figure 2.17 and a example of a needle punching machine is shown in Figure 2.18. Needle punched non-wovens are created by mechanically orienting and interlocking the fibres of a spun bonded or carded web. This mechanical interlocking is achieved with thousands of barbed felting needles repeatedly passing into and out of the web.

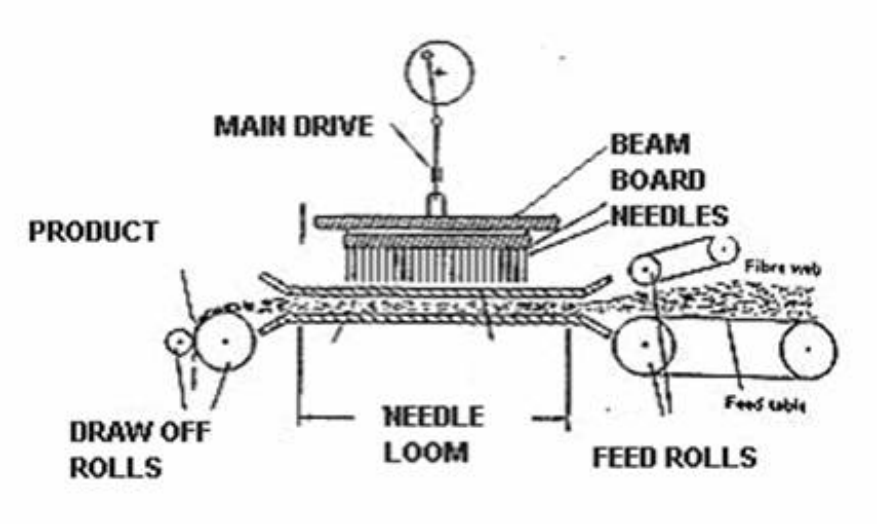

Figure 2.17: Needle punching process [Kamath *et al.*, 2004].

Figure 2.18: An example of a needle punching machine.

The needle board is the base unit into which the needles are inserted and held (see Figure 2.19 and 2.20). The needle board then fits into the needle beam that holds the needle board into place. The feed roll and exit roll facilitate the web

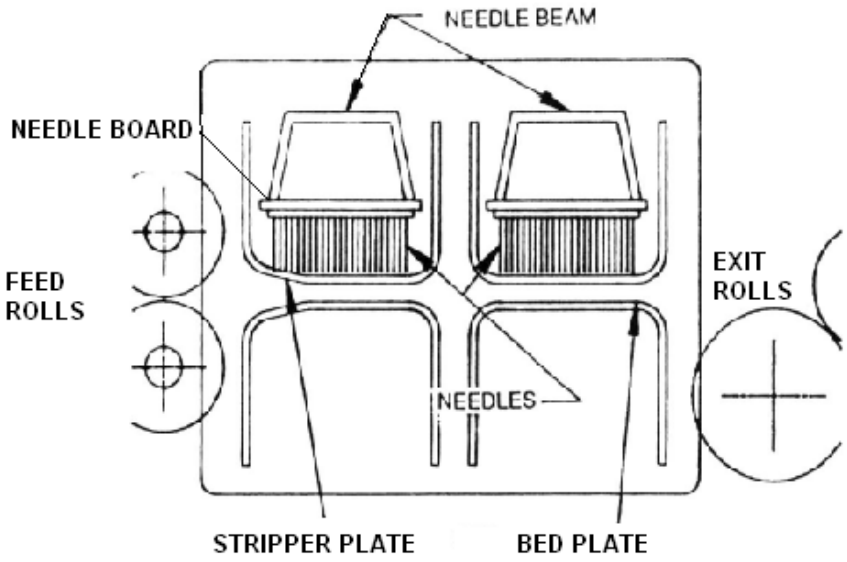

Figure 2.19: Needle loom [Kamath *et al.*, 2004].

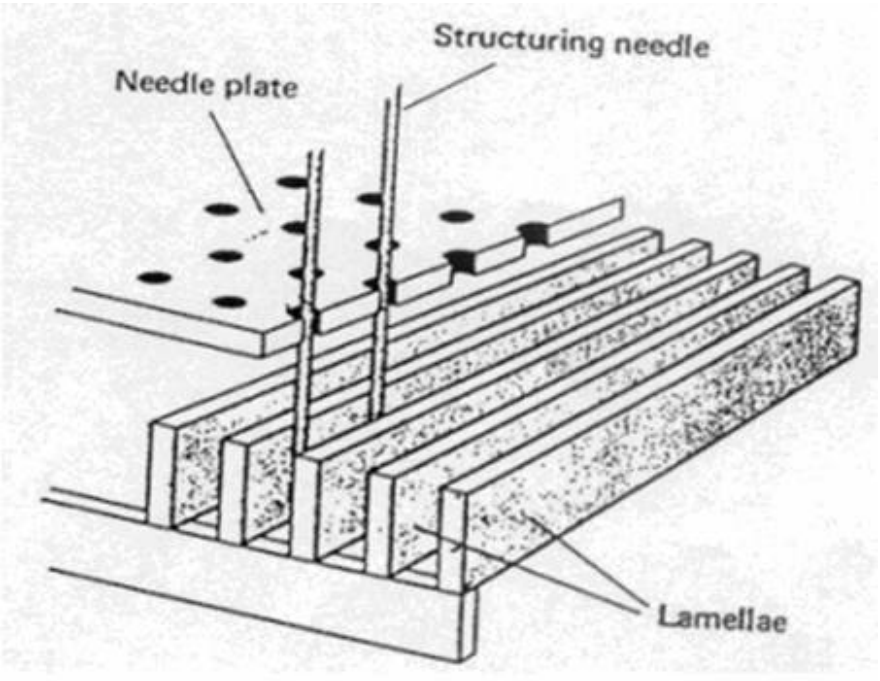

Figure 2.20: Needle penetration [Kamath *et al.*, 2004].

motion as it passes through the needle loom. The web passes through the bed plate on the bottom and a stripper plate on the top. Corresponding holes are located in each plate and it is through these holes the needles pass in and out. The bed plate is the surface the fabric passes over when the web passes through the loom. The needles carry bundles of fibre through the bed plate holes. The stripper plate does what the name implies, it strips the fibres from the needle so the material can advance through the needle loom.

There are many different types of needles that can be used. The gauge of the needles is defined as the number of needles that can be fitted in a square inch area. Thus the finer the needles, the higher the gauge of the needles. Coarse fibres and crude products use the lower gauge needles, and fine fibres and delicate fibres use the higher gauge needles. For example, a sisal fibre product may use a 12 to 16 gauge needle and fine synthetics may use 25 to 40 gauge needle.

As the needle loom beam moves up and down the blades of the needles penetrate the fibre batting. Barbs on the blade of the needle pick up fibres on the downward movement and carry these fibres the depth of the penetration. The draw roll pulls the batt through the needle loom as the needles reorient the fibres from a predominately horizontal to almost a vertical position. The more the needles penetrate the web the more dense and strong the web becomes generally (See Figure 2.21). Beyond some point, fibre damage results from excessive penetration.

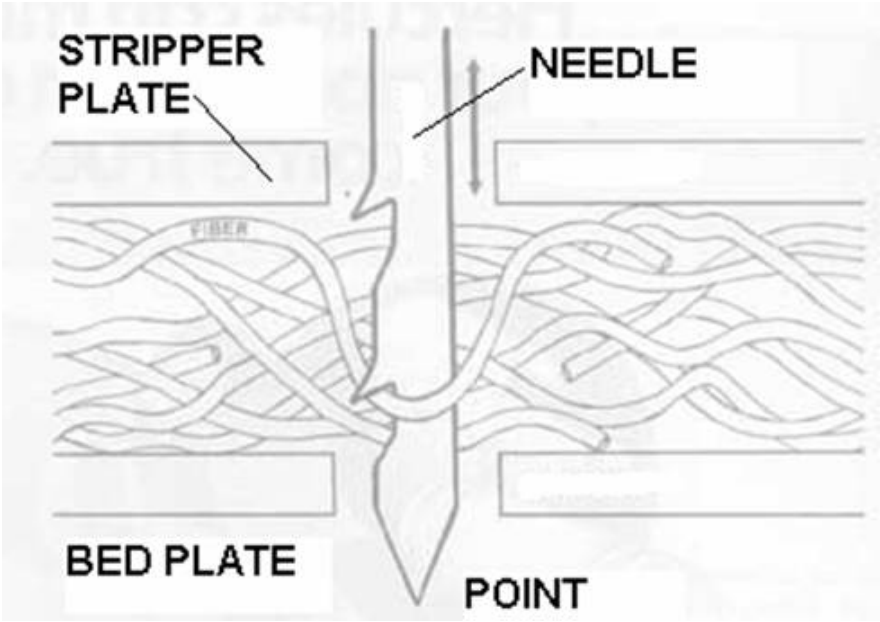

Figure 2.21: Schematic showing the needle action [Kamath *et al.*, 2004].

Machine variables

The most important machine variable is the depth of penetration and puncture density. The fibre travel through the web depends on the depth of penetration of the needle. The maximum penetration is fixed by the needle of the machine and depends on the length of the three sided shank, the distance between the needle plates, the height of stroke, and the angle of penetration. The greater the depth of penetration, the greater is the level of entanglement of fibres within the fabric because more barbs are employed.

The puncture density i.e. number of punches on the surface of the feed in the web is a complex factor and depends on:

- the density of needles in the needle board (Nd)
- the rate of material feed
- the frequency of punching
- the effective width of the needle board (Nb T)

- the number of runs

The puncture density per run Ed_{pass} = [n*F] / [V*W]

where, n= number of needles within a needleboard F = frequency of punching V = rate of material feed W = effective width of the needle board

The puncture density in the needled fabric Ed_{NV} depends on the number of runs N_{pass}; $Ed_{NV} = Ed_{pass} * N_{pass}$.

The thickness, base weight, bulk density and air permeability - which provide information about compactness of fabric are influenced by a number of factors. If the base weight of the web and puncture density and depth are increased, the web density increases and air permeability is reduced (when finer needles and longer, finer and more tightly crimped fibres are used). Web density does not increase when finer fibres are needled with coarser needles. There is neither an increase nor a decrease in air permeability if the puncture density is increased.

As far as the strength of a needled non-woven web, the situation is similar to that for compactness, namely that finer needles, finer and longer fibres, greater web base weight and greater puncture depth and density, result in increased strength of the needled web. However, once a certain critical puncture depth or density has been reached, the rise in strength may be reversed. If the depth of the barb is decreased or the distance between the barbs is increased, the dimensional stability is improved during needling, and the web density and maximum tensile strength in relation to base weight can be raised.

2.10 Mechanical properties of non-woven natural fibre composites

Over the last few years there have been many publications reporting the mechanical properties of various types of natural fibre reinforced composites [Pickering, 2008]. However, in this section only the mechanical properties of non-woven or random fibre reinforced composites will be discussed as this is most relevant to the present study. Most of these publications on these types of reinforcements have been on pure tensile and bending properties.

Tensile properties

Mwaikambo *et al.* [2007] studied compression moulded non-woven hemp/euphorbia composites in tension and obtained tensile strength and modulus of 23 MPa and 2.3 GPa respectively for composites with 21% fibre volume. Mehta *et al.* [2004] investigated non-woven hemp/polyester composites made by compression moulding, with tensile strength and modulus of 36 MPa and 6.4 GPa for composites with 30% fibre volume. Whereas Singleton *et al.* [2003] tested non-woven flax/HDPE made by film stacking and compression moulding method. For 30% fibre volume they reported tensile strength and modulus of 42 MPa and 7.8 GPa, respectively. Pervaiz & Sain [2003] gave tensile strength of 43 MPa for 64% fibre content by weight for non-woven hemp/polyolefin composites made by film stacking method. George *et al.* [1999] reported tensile strength and modulus of 53 MPa and 7.9 GPa for 30% fibre volume of non-woven flax/epoxy composites prepared by autoclave moulding.

Typically the reported tensile properties of non-woven natural fibre reinforced composites range from 20-60 MPa for strength and 2-8 GPa for modulus. This is due to the different matrices and manufacturing methods used. Also further improvement in the tensile properties was reported by many of these authors for fibre composites treated with various chemical fibre surface treatments.

Flexural properties

The flexural properties of non-woven natural fibre composites range from 60-100 MPa for strength and 2.8-4.9 GPa for modulus. Pervaiz & Sain [2003] reported flexural strength and modulus of 63 MPa and 4.9 GPa respectively for 64% fibre content by weight for non-woven hemp/polyolefin composites. Mehta *et al.* [2006] examined the properties of non-woven hemp/polyester composites made by compression moulding and reported a flexural strength and modulus of 100 MPa and 2.9 GPa. Prasad *et al.* [1983] investigated the flexural properties of random coir/polyester composites made by compression moulding. He reported that the flexural strength and modulus of the composite decreased with the introduction of the fibres to the pure resin. Whereas Zarate *et al.* [2003] work on non-woven sisal/resol showed that the flexural strength and modulus increased with increas-

ing fibre volume. They obtained maximum strength and modulus values of 60 MPa and 3.2 GPa respectively at a fibre content of 66 vol.%.

2.11 Summary

The physical and chemical structure of natural fibres has been reviewed in order to understand the factors affecting the mechanical properties of natural fibres. Several factors including: defects and imperfections within the fibres, fibre length and diameter, degree of cellulose crystallinity, microfibril angle, degree of polymerisation and cellulose content as well as growing (climate), harvesting conditions and processing methods have been identified as affecting the mechanical performance of natural fibres. The literature on the process to obtain hemp fibres mats from the hemp plant is thoroughly studied and presented in this chapter. The studies carried out to determine the mechanical properties of non-woven or random natural fibre reinforced composites by various researchers are also reviewed and some of the identified results are presented.

The next chapter describes how the hemp fibre reinforced sheet moulding compounds (H-SMC) was manufactured using a commercially available machine and presents mechanical results of H-SMC composites.

Chapter 3

Mechanical properties of hemp fibre reinforced SMC composites

3.1 Introduction

Sheet moulding compounds (SMCs) are composite materials that, due to their mechanical and aesthetical properties have been employed in a large number of applications from sport and automotive to building applications [Revellino *et al.*, 2000]. However, despite their numerous advantages there are some drawbacks associated with glass fibres used in SMC composites. They are non-renewable and give problems with respect to ultimate disposal at the end of a materials lifetime since they cannot be completely thermally incinerated and leave behind a residue that can damage the incineration furnace [Goutianos & Peijs, 2003]. Additionally these fibres are very abrasive which leads to increased tool wear therefore increasing overall life-cycle cost. Furthermore, glass fibres pose some health and safety problems, like skin irritations during handling of these products [Stamboulis *et al.*, 2000].

An alternative reinforcement for SMC composites could be to use natural fibres such as hemp or flax. Natural fibre composites (NFCs) can be recycled if a thermoplastic matrix is used or thermally incinerated with energy recovery in the case of a thermosetting matrix, since these fibres have a good calorific value compared to glass fibres [George *et al.*, 2001]. Natural fibres have additional

advantages which make them suitable as reinforcement in SMC composites such as low density and high specific mechanical properties [Berglund & Peijs, 2010; Peijs, 2000; Singleton *et al.*, 2003]. Although natural fibres have many advantages, there are certain drawbacks which have restricted their use. Natural fibres have a high rate of moisture absorption [Rouison *et al.*, 2005; Stamboulis *et al.*, 2000] that can affect the durability of the composite in outdoor applications as well as being susceptible to poor dimensional stability and rotting [Peijs *et al.*, 1998; Stamboulis *et al.*, 2001]. Moreover, microcracking of the composite resulting from fibre swelling can cause degradation of mechanical properties. NFCs tend to have low impact strength [Oksman, 2000] and poor fire resistant properties [Hapuarachchi *et al.*, 2007]. Additionally, there is poor compatibility between the hydrophilic natural fibre and the often hydrophobic polymeric resin leading to a weak interface, resulting in inferior mechanical performance [Wambua *et al.*, 2003b] and increased water absorption [Arbelaiz *et al.*, 2005b] of the composite material. Finally, the drawbacks of natural fibres include seasonal growth patterns which affect the supply chain and variability of the product.

The interface plays an important role in transferring the stresses acting on the matrix to the fibre. For the composite to have good mechanical properties the fibre-matrix interface must be relatively strong. However, if the interface is too strong the composite will fail in a brittle mode and have low toughness; therefore it is important to optimise the fibre-matrix interface to accomplish a balance between strength and toughness of the composite [Madhukar & Drzal, 1991; van den Heuvel *et al.*, 1996; Venderbosch *et al.*, 1996]. There have been many studies to improve the bonding between natural fibres and polymer resins through different chemical methods [Doan *et al.*, 2006; Franco & Gonzalez, 2004; Joseph *et al.*, 2000; Mishra *et al.*, 2002; Murkherjee *et al.*, 1993; Qin *et al.*, 2008; Sreekala *et al.*, 2000]. Kalia *et al.* [2009] have reviewed the effect of various surface modification of natural fibres on the properties of fibres and fibre reinforced polymer composites.

One of the most common methods of chemical modification of natural fibres is a treatment with an alkaline solution (also called mercerization), such as NaOH, resulting in a change of fibre properties. Table 3.1 shows some recent studies where alkaline surface treatment was used to enhance the mechanical performance

Table 3.1: Recent studies where alkaline and silane surface treatments have been used to enhance the mechanical performance of natural fibre reinforced composites.

Author	Fibre type	Matrix type	Fibre treatment	Time
Mishra *et al.* [2002]	Sisal	Polyester	Alkaline (5 & 10%)	1h
Qin *et al.* [2008]	Ramie	Cellulose solution	Alkaline (9%)	1h
Sreekala *et al.* [2000]	Oil Palm	Phenol formaldehyde	Alkaline (5%)	72, 48, 24h
Chen *et al.* [2011]	Bamboo	Vinyl ester	Alkaline (20%)	20min
Hu *et al.* [2011]	Flax	PP	Alkaline (2%)	1h
Rokbi *et al.* [2011]	Alfa	Polyester	Alkaline (1,5 & 10%)	24 & 48h
Suradi *et al.* [2011]	Oil palm	PP	Alkaline (15%)	4h
Phuong *et al.* [2010]	Bamboo	PP	Alkaline (0.05,0.1, 0.2,0.25,0.5 & 1M)	-
Lai & Mariatti [2008]	Betel Palm	Polyester	Alkaline (6%)	3h
Franco & Gonzalez [2004]	Henequen	High density PE	Silane (0.05,0.1 & 0.5%)	1h
de Weyenberg *et al.* [2003]	Flax	Epoxy	Silane (1%)	2h
Sreekumar *et al.* [2012]	Sisal	Polyester	Silane (0.6%)	90min
Jandas *et al.* [2011]	Banana	PLA	Sialne (5 wt.%)	3h
Sawpan *et al.* [2011]	Hemp	Polylactide/ Polyester	Silane (0.5 wt.%)	45min
Alix *et al.* [2011]	Flax	Polyester	Silane (0.05M)	24h & 4h(at 100°C)
Kushwaha & Kumar [2010]	Bamboo	Epoxy	Silane (0.5 wt.%)	1h

of natural fibre reinforced composites. Figure 3.1 shows the alkaline reaction of natural fibres. Mercerization directly influences the cellulosic structure, increasing surface roughness of the fibres and resulting in better mechanical interlocking and increasing fibre wetting [Joseph *et al.*, 2000]. Improvements in mechanical performance have been reported by many researchers after alkali treatment of natural fibres [Joseph *et al.*, 2000; Mishra *et al.*, 2002; Qin *et al.*, 2008; Sreekala *et al.*, 2000]. Doan *et al.* [2006] studied the flexural properties of sponge gourd fibre reinforced polyester composites, with alkali treatment of different concentrations. They found that a 5% alkali treatment gave the best flexural properties. Murkherjee *et al.* [1993] found that the use of more than 1% NaOH on cellulose fibres weakens the fibres resulting in a reduction in mechanical properties.

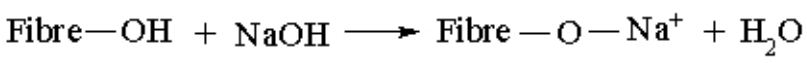

Figure 3.1: Reaction scheme showing alkali reaction of natural fibres.

Another fibre surface modification often used is the use of coupling agents such as silanes [Xie *et al.*, 2010]. Table 3.1 shows some recent studies where silane surface treatment was used to enhance the mechanical performance of natural fibre reinforced composites. Silane coupling agents have been used in glass fibre reinforced composites for a long time and now they are also being evaluated to improve interface properties in wood and natural fibre composites. Hypothetical reaction of natural fibre and silane is shown in Figure 3.2. Many studies have reported the use of silane based coupling agents for natural fibres and found it to be effective in modifying the fibre/matrix interface. Franco & Gonzalez [2004] studied the effect of silane treatment on the mechanical behaviour of high density polyethylene reinforced with henequen fibres. They found that silane coupling agents initially increased the tensile strength of the composite due to improved degree of fibre/matrix adhesion, while at high silane concentrations the tensile strength decreased. The flexural properties of flax fibre reinforced epoxy composites with silane treatment was investigated by de Weyenberg *et al.* [2003]. Again, the tensile strength and modulus of the composites was improved slightly in both longitudinal and transverse directions after silane treatment.

Recently, the interest in thermosets as matrices for natural fibre composites has been increasing [Aziz *et al.*, 2005; Devi *et al.*, 1997; Gassan *et al.*, 1999; Goutianos & Peijs, 2003; Hepworth *et al.*, 2000]. At present around 35% of all natural fibre reinforced composites produced in Europe are based on thermoset matrices compared to 65% for thermoplastic. Thermoset matrices offer better mechanical properties and an improved fibre-matrix adhesion than thermoplastics. Additionally, it is important to understand that the use of a thermoset resin does not necessarily diminish the eco-performance of the produced composites considering they can be recycled through thermal incineration. In fact the use of thermosets could be more complimentary than thermoplastic resin as the addition of natural fibres will considerably lower the mechanical recyclabilty of the

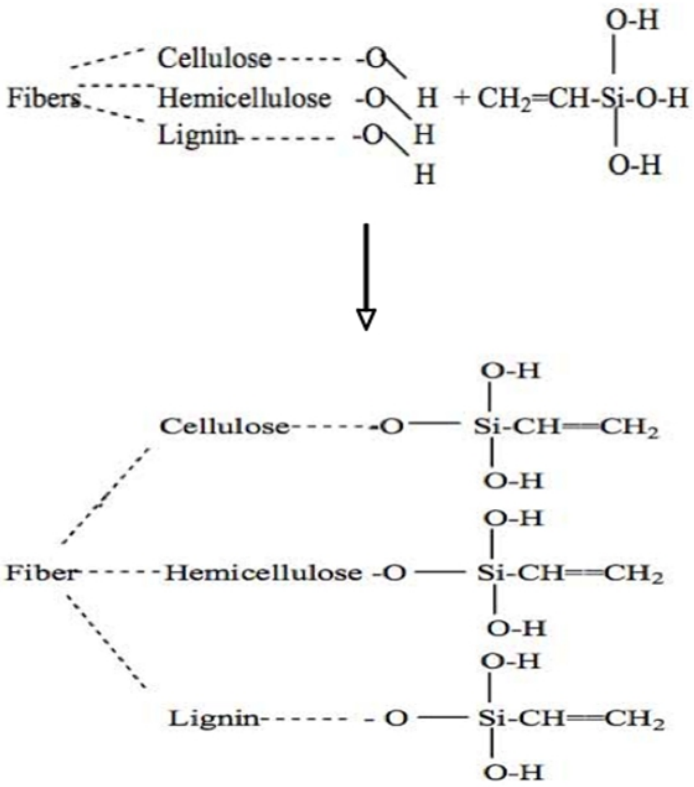

Figure 3.2: Hypothetical reaction of fibre and silane [Sreekala *et al.*, 2000].

thermoplastic. Thermosets also lower the energy required at manufacturing as they are normally cured at lower temperatures. Fully bio-based composites are potentially more eco-friendly, however the current biodegradable polymers are often of modest strength and not always cost-effective at present [Luo & Netravali, 1999; Wibowo *et al.*, 2004]. A relatively new approach is to use cellulose as the matrix material which is reinforced by cellulose or plant fibres together to create all-cellulose composites [Qin *et al.*, 2008; Soykeabkaew *et al.*, 2008]. Natural fibres are nowadays also available in yarn form or as textile reinforcement. Even though textile natural fibre reinforced composites offer better mechanical performance than non-wovens [Goutianos & Peijs, 2003; Heijenrath & Peijs, 1996; Luo & Netravali, 1999; Soykeabkaew *et al.*, 2008; Wibowo *et al.*, 2004] their price is considerably higher; also the embodied energy is considerably increased by the necessary spinning and weaving stages. Therefore non-woven hemp mats are used

in the present investigation.

In this study an attempt has been made to use hemp fibre mats as the principal reinforcement in a SMC composite. Composites with a range of fibre volume fractions and calcium carbonate ($CaCO_3$) filler content were made to determine the optimum fibre and filler content for good mechanical performance. To further improve the mechanical properties of the composite material, hemp fibres have been treated with either NaOH or silane. The composite materials are mechanically tested in tension to determine their strength and Young's modulus. The fracture surface of the tested samples was analysed with SEM technique to understand the failure mechanisms of the composites.

3.2 Experimental

3.2.1 Materials

Needle punched randomly oriented non-woven hemp mats were purchased from Hemptechnology Ltd. (UK) with an areal density of 500 g/m^2 and an average fibre length of 65±15 mm. An orthophthalic unsaturated polyester (UP) was used as resin system (DSM Resins, UK). E-glass roving (2400tex) coated with a silane sizing was used for the glass fibre SMC reference material. Calcium carbonate ($CaCO_3$) with a particle size of 10 μm was used as filler. The E-glass roving and calcium carbonate filler were provided by Menzolit Ltd. (UK). Methyl ethyl ketone peroxide catalyst, p-Benzoquinone polymerisation inhibitor, zinc stearate thickener and butylated hydroxytoluene initiator were also provided by Menzolit. The silane used was an acetoxysilane Z-6075 supplied by Dow Corning. Laboratory reagent grade NaOH pellets were purchased from Fisher Scientific.

3.2.2 Fibre surface treatment

Before treatment the hemp fibre mats were first dried in an oven at 50°C for 24 hrs.

Alkaline treatment: Fibre mats were immersed in NaOH solution (0.5-5 wt.%)

for 1 h and then washed with distilled water several times. Finally the fibre mats were washed with distilled water containing 0.5% of HCl. The washed fibres were then dried at 80°C for 5 hrs.

Silane treatment: Fibre mats were immersed in a water/acetone mixture (5:95 wt.%) containing a silane coupling agent (0.5-5 wt.%). The fibre mats were then dried in an oven at 80°C for 5 hrs.

Alkaline-Silane treatment: Fibre mats were first treated with 2 wt.% alkaline solution and then treated with silane (0.5-5 wt.%).
More detailed description of the hemp fibre surface treatments can be found in Appendix A.

3.2.3 Composite fabrication

Hemp fibre reinforced composites were prepared by a SMC technique using the machine shown in Figure 3.3. The SMC machine comprises of two stations for unwinding polyamide film rolls which serve as a support for the compounds. To make the compound, first an impregnation paste was fed into the bottom resin box of the machine. The machine was then switched on, moving the bottom film along the machine as the resin mixture was deposited on the film with uniform thickness by means of a doctor blade with an adjustable height. In the same way a second film was obtained with an identical procedure to the first and is rotated by 180° to be superimposed on the first one. Simultaneously, the hemp fibre roll located above the top resin box, was fed between the two films, producing a sandwich. This sandwich structure then moved along the machine between a series of compaction rollers, which pressed the layers of resin paste against the hemp fibre layer. The hemp prepreg was then left in a store room of temperature 25°C for one day to pre-cure. The impregnated material was then moulded in a hot-press using a mould of 250 mm × 250 mm. Two layers of the prepreg were used to make one composite plate. A temperature of 140°C and a pressure of 10 MPa was applied for 5 min. The impregnated material was moulded to a notional thickness of 3.5 mm. Composite samples with different fibre volume fractions were produced by varying the doctor blade gap in the SMC machine, resulting in different quantities of resin paste being deposited on the fibre mats.

Details of how the fibre volume fraction of H-SMC composites was calculated is given in Appendix B.

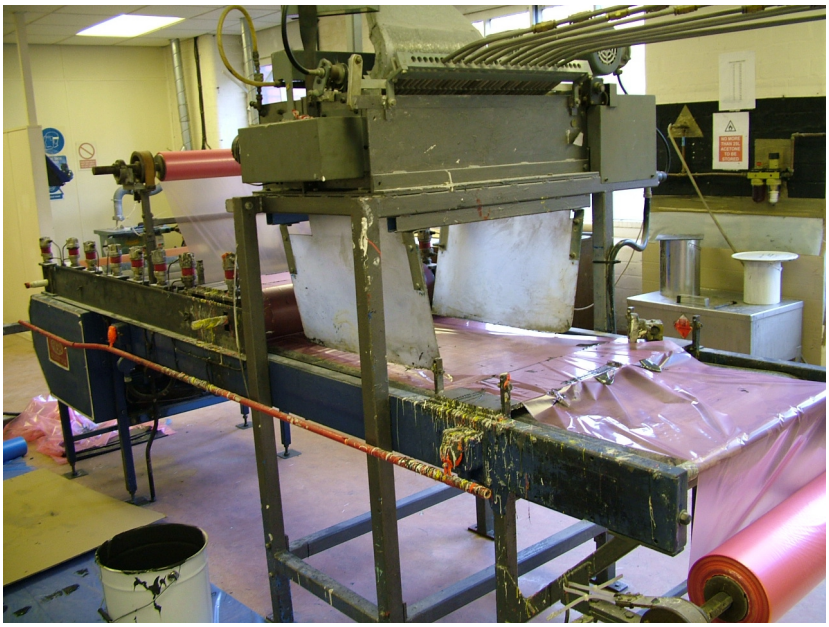

Figure 3.3: Photograph of the machine used to fabricate the SMC composites.

3.2.4 Tensile testing

Tensile tests of hemp fibre reinforced composite samples were carried out according to ASTM D 3039-95. The composite specimens were prepared with end tabs to prevent failure close to the grips. The dimensions of the tensile specimens were 220 mm × 25.4 mm with an average thickness of 3.5 mm. The gauge length was 140 mm. The tensile tests were performed on an Instron 6025 universal tensile testing machine at a cross-head speed of 1 mm/min and a load cell of 10 kN was used. Data reported in this work are calculated as averages of the measurement carried out for three specimens and the error bars shown in the figures represent standard deviation of n=3.

3.3 Micromechanical modelling

Cox-Krenchel [Cox, 1952; Krenchel, 1964] and Kelly-Tyson models [Kelly & Tyson, 1965a,b] are often used to predict the modulus and tensile strength of random fibre reinforced composites. For glass fibre [Thomason & Groenewoud, 1996; Thomason *et al.*, 1996] and even some natural fibre composites [Garkhail *et al.*, 2000] these models give good predictions. However, for most natural fibre reinforced composites these models tend to over estimate the properties, particularly at high fibre content because they do not take into account the effect of porosity and voids in the matrix and the lumen in the plant fibres on the composite mechanical properties.

Madsen & Lilholt [2003] work on unidirectional flax/polypropylene composites suggested that the porosity of the composites can be calculated using:

$$V_f = \frac{1}{1+\alpha} \cdot \left(1 - \left(V_{p(proc)} + V_{p(struc)}\right)\right) \tag{3.1}$$

$$V_f = \frac{\alpha}{1+\alpha} \cdot \left(1 - \left(V_{p(proc)} + V_{p(struc)}\right)\right) \tag{3.2}$$

where V_f and V_m are the volume fractions of fibre and matrix, $V_{p(proc)}$ is the porosity component related to the porosities created during composite processing and $V_{p(struc)}$ is the porosity component assigned to structural mechanisms resulting from the limit of compaction of the plant fibres. α is a factor related to the fibre weight fraction:

$$\alpha = \frac{(1 - W_f) \cdot \rho_f}{W_f \cdot \rho_m} \tag{3.3}$$

where W_f is the fibre weight fraction, ρ_f and ρ_m are the density of fibre and matrix respectively. The Cox-Krenchel model for composite stiffness is given by:

$$E_c = \eta_0 \eta_{LE} V_f E_f + (1 - V_f)\, E_m \tag{3.4}$$

where E_f and E_m are the tensile modulus of fibre and matrix respectively, V_f is the fibre volume fraction, η_0 is the fibre orientation factor of 3/8 for two-dimensional random orientation and 1/5 for three-dimensional random orientation. η_{LE} is the fibre length efficiency factor and is calculate by:

$$\eta_{LE} = \left[1 - \frac{tanh\left(\beta L/2\right)}{\beta L/2}\right] \tag{3.5}$$

where

$$\beta = \frac{2}{D}\left[\frac{2G_m}{E_f ln\left(\sqrt{\pi}/x_i V_f\right)}\right]^{1/2} \tag{3.6}$$

where L is the fibre length, G_m is the shear modulus of the matrix and x_i is the geometrical packing arrangement of the fibres.
The Kelly-Tyson model [Bos *et al.*, 2006; Garkhail *et al.*, 2000; Peijs *et al.*, 1998] for composite strength is given by:

$$\sigma_{uc} = \eta_0 \left(\sum_i \left[\frac{\tau L_i V_i}{D}\right] + \sum_j \left[\sigma_j V_j \left(1 - \frac{L_c}{2L_j}\right)\right]\right) + \left(1 - V_f\right)\sigma_m \tag{3.7}$$

where η_0 is the fibre orientation factor, τ is the interfacial shear strength, σ_m is the strength of matrix, L and L_c is the fibre length and critical fibre length. The first summation is the strength contribution for all fibres of sub-critical length ($L < L_c$) and the second summation for fibres of super-critical length ($L > L_c$). To improve the prediction of strength Fu & Lauke [1996] introduced an additional fitting parameter k:

$$\sigma_{uc} = k\eta_0 \left(\sum_i \left[\frac{\tau L_i V_i}{D}\right] + \sum_j \left[\sigma_j V_j \left(1 - \frac{L_c}{2L_j}\right)\right]\right) + \left(1 - V_f\right)\sigma_m \tag{3.8}$$

The theoretical effect of porosity on the material stiffness [Mackenzie, 1950] can

be given by:

$$E_p = E_d \cdot (1 - V_p)^2 \tag{3.9}$$

where the subscripts d and p represent the fully dense material and the porous material, respectively. Now applying Equation 3.9 to Cox-Krenchel and Kelly-Tyson models gives:

Modified Cox-Krenchel

$$E_c = \eta_0 \eta_{LE} V_f E_f + (1 - V_f)\, E_m \cdot [1 - V_p]^2 \tag{3.10}$$

Modified Kelly-Tyson

$$\sigma_{uc} = k\eta_0 \left(\sum_i \left[\frac{\tau L_i V_i}{D} \right] + \sum_j \left[\sigma_j V_j \left(1 - \frac{L_c}{2L_j} \right) \right] \right) + (1 - V_f)\, \sigma_m \, [1 - V_p]^2 \tag{3.11}$$

3.4 Results and Discussion

3.4.1 Fibre morphology

Scanning electron microscopy (SEM) was used to examine the change in the surface morphology of the surface treated hemp fibres. A SEM micrograph of an untreated hemp fibre is shown in Figure 3.4a. The micrographs show that the untreated fibres have a smooth surface, possibly due to the wax and lignin substances on the fibre surface [Zafeiropoulos *et al.*, 2002]. The SEM micrograph of an alkaline treated fibre is shown in Figure 3.4b. The surface of the fibre has become rough and micro-ridges are visible along the fibre length. The increase in the roughness of the fibre surface after alkaline treatment may be partly due to the removal of the wax layer [Sreekala *et al.*, 1997]. This increased roughness enhances the possibility for mechanical interlocking at the interface. The micro-

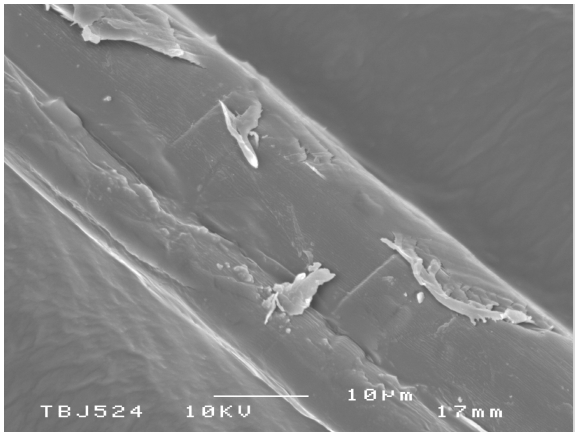

(a) Untreated

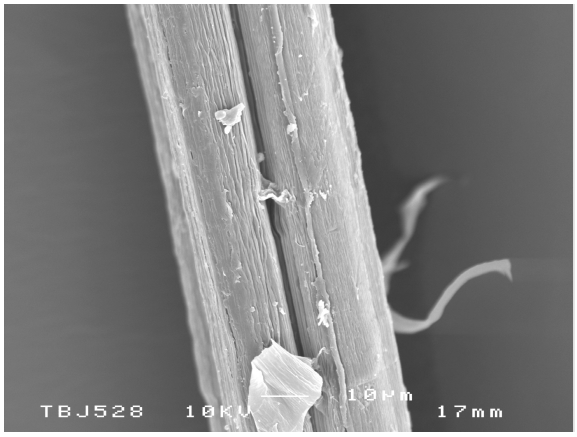

(b) Alkaline

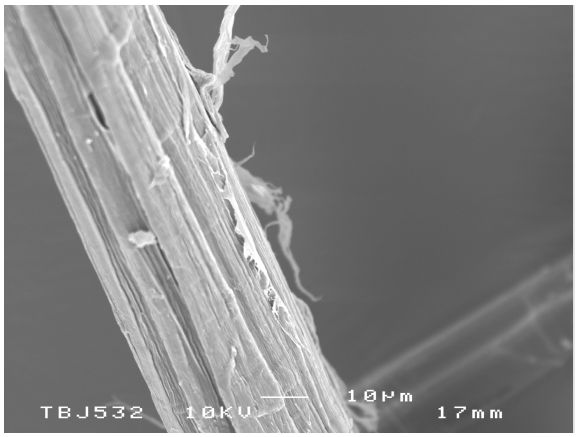

(c) Silane

Figure 3.4: SEM micrographs of different surface treated hemp fibres.

ridges resulting from the separation of the fibres into single fibrils could be due to the removal of lignin material that acts as glue holding individual fibrils together. A SEM micrograph of a silane treated fibre is shown in Figure 3.4c.

3.4.2 Influence of fibre content on mechanical properties

3.4.2.1 Tensile strength

Figure 3.5 shows the tensile strength results of H-SMC and G-SMC composites as a function of fibre volume fraction, together with the Kelly-Tyson (Eq.3.8) and porosity modified Kelly-Tyson (Eq.3.11) predictions for H-SMC composites.

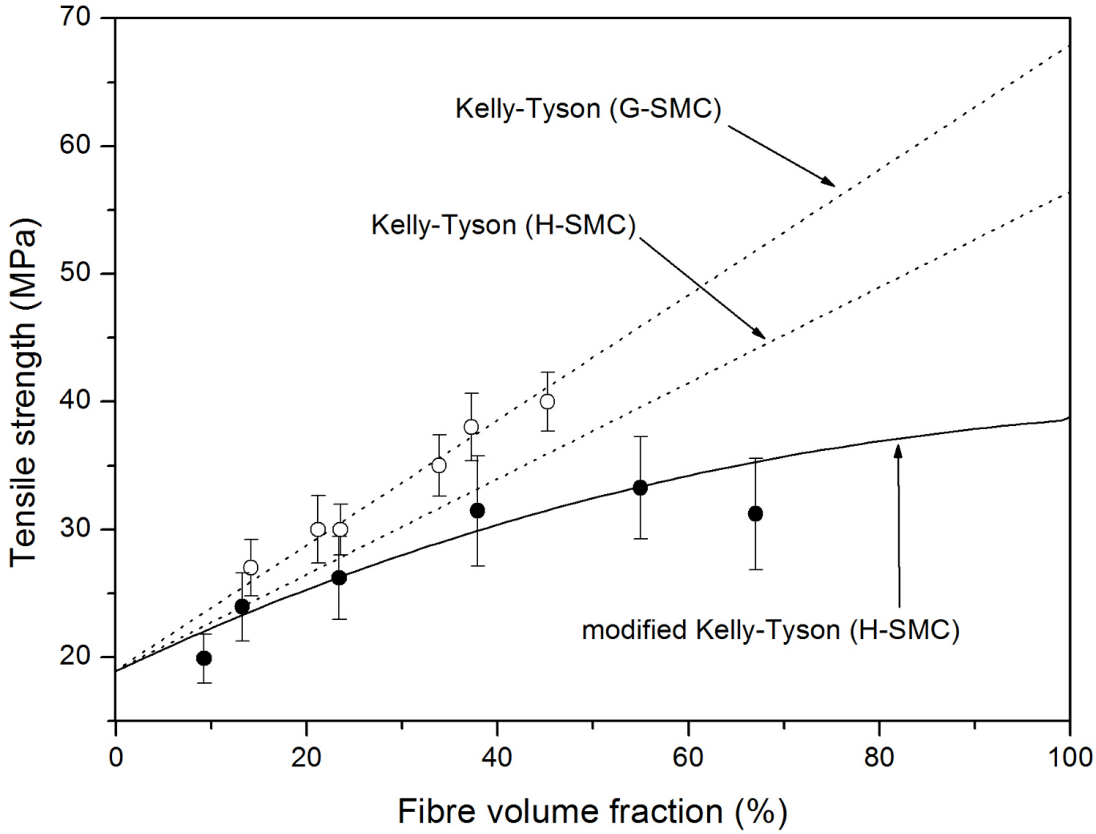

Figure 3.5: Tensile strength of (•) H-SMC composites and (○) G-SMC composites as a function of fibre volume fraction. The dotted lines represent the Kelly-Tyson model predictions for G-SMC and H-SMC and the solid line the modified Kelly-Tyson model predictions for H-SMC.

A constant filler content of 18 vol.% was used. For the Kelly-Tyson model the following parameters are used: fibre strength (σ_f) of 650 MPa (this value was used as it falls within the range of values found in the literature for tensile strength of hemp fibres, see Appendix C), fibre length (L_f) of 65 mm, interfacial shear strength (τ) of 14 MPa [Baley *et al.*, 2006], matrix strength at fibre failure strain of 5.13 MPa ($E_m\sigma_f/E_f = (2000/690)/26900$), critical fibre length (L_c) of 26.5 mm ($\sigma_f D/2\tau = 690 * 0.022/(2 * 14)$), fibre orientation factor (η_0) of 3/8 and a fitting efficiency parameter (k) of 0.18. A similar efficiency parameter of 0.2 was used by Garkhail *et al.* [2000] for flax/PP composites. It is clear from the graph that the reinforcing efficiency of hemp fibres is less than those of glass fibres. The reason for this could be the non-uniformity of natural fibres resulting in large scatter in fibre strength. Another possible reason could be fibre anisotropy resulting in transverse hemp fibre bundle failure. The hemp fibre mats are made of short fibre bundles (technical fibres) which consist of many smaller elementary fibres glued together by a weak pectin-lignin interface. The surface treatment only modifies the fibre bundle surface and not the interface between the elementary fibres within the fibre bundle. The failure of the composite is therefore expected to not only initiate at the fibre-matrix interface but also at the elementary fibre-pectin interface within the fibre bundle. Cracks will propagate not only through the fibre-matrix interface, but also through the interface between the elementary fibres with the technical fibres [Bos, 2004]. Therefore further optimisation of the fibre-matrix interface may have limited influence on the composite mechanical properties. This is displayed schematically in Figure 3.6. A higher efficiency parameter (k) of 0.46 for G-SMC was obtained, possibly because in these isotropic fibres such a failure mode within the fibre cannot occur. G-SMC composite show a good agreement with Kelly-Tyson predictions for all fibre volume fractions, while H-SMC composites have a relatively good agreement at low fibre volume fractions while at high fibre volume fractions the experimental values are considerably lower then the prediction. This is due to the relatively high porosity content in natural fibre composites at high fibre content which the Kelly-Tyson model does not take into account. H-SMC composites have good agreement with the modified Kelly-Tyson prediction for tensile strength at all fibre volume fractions; since this model includes the contribution of porosity content on tensile strength.

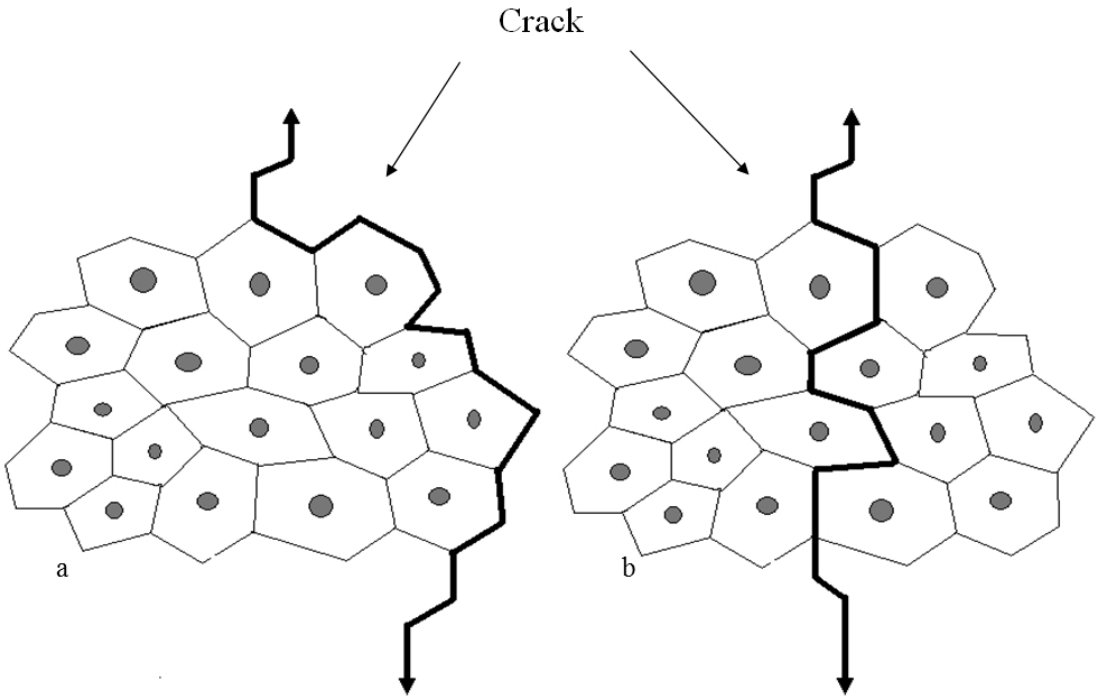

Figure 3.6: Schematic of cross section of a fibre bundle (technical fibre) in a matrix containing a crack. (a) The crack propagating through the fibre-matrix interface. (b) The crack propagating through the interfaces between the elementary fibres. Redrawn from Bos [2004].

The specific properties and price/performance index of G-SMC and H-SMC composites at three different fibre volume fractions are given in Table 3.2. At lower fibre content the specific strength of G-SMC is slightly higher than H-SMC while at higher fibre content the specific strength of H-SMC is higher then G-SMC. A similar trend is noticed for the price/performance index with H-SMC composites having a better price/performance ratio than G-SMC composites at higher fibre loadings. The results indicate that H-SMC composites should be manufactured with relatively high hemp fibre contents to achieve maximum benefits in terms of higher specific properties and price/performance index compared to G-SMC composites.

Table 3.2: Specific properties and price/performance index of G-SMC and H-SMC composites at three different fibre volume fractions.

	Fibre vol.%	G-SMC	H-SMC
Specific strength (MPa/gcm^{-3})	13	13.17	12.47
	23	14.22	14.24
	37	19.00	19.78
Specific modulus (GPa/gcm^{-3})	13	1.07	1.05
	23	1.37	1.48
	37	2.40	2.14
Strength/Price (σ/€m^{-3})	13	4.86	5.96
	23	6.09	6.22
	37	5.54	6.07
Modulus/Price (E/€m^{-3})	13	0.50	0.50
	23	0.59	0.65
	37	0.76	0.66

3.4.2.2 Tensile modulus

Figure 3.7 shows the tensile modulus of H-SMC and G-SMC composites as a function of fibre volume fraction, together with the Cox-Krenchel (Eq.3.4) and modified Cox-Krenchel (Eq.3.10) predictions for H-SMC composites. A constant filler content of 18 vol.% was used. For the Cox-Krenchel model the following parameters are used: fibre modulus (E_f) of 26.9 GPa (this value was used as it falls within the range of values found in the literature for tensile modulus of hemp fibres, see Appendix C), matrix modulus (E_m) of 3.8 GPa, geometrical packing arrangement of fibre of 4, shear modulus of the matrix (σ_m) is 0.71GPa ($E_m/2(1+v) = 2/2(1+0.4)$), a fibre length (L_f) of 65 mm and fibre orientation factor (η_0) of 3/8. Based on the results it can be concluded that the stiffness of H-SMC composites is comparable to G-SMC composites at low fibre volume fractions, while at higher fibre loadings the stiffness of H-SMC composites is slightly lower then that of G-SMC. However, the specific stiffness of H-SMC composites is similar to G-SMC composites (see Table 3.2) considering the low

density of hemp fibres (1.5 g/cm^3 for hemp compared to 2.5 g/cm^3 for E-glass). The price/performance index for tensile modulus is fairly

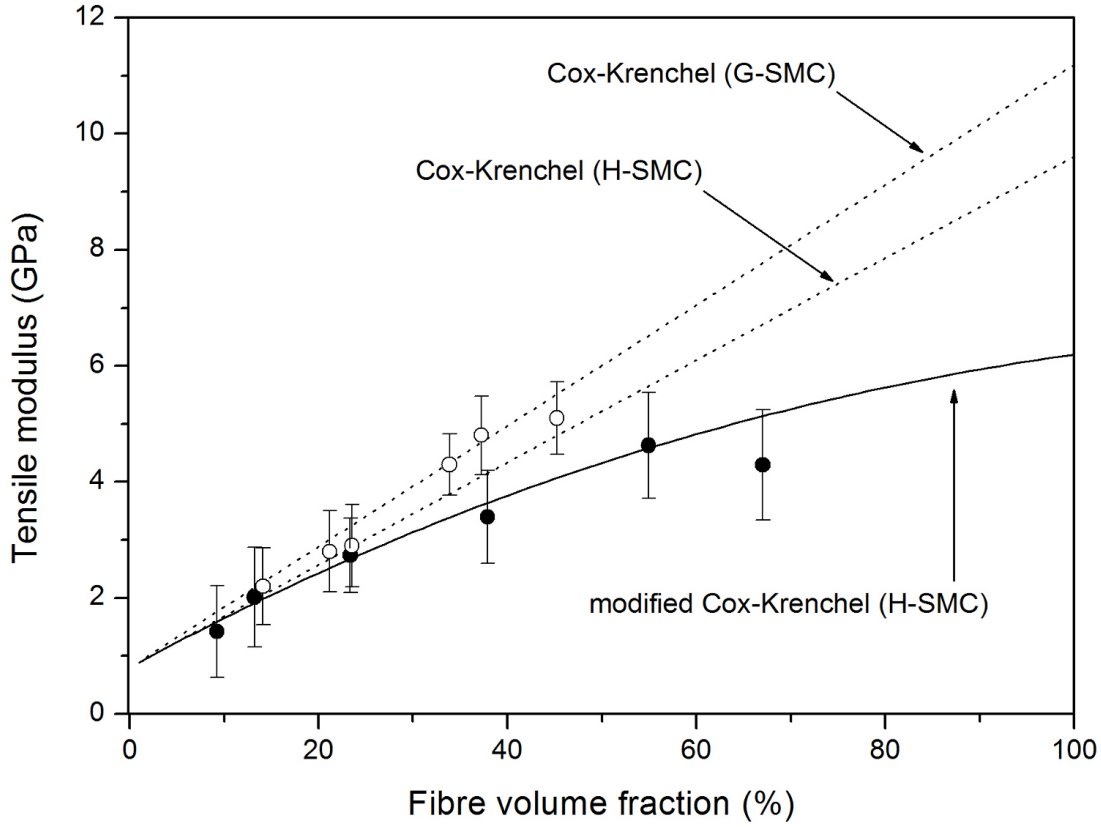

Figure 3.7: Tensile modulus of (•) H-SMC composites and (○) G-SMC composites as a function of fibre volume fraction. The dotted lines represent the Cox-Krenchel model predictions for G-SMC and H-SMC and the solid line the modified Cox-Krenchel model predictions for H-SMC.

similar for both H-SMC and G-SMC. Again the G-SMC composites have a good agreement with the Kelly-Tyson prediction at all fibre volume fractions, while the H-SMC composites only show a good agreement with Kelly-Tyson predictions at low fibre volume fractions. H-SMC composites show good agreement with the modified Kelly-Tyson prediction at all volume fractions.

The models for strength and modulus predictions can be further improved if the porosity content of the composite and other factors of the hemp fibre such as strength and length can be measured more accurately. The results indicate

that further research should focus on trying to reduce the porosity in H-SMC composites by improved processing and compaction methods.

3.4.3 Influence of $CaCO_3$ content on mechanical properties

Figure 3.8 shows the dependence of the tensile strength and modulus of H-SMC composites on the $CaCO_3$ filler content at a constant fibre volume fraction of 23%. Interestingly, the strength of the composite increases with filler content. An improvement of 14% in tensile strength of the composite is obtained with the addition of 26 vol.% filler content compared to the unfilled UP composite

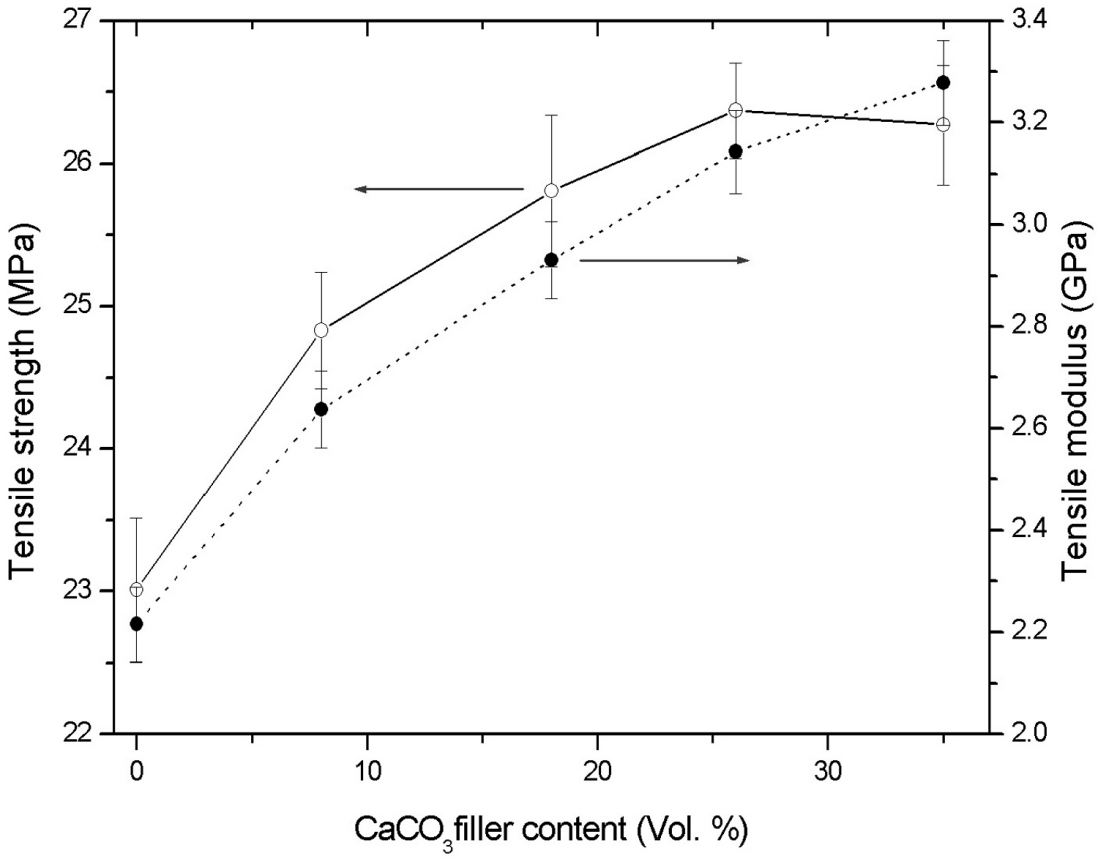

Figure 3.8: (○) Tensile strength and (●) Young's modulus as a function of $CaCO_3$ filler content of H-SMC composites.

specimens. At a filler content of 35 vol.% there seems to be a slight decrease in composite strength, while the stiffness of the composites increases continuously with increasing filler content. Addition of 35 vol.% filler content resulted in a 16% increase in the modulus of the composite. The specific properties and price/performance indexes of H-SMC composites at increasing $CaCO_3$ filler content is given in Table 3.3. The specific properties of H-SMC composites decrease with increasing $CaCO_3$ filler content. This was expected as calcium carbonate has a relatively high density of 2.71 g/cm^3. An alternative to using $CaCO_3$ as filler in H-SMC composites could be to use rice husk powder (RHP). Thanoslip *et al.* [2007] in their work on RHP as a substitute for $CaCO_3$ fillers for glass fibre/polyester moulding compounds showed that weight-for-weight, the composites containing RHP exhibited better or at least comparable mechanical properties to those containing $CaCO_3$ filler. As expected, generally the price/performance index for tensile strength and modulus of H-SMC composites increases with increasing $CaCO_3$ filler content because of the relatively low cost of $CaCO_3$ filler.

Table 3.3: Specific properties and price/performance index of G-SMC and H-SMC composites at different $CaCO_3$ filler content.

Filler content (vol.%)	Specific strength (MPa/gcm^{-3})	Specific modulus (GPa/gcm^{-3})	Strength/Price (σ/€m^{-3})	Modulus/Price (E/€m^{-3})
0	20.54	1.98	6.07	0.58
8	18.53	1.97	6.45	0.68
18	16.03	1.82	6.57	0.75
26	14.49	1.73	6.61	0.79
35	12.69	1.58	6.47	0.81

The fracture surfaces of tensile tested H-SMC composites with different $CaCO_3$ filler content are shown in Figure 3.9. The fracture surface of the unfilled composite (Figure 3.9a) shows a smooth and overlapping matrix phase with sharp edges, while the fracture surface of 8 vol.% $CaCO_3$ filled composite (Figure 3.9b) shows a high level of porosity and the fibres are well embedded in the matrix. The fracture surface of the composite with 26 vol.% filler (Figure 3.9c) shows that fibres are again well embedded in the matrix but the porosity content is

considerably less. This decrease in porosity content is presumably responsible for the increase in tensile strength. The fracture surface of composites with 35 vol.% $CaCO_3$ filler content (Figure 3.9d) shows that the wetting of the fibre becomes poor which results in a reduction in tensile strength. Finally, it is concluded that a filler content of about 25-30 vol.% is optimal to obtain a good balance in tensile strength and stiffness for H-SMC composites.

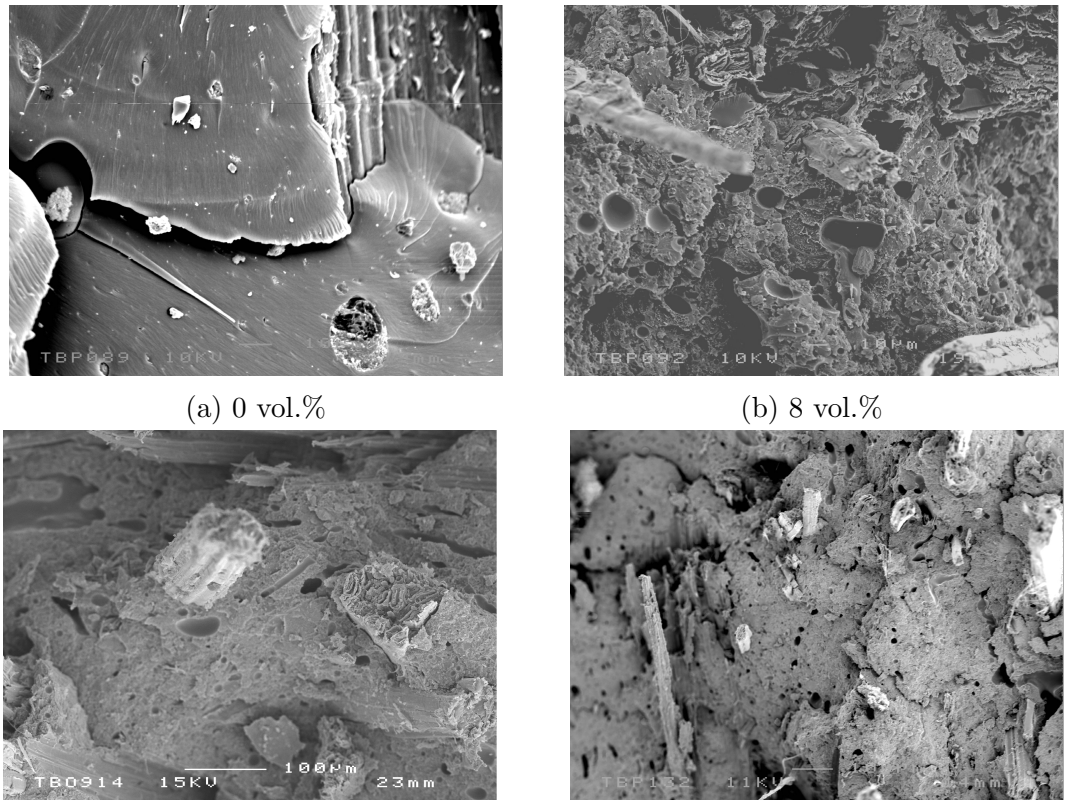

(a) 0 vol.% (b) 8 vol.%

(c) 26 vol.% (d) 35 vol.%

Figure 3.9: SEM micrographs of tensile fracture surface of H-SMC composites with different $CaCO_3$ filler content at a constant fibre volume fraction of 23 vol.%.

3.4.4 Influence of hemp fibre surface treatment

The tensile strength and stiffness of the H-SMC composites based on hemp fibre with different fibre surface treatments are presented in Figures 3.10 and 3.11. Three kinds of hemp fibre surface treatments were used: (i) for fibre cleaning (dewaxing and bleaching) an alkaline (NaOH) treatment was used, (ii) for fibre coating (grafting and coupling) a silane treatment was used and (iii) additionally a combination of these two treatments (constant 2% NaOH concentration with varying silane concentration) was also investigated.

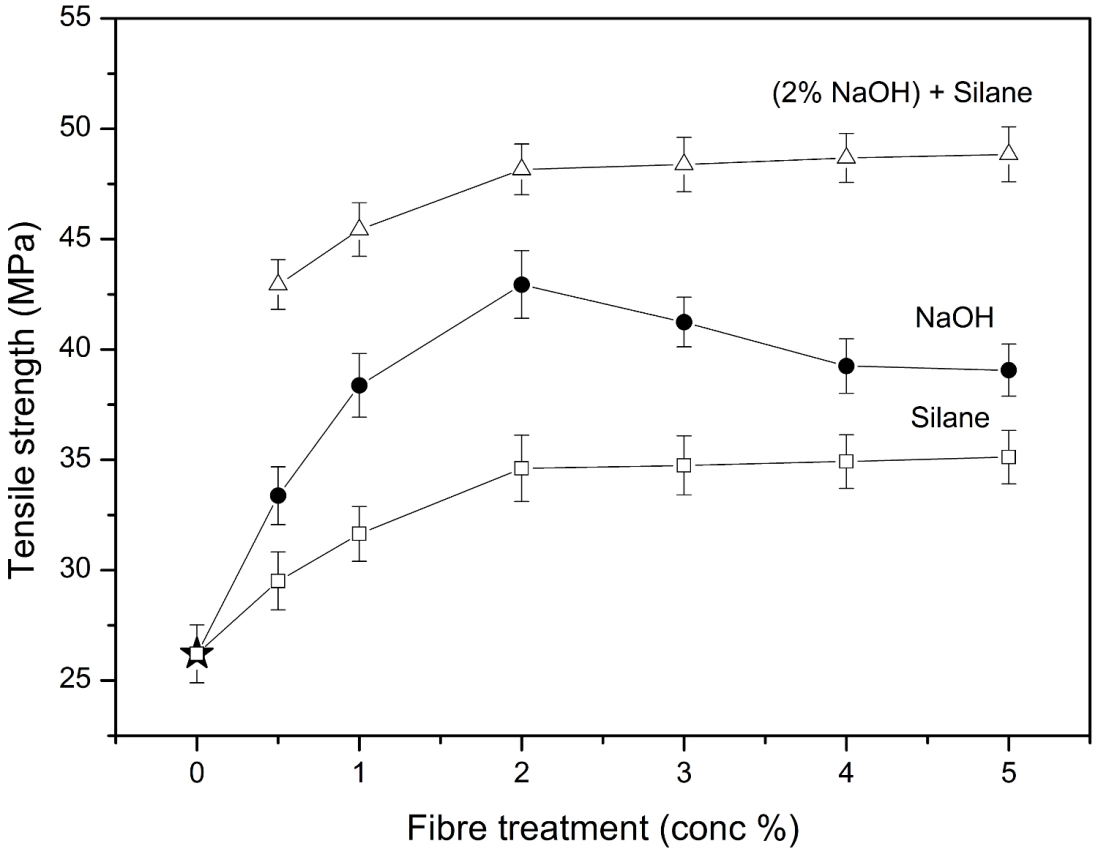

Figure 3.10: Tensile strength of (⋆) untreated, (•) alkaline treated, (□) silane treated H-SMC composites as a function of surface treatment. (△) represents H-SMC composites based on hemp fibres treated with a fixed 2% alkaline treatment and varying concentration of silane treatment.

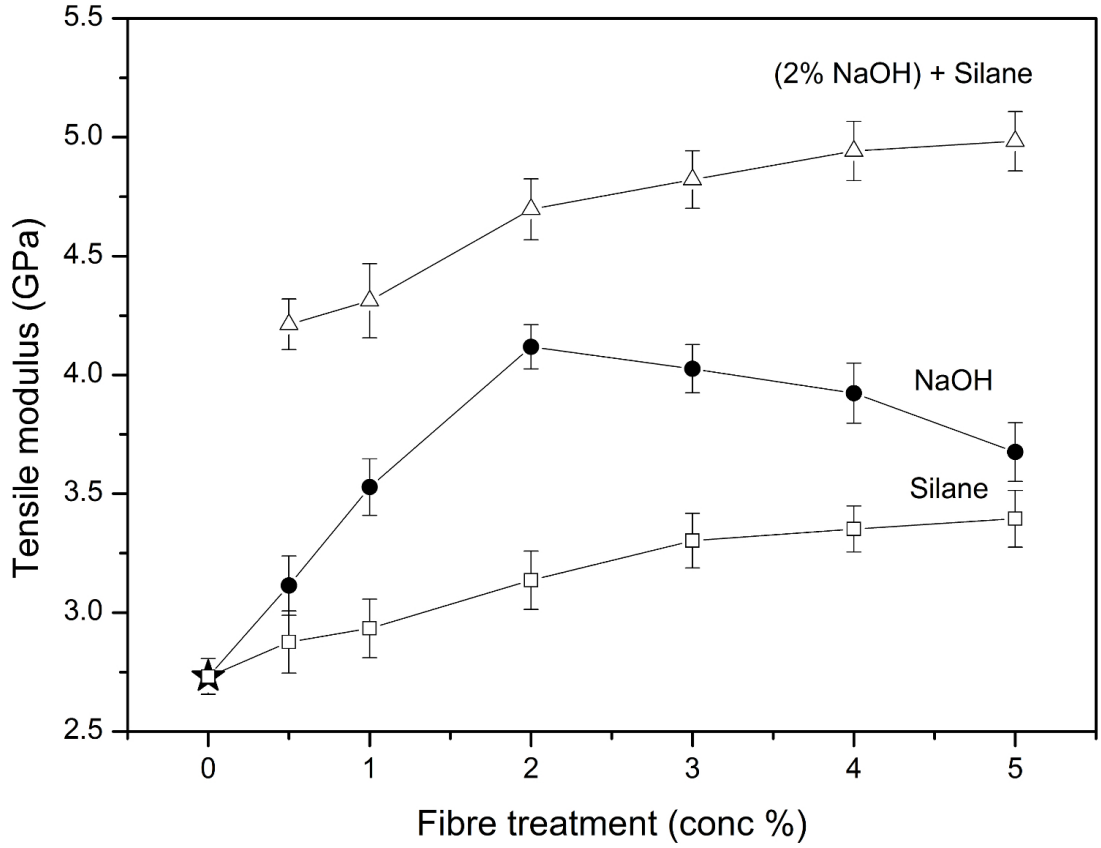

Figure 3.11: Tensile modulus of (⋆) untreated, (•) alkaline treated, (□) silane treated H-SMC composites as a function of surface treatment. (△) represents H-SMC composites based on hemp fibres treated with a fixed 2% alkaline treatment and varying concentration of silane treatment.

3.4.4.1 Alkaline treatment

The tensile strength of the composites increases with alkaline treatment up to a concentration of 2%. However, further increase in alkaline concentration resulted in a decrease in tensile strength. There was, however, a significant improvement of 60% to the tensile strength for composites incorporating hemp fibres treated with 2% alkaline concentration compared to untreated composites. A similar trend to the tensile strength is observed for the composite modulus, with an increase in stiffness with alkaline concentration at a NaOH concentration of 2%, followed by a reduction at higher concentrations. An improvement of 53% in

composite stiffness is obtained for specimens treated with 2% NaOH compared to untreated specimens. As can be seen in Figure 3.4b, the treatment of the hemp fibres with NaOH removed the impurities and waxy substances on the fibre surface thereby making the topography of the fibre surface rougher. This probably enhanced the mechanical interlocking between the fibre and matrix, resulting in an increased tensile strength for alkaline treated fibre composites. Ganan *et al.* [2005] suggested that removal of amorphous components, such as lignin and surface impurities could enhance wetting due to more hydrogen bonds being formed between the purified cellulose fibre surface and the matrix.

3.4.4.2 Silane treatment

The tensile strength of the H-SMC composites increases with increasing silane concentration up to a concentration of 2%, beyond which the strength does not increase any further. An improvement of 32% in tensile strength is achieved for composites treated with 2% silane with respect to the untreated composites. Unlike tensile strength, the composite stiffness continues to increase with increasing silane concentration. An improvement of 24% in stiffness is obtained for composites treated with 5% silane.

3.4.4.3 Alkaline-Silane treatment

The most significant improvement in tensile strength and stiffness of 80% and 82%, respectively is achieved by a combination of an alkaline and silane treatments. The reason for the large increase in tensile properties is that the alkaline treatment as mentioned above removes the impurities on the hemp fibre surface, resulting in more active sites for bonds to form with the silane molecules. In this case considerably more bonds can be formed between the cellulose hydroxyl groups on the fibre surface and the silane molecules than without the alkaline treatment.

3.4.5 Fracture surface analysis

The tensile fracture surfaces of untreated and surface treated H-SMC composites were studied with scanning electron microscopy (SEM). Figure 3.12a shows the

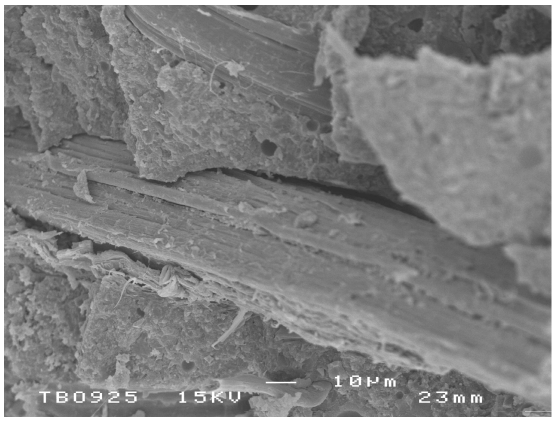

(a) Untreated

(b) Alkaline

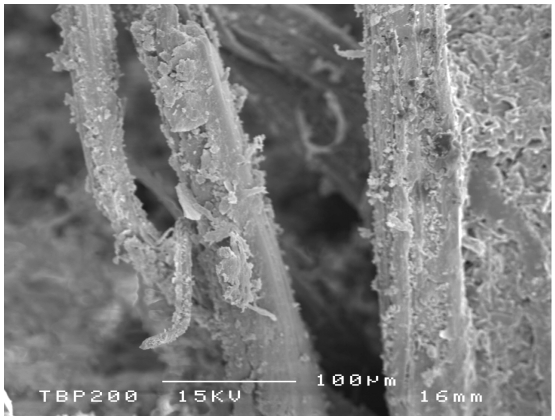

(c) Silane

Figure 3.12: SEM micrographs of tensile fracture surface of H-SMC composites with different fibre surface treatments.

fracture surface of an untreated H-SMC composite. It shows that the surface of the fibres is clean, with little traces of resin adhering to them, suggesting poor adhesion of the polyester resin to the hemp fibres. Furthermore, considerable fibre pull-out is observed in the micrographs of the untreated composite. A SEM fracture surface of an alkaline treated hemp fibre composite is shown in Figure 3.12b. Traces of resin are noticed on the fibre surface, while the embedded fibres are completely surrounded by matrix and fewer gaps are visible between fibre and matrix. This suggests better wetting of the hemp fibres by the polyester resin and considerably less fibre pull-out and debonding is observed. The fracture surfaces of alkaline treated H-SMC composites show that fibrillation of the fibre bundles has occurred, particularly for 2% NaOH concentrations and above. A SEM micrograph of the silane treated fibre composite is shown in Figure 3.12c. The exposed fibre is clearly covered by residue of resin, therefore implying good wetting of the fibre by the polyester resin. Again considerably less fibre pull-out is noticed for the silane treated fibre composite compared to the untreated fibre composite. Again this indicates that silane treatment has enhanced the fibre/matrix adhesion. Furthermore, like the alkaline treated fibre composites the main failure mechanism of the silane treated fibre composites is fibrillation. The fracture surfaces of alkaline-silane treated composites show similarly features to the alkaline and silane fracture surfaces and therefore are not presented here.

3.5 Conclusions

SMC composites were successfully made using random hemp fibre mats and unsaturated polyester resin. Material parameters that were studied for the optimization of the mechanical performance of these H-SMC composites were: fibre volume fraction, $CaCO_3$ filler content and interface modification through the use of alkaline and silane surface treatments. In order to better understand the performance of these H-SMC composites they were compared with glass fibre reinforced composites (G-SMC) manufactured in a similar manner. The mechanical performance of these H-SMC composites was evaluated using modified versions of "Cox-Krenchel" and "Kelly-Tyson" models which included the effect of composite porosity. A rather good agreement between these modified models and the

experimental data was found for both composite tensile stiffness and strength. A significant effect of fibre volume fraction and $CaCO_3$ filler content on the composite mechanical properties was found. The combination of alkaline and silane treatment on the hemp fibres resulted in a significant increase in mechanical properties.

The results demonstrate that the mechanical properties of H-SMC composites are comparable to G-SMC composites especially when considering the low density of hemp fibres compared to glass fibres. Additionally, potential cost savings associated with these H-SMC composites both in terms of raw materials and disposal by incineration after life-time make them a rather attractive alternative to glass fibre based SMCs.

Chapter 4

Impact properties of hemp fibre reinforced SMC composites

4.1 Introduction

Fibre-reinforced composites are increasingly being used in a wide range of low and high technology engineering applications. One of the most paramount are natural fibre reinforced composites (NFCs), which can have higher specific strength and stiffness than more conventional glass fibre composites, therefore making them attractive for numerous weight critical applications [Berglund & Peijs, 2010]. NFCs, however, have relatively poor impact strength [Oksman, 2000]. If NFCs are to be used in large scale applications such as building panels it is necessary to understand the impact behaviour of these composites. The focus of this chapter is to evaluate the impact properties of H-SMC composites using the falling weight test method and compare them to glass SMC. To date there has been little to no impact studies on H-SMC composites. Three composite parameters have been considered for material optimisation: (i) fibre volume fraction, (ii) calcium carbonate filler content and (iii) surface treatment of the hemp fibres by alkali or silane. Impact response of the composites has been studied using a falling weight impact tester and a fundamental understanding of the impact response of the hemp fibre composites has been obtained from the force-deflection curves generated by the impact events.

4.1.1 Low velocity impact

In mechanics, an *impact* is a high force or shock applied over a short time period when two or more bodies collide. Generally, impacts are categorised into either low or high velocity (or sometimes hyper velocity), but there is not a clear transition between categories and authors disagree on the definition. Sjoblom *et al.* [1988] define low-velocity impact as an event which can be treated as quasi-static, the upper limit of which can vary from one to tens of ms^{-1} depending on the target stiffness, material properties and the impactor's mass and stiffness. High-velocity impact response is dominated by stress wave propagation through the material, in which the structure does not have time to respond, leading to very localized damage. Boundary condition effects can be ignored because the impact event is over before the stress waves have reached the edge of the structure. In low-velocity impact, the dynamic structural response of the target is of utmost importance as the contact duration is long enough for the entire structure to respond to the impact and in consequence more energy is absorbed elastically. Cantwell & Morton [1991] conveniently classified low velocity impacts as up to 10 ms^{-1}, by considering the test techniques which are generally employed in simulating the impact event (Instrumented Falling Weight Testing (IFWIT), Charpy, Izod, etc.) whilst, in contrast, Abrate [1998] in his review of impact on laminated composites stated that low-velocity impacts occur for impact speeds of less than 100 ms^{-1}.

4.1.2 Damage modes in random fibre composites

In composites where the fibres are unidirectional it is quite straightforward to predict the orientation of matrix cracking, when the fibres are oriented randomly, then crack patterns are less easy to establish. Clearly, a different approach to defining damage modes is required for these composites. In their research on SMC panels, Liu & Malvern [1987] found that matrix cracks on the impacted surface were short and formed a series of rings away from the point of contact, and deduced that these were caused by the tensile strain wave moving out from the centre of impact. Both Chaturvedi & Sierakowski [1985] and Khetan & Chang [1983] performed work on glass/polyester SMC panels with air-gun equipment

(i.e. high velocity). Whilst the latter authors suggested that damage could be quantified by a 'damage area', the former concluded from tensile residual tests that more information was required on failure modes to be able to predict stiffness and strength degradation. Liu *et al.* [1993] in their work on the repairability of SMC composites for the automotive industry, defined three types of impact-induced damage: (1) indentation (crushing of matrix under the impactor), (2) bending fracture, and (3) perforation (i.e. damage resulting from penetration and associated fracture).

4.1.3 Low velocity impact test methods

The majority of studies on impact response of NFCs have been conducted using either Charpy or Izod pendulum methods, see Table 4.1. Figure 4.1 shows the typical arrangement for Charpy and Izod tests. Although widely used, these tests are not necessarily well suited to an understanding of impact behaviour of natural fibre reinforced composite panels since the test geometry does not represent the end-use application of the composite structure and therefore do not reproduce the failure mode and mechanisms that are likely to occur [Akimoto *et al.*, 2000; Peijs & Venderbosch, 1991].

A better method to study the impact behaviour of NFCs could be falling weight impact as this method gives a closer approximation to a composite material application. Additionally in this method there is no preferential direction of failure and failure can be defined by deformation, crack initiation, or complete fracture, depending on the requirements. These factors suggest that falling weight testing is likely to give a better simulation of impact response of the composite panel which it maybe subjected to in operational service. In a drop weight test an impactor of specific weight is dropped from a pre-determined height. The incident velocity can be determined by equations of motion or by optical sensors on the impactor. Instrumented drop-weight test machines can measure the force/time characteristics and the energy of dissipation can be determined.

Table 4.1: Charpy and Izod are the two most common methods used to test the impact response of various forms of natural fibre composites.

Author	Fibre type	Matrix type	Test method
Garkhail *et al.* [2000]	Flax	PP	Charpy
Hornsby *et al.* [1997]	Flax,Wheat	PP	Charpy
Keener *et al.* [2004]	Flax,Jute	PP	Charpy
Oksman *et al.* [2003]	Flax	PP/PLA	Charpy
Singleton *et al.* [2003]	Flax	PP	Charpy
Wambua *et al.* [2003b]	Sisal,Kenaf, Hemp,Jute,Coir	PP	Charpy
Khalili *et al.* [2011]	Jute	PP	Charpy
Karaduman & Onal [2011]	Jute	Epoxy/Polyester	Charpy
Phuong *et al.* [2010]	Bamboo	PP	Charpy
Joseph *et al.* [2002]	Banana	Phenol formaldehyde	Izod
Mishra *et al.* [2003]	Glass-Biofibre hybrid (Pineapple/Sisal)	Polyester	Izod
Oksman [2000]	Flax	PP	Izod
Rout *et al.* [2001]	Coir	Polyester	Izod
Sanadi *et al.* [1986]	Sunhemp	Polyester	Izod
Sreekala *et al.* [2000]	Oil palm	Phenol formaldehyde	Izod
Kumar & Kumar [2012]	Bamboo	Epoxy	Izod
Goriparthi *et al.* [2012]	Jute	Polylactide/ Polycaprolactone	Izod
Davoodi *et al.* [2012]	Kenaf/Glass hybrid	Epoxy	Izod
Kim *et al.* [2012]	Bamboo	PP/PE	Izod

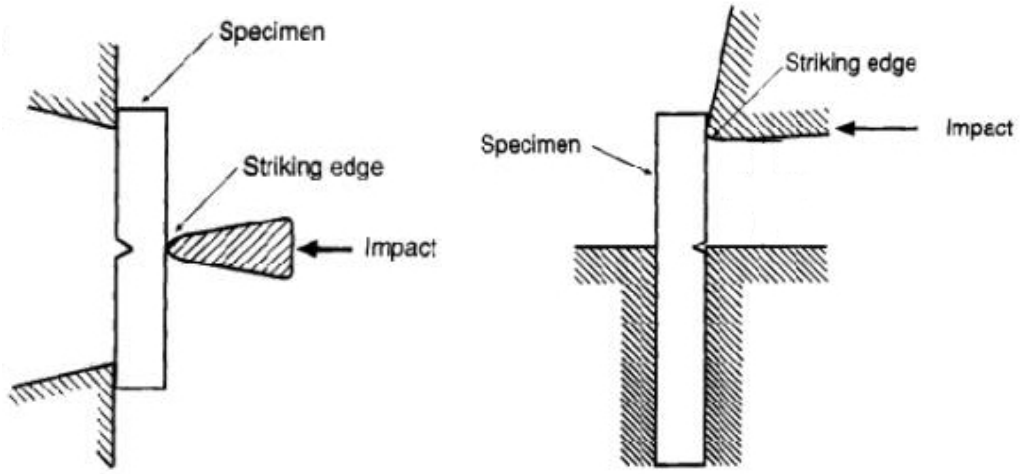

(a) Charpy (b) Izod

Figure 4.1: Specimens and loading configurations for pendulum tests.

4.1.4 Data interpretation

From distinctive portions and peaks on the force-time curve the fracture initiation and propagation of the material can be determined. By using an instrumented impact test, the load-time characteristic, the displacement and energy absorbed during the impact event can be obtained. Load-time response similar to that shown in Figure 4.2 can be recorded.

The important features of the load-time curves include the first point of contact between the striker and the specimen surface, F_C; the point of penetration P_P; the onset of brittle failure, P_f; the load at the incipient point of damage, P_I, and the maximum load point or peak contact force, P_m. Further, inertial load effects, $P_{inertialload} = P_{IL}$: failure initiation phases, and crack propagation phases are also visible. The impact response of the specimen corresponding to each point on the load-time curve is shown in diagrammatic form in Figure 4.3. The deflection at-maximum load, δ_m; time-to-maximum load, t_m: total energy absorbed, E_t: energy absorbed at the incipient and maximum load points, E_i, and E_m, which correspond to P_i and P_m, respectively: impact energy and velocity, E_{imp}, and υ_{imp}, can also recorded.

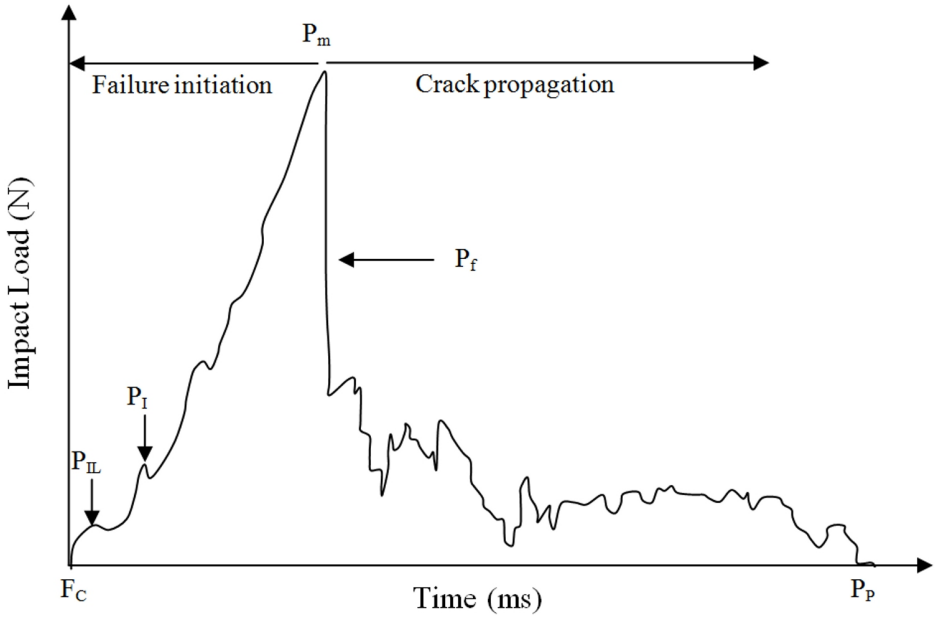

Figure 4.2: Example of load-time curves of an impacted composite material, adapted from Motuku *et al.* [2000].

The incipient point of damage, P_I ; is characterised by a sudden drop (a sharp spike) at the beginning of the load-time curve as shown in Figure 4.3b. It corresponds to the first irreversible damage in the material by subcritical matrix cracking or interface failure and the damage is barely visible at this point. After this point the impact energy corresponds to the damage growth within the composite.

The inertial loads, P_{IL}; also appear as a spike at the beginning of the curve [Aggag & Takahashi, 1996; Bezeredi *et al.*, 1997; Sahraoui & Lataillade, 1990] and can be distinguished from the incipient point of damage by performing the test in question at lower or higher impact velocities. The inertial load spike represents the force required to accelerate the specimen from zero velocity up to the velocity of the tup. The magnitude of the inertial load changes proportionally with impact velocity, whereas the mechanical response of the materials (incipient point of damage) is not usually so strain-sensitive [Aggag & Takahashi, 1996]. The magnitude of the inertial effects and the undesirable oscillations that are often superimposed on the main load curve can be reduced by lowering the impact

velocities, placing a thin sheet of rubber between the specimen (energy absorbed by the rubber sheet can be calculated by subtracting the data of a specimen tested with a rubber sheet from the data of a specimen tested without a rubber sheet present) and the support (mechanical filtering), electrical filtering methods and mathematical filtering treatments. Additionally, the perturbation at point P_{IL}, does not have a sharp load drop and is quite different from the incipient point, P_i, which is identified on the impact load histories.

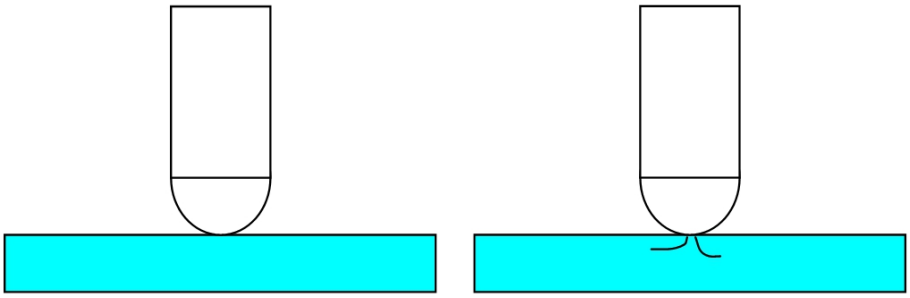

(a) first contact point, F_C (b) first point of damage, P_I

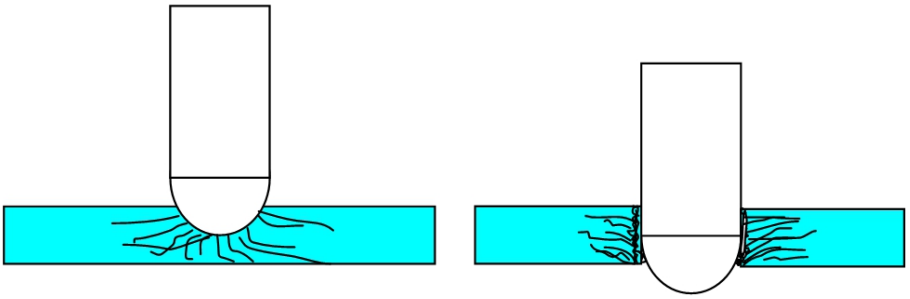

(c) damage at maximum force, P_m (d) specimen penetration, P_P

Figure 4.3: Schematic representation of the falling weight impact event.

The maximum load point or peak contact force, P_m; represents the first visible damage on the composite as shown in Figure 4.3c. This point also represents the highest force the composite can absorb before the onset of major damage. A sudden large drop at P_f, represents the occurrence of significant damage in the material, and failure is of brittle nature in this case. In the case where there was no failure, the kinetic energy of the tup is transferred into the specimen as elastic strain energy, and the maximum load occurs when the tup comes to rest. The unloading portion of the impact load traces corresponds to the rebounding of the

tup. For the case of brittle failure, the tup does not rebound, and some of its kinetic energy is utilized in damage progression. Complete failure occurs when the curve plateaus off in the energy-displacement histories. According to Thanomsilp & Hogg [2003] the peak force is linked to the strength of the reinforcing fibres and strongly influences the energy absorbed by the composite during complete penetration.

4.1.5 Impact studies on natural fibre composites

There have been few impact studies on natural fibre composites using a falling weight impact test method. Antich *et al.* [2006] carried out work on high impact polystyrene reinforced with sisal fibres. Composites of 5, 10, 15, 20 and 25 wt.% of sisal fibres along with a plain matrix panel (HIPS) were manufactured and tested in a falling weight impact machine. A significant decrease in impact toughness was found for the composites in comparison to the plain matrix. In composites, fibre pull-out and debonding are some of the main mechanisms absorbing energy resulting from impact events and the energy required for fibre pull-out increases with fibre length. In their work [Antich *et al.*, 2006] the fibre length was below the critical length (L_c) required for fibre pull-out and therefore, only a small amount of energy was absorbed by this mechanism and it was concluded that matrix yielding was the main energy absorption mechanism.

Santulli [2001] studied impact properties of jute fibre reinforced composite using the falling weight method. Although some useful information on jute fibre reinforced polyester composites was reported by Santulli [2001], he focused more on the acoustic emission activity and the usefulness of this technique in detecting impact damage. However, it was found that the post-impact tensile strength of the composites decreased significantly whereas the Young's modulus showed no significant change. Post-impact cyclic flexural tests exhibited a significant reduction in residual strength. It was suggested that failure modes in the impacted samples did not involve delamination but rather energy absorption by macroscopic matrix cracking. In another study, Santulli *et al.* [2005] examined the falling weight impact behaviour of hybrid composites of E-glass with flax fibre in epoxy matrix (66 vol.% glass and 33 vol.% flax). The hybrids showed

a 25% reduction in impact strength as compared to pure glass fibre composites; however, hybridization with flax fibres lead to a average 12% weight reduction. Rosa *et al.* [2009] have presented a literature review examining the application of acoustic emission technique on studies involving natural fibre composites.

Recently, Dhakal *et al.* [2007a] did some work on impact properties of hemp fibre reinforced composites. Specimens of different fibre volume fraction ranging from 0 to 26 vol.% were impact tested using a falling weight apparatus. They found that peak load and total energy absorption of the specimens increased with increasing fibre volume fraction. Maximum energy absorption was achieved for specimens with a fibre volume fraction of 26%. It was reported that the predominant failure mechanisms were a combination of matrix cracking, delamination and fibre breakage.

4.2 Experimental

For details on materials, composite fabrication and surface treatment the reader is referred to Chapter 3.

4.2.1 Impact testing

Impact properties of the composites were tested using an instrumented DARTVIS falling weight impact tester manufactured by CEAST. Tests were performed according to ISO 6603/2 on specimens of the dimensions 60 mm × 60 mm using a hemispherical striker with a diameter of 20 mm. The specimens were clamped between two plates with a circular opening of 40 mm (no rubber sheet or clamping was used in the present testing). The mass of the striker was 0.780 kg and additional weight was added to generate larger incident energies. A drop height of 0.7 m was used throughout. Both force versus time and impact velocity before impact are recorded and transferred to a data acquisition board in a PC computer. Force was measured using a piezoelectric force transducer. Post processing of data results in the complete energy history during impact and gives a listing of impact velocity, maximum force, total energy, absorbed energy and maximum deflection. Three specimens for each impact condition were tested and the values

plotted in the graphs are averages values of the three specimens. The error bars shown in the figures represent standard deviation of n=3.

4.3 A simple mechanistic model to predict penetration energy

At present there is no general formula available to calculate the penetration energy of a natural fibre reinforced composite under falling weight impact, although some attempts to fulfil this complicated task have been made for glass-fibre-reinforced plastics (GFRP) and carbon-fibre-reinforced plastics (CFRP) thermoset composites [Caprino & Lopresto, 2001; Caprino *et al.*, 2004, 2007] and also for hybrid composites based on carbon-fibres and polyethylene fibres [Peijs & Venderbosch, 1991]. Based on their work on GFRP Caprino & Lopresto [2001] suggested an empirical relationship to predict the penetration energy as:

$$U_p = K \cdot (t \cdot V_f \cdot D_t)^{\alpha} \tag{4.1}$$

where K and α are two fitting parameters, t is the fibre areal weight, V_f is the fibre volume fraction and D_t is the impactor diameter. If the testing parameters are kept constant and the material properties are varied then the parameters which could affect the penetration energy of the composite are matrix type and content, fibre type and architecture, fibre orientations and thickness. According to Caprino & Lopresto [2001] the resin type and content have negligible effect on the penetration energy and similar findings were also reported by Peijs & Venderbosch [1991]; Peijs *et al.* [1994]; Schrauwen & Peijs [2002]. However, for short natural fibre composites the mechanical properties are strongly influenced by the matrix content as at higher fibre volume fraction the mechanical properties tend to decrease due to insufficient wetting and voids. Therefore it is necessary to include a new factor into equation 4.1 which accounts for the effect of matrix content (1-V_f) on the penetration energy:

$$U_p = K \cdot (t \cdot V_f \cdot D_t)^{\alpha} \cdot (1 - V_f) \tag{4.2}$$

Caprino & Lopresto [2000] in another paper studied the energy absorption capability of an in-plane isotropic sheet moulding compound and found that it practically coincided with that of a fabric based laminate having the same fibre areal weight. This suggests that fibre orientation has only a small effect on the penetration energy of the composite while most is related to fibre volume fraction.

Schrauwen & Peijs [2002] investigated the effect of falling weight impact on penetration energy and the influence of laminate construction on damage development of two types of glass reinforcement, i.e. woven and multiaxial non-crimp fabric. They concluded that the penetration energy of both the composite laminates appeared to be mainly influenced by the type of reinforcement, whereas damage development during impact was strongly influenced by both fibre architecture and resin.

Bibo & Hogg [1996, 1998] studied the effect of fibre architecture by employing different forms of glass fibres (unidirectional, quadriaxial warp-knit fabric and eight-harness satin weave) to obtain quasi-isotropic laminates with different spatial distribution of reinforcement. They found that for a given fibre areal weight the penetration energy is approximately the same for all forms of architecture tested, suggesting that penetration energy is independent of fibre architecture.

One problem in using this relationship to determine the penetration energy of NFCs is that this relationship does not take into account the porosity content of the composite, which is relatively high in NFCs compared to GFRP composites. The mechanical properties of NFCs decrease significantly at higher fibre volume fractions due to high porosity content as shown in the previous chapter [Patel *et al.*, 2010]. This porosity content might also significantly affect the energy absorption capabilities of NFCs. The theoretical effect of porosity on the material stiffness [Mackenzie, 1950] can be given by:

$$E_p = E_d \cdot (1 - V_p)^2 \tag{4.3}$$

where the subscripts d and p represent the fully dense material and the porous material. Now applying equation 4.3 to equation 4.1 the following equation is

obtained:

$$U_p = K\,(t \cdot V_f \cdot D_t)^{\alpha} \cdot (1 - V_f) \cdot (1 - V_p)^2 \tag{4.4}$$

4.4 Results and Discussion

4.4.1 Impact event characteristics

Falling weight impact tests were performed to determine the penetration energy of H-SMC composites. Figure 4.4 shows typical force-deflection curves of a penetration test of H-SMC and G-SMC composite specimens with a fibre volume

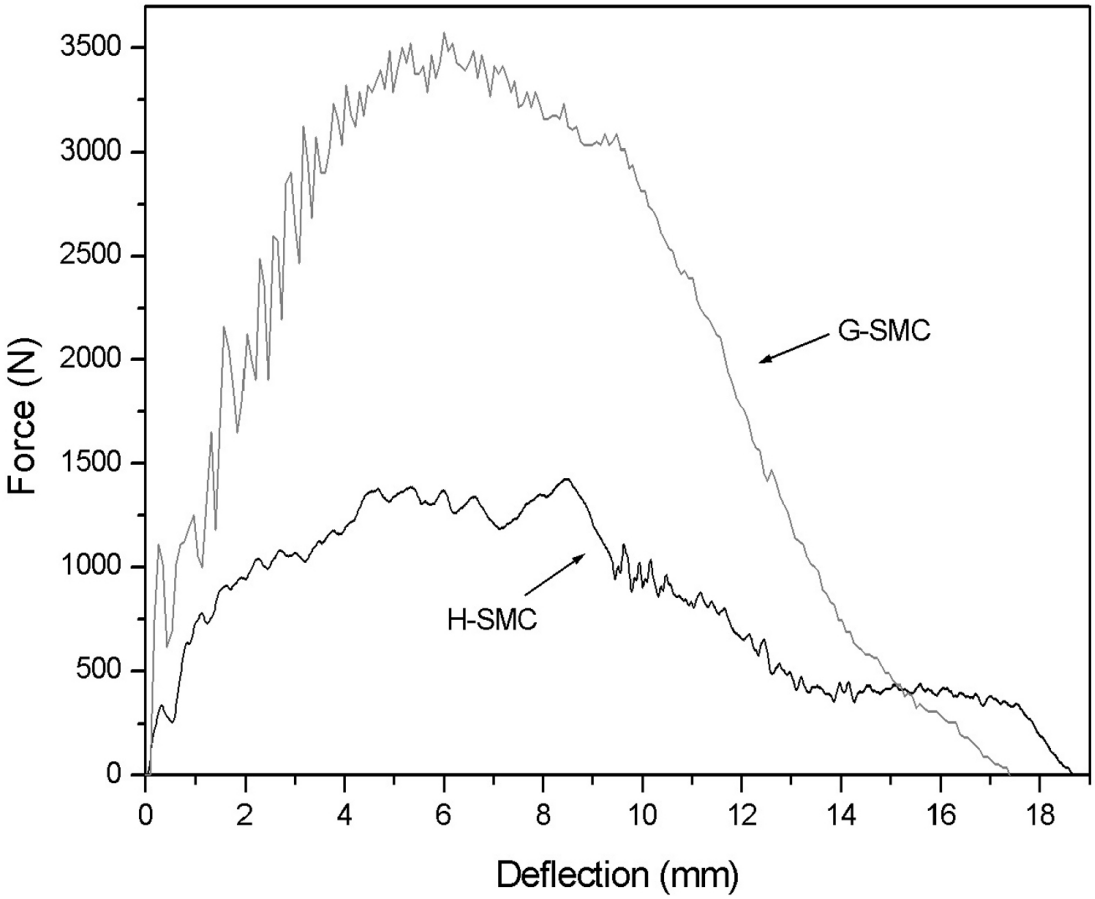

Figure 4.4: Typical force-deflection curves of H-SMC and G-SMC composites with 26 vol.% fibre.

fraction of 26%. Both curves show a sudden drop (a sharp spike) on the force-deflection curve at 0.5 mm which corresponds to the first irreversible damage in the composite specimen by subcritical matrix cracking or debonding. The peak load which represents the first visible damage in the specimen and the highest load the specimen can absorb before the onset of major damage is much higher for the G-SMC specimen (3500 N) compared to the H-SMC specimen (1500 N). The deflection at peak load is slightly higher for the H-SMC specimen (8 mm) than for the G-SMC specimen (6 mm). After maximum load there is a large drop in load for both specimens which indicates the occurrence of significant damage in the specimen. The total deflection of the H-SMC specimen is slightly higher than for G-SMC specimen and the total impact event lasts about 10 ms for both specimens.

4.4.2 Influence of fibre volume fraction

An overview of the penetration energies of H-SMC and G-SMC composites as a function of panel thickness (t) $\times$ fibre volume fraction (V_f) $\times$ impactor diameter (D_t), together with the theoretical prediction for H-SMC and G-SMC using equation 4.1 and the predictions made using the modified model using equation 4.4 are shown in Figure 4.5. For the prediction the following parameters are used: for fitting parameter (K) a value of 0.45 was used for G-SMC and 0.35 for H-SMC (these parameter values were chosen as they most closely match the experimental data, see Appendix D)and for (α) a value of 1 was used, the impactor diameter was 20 mm. The penetration energy of G-SMC composite increases linearly with fibre volume fraction whereas for H-SMC composite the penetration energy initially increases with fibre volume fraction up to 38 vol.%. The penetration energies of H-SMC and G-SMC composites are fairly similar at low fibre loadings while at higher loadings the difference in penetration energy becomes very large. For H-SMC composites the penetration energy increased from 3 J for the pure resin specimens up to 13 J for specimens with 38 vol.% hemp fibre. G-SMC composites show a good agreement with the theoretical model, while H-SMC composites show only a relatively good agreement for composites upto 30 $t.V_f.D_t$ after which the model significantly over predicts the penetration energy.

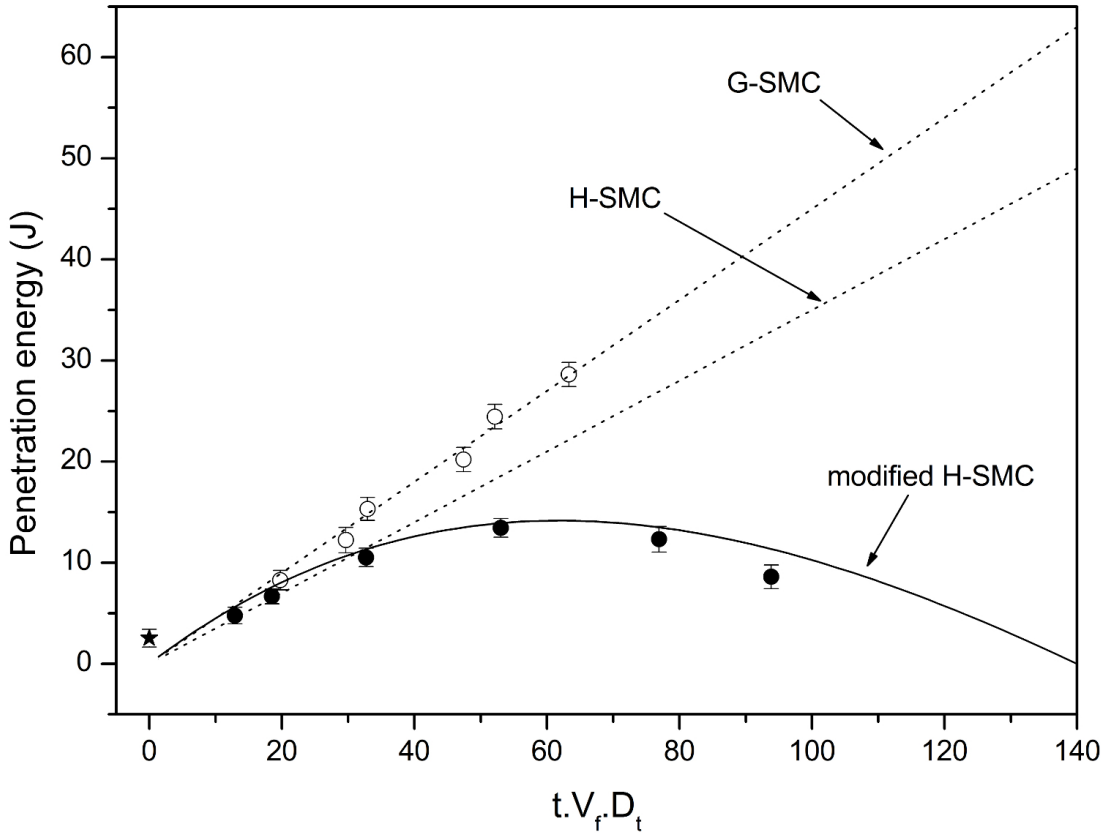

Figure 4.5: Penetration energy of ($\star$) pure resin, ($\bullet$) H-SMC and ($\circ$)) G-SMC composites as a function of panels thickness (t) fibre volume fraction (V_f) impactor diameter (D_t). The dotted lines represent the model predictions (equation 4.1) for G-SMC and H-SMC and the solid line represents the predications made using the modified model (equation 4.4) for H-SMC.

This is because the model does not take into account the poor wetting of the hemp fibres and also the high porosity content at higher fibre contents resulting from insufficient matrix material which might considerably reduce the energy absorbing capabilities of the composites. Apart from data at extremely high fibre content, the H-SMC composites show a relatively good agreement with the modified model at all fibre volume fractions. To further improve the prediction of the penetration energy by the modified model the failure modes of the composites need to be taken into account. There might be a possible change in failure mode from matrix dominated failure at lower fibre loadings to fibre dominated failure

at higher fibre loadings.

The total impact energy involved in an impact event can be divided into two parts: In the first part the elastic potential energy of the composite plate is released by rebounding of the plate after maximum deflection. This elastic energy is transferred back to the impactor. The second part of the impact energy is absorbed by the plate and is made available for damage creation and therefore this part controls the extent of damage and residual strength of the plate after impact [Peijs *et al.*, 1990; Schrauwen & Peijs, 2002]. In Figure 4.6 the absorbed energy (impact energy subtracted by elastic energy) is plotted against the impact energy for H-SMC composites with varying hemp fibre volume fraction.

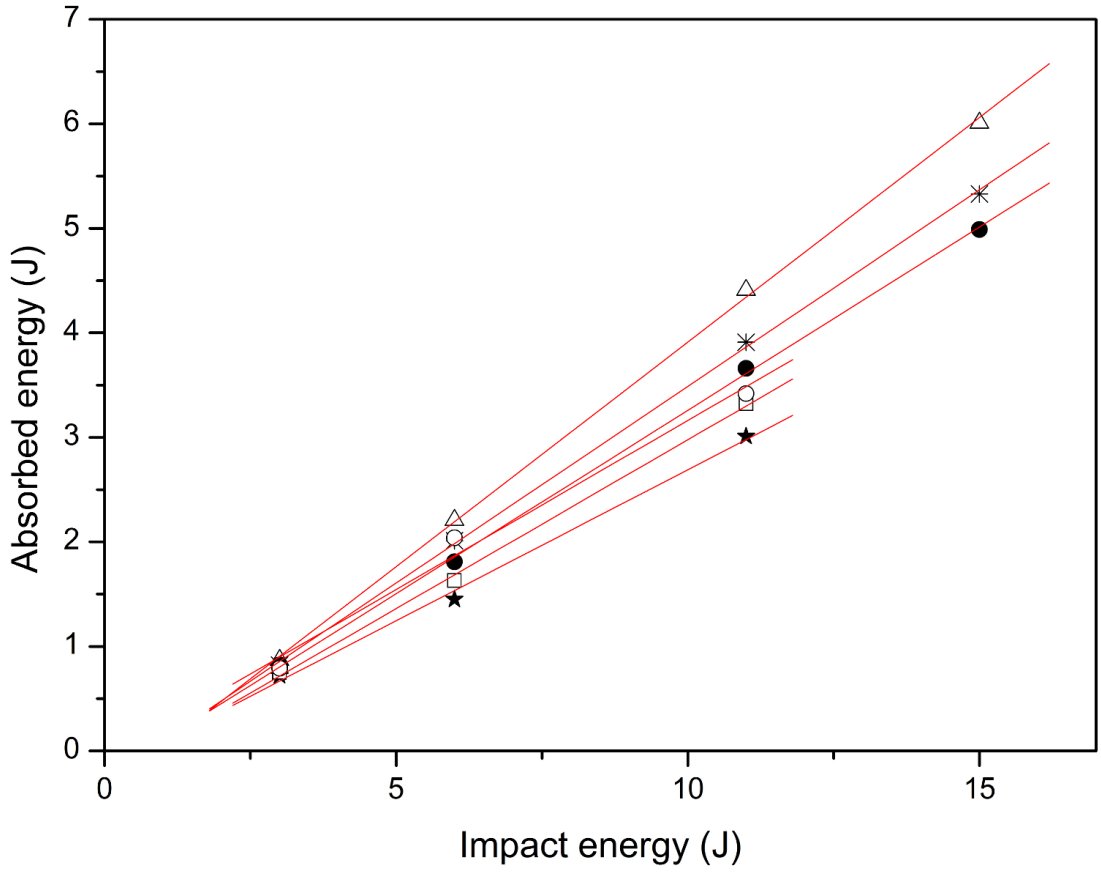

Figure 4.6: Absorbed energy vs. impact energy of H-SMC composites with varying fibre volume fraction (⋆) 9 vol%, (□) 13 vol.%, (∗) 23 vol.%, (△) 37 vol.%, (•) 54 vol.% and (○) 67 vol.%

It is clear that at higher impact energies H-SMC composites with 37 vol.% fibre absorbed the most energy while composites with fibre contents above 37 vol.% absorbed more energy at an impact energy of 6 J; however they failed at much lower impact energy. Generally the energy absorbed by the composites increased with increasing fibre content at an impact energy of 6 J and hence more energy is available for damage as the fibre content increases.

Typical fracture surfaces of H-SMC composites with 23 vol.%, 37 vol.% and 54 vol.% hemp fibre are shown in Figure 4.7. Specimen with 23 vol.% fibre show considerable damage. The fracture surface of 37 vol.% and 54 vol.% fibre specimens is similar. A dome shape protruding material is noticed at the back surface.

(a) 23 vol.% (b) 37 vol.% (c) 54 vol.%

Figure 4.7: Effect of fibre volume fraction on H-SMC impact face damage.

4.4.3 Influence of $CaCO_3$ filler content

Figure 4.8 shows the dependence of the penetration energy and absorbed energy of H-SMC composites on the $CaCO_3$ filler content with a constant fibre volume fraction of 23%. Penetration energy increases with addition of filler content, an improvement of 66% to the penetration energy of the composite is obtained with the addition of 18 vol.% filler content compared to the unfilled composite specimens. At filler content of 18 vol.% filler content the penetration energy of the

composites decreases. The energy absorbed to create damage in the composite shows a similar trend to the penetration energy with an initial increase with filler content upto 18 vol.% and a subsequent decrease with further addition of filler. An improvement of almost 50% is achieved with the addition of 18 vol.% of filler with respect to the unfilled composite.

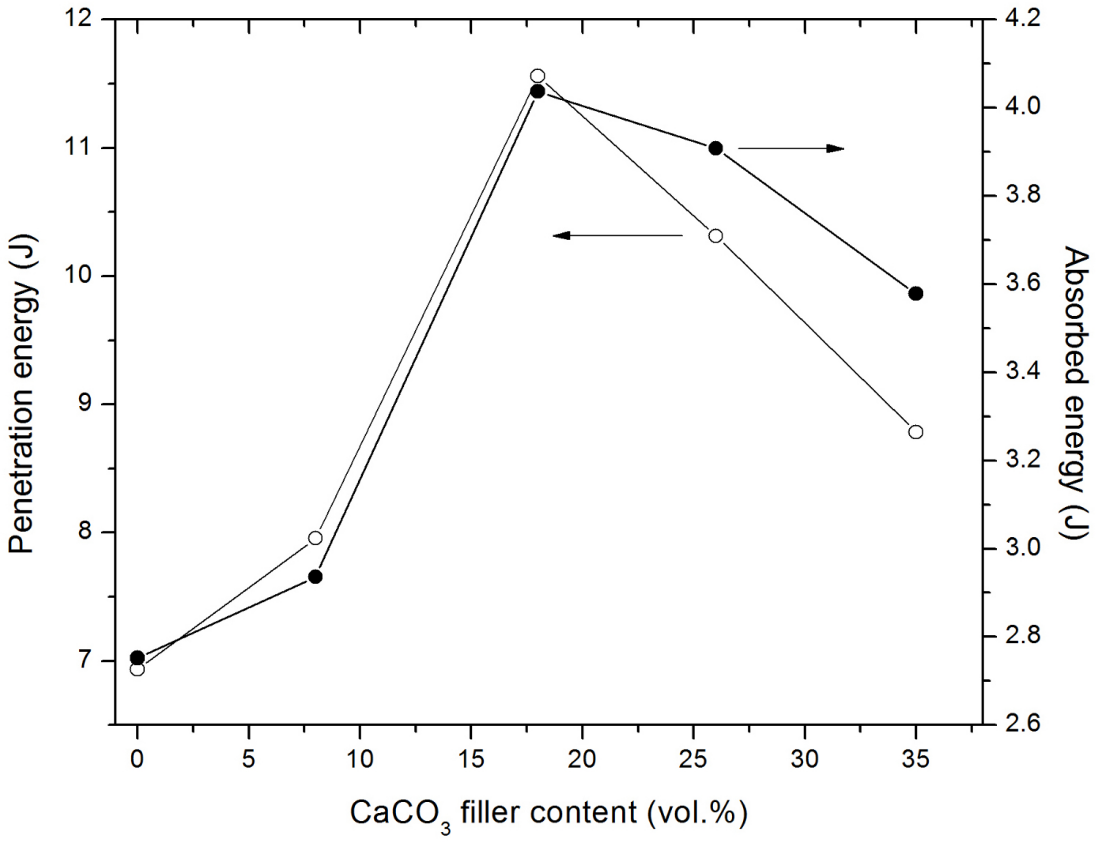

Figure 4.8: (○) Penetration energy and (●) absorbed energy as a function of $CaCO_3$ filler content of H-SMC composites

Fracture surfaces of impacted H-SMC composites were examined using a scanning electron microscope (SEM). The fracture surfaces of tensile tested H-SMC composites with different $CaCO_3$ filler content is shown in Figure 4.9. The fracture surface of the unfilled composite (Figure 4.9a) shows that fracture initiates at the fibre-matrix interface and propagates along the matrix producing sharp cracks, while the fracture surface of 8 vol.% filled composite (Figure 4.9b) shows

a high level of porosity. However, the fibres are well embedded in the matrix which maybe the reason for the increase in penetration and absorbed energy. The fracture surface of 26 vol.% filled composite (Figure 4.9c) shows that the porosity content is considerably less, which could be responsible for the increase in impact performance. The fracture surface of 35 vol.% filled composite (Figure 4.9d) shows that wetting of the fibre is poor due insufficient matrix resulting in the reduced energy absorbing capabilities of the composite.

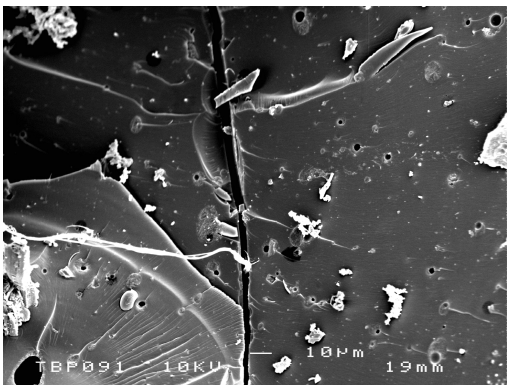

(a) 0 vol.%

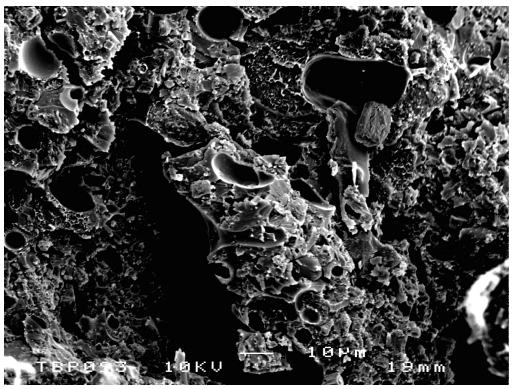

(b) 8 vol.%

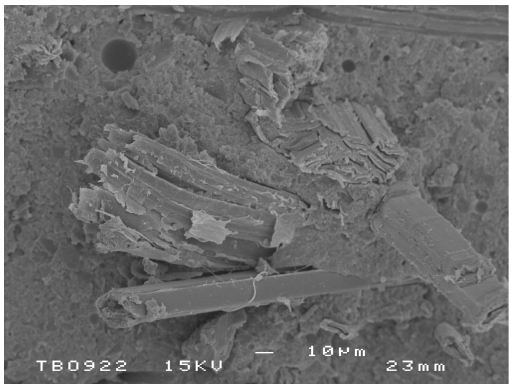

(c) 26 vol.%

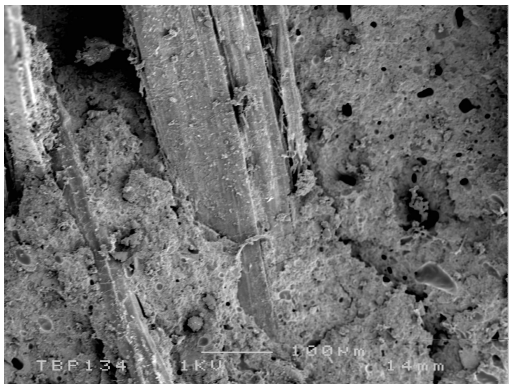

(d) 35 vol.%

Figure 4.9: SEM micrographs of impact fracture surface of H-SMC composites with different $CaCO_3$ filler content.

4.4.4 Influence of fibre surface treatment

Penetration energy and absorbed energy of the H-SMC composites as a function of surface treatment concentration are presented in Figures 4.10 and 4.11. Three different treatments were considered: alkaline, silane and alkaline-silane (constant 2% alkaline concentration with different silane concentration).

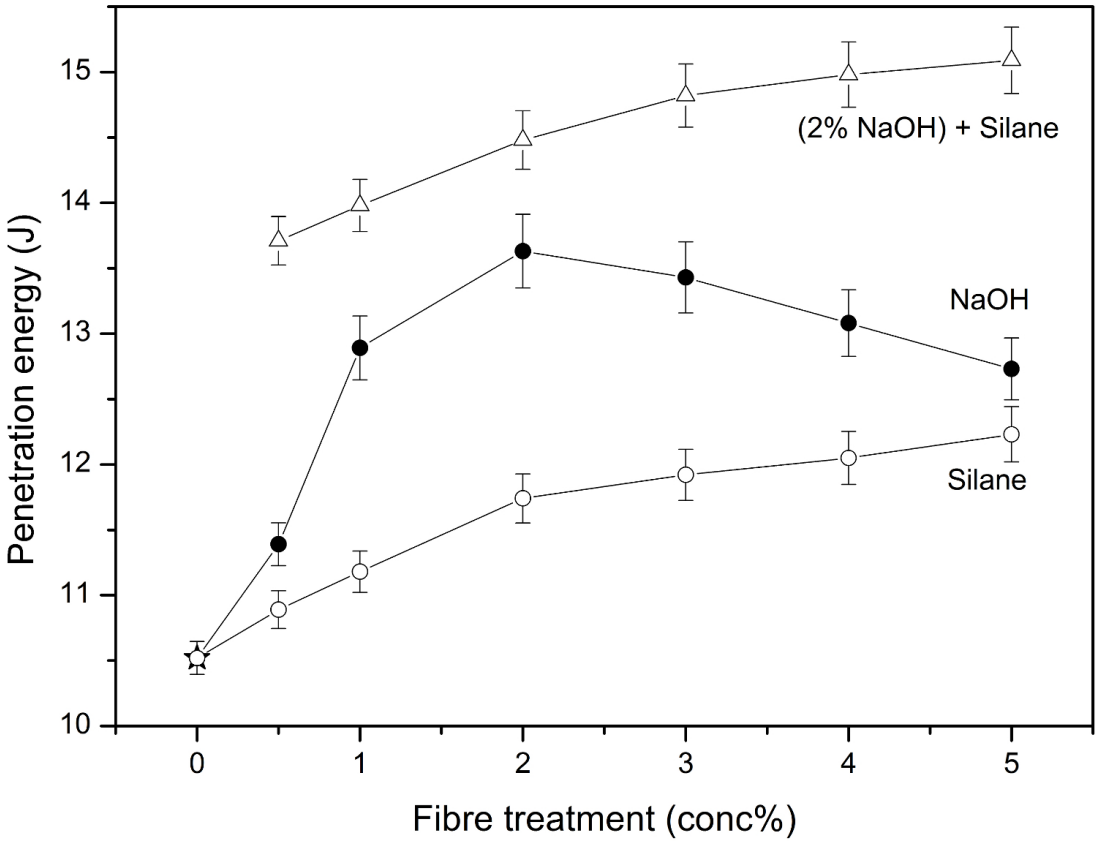

Figure 4.10: Penetration energy of (⋆) untreated, (•) alkaline treated, (○) silane treated H-SMC composites as a function of surface treatment. (△) represents H-SMC composites based on hemp fibres treated with a fixed 2% alkaline treatment and varying concentration of silane treatment.

4.4.4.1 Alkaline treatment

The penetration energy increases with alkaline treatment; at 2% concentration there is an improvement of 3 J in penetration energy compared to the untreated

fibre H-SMC composite, beyond 2% NaOH concentration the penetration energy decreases slightly. The energy absorbed by the composite for damage creation also shows a similar trend to the penetration energy where the composites with hemp fibres treated with 2% concentration of alkali absorbed 20% more energy then untreated hemp fibre composites. As explained in the previous chapter [Patel *et al.*, 2010] the treatment of the hemp fibres with NaOH removes the impurities and waxy substances on the fibre surface thereby making the topography of the fibre surface rougher. This probably enhanced the mechanical interlocking between the fibre and matrix meaning that more energy is absorbed through fibre pullout and debonding mechanisms.

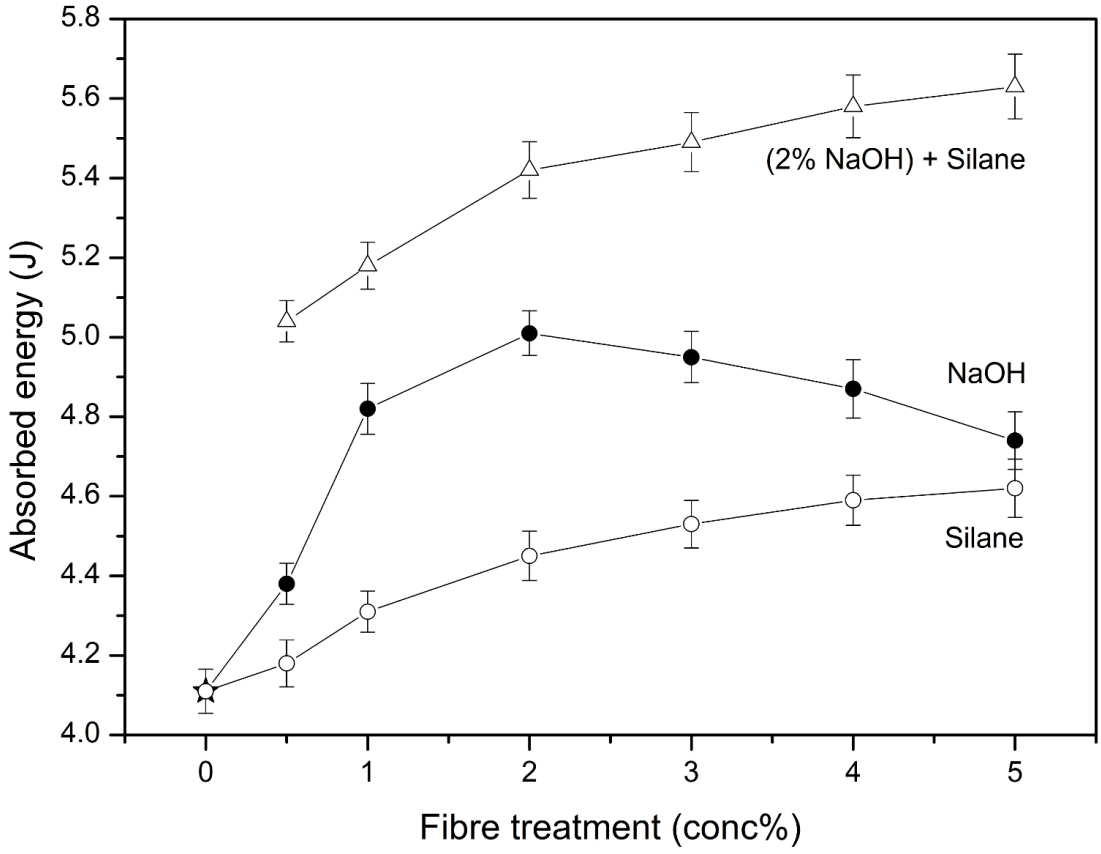

Figure 4.11: Absorbed energy of (⋆) untreated, (•) alkaline treated, (○) silane treated H-SMC composites as a function of surface treatment. (△) represents H-SMC composites based on hemp fibres treated with a fixed 2% alkaline treatment and varying concentration of silane treatment.

4.4.4.2 Silane treatment

There is a considerable increase in the penetration energy of the H-SMC composites between 0 and 2% concentration of silane treatment, while beyond 2% concentration there is only a slight increase in penetration energy. Therefore 2% silane concentration might be considered as sufficient for hemp fibres. At a silane concentration of 5% the penetration energy increased by 15% compared to the untreated fibre composite. The energy absorbed by the composite versus the silane treatment concentration shows a similar trend to the penetration energy, at a silane concentration of 5% the absorbed energy also increased by 20% compared to the untreated fibre composite.

4.4.4.3 Alkaline-Silane treatment

The combination of alkaline and silane treatments on hemp fibre mats significantly improves the penetration and absorbed energy capabilities of the composite. At a silane concentration of 5% the penetration energy of the composite increased by 40% while the energy absorbed increased by 35%. The improvement in fibre-matrix bonding could be responsible for the increased impact properties of the H-SMC composites. Treatment of hemp fibres with alkali removes the impurities on the fibre surface resulting in more sites for the silane molecules to form bonds with the fibre surface which could considerably increase the energy required for fibre pull-out and debonding.

4.4.5 Damage charateristics

The tensile fracture surfaces of untreated and surface treated H-SMC composites are shown in Figure 4.12. The fracture surface of the untreated composite (Figure 4.12a) shows that the fibre surfaces are clean and there is often a gap noticed between fibre and matrix which indicates interfacial failure. The cracks are initiating at the fibre-matrix interface and propagating through the matrix. Considerable fibre pull-out is noticed for all specimens, which again suggests poor fibre-matrix adhesion. Unlike for untreated fibre composites the alkaline and silane (Figure 4.12b and 4.12c) treated composites are covered with residues

of the matrix which indicates that the fibre-matrix adhesion has improved. The predominant failure mechanism of the treated composite was by fibre fracture, fibre pull-out and matrix fracture. Figure 4.12b shows fibre fracture of an alkaline treated fibre composite while Figure 4.12d shows fibre fibrillation of an alkaline-silane treated fibre composite due to the removal of hemicellulose by the alkaline treatment which is probably responsible for the higher energy absorption of this composite.

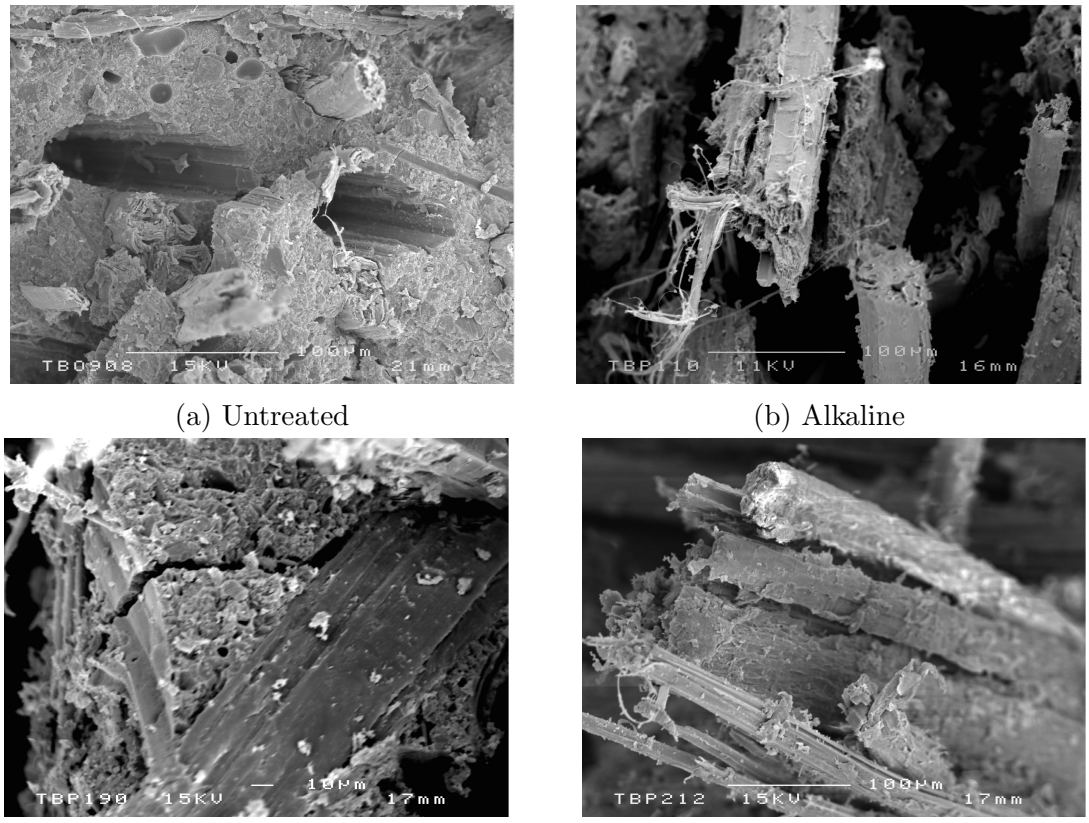

(a) Untreated (b) Alkaline

(c) Silane (d) Alkaline-Silane

Figure 4.12: SEM micrographs of impact fracture surface of H-SMC composites with different fibre surface treatments.

4.5 Conclusions

Response of hemp fibre reinforced SMC composites to low velocity impact loading was investigated. Three different parameters; fibre volume fraction, $CaCO_3$ filler

content and chemical fibre surface treatment were studied. It was found that both peak force and energy absorption by the specimens increased with increasing fibre volume up to a fibre volume fraction of 25% after which it decreased. Therefore the optimum fibre volume fraction of hemp fibre composites for impact applications is about 25%. It was calculated that a maximum of 9.21 J was absorbed by specimens with 25 vol.% fibre. Failure of the specimens was dominated by weak fibre-matrix adhesion while also significant fibre breakage, fibre pull-out and matrix cracking was observed.

There was a significant increase in peak force and energy absorption with the addition of $CaCO_3$ filler. The optimum filler content was found to be around 23% with a maximum energy absorption of 4.51 J. At high filler contents of 45% the peak force and energy absorption decreased due to insufficient fibre wetting. The deformation of the specimens was found to increase with increasing filler content. The specimens with 45% filler content were not completely penetrated by the impactor. The addition of filler was found to improve the stability of the composite by filling the voids noticed in the unfilled specimens. Again, failure of the specimens was observed to be by fibre breakage, fibre pull-out and matrix cracking.

The results demonstrate that there is a small increase in energy absorption of specimens based on hemp fibres treated with both alkaline and silane by approximately 20% and 10% respectively. There is also an increase in the peak force noticed for the treated specimens. A decrease in the deformation of 2.3 and 1.5 mm was noticed for alkaline and silane treated hemp fibre composites. Unlike the untreated specimens which were penetrated, the specimens treated with alkali and silane were not fully penetrated. Both treatments resulted in improved fibre-matrix adhesion. A change in failure mechanism was noticed for treated composites as compared to untreated composites. The predominant failure mechanism of treated composites was by fibre failure resulting from tearing and splitting, while also matrix cracking was noticed. However considerably less fibre pull-out was observed.

Chapter 5

Post-impact damage and flexural properties of hemp fibre reinforced SMC composites

5.1 Introduction

The resistance to impact events plays an important part in the reliability assessment of composites for applications such as building materials as some of these components are likely to experience low velocity impacts during their service life. When a composite material is subjected to impact loading there might be no visible surface damage but internal damage may have already occurred. Even minor damage can have an adverse effect on material performances and structural integrity. To ensure that a damaged structure will not catastrophically fail during service life and maintain maximum structural efficiency, it is necessary to carry out damage-tolerance studies, evaluating the residual properties of the structure after impact.

The aim of this chapter is to study the effect of low velocity impact loading on the post-impact flexural properties of hemp fibre reinforced sheet moulding composites (H-SMC) and compare them to glass fibre based SMC (G-SMC). To date there have hardly been any studies on post-impact response of natural fibre composites in general while no post-impact studies have been carried out on H-

SMC composites. Two composite parameters have been considered for material optimisation: (i) fibre volume fraction and (iii) surface treatment of the hemp fibres by alkali or silane. The influence of impact energy on the residual flexural strength of the composites is analysed. Damage was induced in the mid-section of the simply supported specimens by a falling weight impact tester. The reduction of the flexural residual strength was evaluated by quasi-static three-point bending tests.

5.2 Residual strength

The ability of a structure to sustain defects safely until repair can be effected or the structure needs to be replaced is called *damage tolerance*. The approach to engineering design to account for damage tolerance is based on the assumption that initial flaws exist in any structure and such flaws propagate with usage. An understanding of damage tolerance can be gained through experiments and available models for predicting residual properties. The general trend for the residual strength of laminated composites with impact damage is that, for low initial kinetic energy levels, the strength is not affected since little or no damage is introduced. As damage size increases, the strength drops rapidly and levels off. The effects of impact damage on the residual strength in tension [Cui *et al.*, 2009; Lal, 1983; Wang *et al.*, 2010], compression [Bibo & Hogg, 1996; Cantwell *et al.*, 1983; Prichard & Hogg, 1990; Wong *et al.*, 2010], bending [Peijs *et al.*, 1990, 1993; Schrauwen & Peijs, 2002] and fatigue have been investigated at length and follow the same general trend.

5.2.1 Residual strength of NFCs

As mentioned above, the effects of impact damage on the residual strength of glass and carbon fibre reinforced composites have been investigated at length. However, the effect of impact loading on the residual properties of natural fibre reinforced composites has not been studied extensively. Ahmed *et al.* [2007] studied residual tensile properties after low velocity impact loading of jute-glass reinforced isophthalic polyester hybrid composites. Laminates of four hybrid

combinations of woven jute and glass mat were prepared by a simple hand lay-up technique. The specimens were impacted at energies of 5, 10, 15 and 20 J in a drop weight impactor. A sharp reduction in normalised tensile stress was noticed for laminates with only jute fibre (42.6 vol.% fibre), whereas for hybrid composites there was a more gradual reduction in the normalised tensile stress. For all impact energy levels the loss in normalised tensile stiffness was much less than normalised tensile strength. Yuanjian & Isaac [2007] characterised the residual tensile properties of non-woven hemp fibre mat reinforced polyester composites of fibre content of 44 wt.%. The hemp composites were compared with glass fibre reinforced composites of fibre content of 42 wt.%. The composites were prepared by a simple hand lay-up technique followed by compression moulding. Impact damage was introduced by a drop weight machine with energies up to 10 J. At the same impact energy level of 5 J a significantly higher reduction in tensile strength was noticed for hemp fibre composites of 70% than for glass fibre composites of 30%.

There has been little research in the field of residual flexural properties after low velocity impact of natural fibre composites, even though composite structures are often subject to all kinds of out-of-plane loads in their service such as decking, chair backings, table tops, and building materials. This highlights the significance of research on the residual flexural properties of natural fibre reinforced composites. There are a few studies available reporting on the residual flexure properties of natural fibre reinforced composites. Santulli [2001, 2006] has studied post-impact flexural properties of plain woven jute fibre reinforced polyester composites of 63 vol.% fibre manufactured using a resin transfer moulding (RTM) process. The specimens were impacted at energies of 5, 7.5, 10 and 15 J in a drop weight impactor. As expected, generally the flexural strength decreased with increasing impact energy, for non-impacted, 5 and 20 J impacted specimens the residual flexural strength was 170, 121 and 104 MPa respectively. DeRosa *et al.* [2009a,b] investigated post-impact flexural properties of jute/E-glass hybrid reinforced polyester composites manufactured using an RTM process. A sandwich structure was produced with a stacking sequence of 7 glass/4 jute/7 glass and a fibre content of 50 vol.%. The specimens were impacted at energies of 10, 12.5 and 15 J in drop weight and tested in four-point bending. A significant de-

crease in both flexural strength and modulus with increasing impact energy was reported. The flexural strength and modulus decreased by approximately 75% and 21% respectively at 16 J of impact energy compared to the non-impacted specimens.

5.3 Experimental

5.3.1 Impact testing

Rectangular specimens of overall dimensions of 150 mm × 40 mm × 4 mm were cut from the H-SMC panels (following Zhang & Richardson [2007]). Impact testing was implemented using an instrumented DARTVIS falling weight impact tester manufactured by CEAST. The specimens were pneumatically clamped between a plate with a circular opening of 40 mm and an anvil. A controlled impact was achieved by dropping a hemispherical striker with a diameter of 20 mm and mass of 0.780 kg from prescribed impact heights. The tip of the striker is equipped with a piezo-electric transducer for measurement of velocity and load responses between the striker and specimen. A complete deformation response profile of the specimens during the impact event is provided by the transducer. The impact response information generated by the transducer is collected in a computer for post-processing. The impact machine is fitted with a pneumatic anti-rebound device which switches on when the impactor bounces back to prevent repetitive striking on the specimens. Post-processing of data results in the complete energy history during impact and gives a listing of impact velocity, maximum force, total energy, absorbed energy and maximum deflection. At least three specimens for each condition were impacted. Values plotted in the graphs are averages values of the three specimens and the error bars shown in the figures represent standard deviation of n=3.

5.3.2 Residual flexural strength

The post-impact strength of impacted specimens was evaluated by three-point bending tests under quasi-static conditions. The tests were conducted according

to the standard ASTM D 790-86, since there is no standard to evaluate residual flexural properties. The three-point bending load was applied at a constant cross-head rate of 5.3 mm/min on the impacted side of the specimen, so that the impacted side underwent a compression stress. A support span of 100 mm was used. The tests were performed on a universal Instron 6025 machine with a load cell of 5 kN. The flexural strength (σ_F) and modulus (E_B) were calculated from the measured load-displacement curves by using the beam equations:

$$\sigma_F = \frac{3PL}{2bd^2} \tag{5.1}$$

and

$$E_B = \frac{L^3 m}{4bd^3} \tag{5.2}$$

where, P is the maximum force, L is the support span, m is the slope of load-deflection curve in the elastic regime, and b and d are the width and thickness of the specimen, respectively.

The experimental results were normalised for the flexural properties of non-impacted specimens in order to achieve a straightforward interpretation and comparison of the post impact flexural strength and modulus.

5.4 Results and Discussion

5.4.1 Influence of fibre volume fraction

5.4.1.1 Impact characteristics

Typical load-time curves of H-SMC composites with fibre content of 32 vol.% impacted at six different loading levels are shown in Figure 5.1. All six curves exhibit similar trends with complex series of peaks and troughs. A linear increase of force with time is noticed for all the curves at the start of the impact event. The peak force for all six incident energy levels occurs within a time range of 1.5-3 ms. As expected, the peak force increases with increasing impact energy levels. After the peak value a gradual decrease in force is observed for all six

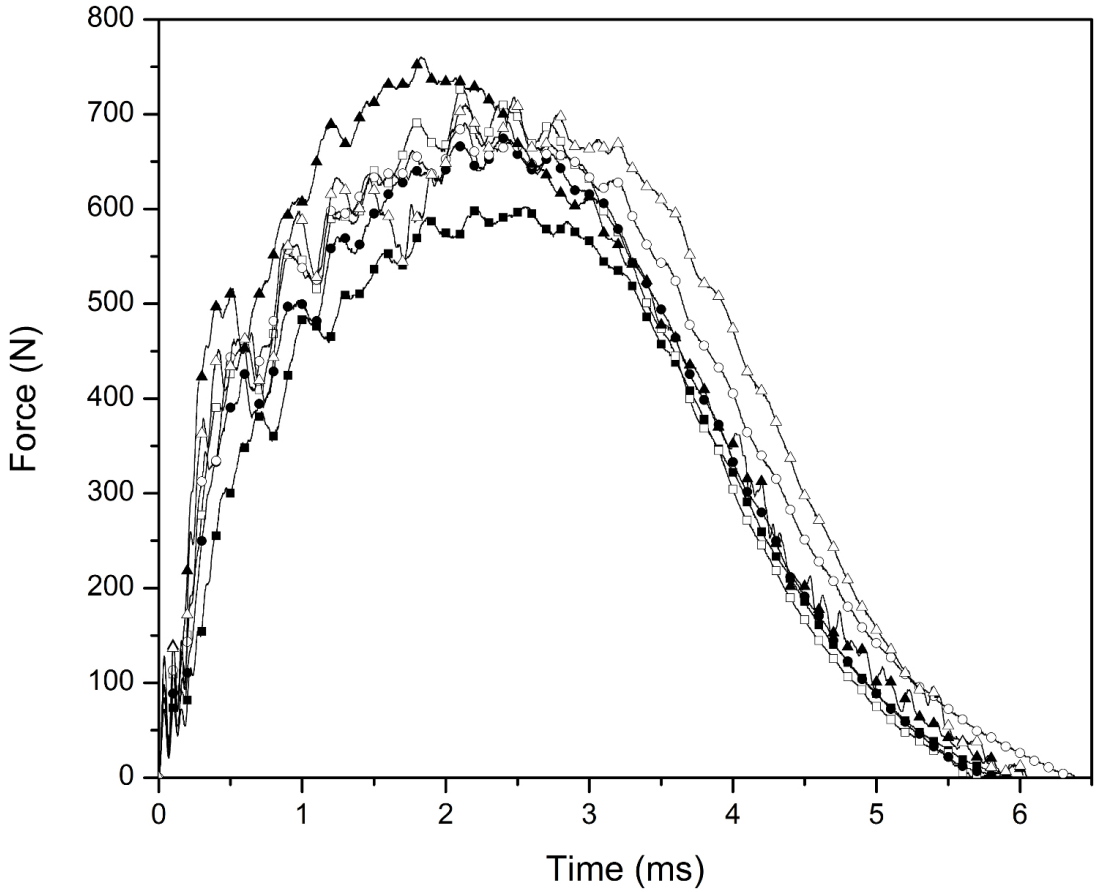

Figure 5.1: Typical force-time curves of H-SMC composite with a constant fibre content of 32 vol.% impacted at six incremental incident energies: (■) 1 J, (□) 1.5 J, (●) 2 J, (○) 2.5 J, (▲) 3 J and (△) 3.5 J.

curves. It is noticed that the non-penetration force-time curves of the H-SMC composites are similar to those of penetration impact tests of these composites (See Figure 4.4). However, in penetration tests the load drops are related to fracture initiation and propagation, whereas in the non-penetration tests they are associated with elastic and plastic deformation of the specimen as the impactor rebounds from the specimen.

Typical load-deflection curves of H-SMC composites with fibre content of 32 vol.% impacted at six different loading levels are shown in Figure 5.2. Load-deflection curves consist of an ascending section for loading and a descending section for unloading. The load-deflection curves for both penetration and non-

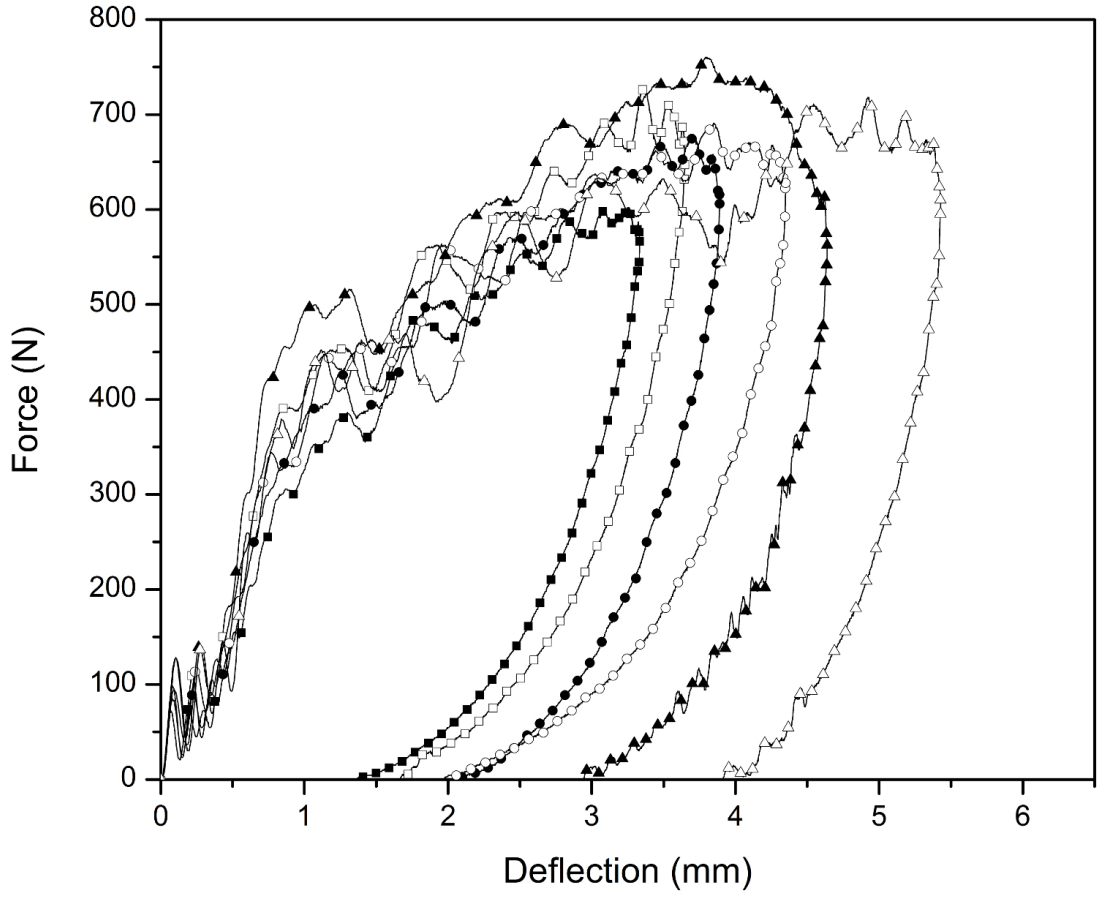

Figure 5.2: Typical force-deflection curves of H-SMC composite with a constant fibre content of 32 vol.% impacted at six incremental incident energies: (■) 1 J, (□) 1.5 J, (●) 2 J, (○) 2.5 J, (▲) 3 J and (△) 3.5 J.

penetration impact testing are similar in the ascending section of the curves. However, for penetration impact tests the descending section of the load-deflection curves would decrease with increasing deflection caused by propagation damage as the impactor passes through the specimen, whereas, for non-penetration impact tests the descending section of the load-deflection curve moves backwards with decreasing deflection as the load decreases which indicates rebounding of the impactor. For non-penetration impact tests the load-deflection curves form a closed loop. For non-penetration impact tests the peak load approximately coincides with the maximum deflection. For specimen impacted at 1 J, the peak

load is the maximum deflection therefore suggesting that complete unloading and return to original specimen state is possible. For specimens impacted at 1.5, 2 and 2.5 J, the maximum deflection occurs slightly after the maximum load indicating partial unloading and return to original specimen state. For specimens impacted at 3 and 3.5 J, the maximum deflection occurs significantly after the peak load, indicating significant damage in the specimen has occurred and the specimen cannot be returned to its original state. Therefore, it is believed that impact loadings with energies exceeding about 1 J will cause irreversible damage to specimens of H-SMC composites.

5.4.1.2 Energy profile

The energy introduced to a composite specimen, i.e the impact energy, is equal to the kinetic energy of the impactor right before contact-impact takes place whereas the energy absorbed by the specimen, i.e the absorbed energy, can be calculated from the associated load-deflection curve. For an impact event having a closed load-deflection curve, such as those shown in Figure 5.2, the absorbed energy is equal to the area surrounded by the load-deflection curve. Absorbed energy as a function of impact energy of H-SMC composites having different fibre volume fractions is shown in Figure 5.3. To better understand the energy absorption of H-SMC composites in impact, they are compared with G-SMC composite specimens containing 25 vol.% of glass fibre (see Figure 5.3). As expected the energy absorbed by both H-SMC and G-SMC composites increased with increasing impact energy. In all cases the curves basically exhibit linear increase. As each data point is associated with a drop height of the impactor, the impact energy increases with drop height. Since a higher impact energy results in more severe damage of the composite specimen, the absorbed energy increases with impact energy. The amount of absorbed energy gives an indication to the damage area of the specimen, since high absorbed energies will result in large damage area. At a low impact energy of 1 J all the H-SMC specimens absorbed a similar amount of energy, however, as the impact energy level increased from 1 J to 3.5 J the difference in absorbed energy increased with increasing fibre volume fraction. At an impact energy of 3.5 J, H-SMC specimens with 46 vol.% fibre content absorbed about

50% more energy than H-SMC specimens with 9 vol.% fibre content. Above impact energy levels of 3.5 J the H-SMC specimens containing 9 vol.% fibre content were fully penetrated, while at an impact energy of 3 J, H-SMC specimens with 20 vol.% fibre content were only partially penetrated whereas G-SMC specimens containing 25 vol.% glass fibre showed no visible damage. G-SMC specimens were able to withstand 6 J of impact energy without being penetrated.

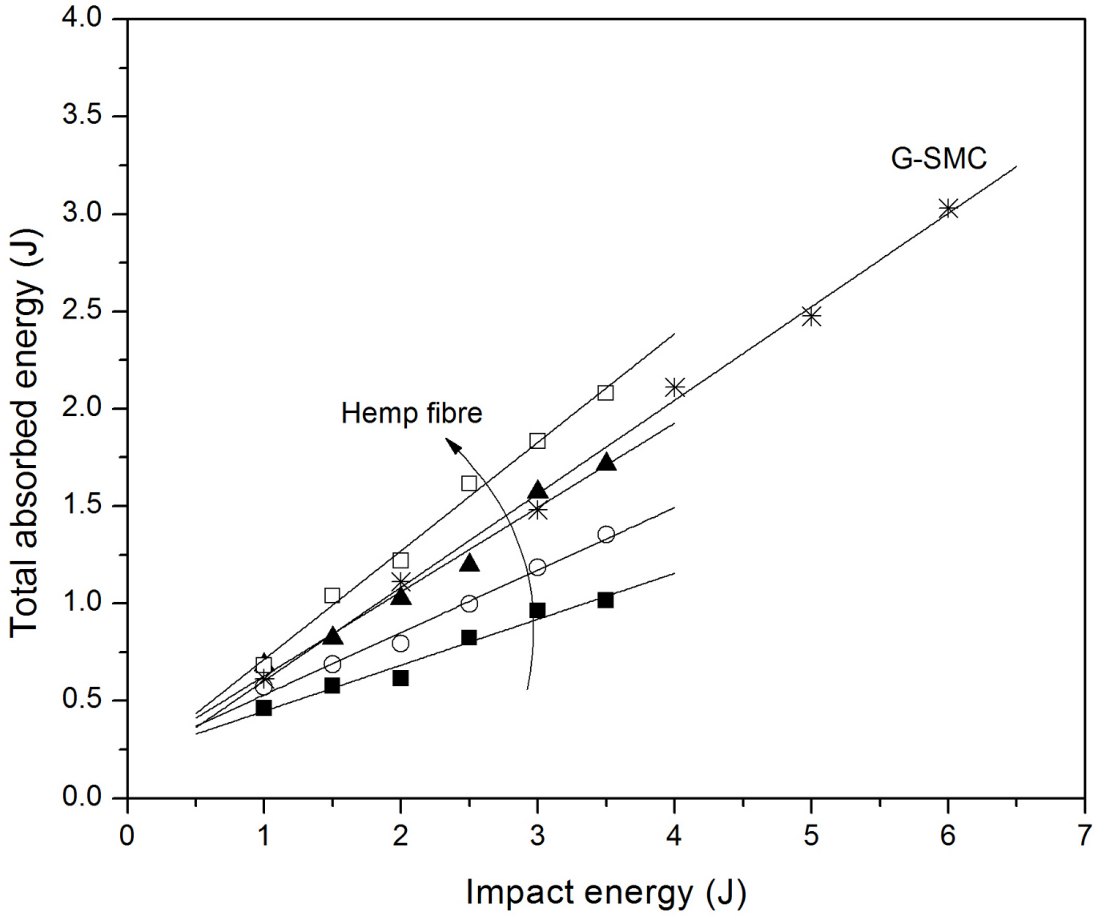

Figure 5.3: Total absorbed energy as a function of incident impact energy of H-SMC composites with varying different fibre volume fraction: (■) 9 vol.%, (○) 20 vol.%, (▲) 32 vol.% and (□) 46 vol.%. (∗) represents G-SMC composite with fibre volume fraction of 25 vol.%.

5.4.1.3 Damage development

H-SMC and G-SMC composite specimens of dimensions 150 mm × 40 mm were impacted such that the damage zone was oriented at the centre of the flexural test specimens. Post-impact visual examination of the H-SMC composites was carried out to determine the extent of damage. It can be expected that higher levels of absorbed energy results in more damage. Figure 5.4 shows the visual observations made on the back (tension) face of the H-SMC composite impacted at energies from 1 to 3.5 J. The cracks on the back face were dyed with a red marker pen to make them easier to visualise. For H-SMC composites a strong increase is seen in visual back face damage with increasing impact energies. Because of the random orientation of the hemp fibres in the composite there appears no preferred direction of crack growth. In this typical case the crack on the back face runs along the whole width of the specimen at an impact energy of 3.5 J. At all impact energy levels the damage on the back face was mainly due to matrix cracking, no significant fibre breakage was observed.

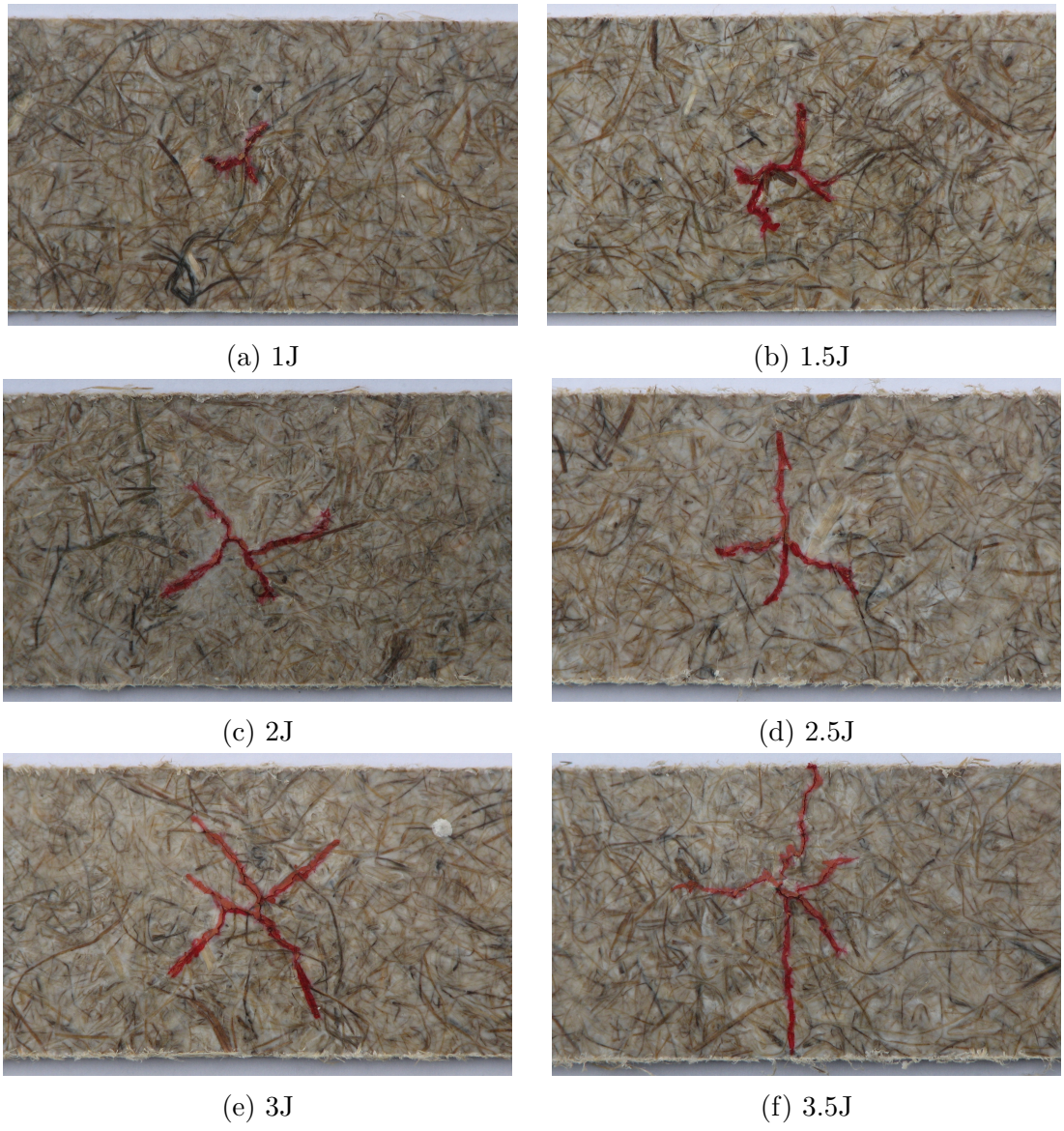

(a) 1J (b) 1.5J

(c) 2J (d) 2.5J

(e) 3J (f) 3.5J

Figure 5.4: Effect of impact energy on visual damage showing H-SMC composite back (tensile) face damage.

5.4.1.4 Post-impact flexural properties

The post-impact flexural tests were conducted in order to determine the degradation in flexural strength and stiffness and retaining flexural load carrying ability of the H-SMC composites. Post-impact flexural properties (flexural strength and modulus) of H-SMC composites with different fibre volume fraction are plotted

as a function of incident impact energy in Figures 5.5 and 5.6. For comparison post-impact flexural properties of G-SMC composites with a fibre volume fraction of 25 vol.% is also plotted. For a better indication of the influence of the impact damage on residual properties, the normalised flexural properties of each specimen was calculated as the strength of the impacted specimen divided by the mean value of the reference test. A sharp linear reduction in the normalised flexural strength of H-SMC composites is noticed indicating that they have poor damage tolerance capability.

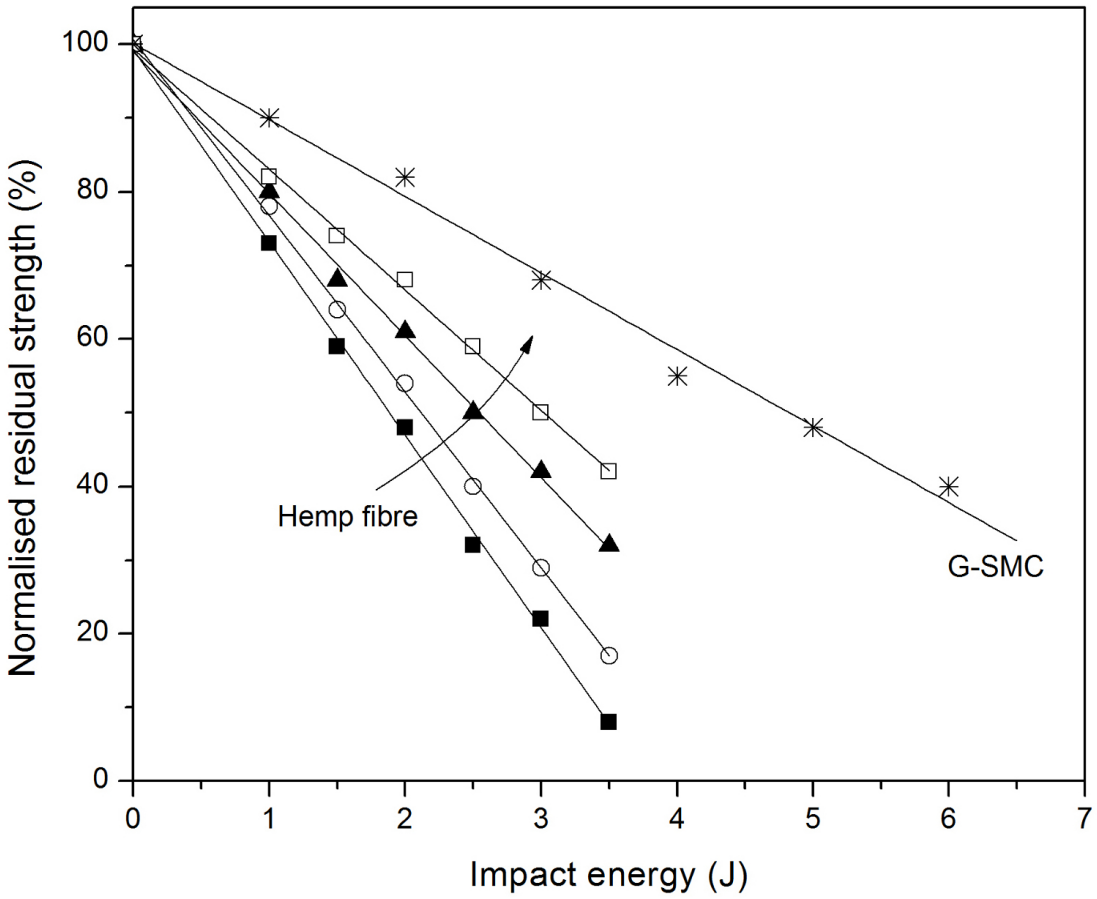

Figure 5.5: Normalised residual flexural strength as a function of impact energy of H-SMC composites with varying fibre volume fraction: (■) 9 vol.%, (○) 20 vol.%, (▲) 32 vol.% and (□) 46 vol.%. (∗) represents G-SMC composite with fibre volume fraction of 25 vol.%

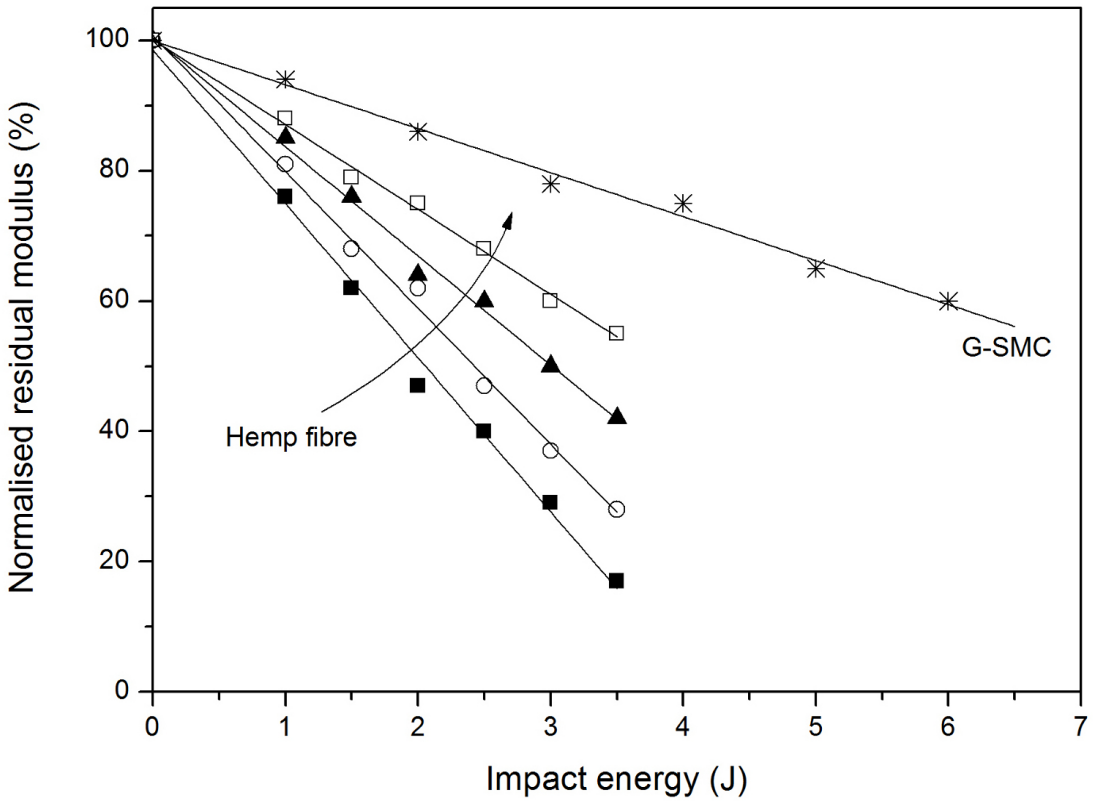

Figure 5.6: Normalised residual flexural modulus as a function of impact energy of H-SMC composites with varying fibre volume fraction: (■) 9 vol.%, (○) 20 vol.%, (▲) 32 vol.% and (□) 46 vol.%. (∗) represents G-SMC composite with fibre volume fraction of 25 vol.%

The damage tolerance of the H-SMC composites was found to improve significantly with increasing fibre volume fraction as indicated by the more gradual reduction in the normalised flexural strength. At an impact energy of 3.5 J, the reduction in normalised flexural strength for H-SMC composites containing 9, 20, 32 and 46 vol.% of fibre was found to be 92, 83, 68 and 58%, respectively. The damage tolerance capability of H-SMC composites is significantly lower than that of G-SMC composites, particularly at higher impact energies. Following an impact of energy 3 J the normalised flexural strength of G-SMC composites (25 vol.% glass fibre) is about 68% of the undamaged material, compared with a figure of about 29% for the undamaged H-SMC composite specimens (20 vol.% hemp fibre) with a slightly lower fibre volume fraction. So the damage tolerance

capability of G-SMC is approximately 2 fold higher than H-SMC composites.

The linear relationship observed between impact energy and absorbed energy is reflected in a linear relationship between the drop in residual strength and impact energy. If the absorbed energy can be considered as an indicator of specimen damage, as higher energy absorption leads to greater damage, then residual flexural strength decreases with increasing specimen damage for H-SMC composites. For G-SMC composites, the absorbed energy is similar to the H-SMC composites at impact energies from 1 to 3.5 J (see Figure 5.3), however, the reduction in residual flexural strength is much lower than for H-SMC composites. This might be due to better fibre wetting and a stronger fibre-matrix interface in G-SMC composites compared to H-SMC composites resulting in better mechanical properties. Also glass fibre are isotropic while hemp fibre bundles are not and the matrix cracking may initiate in the interface between the fibre bundles as shown graphically in Figure 3.6.

As expected, normalised residual flexural modulus of the impact damaged H-SMC and G-SMC composites also decreases with increasing impact energies. Again, a linear relationship between impact energy and normalised residual modulus is noticed. The residual flexural modulus is slightly less reduced with increasing impact energies compared to residual strength for all fibre volume fractions of H-SMC composites and also G-SMC composites. For H-SMC composites with a fibre content of 20 vol.% the maximum reduction (at 3.5 J impact energy) in flexural modulus is approximately 72% compared to 83% in flexural strength. This indicates that flexural modulus is less sensitive to impact damage than flexural strength. Zhang & Richardson [2007] suggested that impact damage is localised and therefore will have less effect on global properties such as modulus, the calculation of which only involve the initial linear part of force-deflection curves. On the other hand localised impact damage has a greater effect on the load bearing capability of materials, referred to as "residual strength", which is calculated using the ultimate force that the specimens could sustain and this is dramatically reduced due to the presence of impact damage. Similar experimental results on residual flexural modulus have been reported by other authors [Ahmed *et al.*, 2007; Zhang & Richardson, 2007].

5.4.2 Influence of fibre surface treatment

5.4.2.1 Energy profile

Figure 5.7 shows the absorbed energy as a function of incident impact energy for the H-SMC composites incorporating alkaline treated, silane treated and alkaline-silane treated hemp fibres. All composites have a constant fibre content of 20 vol.%. The purpose of fibre surface treatments was to improve the level of adhesion between the hemp fibre and matrix. In accordance with the data shown for untreated H-SMC composites there is also an increase in absorbed energy with the addition of treated hemp fibres. All three fibre treatments resulted in a slight

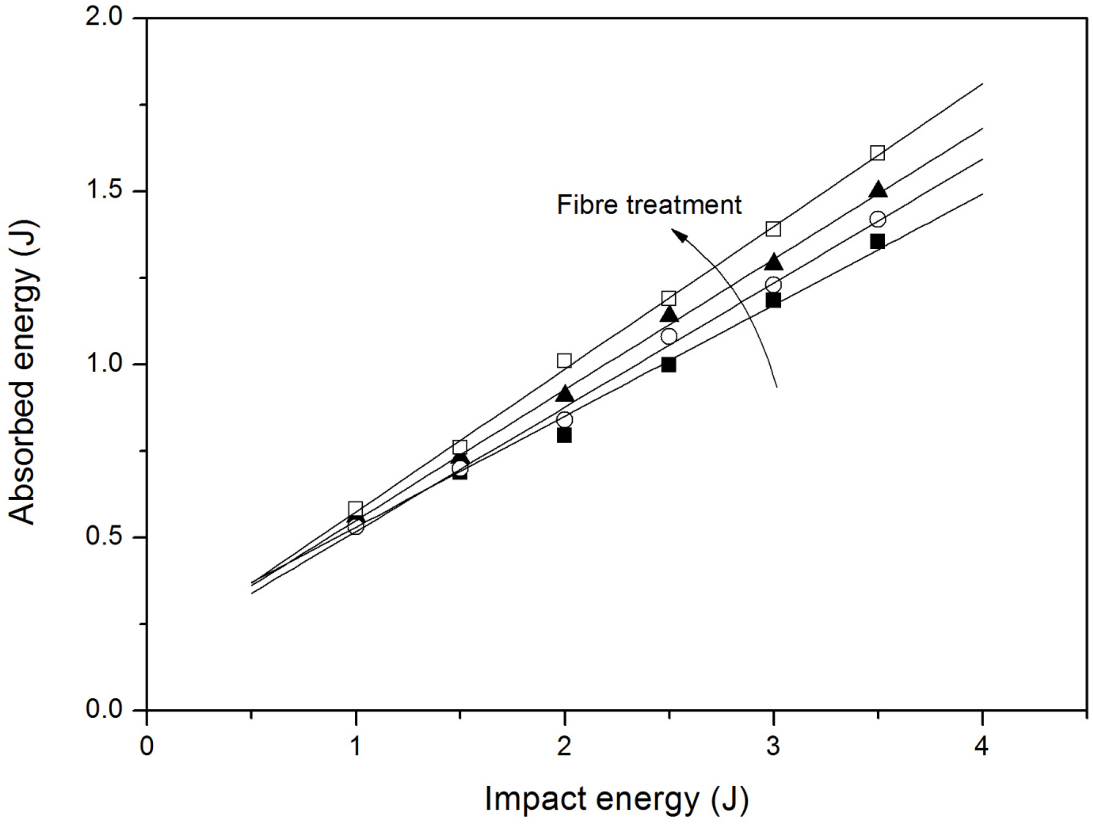

Figure 5.7: Absorbed energy as a function of incident impact energy of (■) untreated, (▲) alkaline treated, (○) silane treated H-SMC composites. (□) represents H-SMC composites based on hemp fibres treated with a fixed 2% alkaline-silane treatment.

increase in the amount of impact energy absorbed. At an impact energy of 3.5 J, the combination of alkaline-silane treatment on the hemp fibres resulted in approximately 20% more energy being absorbed compared to the untreated H-SMC composite. By visual inspection there is no difference in the damage area on the back (tensile) face of H-SMC specimens incorporating surface treated hemp fibres and the specimens incorporating untreated fibres. Treatment of hemp fibre mats with an alkaline solution causes fibre bundle fibrillation as shown in Chapter 3 resulting in greater fibre-matrix interaction which could potentially lead to increased energy absorption through fibre pull-out at the same impact energy level.

5.4.2.2 Post-impact flexural properties

Post-impact flexural properties (flexural strength and modulus) of H-SMC composites incorporating alkaline treated, silane treated and alkaline-silane treated hemp fibres is shown in Figures 5.8 and 5.9. As expected, residual strength decreases with increasing impact energy. However, it is demonstrated that H-SMC composites incorporating surface treated hemp fibres have a significant higher residual strength at higher impact levels than composites with untreated hemp fibres. At an impact energy of 3.5 J, the reduction in normalised flexural strength for H-SMC composites incorporating untreated, alkaline treated, silane treated and alkaline-silane treated hemp fibre was found to be 83%, 71%, 77% and 64%, respectively. A linear reduction in residual flexural modulus with increasing impact energies of H-SMC composites incorporating all different fibre surface treatments is noticed. However, overall fibre surface treatments have very little effect on the residual flexural properties of H-SMC composites.

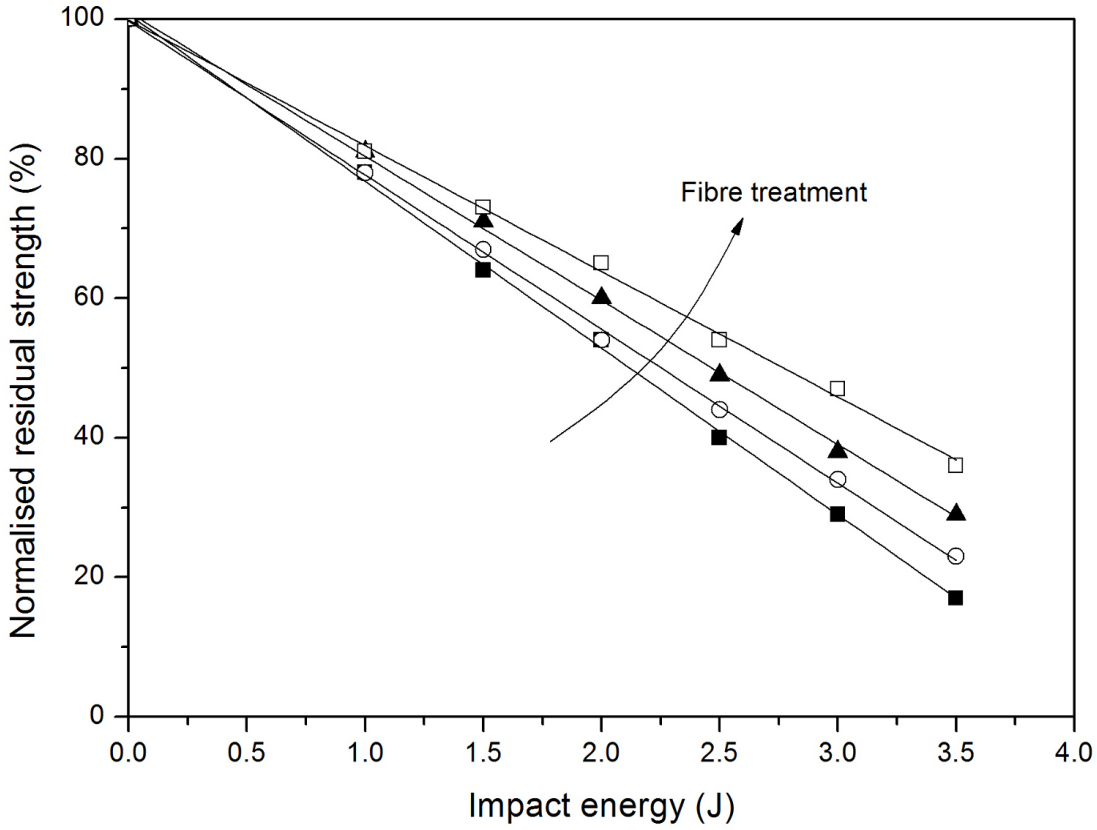

Figure 5.8: Normalised residual flexural strength of (■) untreated, (▲) alkaline treated, (○) silane treated H-SMC composites as a function of impact energies. (□) represents H-SMC composites based on hemp fibres treated with fixed 2% alkaline-silane treatment.

As mentioned above, even though H-SMC specimens incorporating surface treated hemp fibres absorb more impact energy there is no significant difference in the damage area on the back (tensile) face of the specimen compared to the specimens incorporating untreated hemp fibres. Therefore the reduction in residual strength of the H-SMC composite based on the treated fibres is expected to be in a similar or lower range than the reduction in residual strength of H-SMC composites based on untreated fibres. Additionally, it could be that at higher impact energies the damage area of the H-SMC composites incorporating treated fibres is smaller compared to the H-SMC composites based on untreated fibres, therefore resulting in a smaller reduction in residual strength.

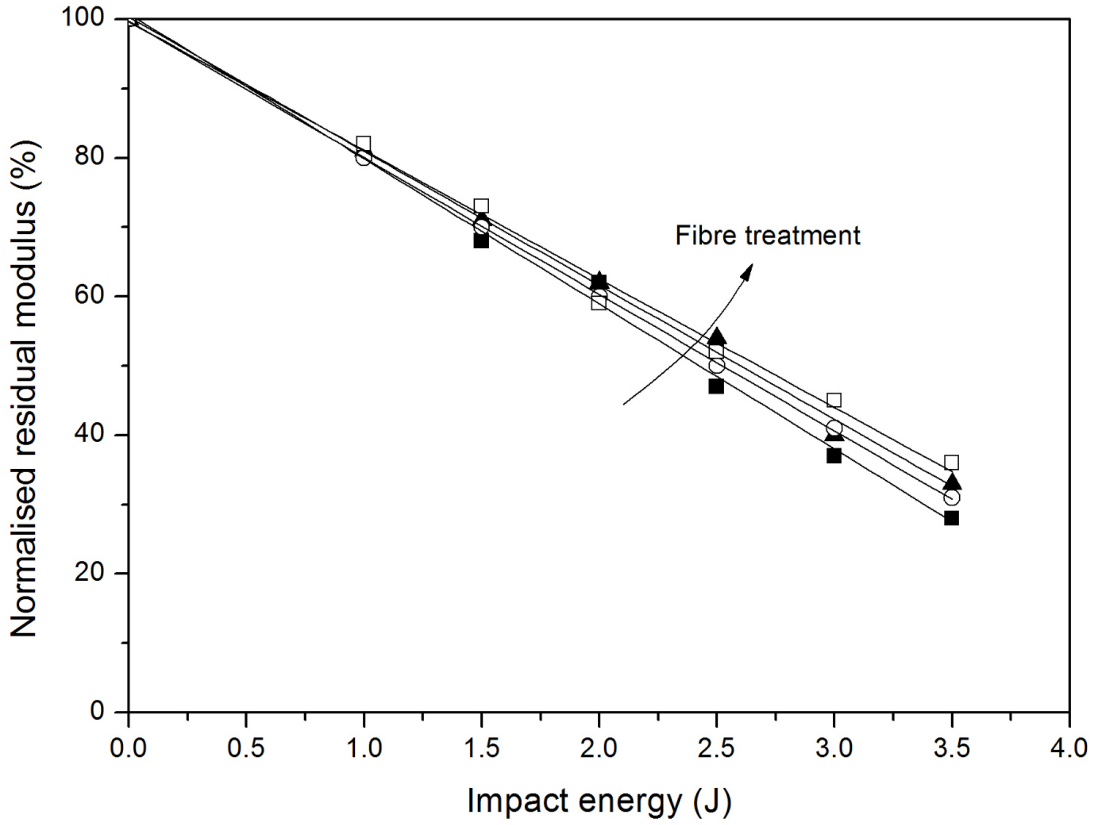

Figure 5.9: Normalised residual flexural modulus of (■) untreated, (▲) alkaline treated, (○) silane treated H-SMC composites as a function of impact energies. (□) represents H-SMC composites based on hemp fibres treated with fixed 2% alkaline-silane treatment.

The interface plays an important role in transferring the stresses acting on the matrix to the fibre. For a composite to have good mechanical properties the fibre-matrix interface must be relatively strong. However, if the interface is too strong the composite will fail in a brittle mode and have low toughness; therefore it is important to optimise the fibre-matrix interface to accomplish a balance between strength and toughness of the composite. In this case an improvement in strength is achieved as there is a smaller reduction in residual flexural strength and also the energy absorption capability is maintained, therefore a good balance between strength and toughness is achieved after these fibre surface treatments.

5.5 Conclusions

This chapter analysed the influence of impact energy, fibre volume fraction and fibre surface treatment on the post-impact flexural properties of hemp fibre reinforced composites (H-SMC). For a better understanding the results were compared with glass fibre reinforced composites (G-SMC). An increase in energy absorption with increasing fibre volume fraction was noticed for H-SMC composites particular at higher impact energies. G-SMC composites absorbed significantly more energy at equal impact energies than H-SMC composites. Visual damage was observed to increase with increasing impact energy levels.

The residual flexural strength of H-SMC composites was found to decrease linearly with increasing impact energy levels. At higher impact energy levels, the damage tolerance of H-SMC composites increased with increasing fibre volume fraction, as the reduction in residual strength significantly decreased at higher fibre volume fractions. Damage tolerance capability of G-SMC was calculated to be approximately 2 times higher than H-SMC composites. The residual modulus also decreased in a linear trend with increasing impact energy levels. Post-impact flexural property testing showed that the flexural strength of H-SMC and G-SMC composites is more sensitive to localised impact damage than flexural modulus.

A slight increase in energy absorption was found with H-SMC composites incorporating surface treated hemp fibres. However, there was no clear increase in damage area noticed on the fracture surfaces of the composites incorporating treated fibres compared to composites based on untreated fibres. H-SMC composites incorporating surface treated hemp fibres did however show improved damage tolerance, particularly for composites based on hemp fibres treated with a combination of alkaline and silane treatments. On the other hand, there was no significant difference noticed on the residual flexural properties of H-SMC composites incorporating surface treated and untreated hemp fibres.

Chapter 6

Fracture toughness of hemp fibre reinforced SMC composites

6.1 Introduction

Toughness is the resistance of a material against fracture and crack propagation. It is one of the most important material properties that have to be considered when designing engineering materials. A useful way of quantitatively describing the toughness of a material is by means of its fracture energy (γ). This is a measure of the resistance of the material to crack propagation, and is defined empirically as the minimum amount of energy required in creating a unit area of fracture surface. An increase in fracture surface energy by inhibiting crack propagation can produce an increased resistance to fracture under static loading or shock.

The amount of energy that a material absorbs during loading can be obtained from the area under the load-displacement curve. The bigger the area underneath the curve, the tougher the material. However, it is important to know how the material responds to the given load before it breaks. A brittle material can be very strong but it cannot deform very much so that energy will not be dissipated when subjected to loading, whereas a ductile material can deform significantly even with a very small load. A tough material should have both the strength to withstand a given load, and an ability to dissipate the energy. Therefore the

controlling variables of material's toughness are critical load and absorbed energy.

6.2 Fracture mechanics

Toughness as a parameter of fracture resistance may be expressed by the critical stress intensity factor, K_{Ic}, or by the critical strain energy release rate, G_{Ic}. Sometimes K_{Ic} is referred to as fracture toughness. Fracture toughness (K_c) and critical strain energy release rate (G_c) can be obtained by three different loading types as shown in Figure 6.1. Mode I is an opening (tensile) mode where the crack surfaces move directly apart. Mode II is a sliding (in-plane shear) mode where the crack surfaces slide over one another in a direction perpendicular to the leading edge of the crack. Mode III is a tearing (anti-plane shear) mode where the crack surfaces move relative to one another and parallel to the leading edge of the crack.

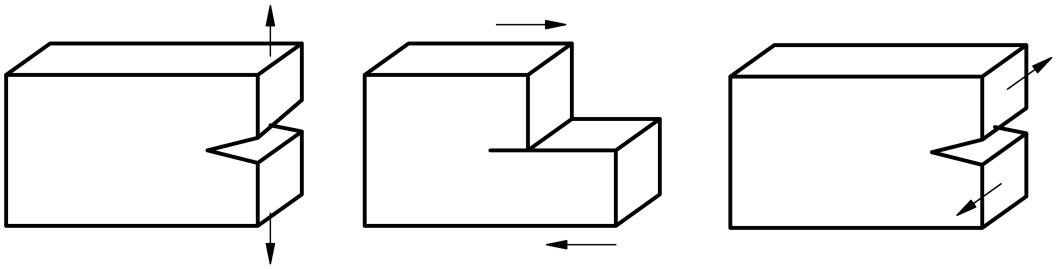

(a) Mode I (b) Mode II (c) Mode III

Figure 6.1: Three loading modes: Mode I (tensile opening mode), Mode II (in-plane shear mode), and Mode III (anti-plane shear mode).

The most common approach is to assume that the material behaves in a linear elastic fashion, thereby allowing the use of linear elastic fracture mechanics (LEFM). The subject relies on the concept that cracks are always present in a material and that the conditions under which they will propagate have to be described.

6.2.1 The energy balance approach

Elastic strain energy is stored in a body when it is deformed elastically. As the crack grow through the body, this energy is released and is used for the creation of new surfaces associated with the crack.

If a load P is applied to a body having thickness B and containing a crack of length, a, and the body deforms elastically (Figure 6.2), then a linear load-deflection (P-u) curve is obtained. The compliance, C, is determined from the curve as the inverse of the stiffness, i.e. $C = u/P$.

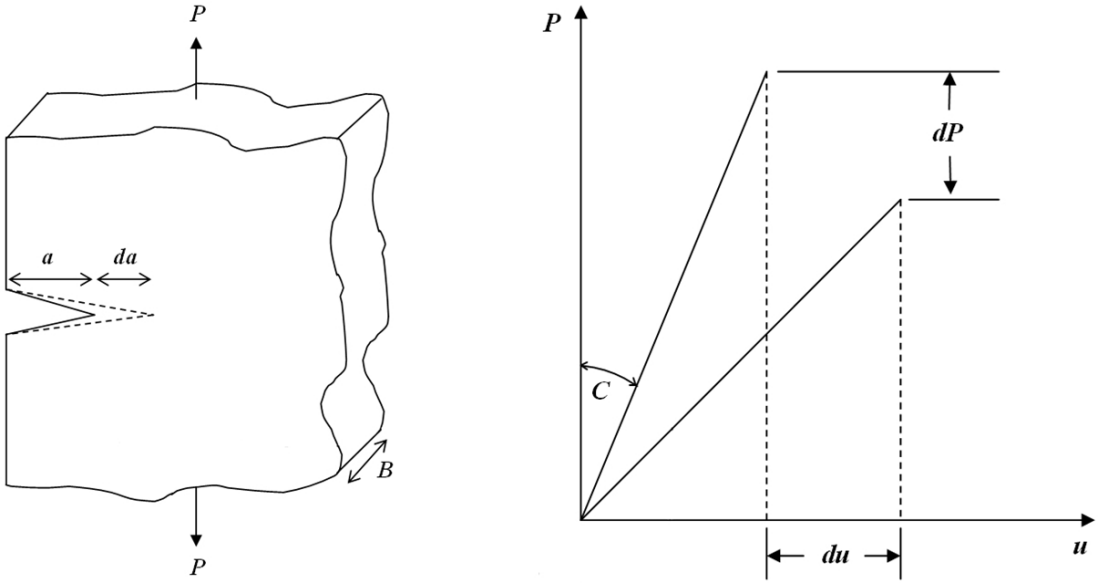

Figure 6.2: General loading on a body of thickness B and crack length, a.

Consider the energy involved as the load changes by dP, and the displacement by du. The crack grows by an amount da, and the crack area increases by Bda. The energy release, dU can be defined as [Kobayashi, 2004]:

$$dU = \frac{1}{2}\left(Pdu - udP\right) \tag{6.1}$$

and the strain energy release rate, G as:

$$G = \frac{1}{2}\frac{dU}{da} = \frac{1}{2B}\left(P\frac{du}{da} - u\frac{dP}{da}\right) \tag{6.2}$$

Differentiating C with respect of a produces:

$$P^2\frac{dC}{da} = P\frac{du}{da} - u\frac{dP}{da} \tag{6.3}$$

Alternatively, G can be rewritten in terms of compliance as:

$$G = \frac{P^2}{2B}\frac{dC}{da} = \frac{u^2}{2BC^2}\frac{dC}{da} \tag{6.4}$$

At fracture, G equals to G_c; where G_c is known as the *critical strain energy release rate*. Both P and u at fracture can be measured experimentally, and both dC/da and G_c can be calculated.

The released strain energy is used to create new surfaces that are formed as the crack propagates. For a completely brittle material G_c can be shown to be equal to twice the surface energy per unit area, γ, allowing for the energy of two faces of the crack.

$$G_c = 2\gamma \tag{6.5}$$

6.2.2 The stress approach

In this approach, the local stresses around the crack tip are considered. The crack acts as a stress concentrator giving high stresses at the crack tip as shown in Figure 6.3.

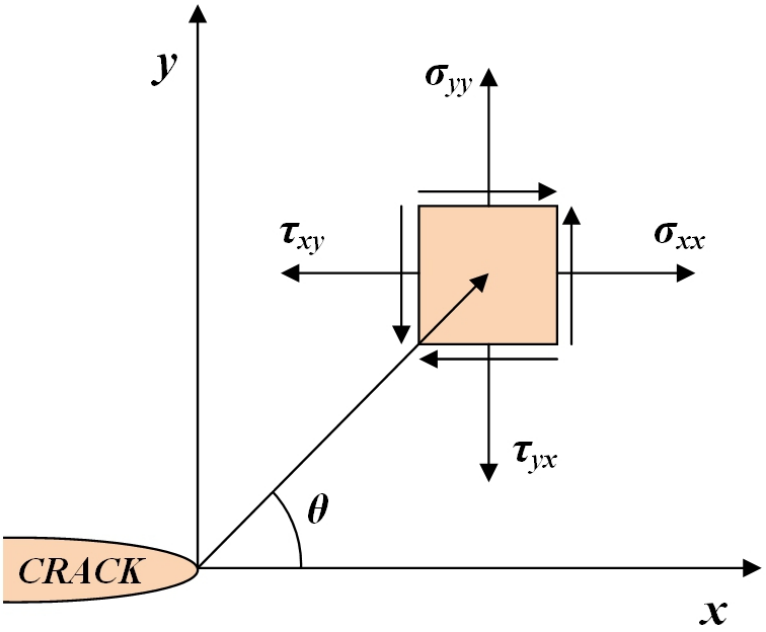

Figure 6.3: The co-ordinate system used to describe the local stress around the crack tip.

Using elasticity theory to calculate the stresses at any point (r,θ) in the vicinity of the crack tip, the results of such analysis are [Thanomsilp, 2001]:

$$\alpha_{yy} = \frac{K}{(2\pi r)^{\frac{1}{2}}} cos\frac{1}{2}\theta \left(1 + sin\frac{1}{2}\theta sin\frac{3}{2}\theta\right) \tag{6.6}$$

$$\alpha_{xx} = \frac{K}{(2\pi r)^{\frac{1}{2}}} cos\frac{1}{2}\theta \left(1 - sin\frac{1}{2}\theta sin\frac{3}{2}\theta\right) \tag{6.7}$$

$$\tau_{xy} = \frac{K}{(2\pi r)^{\frac{1}{2}}} \left(cos\frac{1}{2}\theta sin\frac{1}{2}\theta sin\frac{3}{2}\theta\right) \tag{6.8}$$

where K is the stress intensity factor. The crack propagates when K equals K_c, which is termed the critical stress intensity factor. K_c is a measure of fracture toughness, while G_c is a measure of fracture energy. The relationship of K_c and G_c can be shown in the equations below:

$$K_c^2 = EG_c \qquad \text{for plane stress conditions} \tag{6.9}$$

$$K_c^2 = \frac{EG_c}{(1-\nu^2)} \qquad \text{for plane strain conditions} \tag{6.10}$$

For an infinite plate containing a central crack of length $2a$, then

$$K^2 = \pi\sigma^2 a \tag{6.11}$$

$$G = \frac{\pi\sigma^2 a}{E} \tag{6.12}$$

At fracture, σ=σ_F, $G = G_c$ and $G_c = 2\gamma$; where σ_F is the fracture stress and γ is the surface energy per unit area. Therefore, the above equation can be rewritten as:

$$\sigma_F = \left(\frac{2\gamma E}{\pi a}\right)^{\frac{1}{2}} \tag{6.13}$$

This equation is known as the Griffith equation. π is the calibration factor for the infinite plate. However, typical specimens have finite dimensions, resulting in a crack that is not small in comparison with the specimen. Hence, a different calibration factor needs to be used, such that the equation becomes:

$$K^2 = Y^2\sigma^2 a \tag{6.14}$$

where Y is a calibration factor that depends on the crack length and specimen dimensions.

6.2.3 Fracture toughness testing

Fracture toughness (K_c) and critical strain energy release rate (G_c) can be obtained by several tests. Different loadings give different values. However, there are three main modes according to loading type as shown in Figure 6.1.

The fracture toughness and critical strain energy release rate are named after the loading mode such as K_{Ic} and G_{Ic} for Mode I, and K_{IIc} and G_{IIc} for Mode II. The specimen geometry varies from test to test. The recommended specimens in ASTM D5045-99 and E1820-99a are single-edge-notch bending (SENB) and compact tension (CT) for fracture toughness testing of plastics and metals. For the translaminar fracture toughness testing of laminated polymer matrix composites, ASTM E1922-97 uses a single-edge-notch tension (SENT) specimen geometry. There are various specimen geometries for interlaminar fracture toughness testing of fibre-reinforced composites such as a double cantilever beam (DCB) for Mode I, an end-notched flexure (ENF), an end-loaded split (ELS), a four point ENF (4ENF) for Mode II, and an edge crack torsion (ECT) for Mode III. The test configuration for some of these fracture toughness test methods are shown in Figure 6.4.

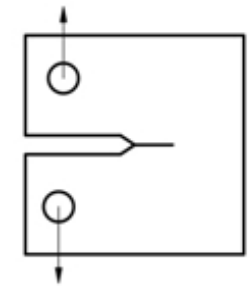

Compact tension (CT)

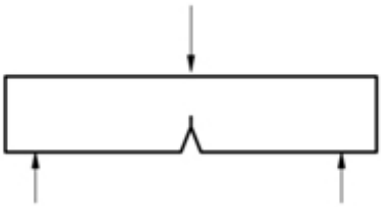

Single-edge-notched bending (SENB)

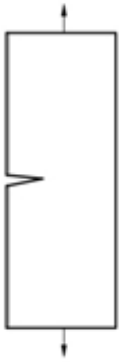

Single-edge-notched tension (SENT)

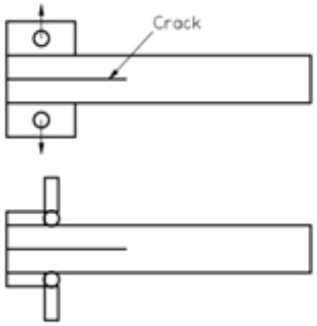

Double cantilever beam (DCB)

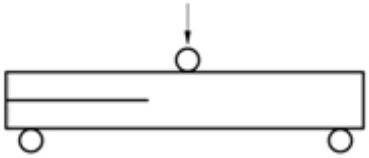

End-notched flexure (ENF)

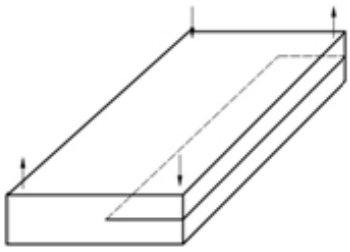

Edge crack torsion (ECT)

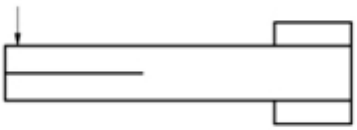

End-loaded split (ELS)

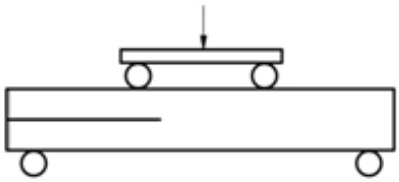

4-point ENF (4ENF)

Figure 6.4: Examples of test configurations for fracture toughness testing of composites.

6.3 Fracture toughness of NFCs

There are only a few studies available in the literature investigating various types of natural fibre reinforced composites with different specimen geometries [Joffe *et al.*, 2001; Li *et al.*, 2005; Okubo *et al.*, 2005; Romhany *et al.*, 2006; Sawpan *et al.*, 2009; Wong *et al.*, 2004]. Hughes *et al.* [2002] studied the fracture toughness of compression moulded non-woven hemp and jute fibre mat reinforced polyester composites of fibre content up to 45 vol.%. The fracture tests were carried out using single edge notched (SEN) specimens in three point bending. It was found that the K_{Ic} was approximately 3 times lower and the G_{Ic} an order of magnitude lower than that of glass fibre chopped strand mat (CSM) composites. It was hypothesised that the lower fracture toughness of NFCs was due to a smaller crack-tip plastic zone of these composites compared to CSM reinforced composites. Similar findings for glass fibre reinforced composites were found by Geers *et al.* [1996]. Liu & Hughes [2008] investigated the effect of reinforcement architecture of vacuum infusion prepared woven flax/epoxy composites. Fracture toughness testing was conducted on compact tension (CT) specimens of a fibre volume fraction between 32-34 vol.%. An improvement of 2-4 times in K_{Ic} was found with addition of woven textile over that of the unreinforced epoxy. They concluded that toughness was dominated by fibre volume fraction rather than reinforcement architecture. Alvarez *et al.* [2003, 2005] examined the fracture behaviour of sisal/starch compression moulded composites of fibre content ranging from 5 to 20 wt.%. Single edge notched (SEN) specimens were tested in three point bending to obtain the fracture toughness of the composites. A significant increase in crack initiation resistance was noticed while a modest increasing trend of the resistance to crack initiation with fibre loading was detected. Silva *et al.* [2006] studied the fracture toughness of compression moulded sisal and coconut fibre reinforced castor oil polyurethane composites tested in compact tension (CT) geometry. Here, the natural fibres were also treated with alkaline solution. They found that the fracture toughness in terms of G-P_{max} decreased for alkaline treated sisal fibre composites due to improved interfacial adhesion which probably impaired the main energy absorption mechanisms like pull-out and debonding. However, an improvement in fracture toughness was noticed for alkaline treated

coconut fibre composites due to fibrillation which might have created additional fracture mechanisms.

More recent studies on fracture toughness of natural fibre composites include: cellulose nanofibres (Masoodi *et al.* [2012]), cellulose fibres (Gamstedt *et al.* [2011]), sisal fibre (Argento *et al.* [2011]; Tan *et al.* [2012]), cotton (Yusliza *et al.* [2008]) and kenaf (Ahmad *et al.* [2011]).

6.4 Experimental

Information about the materials used, the composite fabrication process and surface treatment applied can be found in Chapter 3, Section 3.2.

6.4.1 Specimens preparation and experimental setup

The compact specimen (CT) specimens were machined from a composite sheet as recommended in ASTM 5045. The thickness of the specimens was approximately 3 mm and the width, W, was set at 40 mm. The geometry of the CT specimens used for fracture toughness tests is shown in Figure 6.5.

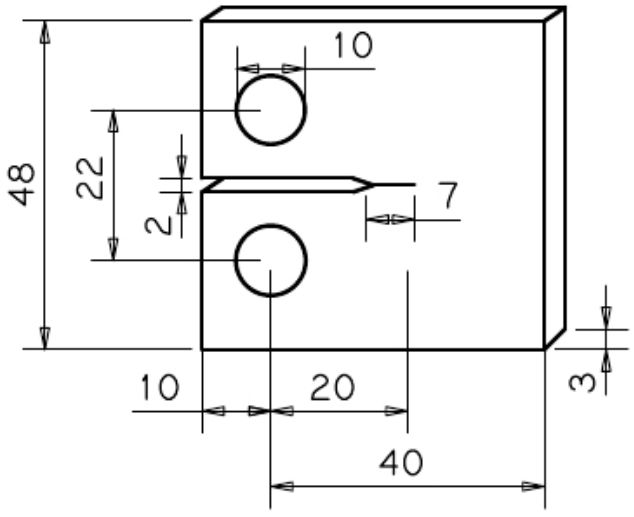

Figure 6.5: Test specimen nominal dimensions (in mm) for compact tension (CT) fracture toughness test.

A sharp notch in the specimens was prepared by machining and subsequently an initiator crack was introduced using a razor blade. Figure 6.6 shows a photograph of the initiator crack in an H-SMC specimen. A crack length, a, of 20 mm was selected such that the crack length to specimen width ratio was the within $0.45 < a/W < 0.55$.

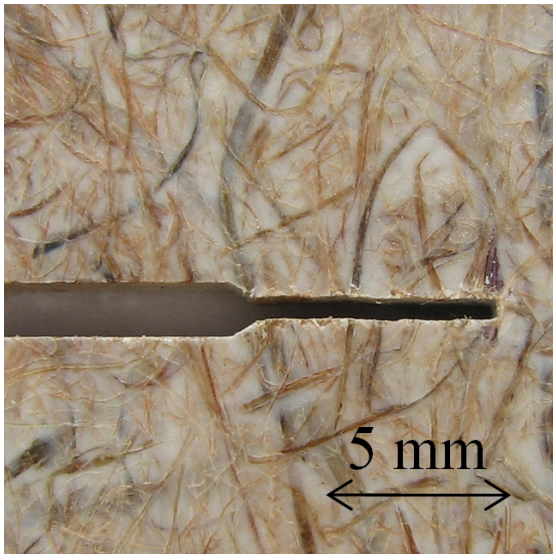

Figure 6.6: Photograph of the initiator crack in an H-SMC composite specimen.

Since there is not standardized procedure for testing fracture toughness of composite materials, most of the recommended conditions given for fracture toughness testing of non-reinforced plastic materials ASTM D 5045 were followed. Testing was carried out on an Instron 6025 universal testing machine with a 5 kN load cell, at room temperature. To observe the effect of strain rate on the H-SMC composites two different loading rates of 5 mm/min and 10 mm/min were used. The tests were carried out until 50% load drop from the maximum load was reach for each specimen. Five specimens were tested for each material condition.

6.4.2 Data analysis

Mode I critical stress intensity factor, K_{Ic}, of CT specimens was calculated with the following relations [ASTM-D5045, 1999]:

$$K_{Ic} = \left(\frac{P_Q}{BW^{\frac{1}{2}}} \right) f(x) \tag{6.15}$$

where $(0.2 < x < 0.8)$

$$f(x) = \frac{(2+x)\left(0.886 + 4.64x - 13.32x^2 + 14.72x^3 - 5.6x^4\right)}{(1-x)^{\frac{3}{2}}} \tag{6.16}$$

where P_Q, B and W are critical load, specimen thickness and width, respectively. Here, f is the geometrical correction factor expressed as a function of a/W, where a is the initial crack length.

Critical load, P_Q, was determined from the load vs. displacement curve of the specimens. A best fit straight line (AB) was drawn to determine the initial compliance, C. A second line (AB') with a compliance of 5% greater than that of line (AB) was drawn. As the maximum load, P_{max}, of the specimens fell outside the line (AB) and line (AB'), therefore the intersection of line (AB') and the load curve was used as P_Q.

Critical strain energy release rate, G_{Ic}, was measured directly from the energy derived from integration of the load vs. displacement curve up to the same load point, P_Q, as used for K_{Ic} by the following relation:

$$G_{Ic} = \frac{U}{BW\phi} \tag{6.17}$$

where U is the energy up to a critical point obtained as the area under the load-displacement curve and ϕ is the energy calibration factor. Values of $f(x)$ and ϕ are available in the literature (ASTM D 5045-99).

6.5 Results and Discussion

6.5.1 Fracture characteristics

Typical load versus displacement curves for a CT specimen of H-SMC and G-SMC composites at two different loading rates of 5 and 10 mm/min are shown in Figure 6.7. H-SMC composites exhibit non-linear behaviour followed by a gradual decline of load from the maximum point as the displacement increases indicating that crack propagation is occurring in a stable and continuous manner. G-SMC composites display a more linear behaviour followed by a more rapid load drop after maximum load. Generally, for G-SMC composites the load also decreases continuously with some unstable points as the displacement increases after the maximum load. This may result in continuous crack propagation along with

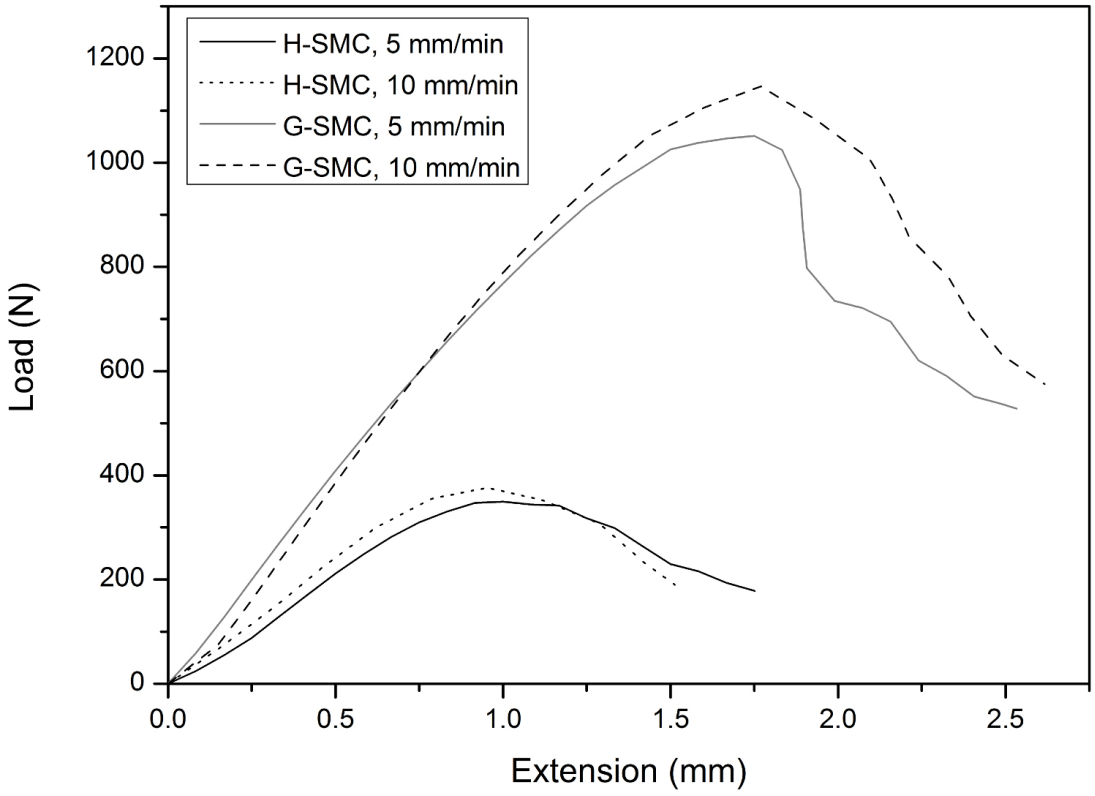

Figure 6.7: Typical CT specimen load-displacement curves for H-SMC and G-SMC composites at two distinct loading rates of 5 and 10 mm/min.

stages of crack initiation and crack arrest [Wong *et al.*, 2004]. The results suggest that H-SMC and G-SMC composites are strain rate dependent as higher maximum load point were obtained at 10 mm/min than 5 mm/min loading conditions. Typical fracture patterns of H-SMC and G-SMC specimens are shown in Figure 6.8.

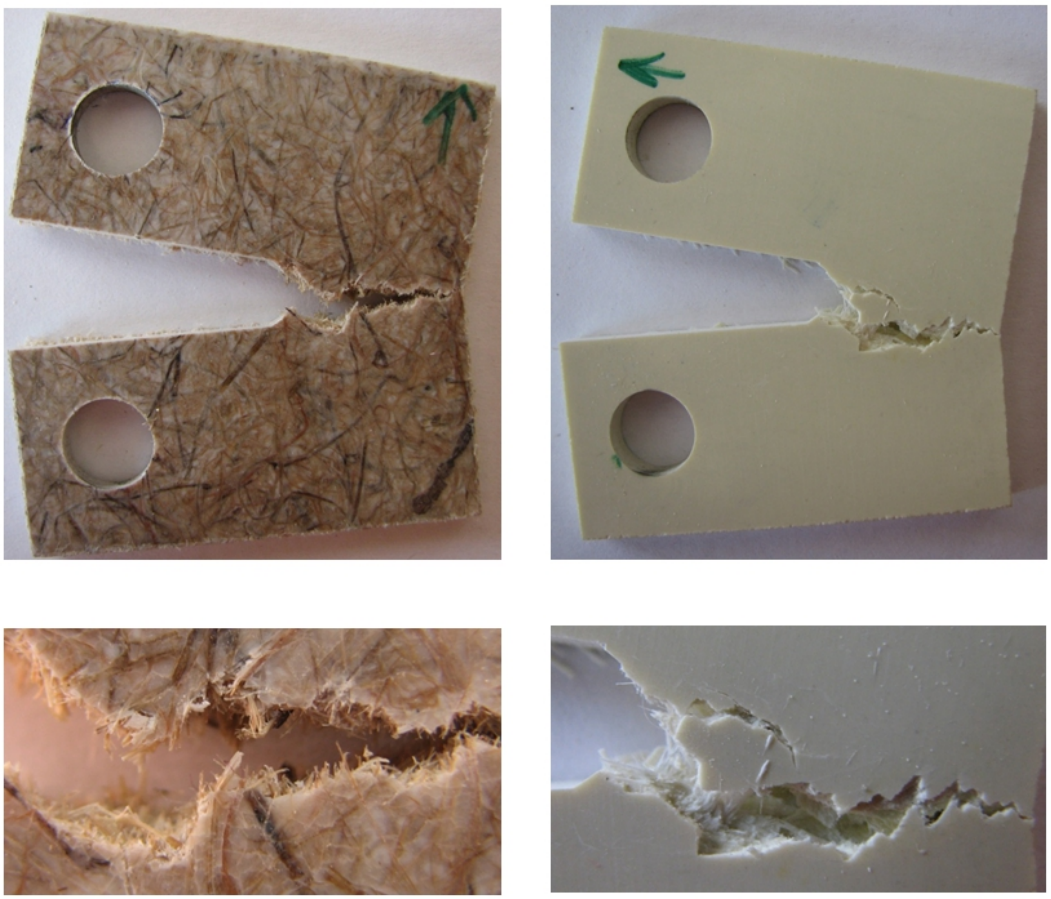

(a) H-SMC (b) G-SMC

Figure 6.8: Typical fracture patterns of H-SMC and G-SMC specimens.

6.5.2 Influence of fibre volume fraction

Since these materials exhibit a non-linear behaviour before maximum load is attained, an offset method of 5% from the gradient of the linear portion of the load-displacement curve was used to calculate the K_{Ic} using eq.4.2 as recom-

mended by ASTM D 5045-99. Figure 6.9 shows the fracture toughness in terms of the critical-stress-intensity factor, K_{Ic}, of H-SMC and G-SMC composites as a function of fibre volume fraction, together with the curve fitting for both composites. A constant $CaCO_3$ filler content of 18 vol.% was used.

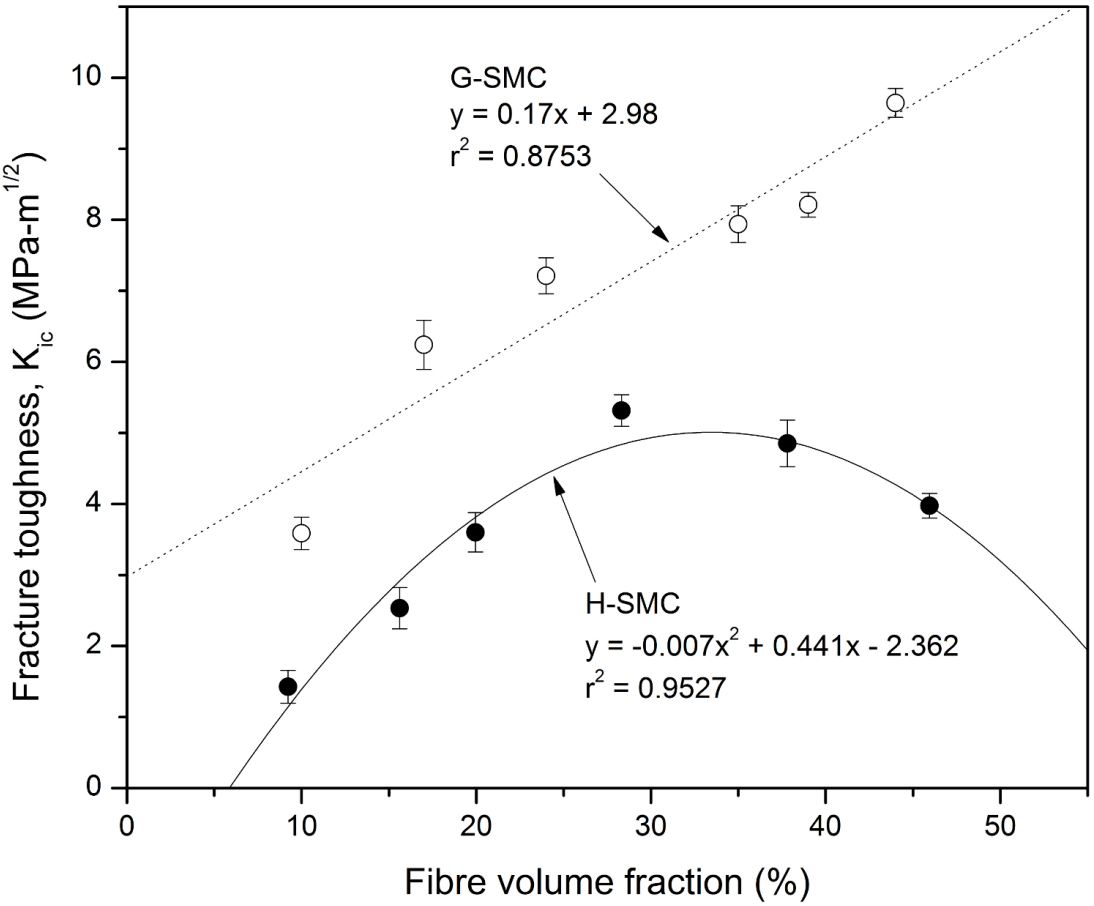

Figure 6.9: Fracture toughness, K_{Ic}, as a function of fibre volume fraction of (•) H-SMC and (∘) G-SMC composites, together with the linear regression fitting for both composites.

It is clear from the graph that the fracture toughness of both composites show a different trend. For G-SMC composites K_{Ic} increases with increasing fibre content, however for H-SMC composites the K_{Ic} increases to a maximum at about a hemp fibre content of 30 vol.% and then it decreases. The K_{Ic} of G-SMC is significantly higher than H-SMC for all fibre volume fractions. An attempt was

made to predict the K_{Ic} of both composites using regression equations. A good fitting of the linear regression to the experimental data is noticed for G-SMC composites, however the linear fit overestimates the K_{Ic} value at low fibre volume fractions. Linear regression clearly overestimates the K_{Ic} values at high fibre volume fractions for H-SMC composites and therefore a polynomial regression fitting is used for H-SMC composites which is in good agreement with experimental data at all fibre volume fractions. At fibre loading of 10 and 40 vol.% the K_{Ic} of G-SMC is about 70% and 50% higher than H-SMC composites. The K_{Ic} value of about 6 MPa-m$^{1/2}$ for 20 vol.% G-SMC composite is in good agreement with those published in literature of about 9 MPa-m$^{1/2}$ [Hughes *et al.*, 2002] considering the effect of $CaCO_3$ filler and no resin degassing during composite manufacturing.

The critical stress intensity factor describes the stress intensity of the stress field ahead of the crack tip and therefore gives the value of force required to overcome crack resistance. This could be thought of as measure of a material's strength with a crack present. This suggests that the lower values of K_{Ic} for H-SMC composites compared to G-SMC composites at all fibre volume fractions maybe due to the lower tensile strength of hemp fibres compared to E-glass fibres (approximately 650 MPa for hemp fibres verus 2000 MPa for glass fibre). Additionally, these H-SMC composites have been shown to have poor interfacial strength when the fibres are untreated due to presence of wax on the hemp fibre surface that could lead to crack propagating through the weak interface [Patel *et al.*, 2010] and see Chapter 3. At low fibre loading there are insufficient fibres to stop crack propagation, whereas at higher fibre loading the wetting of fibres is poor, resulting in low fracture toughness of the composite. Also, at higher fibre volume fractions H-SMC composites have high levels of porosity and voids that are present in the fibre themself in the form of lumen or introduced during composite processing. All of this will probably influence the fracture toughness properties. However, at an optimum fibre loading the level of porosity is low which may lead to enhanced wetting of the fibres and the combination of these two methods could result in a stronger fibre-matrix interface and increase the fracture toughness of the composite.

Figure 6.10 shows the critical strain energy release rate, G_{Ic}, of H-SMC and G-SMC composites as a function of fibre volume fraction, together with the curve

fitting for both composites. Again, a linear regression is used to predict the G_{Ic} of G-SMC composites and a polynomial regression is used to predict the G_{Ic} of the H-SMC composite. A good agreement of the experimental data with the curves is found for both composites. Critical strain energy release rate is a measure of the energy necessary for crack initiation. Generally, G_{Ic} increases with fibre volume fraction for G-SMC composites, while the trend for H-SMC is similar to the K_{Ic} results. The G_{Ic} increases almost linearly upto a maximum value at about 30 vol.% fibre loading and then decreases with further fibre loading. The energy required for crack initiation is significantly higher for G-SMC composites than

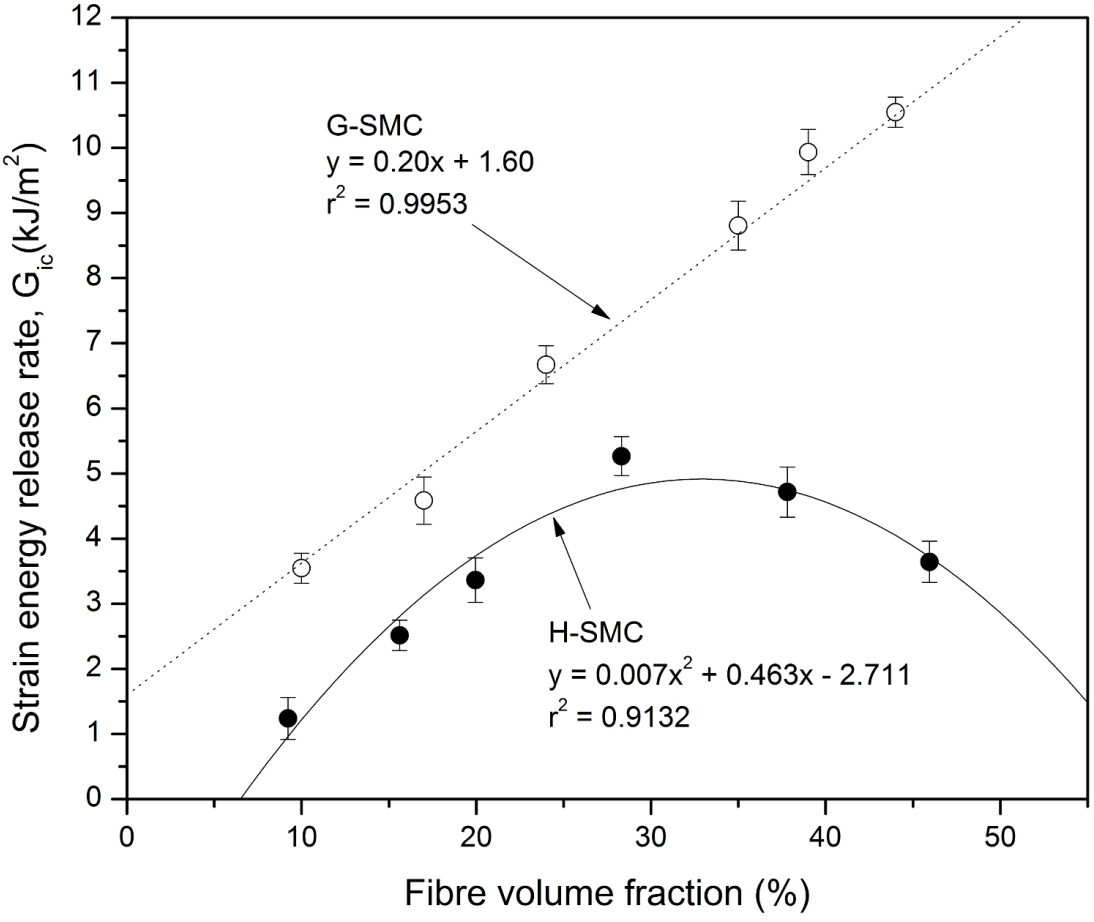

Figure 6.10: Strain energy release rate, G_{Ic}, as a function of fibre volume fraction of (•) H-SMC and (○) G-SMC composites, together with the linear regression fitting for both composites.

H-SMC composites at all fibre volume fractions. The low crack initiation energy maybe due to the poor fibre-matrix interface of H-SMC composites and presence of cracks as described above. Additionally, failure of the interface holding the hemp bundles together may also lead to low crack initiation energy as shown in Chapter3, Section 3.4.2. The difference in fracture toughness properties for H-SMC and G-SMC is the smallest at a fibre content of 15-30 vol.%.

6.5.3 Influence of $CaCO_3$ filler content

Figure 6.11 show the fracture toughness and critical strain energy release rate of H-SMC composites as a function of $CaCO_3$ filler content at a constant fibre loading of 20 vol.%. It clear from the curves that K_{Ic} and G_{Ic} are sensitive to the incorporation of $CaCO_3$ particles. Both K_{Ic} and G_{Ic} increase to a maximum value at 18 vol.% filler content but after this maximum the K_{Ic} plateaus off whereas the G_{Ic} decreases as the filler content increases. Incorporation of $CaCO_3$ filler into the unfilled unsaturated polyester (UP) composite specimens increases the K_{Ic} and G_{Ic} by about 40 and 30%, respectively.

The filler particles may become an obstacle for a growing crack and force it to go around the particle thereby increasing the crack propagation energy. Addition of $CaCO_3$ to a virgin thermoset resin may change the fracture mode from brittle to ductile fracture for a filled composites caused by the changes of stress fields in the matrix around the filler particles. The particle-matrix debonding may promote the yielding of the brittle thermoset matrix. At higher filler content the wetting of the fibre becomes poor leading to a weak fibre-matrix interface and may result in lower fracture energy.

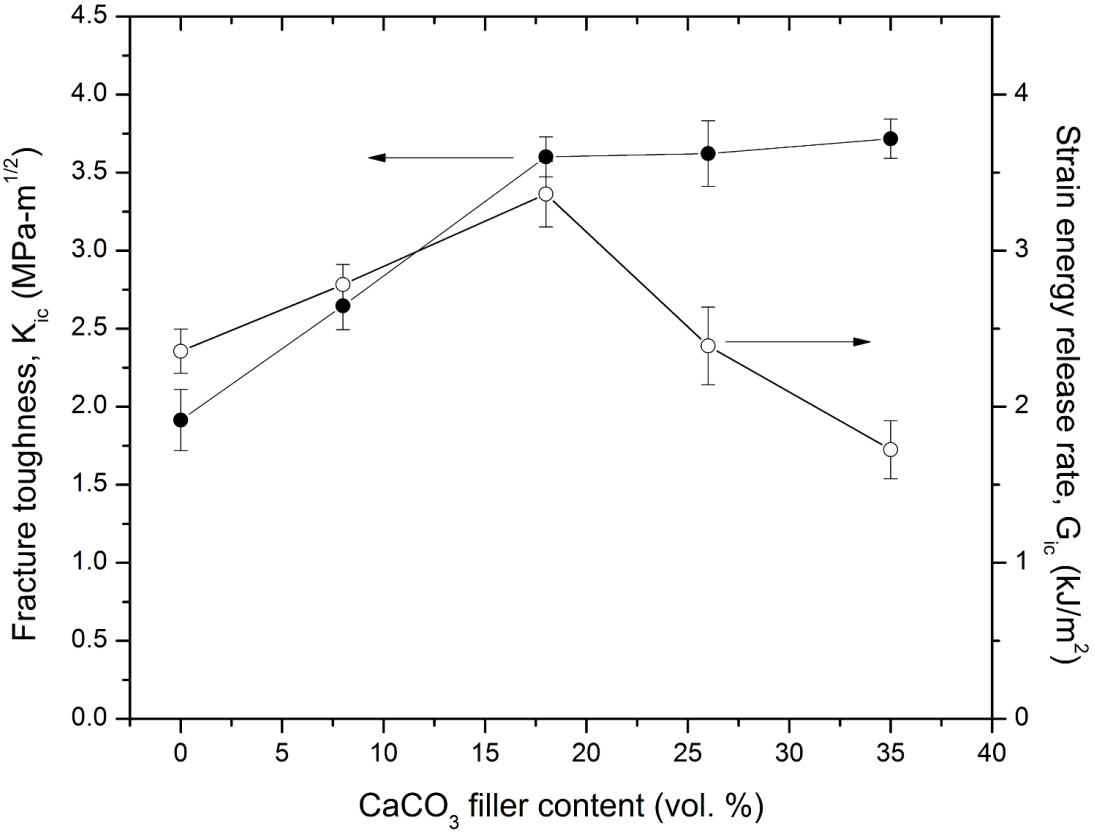

Figure 6.11: (•) Fracture toughness, K_{Ic}, and (○) strain energy release rate, G_{Ic}, of H-SMC composites as a function of $CaCO_3$ filler content at a constant fibre loading of 20 vol.%.

6.5.4 Influence of fibre surface treatment

The normalised values of fracture toughness, K_{Ic}, and critical strain energy release rate, G_{Ic}, of the H-SMC composites based on hemp fibre mats with different fibre surface treatments are presented in Figures 6.12 and 6.13 (the values are normalized by the untreated H-SMC composite of similar composition). Three kinds of hemp fibre surface treatments were used: (i) for fibre cleaning (dewaxing and bleaching) an alkaline (NaOH) treatment was used, (ii) for fibre coating (grafting and coupling) a silane treatment, while (iii) additionally a combination of these two treatments (constant 2% NaOH concentration with varying silane concentration) was also investigated.

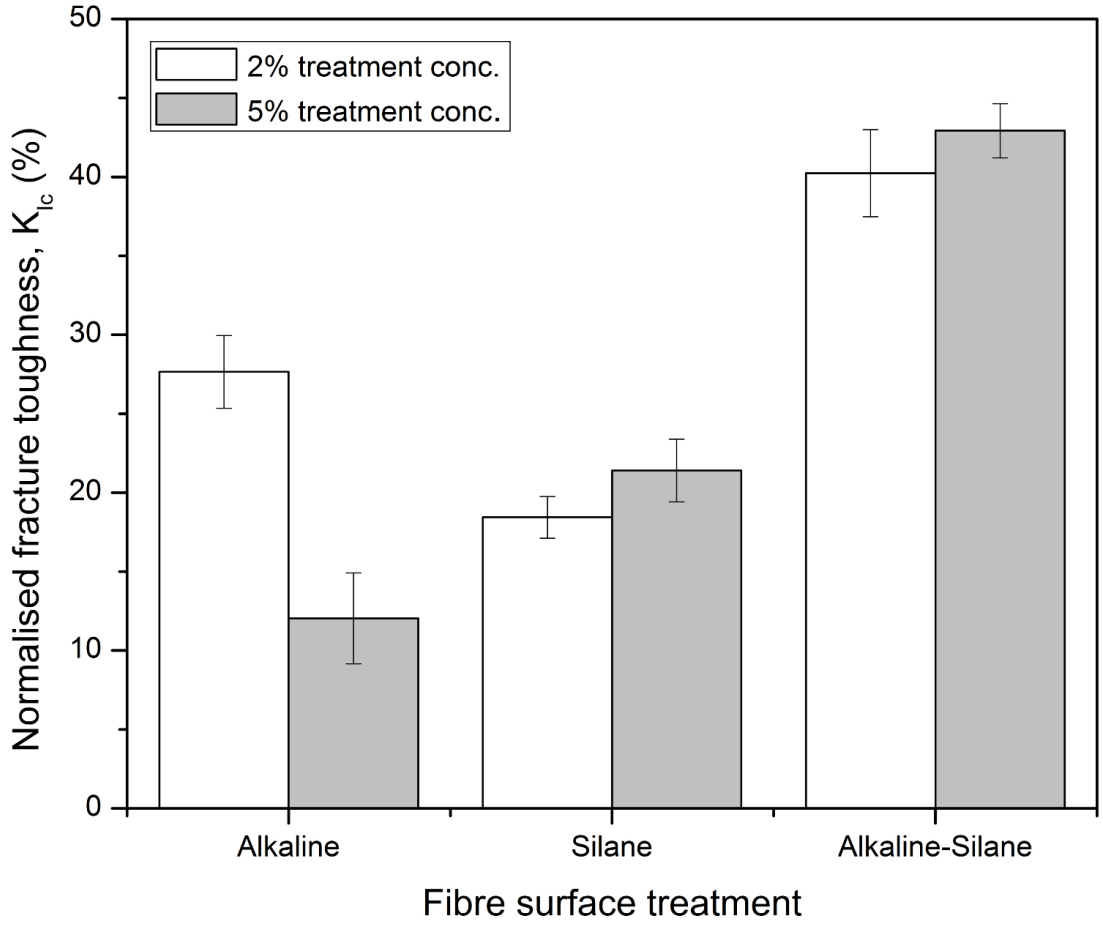

Figure 6.12: Normalized fracture toughness, K_{Ic}, of H-SMC composites as a function of different surface treatments. Alkaline-Silane (right column) treatment represents H-SMC composites based on hemp fibres treated with a fixed 2% alkaline treatment and varying concentration of silane treatment.

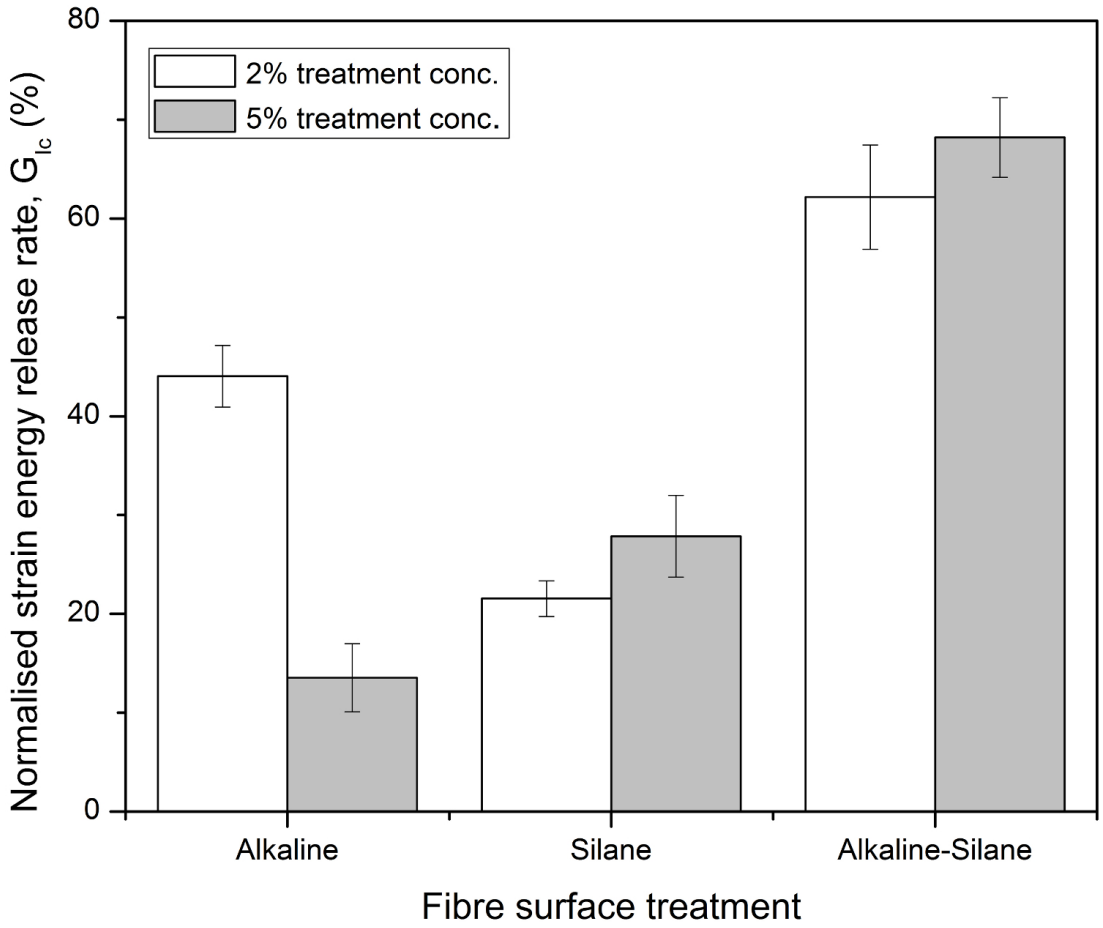

Figure 6.13: Normalized strain energy release rate, G_{Ic} , of H-SMC composites as a function of different surface treatments. Alkaline-Silane (right column) treatment represents H-SMC composites based on hemp fibres treated with a fixed 2% alkaline treatment and varying concentration of silane treatment.

It can be seen that K_{Ic} and G_{Ic} increases when the hemp fibres are treated with 2% concentration of alkaline treatment. This treatment can remove natural and artificial impurities and produce a rough surface topography which enhances the possibility for mechanical interlocking at the interface [Patel *et al.*, 2010]. The increased fibre surface roughness may result in greater friction energy through higher resistance to pull-out and debonding of the fibre from the matrix. Additionally, alkaline treatments can lead to fibre fibrillation therefore increasing the effective surface area available for wetting by the polymer matrix. Fibrillation

can provide an easier path for crack propagation resulting in increased fracture surface being created and also more energy absorption through mechanical friction between the fibre and matrix [Silva *et al.*, 2006]. A combination of all these factors can result in increased crack resistance K_{Ic} and a higher energy per unit crack surface G_{Ic}. Treatment of hemp fibres with 5% alkaline concentration decreased both the K_{Ic} and G_{Ic} of the H-SMC composites. Murkherjee *et al.* [1993] found that the use of more than 1% NaOH on cellulose fibres weakens the fibres resulting in a reduction in mechanical properties. Furthermore, severe alkaline treatment results in excessive fibrillation meaning there are more fibre ends for crack initiation. Silane treatment of the fibres also increased the K_{Ic} and G_{Ic} of H-SMC composites by about 20%. Silane treatment acts as a bridging material that forms chemical links between the fibre and matrix leading possibly to an improved fibre-matrix interface which could lead to increased fracture toughness of the H-SMC composites. Treatment of the hemp fibre mat with 2% alkaline treatment followed by a varying silane treatment resulted in a significant improvement in the K_{Ic} and G_{Ic} of the H-SMC composites. The combination of factors described above for both treatments will possibly lead to increased fracture toughness properties of (2% alkaline)-silane treated H-SMC composites. The alkaline treatment first removes impurities on the hemp fibre surface therefore allowing more fibre-silane chemical links to be formed.

6.6 Conclusions

This chapter investigated the fracture toughness of hemp fibre mat reinforced sheet moulding compound (H-SMC) in terms of the critical-stress-intensity factor, K_{Ic} and critical strain energy release rate, G_{Ic}. Three materials parameters: fibre volume fraction, $CaCO_3$ filler content and fibre surface treatment were studied using compact tension test method. It was shown that fracture toughness of H-SMC composites is significantly lower than that of glass fibre reinforced composites (G-SMC). The H-SMC composites show a peak in fracture toughness properties at a fibre content of about 30 vol.%, while G-SMC composite increases continuously. At extreme high fibre volume fractions the fracture toughness properties of H-SMC composites are low due to the presence of a high level of porosity

and poor fibre wetting. It is noticed that the fracture toughness properties of H-SMC composites are sensitive to the incorporation of the $CaCO_3$ filler. The combination of alkaline and silane treatments on the hemp fibres resulted in a significant increase in fracture toughness properties of H-SMC composites.

The results show that with the optimal combination of fibre volume fraction, $CaCO_3$ filler and fibre surface treatment can result in H-SMC composites that have fracture toughness properties that can be exploited for low to medium range engineering applications. It is recommended that to further improve the fracture toughness properties of these natural fibres reinforced composites more research needs to be devoted on the optimization of fibre-matrix interfacial properties and ways of reduce porosity content in these composites.

Chapter 7

Environmental impact of hemp fibre reinforced SMC composites

7.1 Introduction

The preceding chapters focused on the development of natural fibre reinforced composites (NFCs) partly based on the promises that NFCs are more environmentally friendly than conventional glass fibre reinforced composites. However, the question should be asked if these claims and assertions about NFCs are really justified? The answer is not as straight forward as it seems and a better understanding of the fundamental loops and processes of the entire life cycle of these materials, such as the stages of extraction, use and disposal (from cradle to grave) is necessary to make a real judgment about the environmental characteristics of these material.

In Chapters 3 and 4 it was found that the mechanical properties (strength and impact) of hemp fibre reinforced sheet moulding compounds (H-SMC) is much lower when compared with glass fibre reinforced sheet moulding compounds (G-SMC), but the effect of these materials on the environment was not studied. The environment impact is having increasing importance due to an increasing population and an increasing consumption. This makes clear that the environment cannot keep supporting this ever increasing burden. In this chapter the effect of H-SMC on the environment is studied through Life Cycle Analysis (LCA)

computer program and compared with the existing material i.e. G-SMC.

LCA is a methodology for assessing the environmental aspects associated with a product over its life cycle. This is achieved by examining the inputs and outputs of materials along with energy and the associated environmental impacts directly attributable to the functioning of a product or service system throughout its life cycle. The emissions are quantified in a number that indicates its 'damage to the environment'. The advantage of this method is that it not only considers the emissions during production of the investigated product, but also emissions during: production/mining of the needed raw materials, use and post-use i.e. disposal of the product. The disposal could include dumping or land filling, incineration to produce energy e.g. electricity, reuse of the product or recycling the material i.e. using the material as a raw material to produce same or another product. Figure 7.1 shows an example of a life cycle of an automobile.

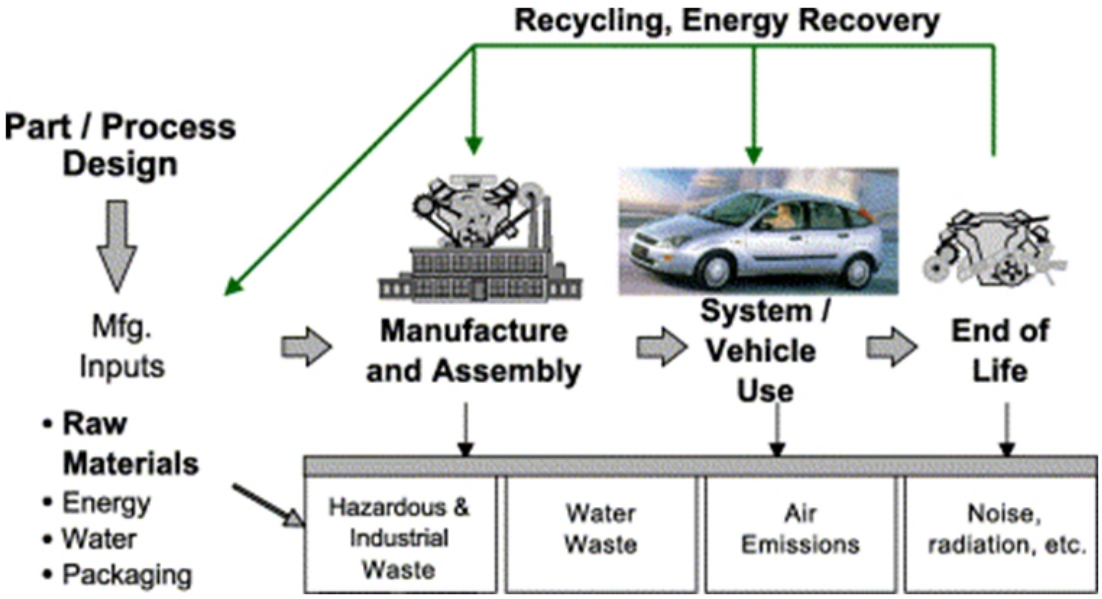

Figure 7.1: Life cycle of an automobile [Rebitzer *et al.*, 2004].

The results of the contribution of the life cycle stages to the overall environmental load can be used to optimise the environmental performance of a product or process. LCA can also be used to compare two or more products to determine which of them is more preferable from an environmental point of view. Although

natural fibres do not have clear advantages with respect to mechanical recycling issues, they do have ecological advantages over glass fibres, since they can be incinerated. It is especially for the incineration aspect that natural fibres such as flax and hemp are considered as an interesting environmentally safe - alternative for the use of glass fibres as reinforcement in engineering polymeric materials [Berglund & Peijs, 2010; Garkhail, 2001; Peijs, 2000].

The aim of this LCA study is to compare the environmental impact of using natural fibre instead of glass fibre as reinforcement in plastics. The environmental issues analysed in LCA are:

- carcinogens
- respiratory organics
- respiratory inorganic
- climate change
- radiation
- ozone layer
- ecotoxicity
- acidification/eutrophication
- land use
- minerals
- fossil fuel

as outlined in eco-indictor 99 method [Goedkoop & Spriensma, 2000] and complies with ISO/TR14047 [2003].

7.1.1 LCA of natural fibre composites

Some life cycle assessment (LCA) studies of plant and wood based composites can be found in the literature [Ardente *et al.*, 2008; Bos, 2004; Miao & Finn, 2008; Shen & Patel, 2008; Thamae *et al.*, 2008; Vidal *et al.*, 2009]. Wotzel *et al.* [1999] carried out a study of an automotive side panel made of ABS copolymer and another of hemp fibre (66 vol.%) reinforced epoxy composite. It takes about 59 MJ/basic-component less energy to produce the hemp fibre component than the ABS component, which is an energy saving of 45%. For the hemp component the epoxy resin accounts for about 78% of the energy demands and is far the largest contributor to emissions, mainly due to acidification potential caused by emissions of NOx and SO_2. Corbiere-Nicollier *et al.* [2001] compared the environmental performance of China reed fibre and glass fibre as reinforcement with polypropylene (PP) and found that energy consumption and other environmental impacts were reduced by the use of raw renewable fibres due to: substitution of glass fibres with natural fibres, indirect reduction in PP due to higher fibre volume fractions and reduced weight of the final part resulting in low fuel consumption. Other studies on natural fibre for automotive application include Zah *et al.* [2007] and Schmehl *et al.* [2008]. Joshi *et al.* [2004] reviewed the existing literature on LCA to compare the impacts of natural fibre and glass fibre composites and concluded that NFC are likely to be environmentally superior to GRP in most applications due to (1) lower environmental impact of producing hemp fibre compared to glass fibre; (2) NFC tend to have higher fibre content for equivalent performance therefore reducing more polluting base polymer content; (3) lower weight of the NFC improves fuel efficiency and reduces emissions; and (4) energy recovery and carbon credits at end of life. Puettmann & Wilson [2005] have documented LCAs of wood products: glulam, softwood lumber, laminated veneer lumber, softwood plywood. Xu *et al.* [2008] have studied wood-plastic-composites (WPC) based on polypropylene with 10%, 30% and 50% wood fibre content by mass. It was found that when the material service density (volume of material satisfying property requirement) is used as the functional unit, WPC demonstrate superior environmental friendliness compared to pure polypropylene.

7.1.2 LCA methodology

The LCA methodology has four components: goal and scope definition, life cycle inventory (LCI), impact assessment, and improvement assessment [ISO14044, 2006]. A full life cycle assessment includes each of the four components as discussed below and shown in Figure 7.2.

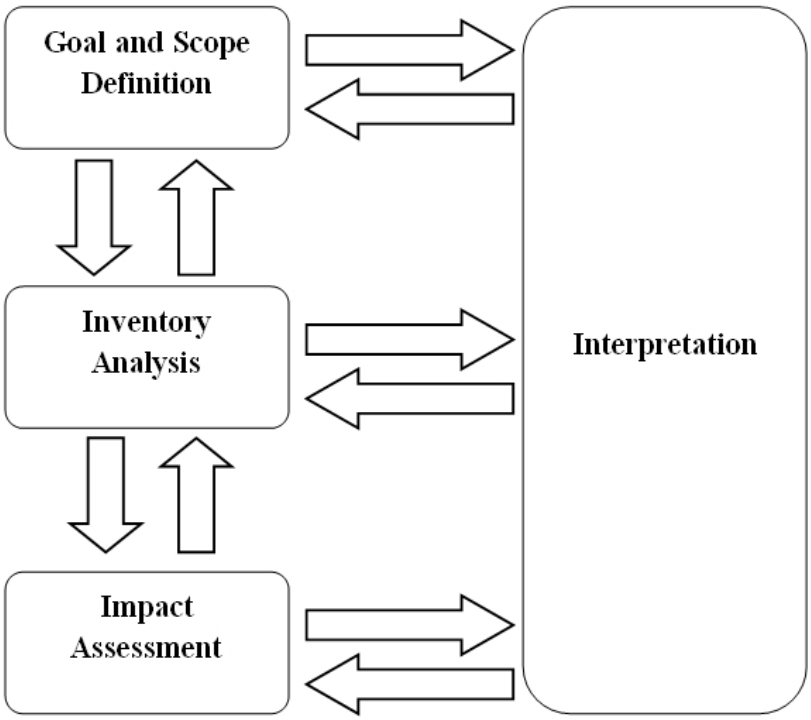

Figure 7.2: Framework for life cycle assessment [ISO14044, 2006].

The *goal* defines the purpose of the study. The execution of the LCA method will vary according to the goal of the study. Some of the factors that need to be considered when defining the goal include: (1) intended audience, for example if the study is for company decision-makers it needs to be less rigorous than if it was for informed policy-makers. (2) purpose of study, for example a streamlined study is adequate when deciding between two materials as the risk involved and the level of certainty required is low. However, a full study is required when significant revenue or major implications are involved as the risk is high. (3) critical review, if the study needs to be reviewed by an independent third party

of experts or not.

The *scope* of the study determines how the data is to be collected and input, what the boundary conditions and the functional units of the study are. The boundary conditions are defined by the intended goal, they are used to determine which processes are included or excluded from the study. Functional unit (comparison basis) is used to compare the service or function provided by the system. The results of the LCA study will relate directly to the functional unit; e.g. if the functional unit is 1kg of a product, the results will include the amount of pollutants released for every kg of product that is made. Finally the scope phase includes a description of the method applied for assessing potential environmental impacts of each category.

Life cycle inventory analysis involves compiling an inventory of the relevant inputs and outputs of a product system, including polluting emissions and consumption of resources (and energy) per functional unit into a flowchart according to the system boundaries decided on in the goal and scope definition (Figure 7.3). The data inventory for each unit process is defined by the system. Depending on the study and aims, first hand data may be collected through measurements and estimates of key energy and materials usage, which relate directly to process optimisation and to economic savings.

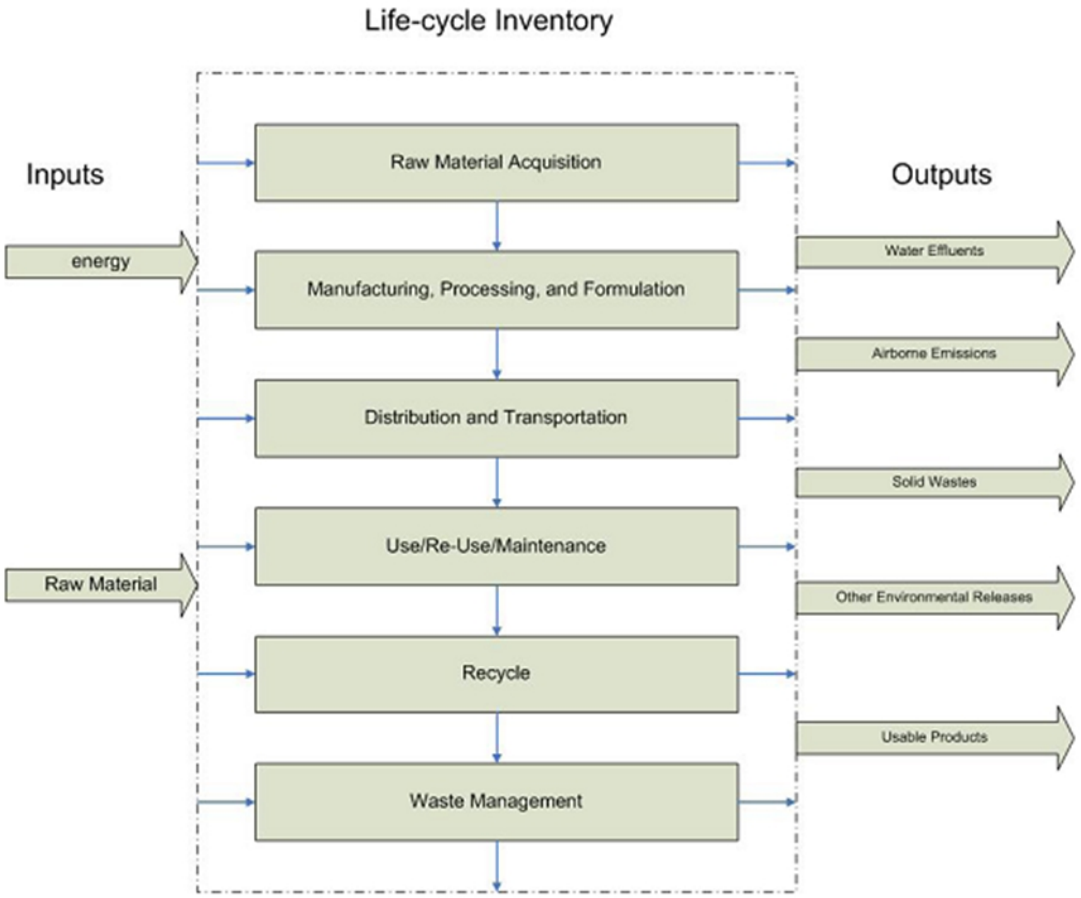

Figure 7.3: Life cycle inventories account for material use, energy, wastes, emissions, and by-products over all of the stages of a product's life cycle [Zhu, 2004].

Life cycle impact assessment (ISO 14042) evaluates the possible environmental impacts associated with measured environmental inputs and outputs. This stage consists of three stages: classification, normalisation and evaluation. In classification all impacts are sorted into classes according to the effect they have on the environment. The environmental impacts are aggregated within each class to produce an effect-score. Classification enables the environmental effects of two or more products to be compared. In normalisation the effects are set off against a "normal" effect. The normalisation values are based on average European data in the Eco-indicator 95 method. Normalisation reveals which effects are large and

which are small with respect to other effects in relative terms. However, it does not yet say anything about the relative importance of the terms. A small effect can very well be the most important. A weighing step is therefore necessary to achieve an overall result. In the evaluation step the impact profiles are converted into environmental score, which are useful when more alternatives are being compared. In the Eco-indicator 95 method the weighing factors are based on the distance between the current level and target level. Weighing factors may differ from country to country depending on the political views and opinions concerning the relative importance of local or regional impact categories.

In the *interpretation* stage the results of the impact assessment are analysed in order to draw conclusions and suggest improvements. Interpretation is performed in interaction with the three other phases of the life cycle assessment, as seen Figure 7.2. If the results of the inventory analysis or the impact assessment are found not to fulfill the requirements defined in the goal and scope phase, the inventory analysis must be improved by e.g. revising the system boundaries, further data collection, etc., followed by an improved impact assessment. This iterative process must be repeated until the requirements in the goal and scope are fulfilled.

7.1.3 LCA drawbacks

There are certain drawbacks with the use of SimaPro 7.0; the LCA software package used in this study.

- Processing machines: Additional emissions to the environment caused by maintenance of machines are not incorporated in the analysis. This would lead to an interpretation that is slightly unfavourable for H-SMC, because glass is harder and causes more wear.

- Growth: Additional herbicides, fungicides, insecticides and pesticides needed to grow the plants from which flax or hemp fibres are produced. Emissions that occur during the production of oil or mineral ores are not considered and only emissions that take place during extraction and purification of oil and mineral-ore based materials are considered.

- Non-renewable sources: As is the case with fuels, the stocks of some metal ores are very limited. In a theoretical sense metal never disappears from the earth and metal can always be recycled. In practice, exhaustion of ore reserves will have a significant economic impact.
- Renewable sources: Renewable sources cannot be exhausted, but the production potential of renewable sources such as hemp is limited, due to agricultural area.

7.2 Materials and Methods

The specialised software package SimaPro 7.1 was chosen for this investigation. SimaPro has a large database of materials and processes and has been successfully used to analyse the effect of various products on the environment. The Eco-indicator '95 (the normalisation/evaluation method, explained in the below section) has been developed by Pre (The Netherlands) in collaboration with Philips, NedCar, Oce, Schuurink and several universities (Amsterdam, Leiden and Delft) as well as consultancies (TNO, Centrum voor Energiebesparing en Schone Energie).

The BUWAL 250 and IDEMAT 2001 database was selected because it covers more data related to the products under study. These two databases are based on European scenarios. The BUWAL 250 is a Swiss database for packaging materials (plastic, carton, paper, glass, tin plated steel, aluminium), energy, transport and waste treatment. IDEMAT 2001 database was developed by the Faculty of Industrial Design Engineering, Technical University of Delft, The Netherlands. This database focuses on the production of materials (metals, alloys, plastics, wood), energy and transport.

7.2.1 Goal and scope

The goal of this LCA study is to compare the environmental impact of using natural fibres (H-SMC) instead of glass fibre (G-SMC) as reinforcement in polymer matrix composites, and to identify major environmental impact categories to which these two composites have most significant effect.

7.2.2 Functional unit and system boundaries

Defining the functional unit is one of the most important steps in a life cycle analysis. The impact is considered for the entire life cycle of the component, i.e. (1) assembly (raw material extraction, raw material processing, and panel fabrication), (2) the use phase and (3) the end-of-life (disposal). The system boundaries are depicted in Figure 7.4. The environmental emissions during the procurement of the raw materials is either included in the database or must be found in literature. The database should contain all relevant emissions that took place to obtain the raw materials (including mining, purification and production).

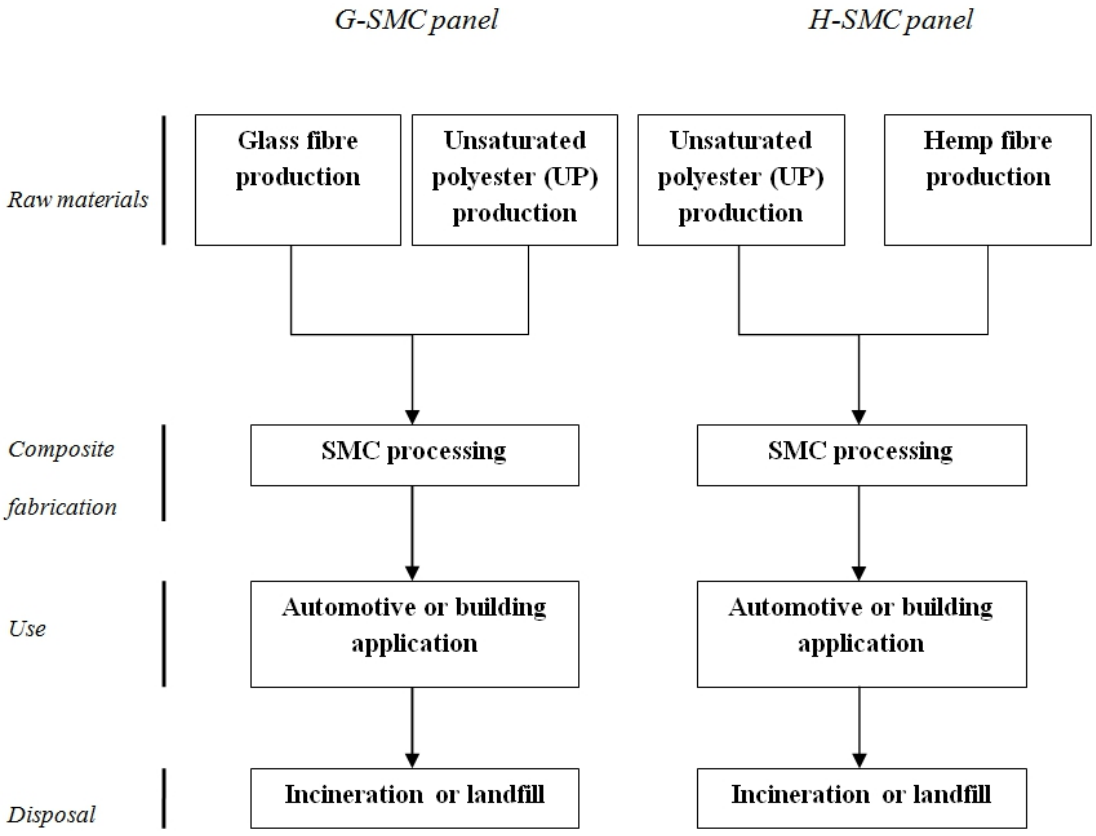

Figure 7.4: Process steps included in this study for the production of H-SMC and G-SMC (reference material).

To compare components, both G-SMC and H-SMC composite panels must perform the same function meaning they should have the same mechanical prop-

erties. In reality, glass fibre composites have higher mechanical properties than hemp fibre composites as shown in Chapter 3. In this study it is assumed that the material is required for certain applications (e.g. automotive applications) for which a particular property is specified. Only basic mechanical properties are considered and environmental properties like durability, moisture pick-up etc. are ignored. These environmental properties are likely to reduce the life span of H-SMC composite compared to G-SMC composites; however it is not yet possible to understand by how much the life span will be reduced. To determine this water absorption and environmental weathering experiments on H-SMC and G-SMC composites need to be carried out first and the result analysed before they can be included in the LCA study.

The mechanical properties considered are tensile strength and Youngs modulus (stiffness). The required tensile properties of a composite material for an automotive application are given in Table 7.1.

Table 7.1: Required properties for an automotive application [Vissers, 2000].

Composite	Tensile strength (MPa)	Young's modulus (GPa)
Automotive application	45	3

Based on rule of mixtures an estimate of the required fibre volume fraction (and weight fraction) for each material property was made and is presented in Table 7.2. The material parameters used for the calculations were: hemp fibre strength and modulus of 628.28 MPa and 36.75 GPa respectively (based on mean values found in the literature, see Appendix C), glass fibre strength and modulus of 2500 MPa and 70 GPa respectively, hemp and glass fibre densities of 1.5 g/cm^3 and 2.5 g/cm^3 respectively and fibre orientation factor (η_0) of 0.375 for random fibre orientation.

Table 7.2: The estimated (approximate) fibre volume fraction (V_f) and weight fraction (W_f) of H-SMC and G-SMC required to obtain the required property for an automotive application.

Property	Value	Hemp fibre (V_f)	Glass fibre (V_f)	Hemp fibre (W_f)	Glass fibre (W_f)
Tensile strength	45 MPa	0.19	0.048	0.21	0.053
Stiffness	3.0 GPa	0.22	0.11	0.24	0.12

Based on the fibre volume fractions from Table 7.2 the composite weight for H-SMC and G-SMC composites for each property criterion was calculated (see Appendix E for calculations). In order to compare the impact of life cycle of the two composites, 1 kg of G-SMC composite is taken as a reference material and the equivalent weight of H-SMC for each property criterion are calculated and mentioned in Table 7.3.

Table 7.3

Property	Value	Hemp fibre (V_f)	Glass fibre (V_f)	Weight of G-SMC (kg)	Weight of H-SMC (kg)
Tensile strength	45 MPa	0.19	0.048	1	0.996
Stiffness	3.0 GPa	0.22	0.11	1	0.943

7.2.3 Raw materials

Unsaturated polyester

UP is produced by cracking of natural gas or light oils. The cracking results in the monomer, ester, which is reacted with a alcohol to form UP. The production of UP that includes the extraction process (drilling for oil, or mining of coal) and refining is very energy intensive. Hydrocarbons are combined with steam and heat at temperatures above 900°C. IDEMAT 2001 database shows that the main impact due to the production of UP include release of nitrogen oxides (impact on eutrophication and potential for acidification from nitrogen oxides into water)

and hydrocarbons (impact on photochemical oxidation). Other emissions include CO_2 and methane which have impact on global warming.

Glass fibre

Glass fibre is mainly made of silica (SiO_2) but includes other impurities such as soda and lime. Sodium carbonate (Na_2CO_3) is added to lower the melting temperature to about 1000-1500°C. Calcium carbonate ($CaCO_3$) or calcium oxide (CaO) is added to make the mixture more durable. These raw materials are maintained in a molten state inside a bushing (commonly made of rhodium-platinum alloy) and flows slowly through orifices with a network of small round holes under the influence if gravity. The glass emerging from the holes is drawn mechanically downwards at a speed of up to about a thousand meters per minute to give very fine filaments. In this study Glass fibres I from the IDEMAT 2001 data is used to represent the glass fibres used in the SMC process. This includes the raw materials extraction, energy input and the emissions to the environment during the production of the glass fibres.

Hemp fibre

The cultivation of hemp consists of several phases. The land needs to be plowed, before that seeds are sown. The crop has to be protected against different pests/weeds, and the crop needs nutrients in the form of fertilizers. In this study the input data for hemp fibre was based on [van der Werf & Turunen, 2008].

Other additives such as styrene and sodium silicate are also added to the SMC paste, however they will not be described in detail here.

Transport of raw materials

Transport of hemp and glass fibres to the composite manufacturing site at Menzolit was modelled using the BUWAL 250 database with a 28 ton truck (Truck 28t). Transports of final products to consumers is not included in the LCA study.

7.2.4 Composite fabrication

Identification of the required processing steps and their corresponding energy and material consumption as well as emissions are often the most important steps in LCA.

Roughly two steps are identified in the production of G-SMC and H-SMC products out of glass fibres and unsaturated polyester resin:

1. Production of prepreg sheets out of the corresponding materials using SMC process
2. Production of the product out of G-SMC or H-SMC sheets via compression moulding

As the data for compression moulding process is not available in the SimaPro software this step was not included in the LCA study. It is assumed that the same amount of energy will be required for both G-SMC and H-SMC composite moulding process.

Prepreg sheet production using SMC process
In this study SMC 25% GL I from the IDEMAT 2001 data is used to represent the prepreg sheet production using the SMC process. This includes: 0.12 kg unsaturated polyester resin, 0.13 kg styrene, 0.25 kg glass fibres and 0.5 kg sodium silicate. The production of 1 kg of G-SMC sheets with 25% weight glass requires the 2.65 MJ of energy. It is assumed that the production of G-SMC and H-SMC sheets with different weight % of reinforcement (glass or hemp) requires the same amount of energy.

7.2.5 Use phase: additional emissions and savings

An inventory of the emissions that take place during the use of the investigated product is also an important part of LCA. For the present study two different criterion are used which would mean two different applications are considered i.e. application where the design criterion is either stiffness or strength.

As mentioned earlier for an automotive application, e.g. car bumper beam where the material should satisfy both design criterion i.e. strength and stiffness

(Table 7.3), the weight of the objects would contribute in the fuel consumption of an automobile. Thus a weight saving of the product is beneficial to the environment. For every kilogram that is saved in the weight of a car, approximately 6 kg of fuel is saved over the entire lifetime of the automobile. Higher savings are even possible if secondary weight savings are considered. A primary weight saving reduces the load in the other components leading to secondary savings. For an average European car these secondary weight effect can be as high as 150%, meaning that 1 kg primary weight reduction allows for 1.5 kg secondary weight savings. The weight of a product made from reference material (G-SMC) is taken as 1 kg, and the equivalent weight of H-SMC for tensile strength and stiffness criterion is 0.996 and 0.943 kg respectively. The extra fuel required to satisfy the tensile strength and stiffness criteria is given in Tables 7.4 and 7.5. In both design criterion H-SMC composite is lighter in weight than the G-SMC composite. The reduced weight of H-SMC would lead to saving in fuel therefore negative sign is placed.

Table 7.4: Calculation of additional fuel consumption because of added weight, for strength criterion

Property	G-SMC	H-SMC	Units
Weight	1	0.996	kg
Density	1.262	1.257	g/cc
Additional fuel use	0	-0.024	kg
Diesel use*	0	-1.021	MJ

Table 7.5: Calculation of additional fuel consumption because of added weight, for stiffness criterion

Property	G-SMC	H-SMC	Units
Weight	1	0.943	kg
Density	1.343	1.266	g/cc
Additional fuel use	0	-0.342	kg
Diesel use*	0	-1.455	MJ

For applications not in automotive industry e.g. office furniture, the effect of life cycle, 'during usage', of the product on the environment is considered same in both the cases i.e. H-SMC as well as G-SMC.

7.2.6 Life cycle assessment methods

The ISO 14040 standard defines an LCA as a compilation and evaluation of the inputs and outputs and the potential environmental impacts of a product system through its life cycle. In this definition, it is clear that the impact assessment is an integral part of LCA. Life cycle impact assessment is defined as the phase in the LCA aimed at understanding and evaluating the magnitude and significance of the potential environmental impacts of a product system.

In Simapro software there are many methods available to evaluate the possible environmental impacts of the product or process. An important step is the selection of the appropriate impact categories and the definition of so-called endpoints. Endpoints are issues of environmental concern, like human health, extinction of species, availability of resources for future generations etc. For this study the SimaPro method selector (http://www.pre.nl) is used to choose the best among available impact assessment methods. The criteria used to select the impact assessment method is given in Table 7.6.

Table 7.6: The criteria used for selecting the most suitable impact assessment methods (http://www.pre.nl).

Categories	Preferred selection
Single scores	Able to switch between single scores and separate impact category indicator.
Weighting set	Use panel (group of experts) to determine weighting.
Time perspective	A very long time perspective should be applied to factors in the modelling (future generations are very important).
Geographic coverage and acceptance	Validity in Europe is of prime importance
Simplicity versus scientific quality	State of the art modelling techniques, like fate exposure for toxicity.
Completeness	As complete as possible, including land use, small particulates, radioactive substances, solid waste etc.

Eco-indicator 99 egalitarian version (EI99E/E) was chosen as the impact assessment method for this study as it scored the most points in the SimaPro method selector as shown in Table 7.7. Here only a brief description of the Eco-indictor 99 method is given, a detailed description of this method and other possible methods can be found in the SimaPro database manuals [Goedkoop & Spriensma, 2000].

Table 7.7: Results of Simapro method selector (http://www.pre.nl)

	Total	Single scores	Weighting set	Time perspective	Geographic coverage acceptance	Simplicity vs. scientific quality	Completeness
EI99E/E	18	3	3	3	3	3	3
EI99H/A	17	3	2	2	3	3	3
EI99I/I	16	3	3	1	3	3	3
EPS	14	3	0	3	2	3	3
EDIP	14	3	3	3	1	3	1
Impact 2002+	13	2	0	3	3	3	3
CML2000	10	0	0	3	3	3	1
EI95	9	3	2	1	2	1	0
GWP	6	1	0	1	3	1	0
CML92	5	0	0	2	2	1	0
UBP	5	2	0	0	1	1	1

The Eco-indictor is a weighting method that determines the contribution of a products life cycle to the greenhouse effect, acidification and other environmental problems to give a total environmental impact in one single score. Data have been collected in advance for the most common materials and processes and used to calculate the Eco-indicator. The higher the indicator score, the greater the environmental impact.

In Eco-indicator 99 the term "environment" has been defined with types of damage:

1. Human health: this category includes the number and duration of diseases, and life years lost due to premature death from environmental causes and it is measured in DALY (Disability adjusted life years). The effects included are: climate change, ozone layer depletion, carcinogenic effects, respiratory effects and ionising (nuclear) radiation.

2. Ecosystem quality: this category includes the effect on species diversity, especially for vascular plants and lower organisms. It is measured in PDF*m2yr, which is the Potentially Disappeared Fraction of plant species. The effects included are: ecotoxicity, acidification, eutrophication and land-use. In terms of ecotoxicity, this is measured as the percentage of all species present

in the environment living under toxic stress (Potentially Affected Fraction or PAF*m2yr).

3. Resources: this category includes the surplus energy needed in future to lower quality mineral and fossil resources. The depletion of agricultural and bulk resources as sand and gravel is considered under land use. This damage category is measured in MJ surplus energy.

The normalization and weighting values are displayed in Table 7.8

Table 7.8: Eco-indicator 99 normalization and weighting values for egalitarian perspective.

Environmental impact categories	Damage category	Normalized values	Weight
Climate change (DALY)	Human health	0.0155	30%
Respiratory inorganics (DALY)			
Ecotoxicity (PAF*m2yr)	Ecosystem quality	5130	50%
Acidification (PDF*m2yr)			
Fossil fuels (MJ Surplus)	Resources	5940	20%

The standard Eco-indictor values are dimensionless figures given as Eco-indicator point (Pt). The absolute value of the points is not very relevant as the main purpose is to compare relative differences between products or components. One Eco-indicator point is representative for one thousandth of the yearly environmental load of one average European inhabitant.

To deal with the uncertainties in the Eco-indicator 99 model three different perspectives are created: hierarchist, individualist and egalitarian. The different characteristics of each perspective is given in Table 7.9.

Table 7.9: The different characteristics of the three different perspectives in Eco-indictor 99 method.

Perspective	Time view	Manageability	Level of evidence
Hierarchist	Balance between short and long term	Proper policy can avoid many problems	Inclusion based on consensus
Individualist	Short term	Technology can avoid many problems	Only proven effects
Egalitarian	Very long term	Problems can lead to catastrophe	All possible effects

7.2.7 Waste phase

The waste disposal is the last step of product life cycle. The environmental impact of a product is influenced by the treatment (disposal scenario) after its use by the consumer. A product can be reused, recycled, incinerated or it may end up with the landfill waste. Recycling of post-consumer material depends on the application since the cleanliness of the material is very important. The material would be difficult to clean if it has come in contact with e.g. oil. If the material is cleaned with a shredding step should be sufficient to recycle the material. The landfill waste describes what happens if a consumer puts a product into the waste bin. In the incineration scenario the emissions and useful outputs such as heat are taken into account.

Different configurations varying in disposal scenario were examined by Sima Pro 7.1 with the Eco-Indicator 99. The various disposal scenarios considered include landfill waste, incineration and landfill waste with an additional impact of extra/reduced fuel required during the use of H-SMC product because of its extra volume/reduced weight, when compared to G-SMC, for automotive applications.

The notations used for various combinations of H-SMC and G-SMC products, involving various use and disposal methods, are given in Table 7.10.

Table 7.10: Codes used for various combinations of composite criterion, use and disposal.

Description	Codes used
Automotive applications (diesel savings during use included)	
G-SMC- Strength criterion- Extra diesel use- disposal through landfill	GDL
G-SMC- Strength criterion- Extra diesel use- disposal through incineration	GDI
H-SMC- Strength-Diesel-Landfill	HSDL
H-SMC-Strength-Diesel-Incineration	HSDI
H-SMC-Modulus-Diesel-Landfill	HMDL
H-SMC-Modulus-Diesel-Incineration	HMDI
Non-automotive applications	
G-SMC-Landfill	GL
G-SMC-Incineration	GI
H-SMC-Strength-Landfill	HSL
H-SMC-Strength-Incineration	HSI
H-SMC-Modulus-Landfill	SML
H-SMC-Modulus-Incineration	HMI

7.3 Results and discussions

Glass fibre reinforced SMC and hemp fibre reinforced SMC for automotive and non-automotive applications were investigated for their environmental impact. The two materials materials were compared having to fulfil criterion of: tensile strength and stiffness.

7.3.1 Non-automotive applications

For non-automotive application the results are presented in three steps as discussed in life cycle impact assessment Section 7.1.2, with classification chart (Figure 7.5), normalised-effect score (Figure 7.6) and evaluated effects (Figure 7.7).

In the classification chart the relative size of the effect is compared to the size of the other effects and the effect with the highest score is scaled to 100%. The

absolute value of the classification chart are given in Appendix F. Interpretation of classification chart may be difficult because comparison between impact categories is impossible. Therefore a normalisation step is performed, in order to gain a better understanding of the relative size of an effect. In the normalised-effect score chart the damage categories are normalised based on average European data (damage caused by 1 European per year), mostly using 1993 as base year and this is part of the Eco-indicator 99 method. Normalisation and weighting values of Eco-indicator 99 are given in Table 7.8. Normalisation considerably improves our insight into the results. However, no final judgement can be made since not all effects will be considered to be of equal importance. In the evaluation phase the normalised effect scores are multiplied by a weighting factor representing the relative importance of the effect. Eco-indicator 99 with a egalitarian perspective was used as the weighting factor. The relative contribution of the impact categories to the European damage according to the egalitarian perspective is given in Table 7.8.

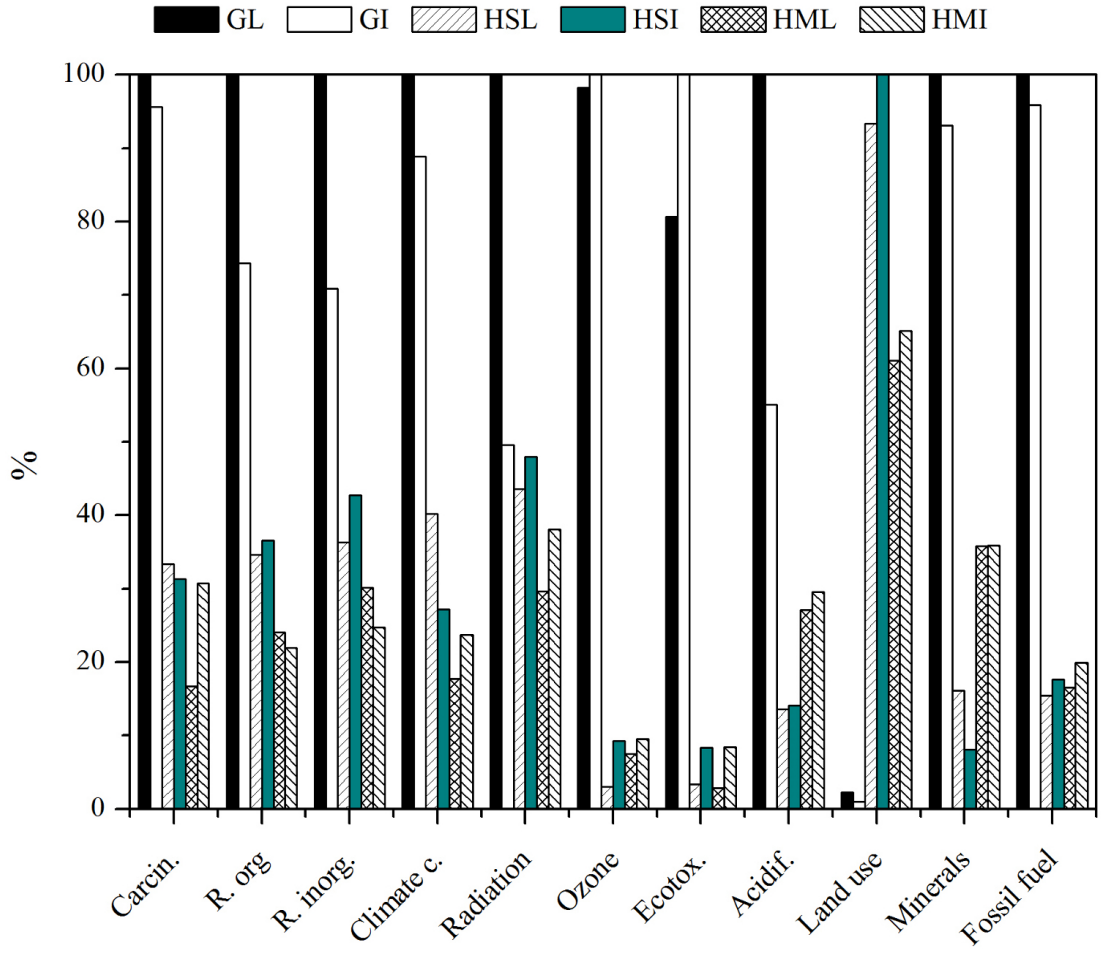

Figure 7.5: Graphical representation of the characterisation obtained by scaling the effects due to various combinations of composite use (for non-automotive applications) and disposal. The sequence of bars in each category is the same as the sequence of codes, mentioned above the figure, starting from left top (GL) and ending at bottom right (HMI).

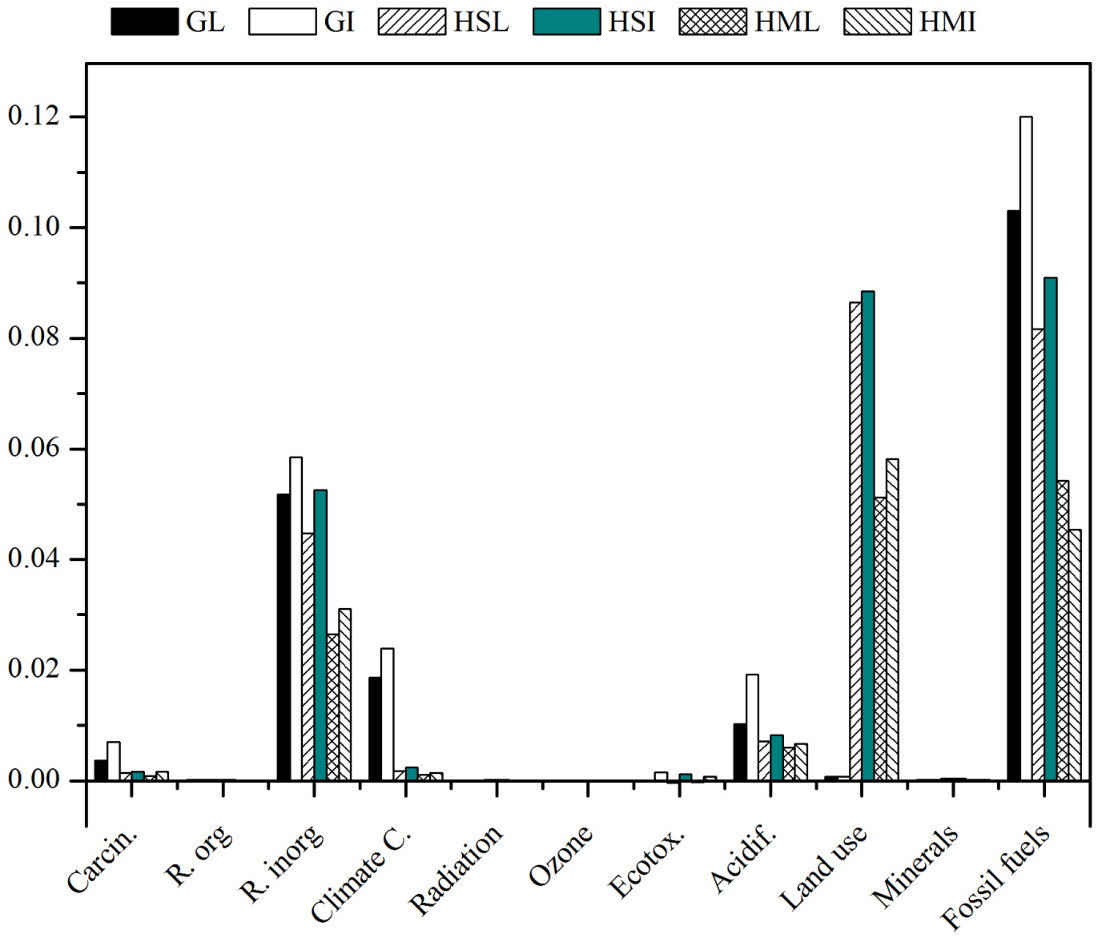

Figure 7.6: Graphical representation of the normalised effect score due to various combinations of composite use (for non-automotive applications) and disposal. The sequence of bars in each category is the same as the sequence of codes, mentioned above the figure, starting from left top (GL) and ending at bottom right (HMI).

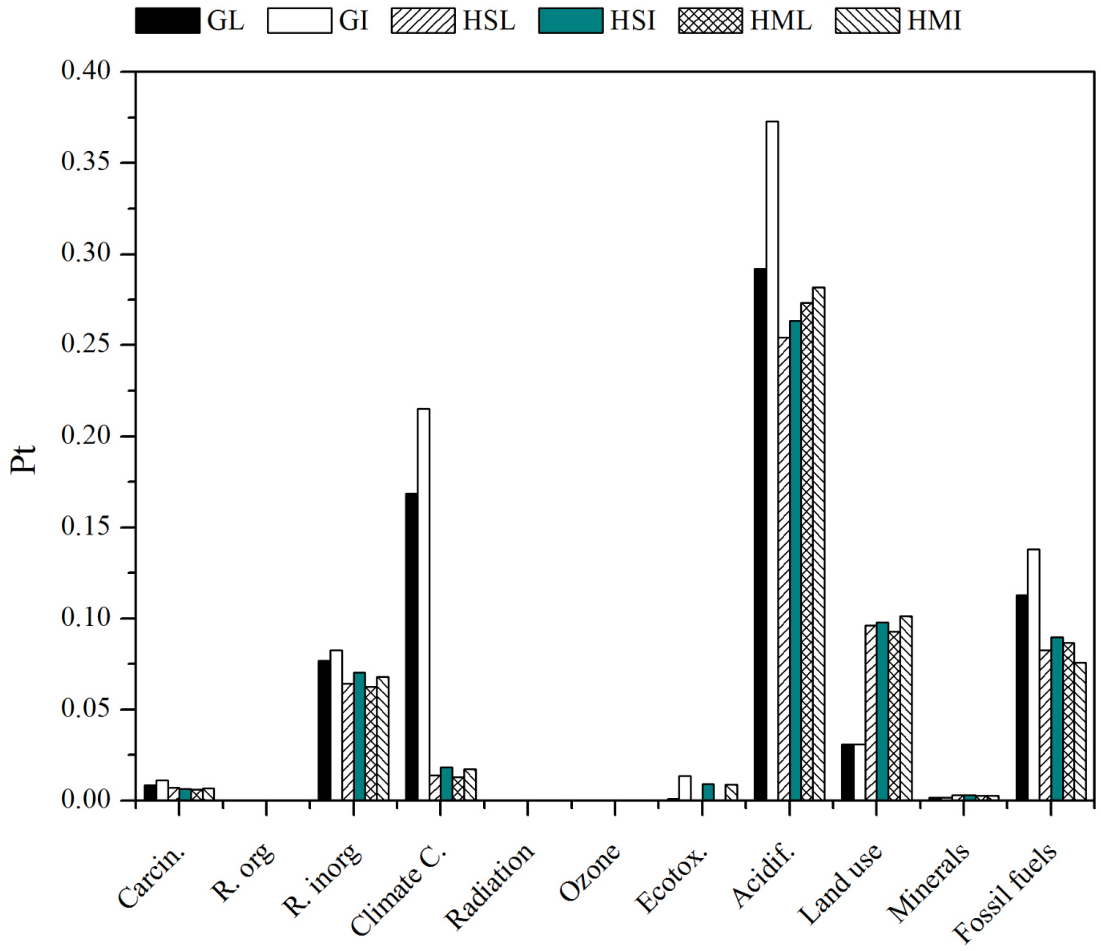

Figure 7.7: Graphical representation of the evaluated effect score due to various combinations of composite use (for non-automotive applications) and disposal. The sequence of bars in each category is the same as the sequence of codes, mentioned above the figure, starting from left top (GL) and ending at bottom right (HMI).

The evaluated impacts per category can be added together to give one indicator: the total interpretation of the environmental impact (Figure 7.8). From the indicator it can be seen that the environmental impact of H-SMC composite is lower than the reference G-SMC composite alternative. G-SMC composites have a much higher environmental impact on climate change, acidification and fossil fuels than H-SMC composites. In G-SMC case the environmental impact of the production of glass fibre is larger, as compared to H-SMC composite due to the

energy consumption needed for glass fibre production, therefore higher impact on fossil fuels. As expected H-SMC composite have a higher impact on land use than G-SMC composites. H-SMC composites also shown higher impact on ecotoxicity than G-SMC composites. The results show that disposal of composite through incineration is slightly more harmful to environment than compared to landfill (composite materials are assumed to be inert in this LCA study).

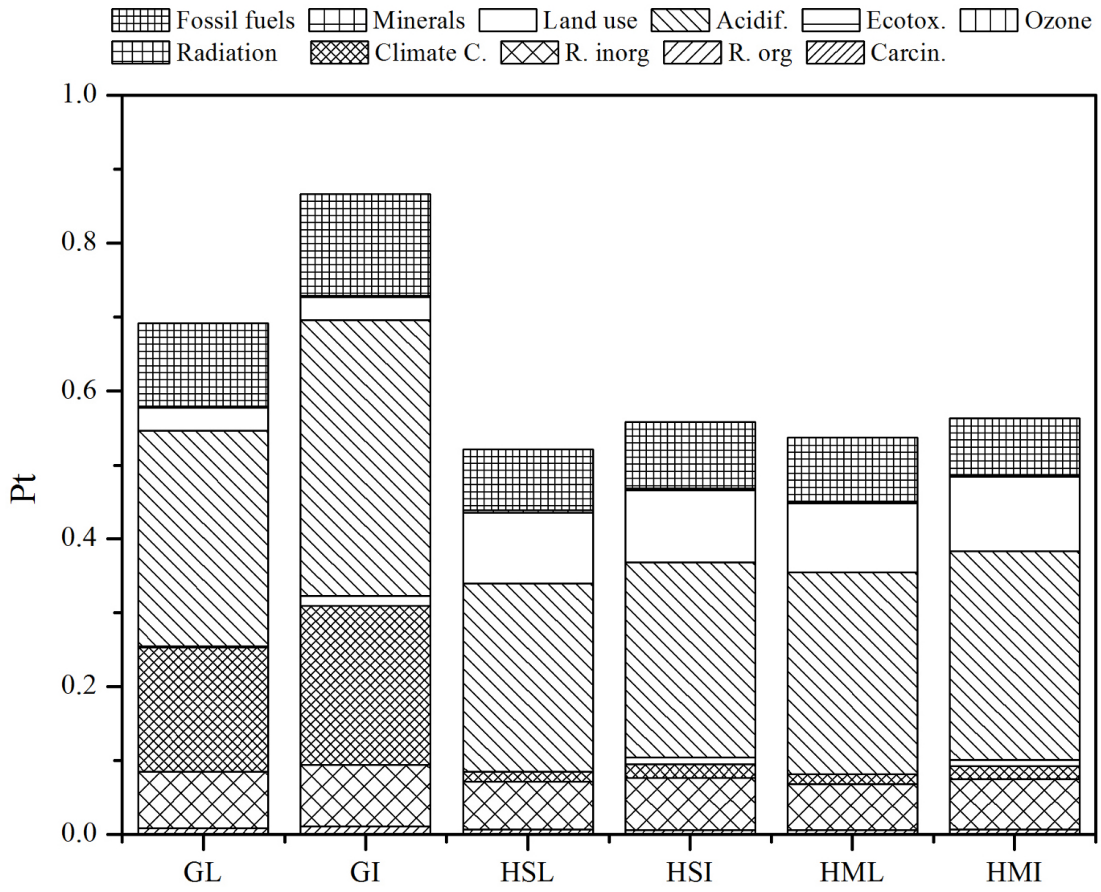

Figure 7.8: Graphical representation of the indicator obtained by summarising the evaluated numbers for non-automotive applications.

7.3.2 Automotive applications

Similar to non-automotive applications an LCA study was also conducted on automotive applications. For automotive applications the effect of extra/reduced

weight of composite product on fuel consumption and hence its effect of environment is also considered. Figure 7.9, 7.10 and 7.11 show the classification chart, normalised effect score and an evaluation chart, respectively.

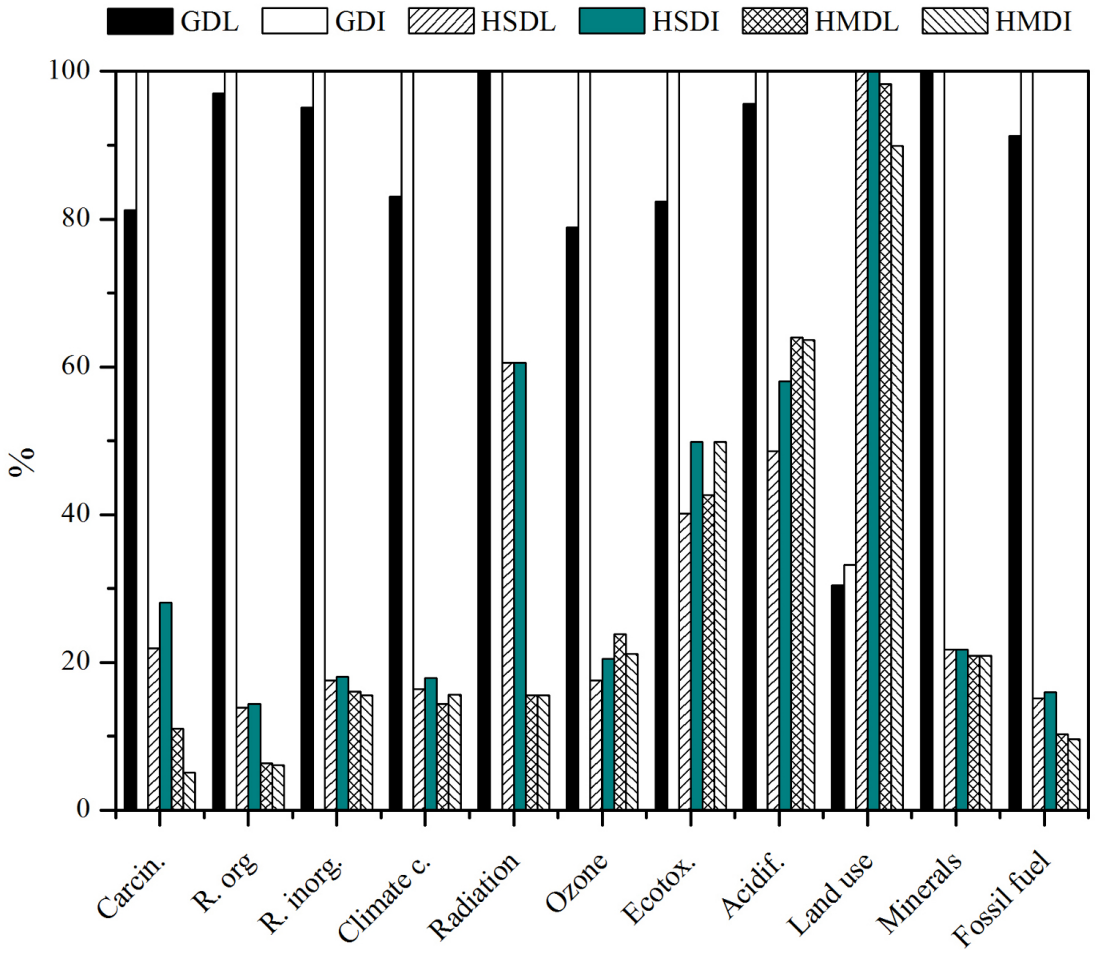

Figure 7.9: Graphical representation of the characterisation obtained by scaling the effects due to various combinations of composite use (for automotive applications) and disposal. The sequence of bars in each category is the same as the sequence of codes, mentioned above the figure, starting from left top (GDL) and ending at bottom right (HMDI).

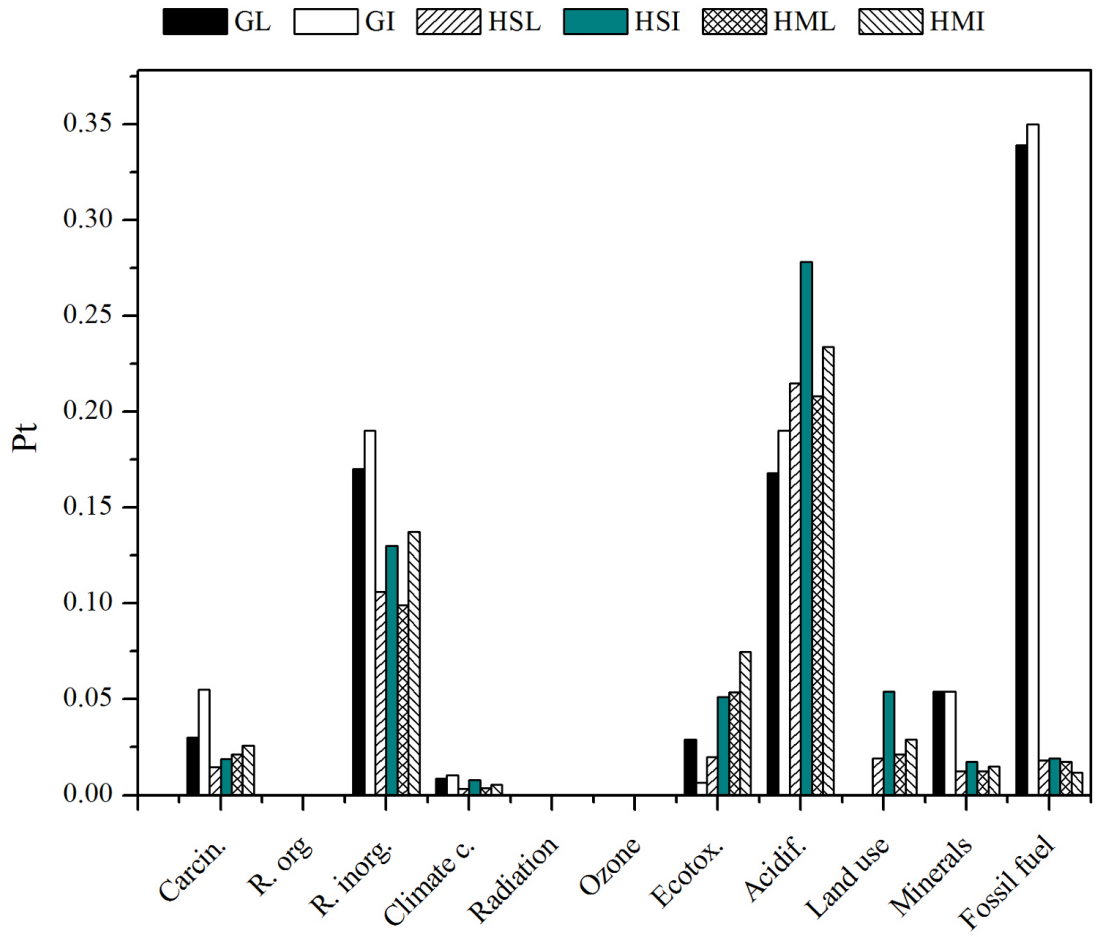

Figure 7.10: Graphical representation of the normalised effect score due to various combinations of composite use (for automotive applications) and disposal. The sequence of bars in each category is the same as the sequence of codes, mentioned above the figure, starting from left top (GDL) and ending at bottom right (HMDI).

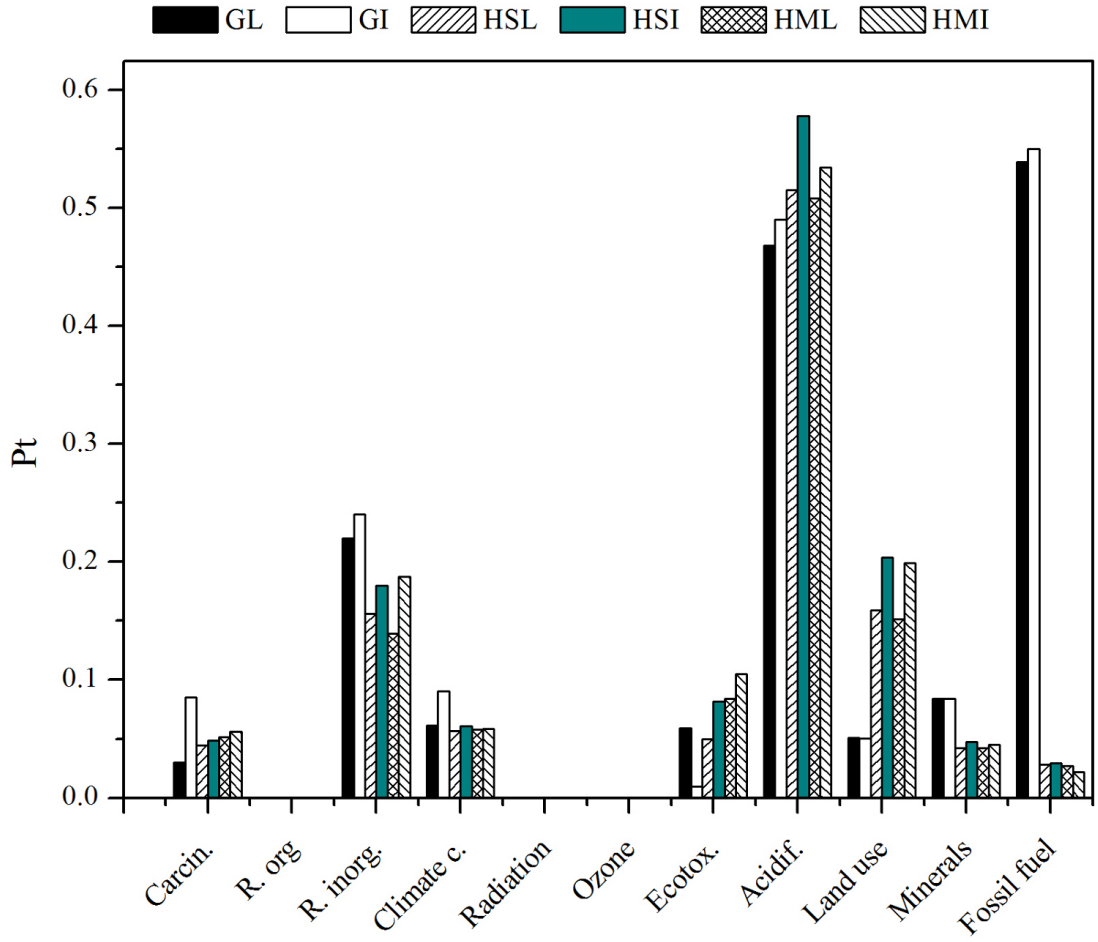

Figure 7.11: Graphical representation of the evaluated effect score due to various combinations of composite use (for automotive applications) and disposal. The sequence of bars in each category is the same as the sequence of codes, mentioned above the figure, starting from left top (GDL) and ending at bottom right (HMDI).

Figure 7.12 shows the graphical representation of the indicator obtained by summarising the evaluated numbers, for automotive applications. As seen from Figure 7.12, similar to non-automotive applications, the environmental impact of H-SMC composites is lower than G-SMC composites. Due to reduced fuel consumption, which is because of lower weight of H-SMC composites, these composites seem to be attractive for automotive applications than compared to G-SMC composites, as far as environmental impact is considered. Again like for non-

automotive application G-SMC composites have a much higher environmental impact on climate change, acidification and fossil fuels than H-SMC composites, where as H-SMC composites have a higher impact on land use and ecotoxicity than G-SMC composites.

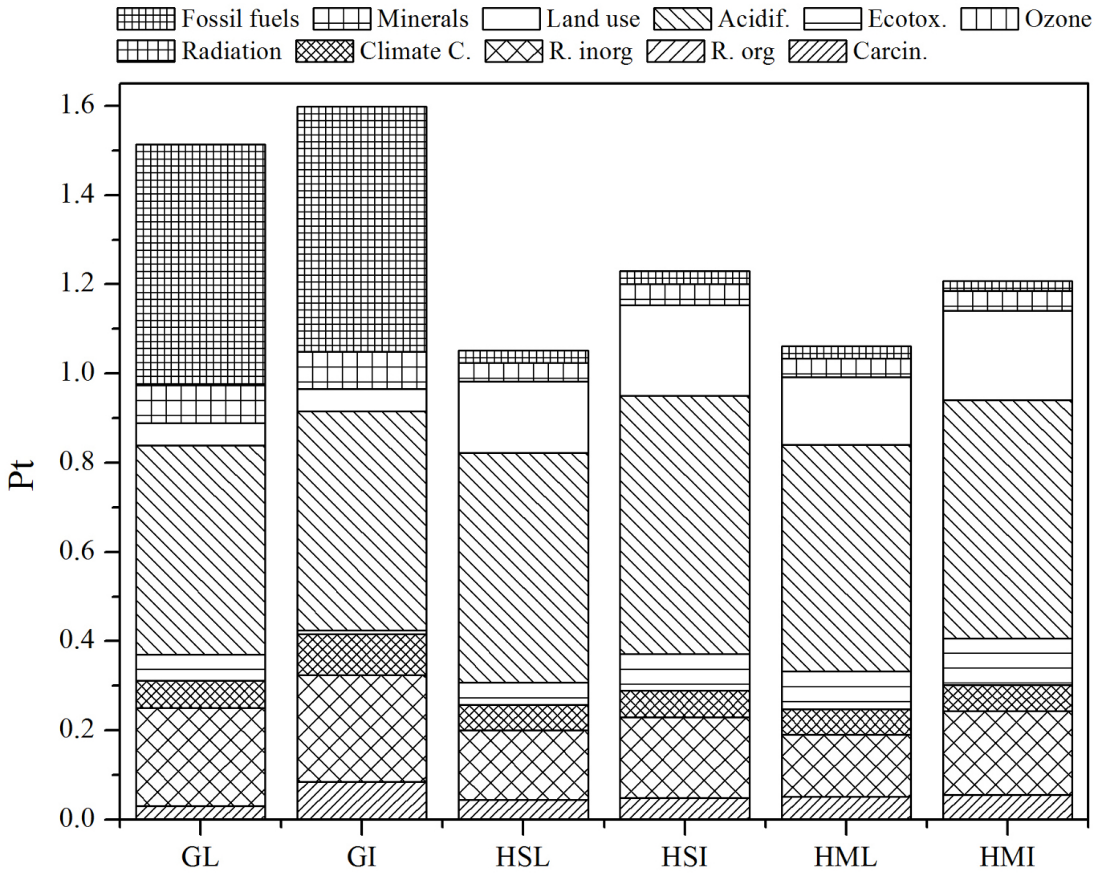

Figure 7.12: Graphical representation of the indicator obtained by summarising the evaluated numbers for automotive applications.

7.4 Conclusions

The goal of this LCA study was to compare the environmental impact of using natural fibres (H-SMC) instead of glass fibre (G-SMC) as reinforcement in polymer matrix composites, and to identify major environmental impact categories to which these two composites have most significant effect.

The environmental impact of H-SMC composite with conventional G-SMC composite for automotive and non-automotive applications was compared. The composites were assumed to be made in a traditional SMC manufacturing method. Two different types of performance requirements; i.e. stiffness and strength were investigated for both the non-automotive and automotive parts. Two different disposal scenarios: landfill and incineration of the SMC product at the end of life was considered.

The LCA results demonstrate that the environmental impact of H-SMC composites is low than the reference G-SMC composites. G-SMC composites have a significantly higher environmental impact on climate change, acidification and fossil fuels than H-SMC composites. Where as H-SMC composites have a much higher impact on land use and ecotoxicity than G-SMC composites.

This study presents an outline of a method which results in a relative indication of the environmental impact of a composite material, without performing an exhaustive LCA. The method can assist designers in making decisions regarding environmental aspects. It should be noted that the results of LCAs are never certain due to the inevitable complexity of the "environment". So the conclusion as to whether natural fibres are better or worse environmentally than glass fibres for use in composites may not be viewed in light of a single study but a series of studies like this one which use different sources of data.

Chapter 8

General Conclusions and Future Work

Glass fibres are by far the most extensively used fibre reinforcement in thermosetting composites because of their excellent cost-performance ratio. However, glass fibres have some disadvantages such as they are non-renewable and give problems with respect to ultimate disposal at the end of a materials lifetime since they cannot be completely thermally incinerated and leave behind a residue that can damage the incineration furnace. Additionally these fibres are very abrasive which leads to increased tool wear therefore increasing overall life-cycle cost. Furthermore, glass fibres pose some health and safety problems, like skin irritations during handling of these products. In light of all these environmental concerns, composite manufactures are turning their attention to more environmental friendly reinforcements such as plant fibres like flax, hemp, jute, kenaf and sisal.

This thesis has investigated the possibility of replacing glass fibres with natural (plant based) fibres as reinforcement in composite materials. In particular, hemp fibres were examined as potential alternatives to E-glass fibre in sheet moulding compounds (SMC). The composite materials were manufactured with existing SMC processing technique and similar resin formulation as used in the commercial industry. An attempt was made to enhance/optimise composite the mechanical properties of hemp/polyester composites by modifying the fibre-matrix interface via chemical modifications with alkaline and silane treatments. Influence of hemp fibre volume, calcium carbonate ($CaCO_3$) filler content and fibre-matrix

interface modification on the mechanical propertites of hemp-fibre-mat-reinforced sheet moulding compounds (H-SMC) were studied. The results of H-SMC composites were compared to conventional E-glass-fibre-reinforced sheet moulding compounds (G-SMC).

The novel contribution to knowledge that has been made in this thesis:

1. *Equations 4.2 and 4.4*: These equations have been developed and successful used to model the penetration energies of G-SMC and H-SMC composites under falling weight impact. The development of these models has given greater understanding of factors affecting the impact response of natural fibre reinforced composites such as: matrix and void contents.

2. *Effect of calcium carbonate $CaCO_3$ filler incorporation*: until know studies on natural fibre reinforced composites have focused on trying to characterise the fibre or its composites by varying factors such as fibre volume fraction. Additionally, most of these studies have been pure research based with no commercial aspect to them. In this study the incorporation of $CaCO_3$ filler content on the mechanical and economical (see Table 3.3) performance of H-SMC composites from a commercially viable point of view has been investigated.

3. Furthered a model developed for unidirectional natural fibre reinforced composites to predict mechanical properties of *random short-fibre-reinforced natural fibre reinforced composites*.

4. A detailed examination of the impact strength capability and post-impact damage tolerance of these new H-SMC composites through testing and theoretical analysis.

5. *Fracture toughness of H-SMC composites*: This is the first study to investigate the fracture toughness of natural fibre reinforced sheet moulding compounds in terms of K_{Ic} and critical strain energy release rate, G_{Ic}. Additionally, to examine the effect of $CaCO_3$ filler content and fibre surface treatment on these developed H-SMC composites.

The next section reviews the key findings in this thesis in more detail and the last section in this chapter presents future work directions.

8.1 Summary of results

SMC composites were successfully made using random hemp fibre mats and unsaturated polyester resin. Mechanical performance of these composites were studied using tensile testing, three different material parameters: fibre volume fraction, $CaCO_3$ filler content and interface modification through the use of alkaline and silane surface treatments were studied for the optimization of the mechanical performance. In order to better understand the performance of these H-SMC composites they were compared with glass fibre reinforced composites (G-SMC) manufactured in a similar manner. The experimental data of these H-SMC composites were compared with modified versions of "Cox-Krenchel" and "Kelly-Tyson" models which included the effect of composite porosity. A rather good agreement between these modified models and the experimental data was found for both composite tensile strength and stiffness. A significant effect of fibre volume fraction and $CaCO_3$ filler content on composite mechanical properties was found. The combination of alkaline and silane treatment on the hemp fibres resulted in a significant increase in mechanical properties.

The mechanical testing results demonstrate that the mechanical properties of H-SMC composites are comparable to G-SMC composites especially when considering the low density of hemp fibres compared to glass fibres. Additionally, potential cost savings associated with these H-SMC composites both in terms of raw materials and disposal after life-time make them a rather attractive alternative to glass fibre based SMCs.

Response of hemp fibre reinforced SMC composites to low velocity impact loading was investigated using a falling weight impact tester. Understanding of the impact response of the hemp fibre composites was obtained from the force-deflection curves generated by the impact events. It was found that both peak force and energy absorption by the specimens increased with increasing fibre volume up to a fibre volume 25% after which it decreased. Therefore the optimum

fibre volume fraction of hemp fibre composite for impact applications is about 25%. The failure of the specimens was dominated by weak inter-bundle failure or fibre-matrix adhesion, while also significant fibre pullout and matrix cracking was observed.

There was significant increase in the peak force and energy absorption with the addition of filler. The optimum filler content was found to be around 23% with energy absorption of 4.51 J. At a higher filler content of 45% the peak force and energy absorption decreased due to insufficient resin for fibre wetting. The deformation of the specimens was found to increase with increasing filler content. The specimens with 45% filler content were not completely penetrated by the impactor. The addition of $CaCO_3$ filler was found to improve the stability of the composite by filling the voids which occur in the unfilled specimens. Again failure of the specimens was observed to be by fibre pullout and matrix cracking.

The impact testing results demonstrate that there is a small increase in energy absorption of specimens treated with both alkaline and silane. There is also an increase in the peak force noticed for the treated specimens. A decrease in the deformation of 2.3 and 1.5 mm was noticed for alkaline and silane treated specimens. Unlike the untreated specimens which were penetrated the specimens treated with alkaline and silane were not completely penetrated. Both treatments resulted in improved fibre-matrix adhesion. A change in failure modes was noticed for the treated composites as compared to the untreated composites. The predominant failure mechanism of the treated composites was by fibre failure resulting from tearing and splitting, while also matrix cracking was notice. However considerably less fibre pullout was observed.

The influence of impact energy, fibre volume fraction and fibre surface treatment on the post-impact flexural properties of hemp fibre reinforced composites (H-SMC) was investigated. Damage was induced in the mid-section of the simply supported specimens by a falling weight impact tester. The reduction of the flexural residual strength was evaluated by quasi-static three-point bending tests. An increase in energy absorption with increasing fibre volume fraction was noticed for H-SMC composites particular at higher impact energies. G-SMC composites absorbed significantly more energy at similar impact energy than H-SMC composites. The visual damage area was observed to increase with increasing impact

energy levels.

The residual flexural strength of H-SMC composites was found to decrease linearly with increasing impact energy levels. At higher impact energy levels, the damage tolerance of H-SMC composites increased with increasing fibre volume fraction, as the reduction in residual strength significantly decreased at higher fibre volume fractions. Damage tolerance capability of G-SMC was calculated to be approximately twice that of H-SMC composites. The residual modulus also decreased in a linear trend with increasing impact energy levels. Post-impact flexural property testing shows that flexural strength of H-SMC and G-SMC composites is more sensitive to the localised impact damage than flexural modulus.

A slight increase in energy absorption was found for H-SMC composites incorporating surface treated hemp fibres. However, there was no increase in damage area noticed on the fracture surfaces of the composites incorporating treated fibres compared to composites based on the untreated fibres. H-SMC composites incorporating surface treated hemp fibres also showed improved damage tolerance, particularly composites based on hemp fibre treated with a combination of alkaline and silane treatments. There was no significant difference noticed in residual flexural properties of H-SMC composites incorporating surface treated and untreated hemp fibres.

The fracture toughness of hemp fibre mat reinforced sheet moulding compound (H-SMC) in terms of the critical-stress-intensity factor, K_{Ic} and critical strain energy release rate, G_{Ic} were investigated. Fundamental understanding of the fracture toughness of H-SMC composites was obtained through the analysis of typical load-displacement curves. It was shown that fracture toughness of H-SMC composites is significantly lower than that of glass fibre reinforced composites (G-SMC). The influence of hemp fibre volume fraction on H-SMC composites show a peak in fracture toughness properties at a fibre content of about 30 vol.%. At extreme high and low fibre volume fractions the fracture toughness properties of the H-SMC composites is low due to possibly the presence of high level of porosity and poor fibre wetting. It is noticed that the fracture toughness properties of H-SMC composites are sensitive to the incorporation of the $CaCO_3$ filler. A optimum value of K_{Ic} and G_{Ic} was obtained at a $CaCO_3$ filler content of 18 vol.%.

Improvement in K_{Ic} and G_{Ic} for H-SMC composites was obtained for composites treated with both alkaline and silane treated hemp fibre mats. However, the most significant increase in fracture toughness properties of H-SMC composites was obtained by combination of alkaline and silane treatments.

The fracture toughness results show that with the optimal combination of fibre volume fraction, $CaCO_3$ filler and fibre surface treatment can result in H-SMC composites that have fracture toughness properties that can be exploited for low to medium range engineering applications.

LCA methodology was used to compare the environmental impact of hemp fibre reinforced composites (H-SMC) with conventional glass fibre reinforced composite (G-SMC) for automotive and non-automotive applications. The composites were assumed to be made in a traditional SMC manufacturing method. Two different types of performance requirements; i.e. stiffness and strength were investigated for both the non-automotive and automotive parts. Two different disposal scenarios: landfill and incineration of the SMC product at the end of life was considered.

The LCA results demonstrate that the environmental impact of H-SMC composites is low than the reference G-SMC composites. G-SMC composites have a significantly higher environmental impact on climate change, acidification and fossil fuels than H-SMC composites. Where as H-SMC composites have a much higher impact on land use and ecotoxicity than G-SMC composites.

The LCA study presented an outline of a method which results in a relative indication of the environmental impact of a composite material, without performing an exhaustive LCA. The method can assist designers in making decisions regarding environmental aspects. It should be noted that the results of LCAs are never certain due to the inevitable complexity of the "environment". So the conclusion as to whether natural fibres are better or worse environmentally than glass fibres for use in composites may not be viewed in light of a single study but a series of studies like this one which use different sources of data.

8.2 Direction for future work

One of the major factors noticed in this current study is that natural fibre reinforced composites tend to have higher porosity content particularly at higher fibre volume fractions compared to glass fibre reinforced composites. This is because plant fibres have an inherent central void called the lumen. The increased porosity content leads to decrease in mechanical properties of the composites. It would be beneficial to look at ways of reducing the porosity content in these composites which could probably improve the mechanical performance of natural fibre reinforced composites further.

The majority of this work focused on random fibre orientated non-woven hemp fibre mats to produce SMC composites. For low strength applications such as false panelling and upholstery non-woven mats provide reasonably acceptable mechanical properties. However, for highly loaded engineering applications composites with non-woven natural fibre mats are not suitable due to their limited mechanical properties caused mainly by short fibre lengths and orientation. It would be advantageous to extend the SMC technology to include textiles based on natural fibres. If the cost of manufacturing woven fabrics based on natural fibres could be reduced further then it would be possible to use them as reinforcement in SMC composites. This would provide natural fibre reinforced composites with superior mechanical properties than non-woven mat reinforced SMC composites and hence the application area of natural fibre reinforced composites would be considerably expand.

Unsaturated polyester resin was used as the matrix for the H-SMC composites manufactured in this study. Polyester resins are produced from petroleum based chemical and are therefore a non-renewable resource also composites based on polyester polymer cannot be recycled like thermoplastic polymer based composites. It would be interesting to use a natural resin based on renewable resources such as soybean oil polymers [Lu & Wool, 2001] or cashew nut shell liquid polymers [Mwaikambo & Ansell, 2003] and also rice husk as replacement for $CaCO_3$ [Thanoslip *et al.*, 2007] which would truly allow a "fully natural and renewable" composites to be produced. Further research needs to develop matrices that are natural or renewable and provide good mechanical properties and durability as

well.

Although natural fibres have some ecological advantages over glass fibres they also possess some disadvantages. Natural fibres can easily compete with glass fibres in terms of specific stiffness. However, the tensile strength and impact strength of natural fibre composites are relatively low compared to glass fibre composites. At this moment much research has focused on the interfacial bond strength by trying to modify the fibre surface with physical, chemical or other treatments as a way to improve the properties of natural fibre composites. These interface modification schemes often follow schemes similar to the ones used in the past for glass fibre. However, unlike isotropic glass fibres natural fibres exhibit an anisotropic hierarchical composite-like structure. Figure 8.1 shows the cross-sectional view of flax fibre bundle. Natural fibre mats are made of such fibre bundles (technical fibres) which consist of many smaller elementary fibres glued together by a pectin interface. Surface treatments only modify the fibre bundle surface and not the interface between the elementary fibres within the fibre bundle. The failure of the composite is therefore expected to not only initiate at the fibre-matrix interface but also at the elementary fibre-pectin interface within the fibre bundle. Cracks will propagate not only through the fibre-matrix interface, but also through the interface between the elementary fibres with the technical fibres. Therefore further optimisation of the fibre-matrix interface will have limited influence on the composite mechanical properties. Findings ways to improve the interfaces within the elementary fibres may turn out to be more important for bridging the (impact strength) gap with glass fibre systems than finding ways to improve the interface with the between the technical fibres and the matrix.

Figure 8.1: The cross-sectional view of flax fibre showing around 7 fibre cells together forming a technical flax fibre (fibre bundle)(Source: [Garkhail, 2001]).

Appendix A: Fibre surface treatment

Alkaline treatment

First the hemp fibre mats were cut into a size of 300 × 300 mm^2 and dried in an oven at 50°C for 24 hours. The fibre mats were then immersed in sodium hydroxide (NaOH) solution of 0.5, 1, 2, 3, 4 and 5 wt.% for 1 hour. The concentrations were ensured by the addition of distilled water at certain percentages of the NaOH pellets as shown in Table 3. The fibre mats were then washed three times with distilled water containing 0.5 wt.% of hydrochloric acid to remove any remaining NaOH on the fibre surface. The washed fibre mats were then dried at 80°C for 5 hours. The dried fibre mats were then stored in a sealed plastic bag for use.

Table 1: Formulation of different concentrations of alkaline treatment.

NaOH, ml	Distilled water, ml	NaOH, wt.%
0.5	99.5	0.5
1	99	1
2	98	2
3	97	3
4	96	4
5	95	5

Silane treatment

First the hemp fibre mats were cut into a size of 300 × 300 mm^2 and dried in an oven at 50°C for 24 hours. The fibre mats were then immersed in acetoxysilane solution of 0.5, 1, 2, 3, 4 and 5 wt.% for 1 hour. The silane concentrations were ensured by dissolving silane in a water/acetone mixture (5:95 wt.%) as shown in Table **??**. The fibre mats were removed from the solution and left to drain the excess solution for 5 min. The washed fibre mats were then dried at 80°C for 5 hours. The dried fibre mats were then stored in a sealed plastic bag for use.

Table 2: Formulation of different concentrations of silane treatment.

Silane, ml	Distilled water: acetone mixture, ml	Silane, wt.%
0.5	99.5	0.5
1	99	1
2	98	2
3	97	3
4	96	4
5	95	5

Alklaine-Silane treatment

Hemp fibre mats of dimensions 300 × 300 mm^2 was first dried in an oven at 50°C for 24 hours. The fibre mats were then immersed in sodium hydroxide (NaOH) solution of 2 wt.% for 1 hour. The fibre mats were then washed three times with distilled water containing 0.5 wt.% of hydrochloric acid. The washed fibre mats were then dried at 80°C for 5 hours. The fibre mats were then immersed in a water/acetone mixture (5:95 wt.%) containing acetoxysilane solution of 0.5, 1, 2, 3, 4 and 5 wt.% for 1 hour. The fibre mats were removed from the solution and left to drain the excess solution for 5 minutes. The washed fibre mats were then dried at 80°C for 5 hours. The dried fibre mats were then stored in a sealed plastic bag for use.

Appendix B: Fibre volume fraction

Fibre volume fraction was calculated by:

$$V_f = \frac{\rho_m \times W_f}{(\rho_f \times W_m) + (\rho_m \times W_f)} \tag{1}$$

where ρ_m is density of matrix (1.2 g/cm^3), ρ_f is density of fibres (1.5 g/cm^3), W_m is weight of matrix and W_f is the weight of fibres which is calculated by:

$$W_f = W_c - W_m \tag{2}$$

where W_c is the weight of the composite sheet which was simply measured. The weight of the matrix (W_m) was calculated by:

$$W_m = [(D_g \times C_A) \times 2] \times 2 \tag{3}$$

where D_g is the doctor blade gap, C_A is the area of the composite plate (250 mm $\times$ 250 mm). It is multiplied by two because the resin paste is deposited in two layers on the top and bottom of the hemp fibre mat during SMC processing. It is further multiplied by two because two prepreg sheets were used to make one composite plate.

Appendix C: Hemp fibre properties

Table 3: Tensile strength and modulus values quoted in the literature.

Authors	Tensile strength, MPa	Tensile modulus, GPa
Li *et al.* [2009]	660 ± 83	24 ± 0.85
Placet *et al.* [2012]	636 ± 253	24.7 ± 11.4
Beckermann & Pickering [2008]	514 ± 274	24.8 ± 16.3
Li *et al.* [2006]	900	34
Symington *et al.* [2009]	650 ± 350	64 ± 55.5
Eichhorn & Young [2004]	270 ± 40	19.1 ± 4.3
Ku *et al.* [2011]	690	70
Ali [2012]	690	-
Bodros & Baley [2008]	389 - 900	35

Appendix D: K fitting parameter

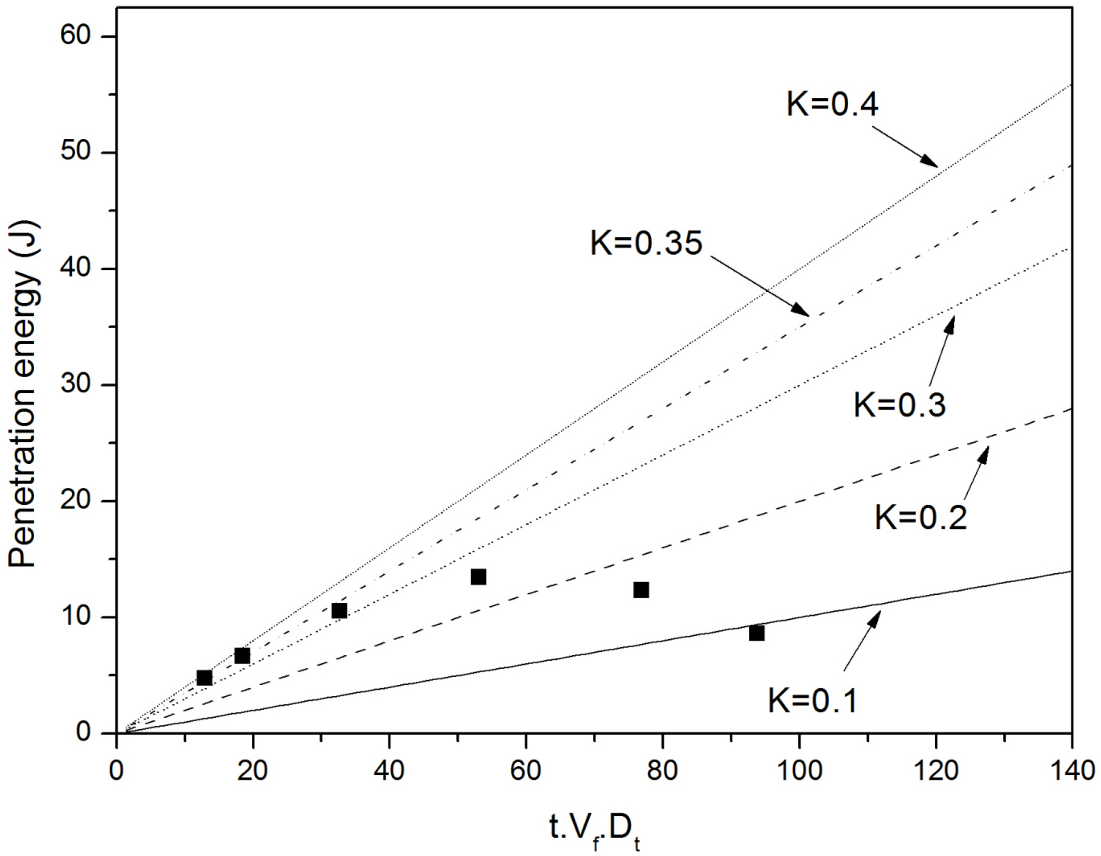

Figure 2: Different K fitting parameters for H-SMC composites.

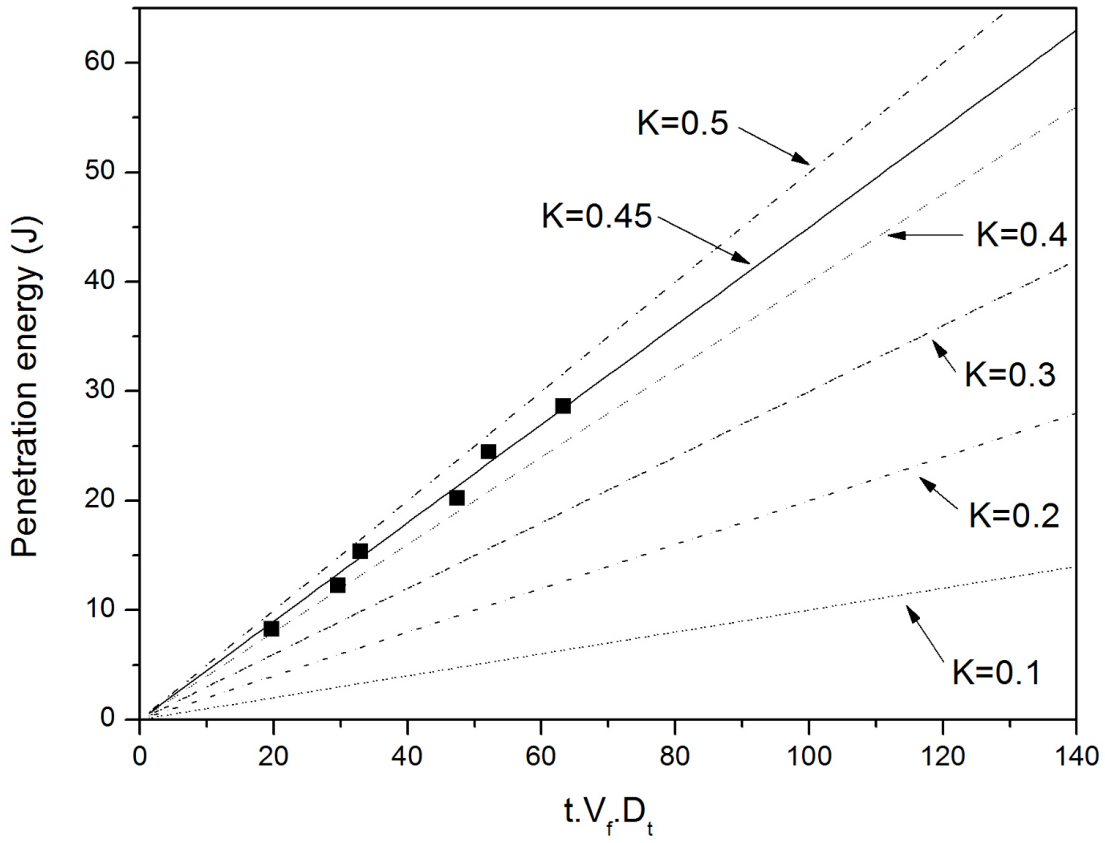

Figure 3: Different K fitting parameters for G-SMC composites.

Appendix E: Weight of H-SMC and G-SMC for tensile strength and modulus

Composite panel having dimensions of 0.35 cm × 25 cm × 25 cm were manufactured.
Therefore the volume of the composite panel is:

$$0.35 \times 25 \times 25 = 218.75 \text{ cm}^3$$

G-SMC tensile strength criterion

Glass fibre volume fraction (V_f) = 0.048
Polyester matrix volume fraction (V_m) = 0.952

Therefore volume of glass fibre is:

$$218.75 \times 0.048 = 10.5 \text{ cm}^3$$

and volume of polyester matrix is:

$$218.75 \times 0.952 = 208.25 \text{ cm}^3$$

Therefore weight of glass fibre is:

$10.5 \times 2.5 = 26.25$ g

and weight of polyester natrix is:

$208.25 \times 1.2 = 249.9$ g

where 2.5 g/cm^3 and 1.2 g/cm^3 are density of glass fibre and polyester resin.

Hence weight of G-SMC composite is:

$26.25 + 249.9 = 276.15$ g

H-SMC tensile strength criterion

Hemp fibre volume fraction (V_f) = 0.19
Polyester matrix volume fraction (V_m) = 0.81

Therefore volume of hemp fibre is:

$218.75 \times 0.19 = 41.56$ cm^3

and volume of polyester matrix is:

$218.75 \times 0.81 = 177.19$ cm^3

Therefore weight of hemp fibre is:

$41.56 \times 1.5 = 62.34$ g

and weight of polyester natrix is:

$177.19 \times 1.2 = 212.628$ g

where 1.5 g/cm^3 and 1.2 g/cm^3 are density of hemp fibre and polyester resin.

Hence weight of H-SMC composite is:

$62.34 + 212.628 = 274.968$ g

To compare the LCA of both the composites, 1 kg of G-SMC is used as the reference materials. The equivalent weight for H-SMC composite is:

$(1/276.15) \times 274.968 = 995.71$ g

G-SMC stiffness criterion

Glass fibre volume fraction (V_f) = 0.11
Polyester matrix volume fraction (V_m) = 0.89

Therefore volume of glass fibre is:

$218.75 \times 0.11 = 24.063$ cm^3

and volume of polyester matrix is:

$218.75 \times 0.89 = 194.688$ cm^3

Therefore weight of glass fibre is:

$24.063 \times 2.5 = 60.156$ g

and weight of polyester natrix is:

$194.688 \times 1.2 = 233.625$ g

where 2.5 g/cm^3 and 1.2 g/cm^3 are density of glass fibre and polyester resin.

Hence weight of G-SMC composite is:

$60.156 + 233.625 = 293.781$ g

H-SMC stiffness criterion

Hemp fibre volume fraction (V_f) = 0.22
Polyester matrix volume fraction (V_m) = 0.78

Therefore volume of hemp fibre is:

$218.75 \times 0.22 = 48.125$ cm^3

and volume of polyester matrix is:

$218.75 \times 0.78 = 170.625$ cm^3

Therefore weight of hemp fibre is:

$48.125 \times 1.5 = 72.188$ g

and weight of polyester natrix is:

$170.625 \times 1.2 = 204.750$ g

where 1.5 g/cm^3 and 1.2 g/cm^3 are density of hemp fibre and polyester resin.

Hence weight of H-SMC composite is:

$72.188 + 204.750 = 276.938$ g

To compare the LCA of both the composites, 1 kg of G-SMC is used as the reference materials. The equivalent weight for H-SMC composite is:

$(1/293.781) \times 276.938 = 0.943$ g

Appendix F: Values for classification chart

Table 4: Classification scores for non-automotive applications

	GL	GI	HSL	HSI	HML	HMI
Carcin.	3.40E-08	3.25E-08	1.13E-08	1.06E-08	5.68E-09	1.05E-08
R. org	1.96E-08	1.46E-08	6.80E-09	7.18E-09	4.72E-09	4.31E-09
R. inorg.	4.85E-06	3.44E-06	1.76E-06	2.08E-06	1.46E-06	1.20E-06
Climate c.	1.75E-06	1.56E-06	7.06E-07	4.77E-07	3.11E-07	4.16E-07
Radiation	5.27E-10	2.61E-10	2.30E-10	2.53E-10	1.56E-10	2.01E-10
Ozone	3.09E-11	3.14E-11	9.42E-13	2.90E-12	2.34E-12	2.98E-12
Ecotox.	4.02E-02	4.98E-02	1.65E-03	4.14E-03	1.41E-03	4.19E-03
Acidif.	1.72E-01	9.46E-02	2.33E-02	2.42E-02	4.65E-02	5.07E-02
Land use	1.53E-02	6.88E-03	6.34E-01	6.80E-01	4.15E-01	4.42E-01
Minerals	1.05E-02	9.73E-03	1.69E-03	8.43E-04	3.74E-03	3.75E-03
Fossil fuel	5.60E+00	5.37E+00	8.66E-01	9.88E-01	9.26E-01	1.11E+00

Table 5: Classification scores for automotive applications

	GDL	GDI	HSDL	HSDI	HMDL	HMDI
Carcin.	6.40E-07	7.88E-07	1.72E-07	2.21E-07	8.70E-08	4.04E-08
R. org	1.31E-07	1.35E-07	1.88E-08	1.94E-08	8.54E-09	8.18E-09
R. inorg.	6.63E-05	6.97E-05	1.23E-05	1.26E-05	1.12E-05	1.09E-05
Climate c.	1.32E-05	1.59E-05	2.60E-06	2.84E-06	2.29E-06	2.49E-06
Radiation	1.72E-08	1.72E-08	1.04E-08	1.04E-08	2.68E-09	2.68E-09
Ozone	2.98E-09	3.78E-09	6.64E-10	7.74E-10	9.00E-10	7.98E-10
Ecotox.	2.39E-01	2.90E-01	1.16E-01	1.44E-01	1.24E-01	1.45E-01
Acidif.	2.40E+00	2.51E+00	1.22E+00	1.46E+00	1.61E+00	1.60E+00
Land use	2.24E-01	2.44E-01	7.36E-01	7.36E-01	7.23E-01	6.61E-01
Minerals	3.22E-01	3.22E-01	6.99E-02	6.99E-02	6.74E-02	6.74E-02
Fossil fuel	4.99E+01	5.47E+01	8.27E+00	8.73E+00	5.63E+00	5.23E+00

Appendix G: Economic feasibility of NFCs composites

Introduction

Previous chapters in this thesis focused on creating enhanced performance and high-value composite materials by using natural fibres as reinforcements. However, it is also important to ask the question "what is the future for these natural fibre reinforced composites?" To shed some light on this question, in this chapter first an analysis of the natural fibre industry in Western Europe is made, to understand the economic situation in regard to producing large quantities of natural fibre for technical applications. Next, the market share of different production methods and matrix type used for producing natural fibre composites (NFCs) is reviewed to understand where new opportunities for NFCs lies. Finally, an attempt is made to analyse the possible factors that might affect a product or material made from natural fibre composites entering a market. For this Porter's five forces marketing model is used to discuss the possible strategies required to enter the market place. The focus of this thesis is on hemp fibres, however, where literature is not available for hemp fibre, data based on other natural fibres is used. Furthermore, some of the data used in this chapter is based on studies carried out by the Nova-Institute GmbH, Furth, Germany.

Hemp cultivation in the EU

Figure 4 and Table 6 shows the cultivation area of hemp on land with EU aid. In most EU countries the cultivation on other land is small. It should be noted

that in Sweden hemp is grown in 512 ha of land with no EU state aid for mainly energy purpose and therefore is not shown in Figure 4 or Table 6. From 1999 to 2006 several hemp fibre extraction businesses failed due to technical problems and the economic challenges of the market (especially as the EU Commission significantly lowered the aid in this period), while other producers mastered the technical problems and maintained their production levels and even expanded.

From 2001-2006 the hemp production areas were largely stabilised in important producers in The Netherlands and Germany. Due to the growing interest in natural fibre materials and natural fibre insulation, the price of exotic natural fibres, the emergence of new hemp production industries in the Czech Republic, Poland and other Eastern European countries and also new investment in Britain, France and Germany the production area is expected to increase from 15,000 ha at present to 20,000 ha in the next few years.

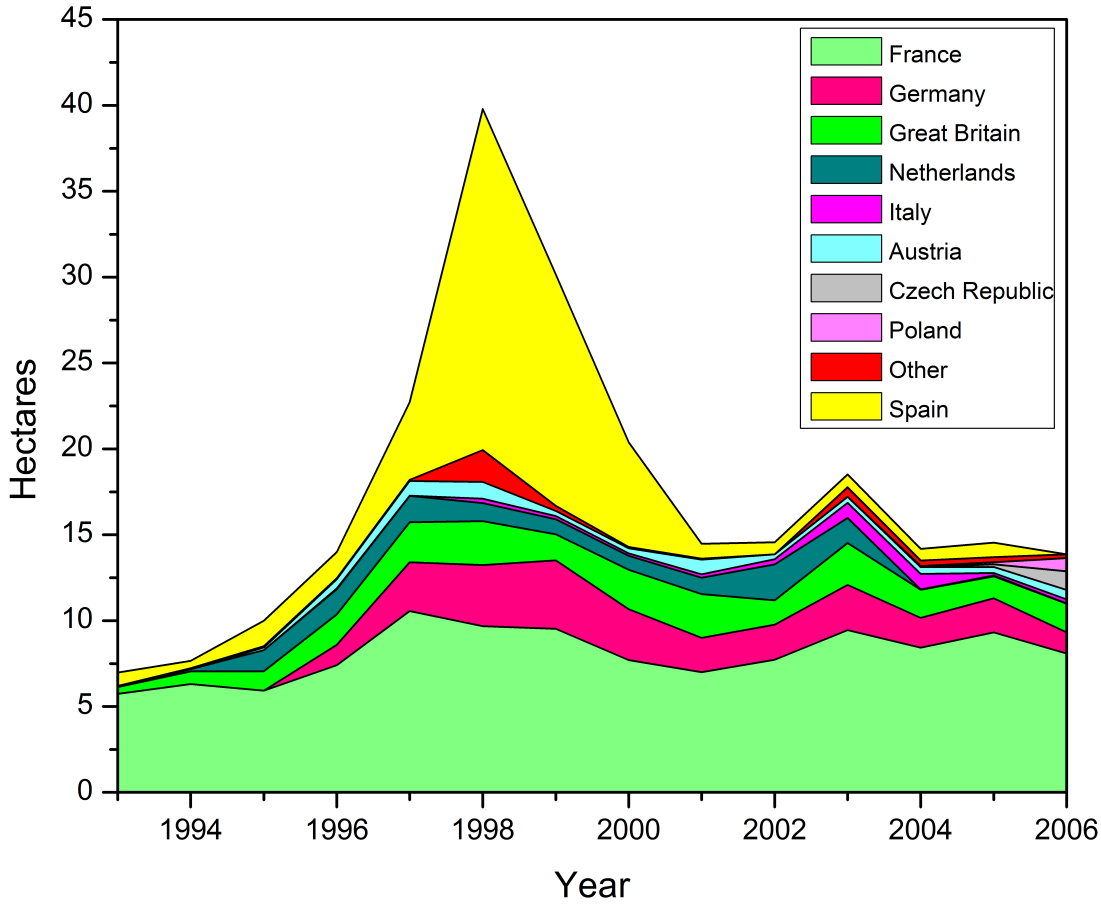

Figure 4: Annual cultivation rate of hemp on EU land since 1993. Source: Carus *et al.* [2008].

Table 6: Annual cultivation rate of hemp on EU land since 1998 (values in hactares). Source: Carus *et al.* [2008].

	1998	1999	2000	2001	2002	2003	2004	2005	2006
Denmark	26	23	7	7	0	5	0	0	1
Germany	3.553	3.993	2.967	1.993	2.035	2.628	1.730	1.985	1.233
Finland	1.218	93	75	116	39	10	6	0	75
France	9.682	9.515	7.700	7.000	7.729	9.452	8.427	9.315	8.083
G.B	2.556	1.517	2.298	2.556	1.413	2.438	1.640	1.274	1.671
Ireland	28	22	5	1	-	0	0	0	0
Italy	255	197	151	200	300	872	885	157	236
Luxemburg	13	-	-	-	-	0	0	0	-
Holland	1.055	872	806	946	2.100	1.470	27	49	16
Austria	974	289	287	860	277	352	397	342	546
Poland	-	-	-	-	-	-	81	129	762
Portugal	770	185	5	0	-	0	0	0	0
Sweden	-	-	-	-	-	30	147	-	-
Spain	19.860	13.473	6.103	850	691	744	678	853	3
Czech Republic	-	-	-	-	-	-	0	156	1.086
Hungary	-	-	-	-	-	-	539	277	198
EU	39.990	30.179	20.404	14.529	14.584	18.001	14.557	14.538	13.911

Production volumes and markets for hemp

The older and younger hemp industry in the EU has very different markets. For decades the older French hemp fibre was used to produce short fibres for speciality papers, in particular cigarette papers. The fibres were extracted with hammer mills which caused fibre damage, therefore application outside the pulp and paper industry was very limited. Table 7 shows the use of hemp for "specialty papers" in the EU was almost 83%. Ten years ago, before the new hemp industry started the proportion was even higher then 95% mainly due to the dominance of French hemp industry.

Table 7: Quantities, prices and sales of hemp fibres in the EU for year 2003.

Hemp	Volume (ton)	Price (€/ton)	Turnover (million, €)	Revenue share (%)
Fibres for specialty paper	20.706	371	7.7	82.8
Fibre for nonwovens and felts	824	500	0.4	4.3
Fibre for composite materials (mostly automotive industry)	2.470	500	1.2	12.9
Total	**24.000**	**-**	**9.3**	**100**

In recent years, the younger industries from Britain, The Netherlands and Germany have applied hemp fibre in new applications, especially composites for the automotive industry. An interesting and fairly young market for hemp application is insulation. In Germany the launch of the Program Agency Renewable Resources Association (FNR) in 2005 heavily promoted use of hemp fibre for insulation. Britain and France are currently very committed to introducing hemp fibres as insulation meaning this market has enormous potential. Currently the prices for short-hemp fibres are 0.55 to 0.60 €/kg, well above the prices for speciality paper quality.

Figure 5 show that the area and hence production quantities of raw hemp has changed little in the last five years. The symmetric correlation between cultivation and production can be explained by the fact that hemp can be stored several years without any problem. The slight decline in the last three years was due to the closure of a Dutch hemp pioneering industry.

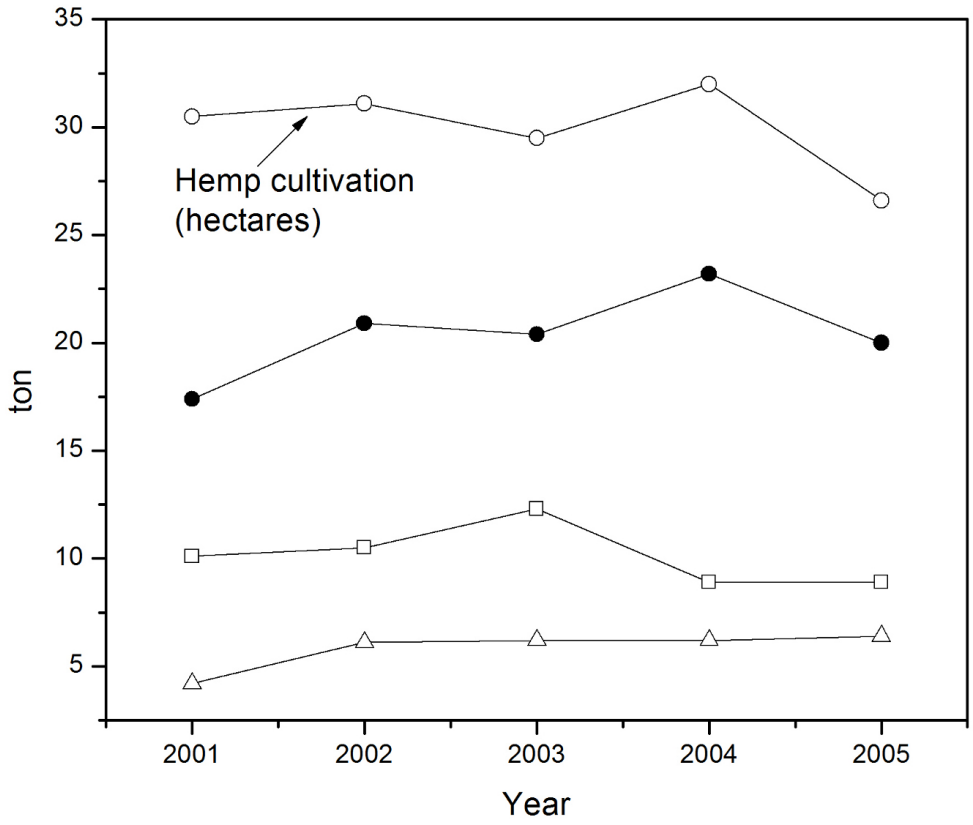

Figure 5: Arable land and raw materials production of EIHA (European Industrial Hemp Association) members. (○) hemp cultivation in hectares, (●) fibre production in ton, (□) scrap production in ton and (△) joint production.

Figure 6 shows that the application of hemp is dominated by the speciality paper industry in France and Spain. In recent years, the new applications for hemp have been developed like composites and insulation. At the beginning the main application for this new hemp industry was the automotive market for composites. However, since 2003 the insulation market has grown steadily and has now overtaken the composite market value.

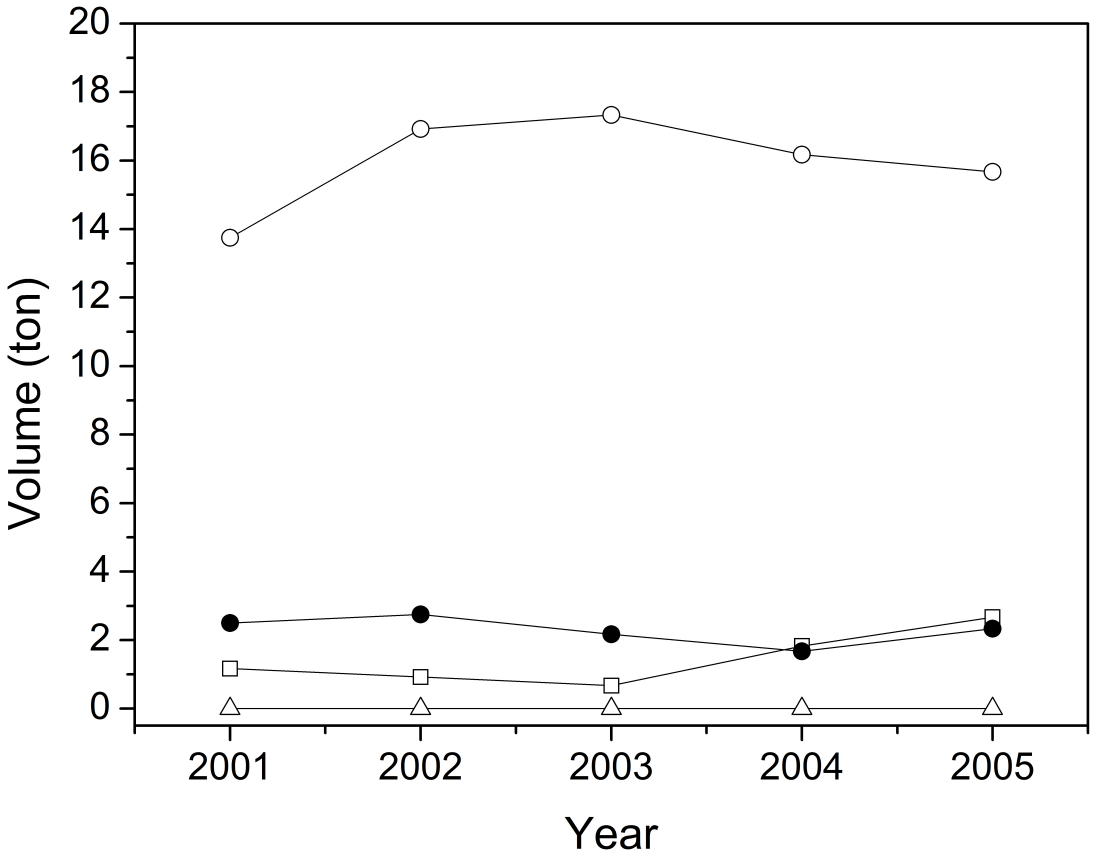

Figure 6: Outlets for hemp members of EIHA. (○) pulp and paper, (□) construction and insulation materials, (●) composites (mainly automotive sector), and (△) other applications.

Figure 7 shows the quantities and areas of application of hemp for all European hemp production in 2006. As a general estimate about 22,000-24,000 tons of hemp was produced in the EU in 2006. The pulp sector still dominates (66%) while its relative importance has been declining, with the steadily growing insulation sector making up about 20%. The composite sector makes up about 12% while it has stagnated in recent years.

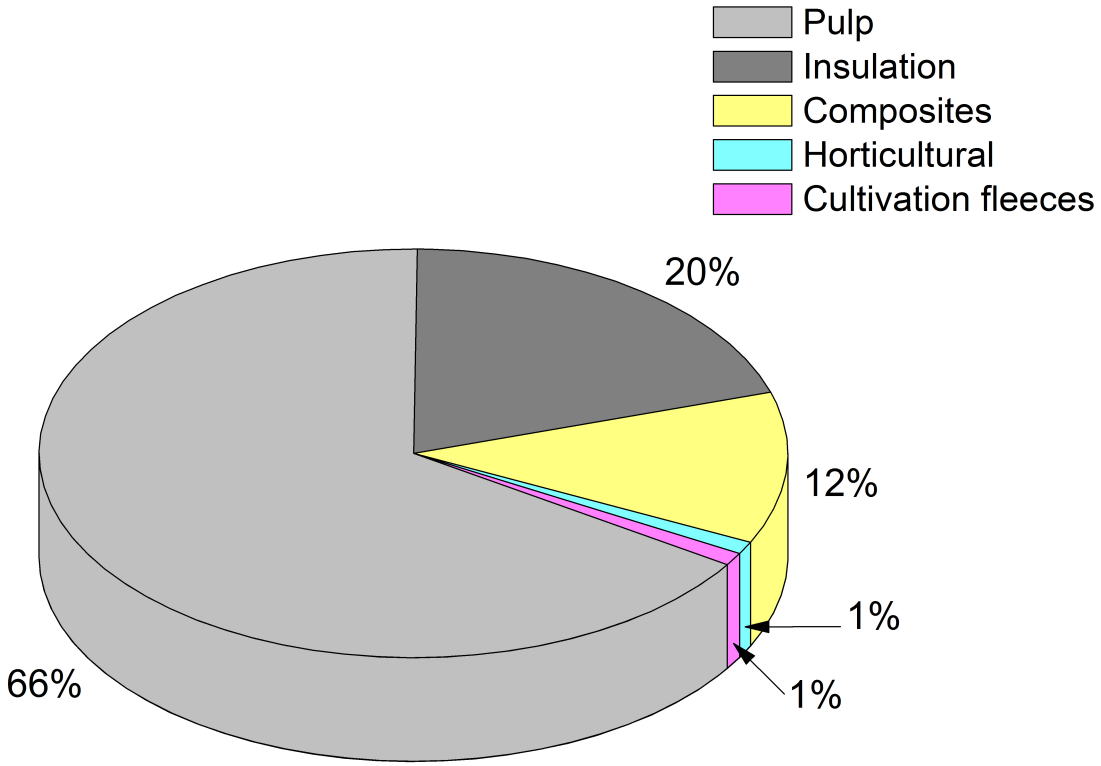

Figure 7: Application areas of hemp in percentages produced in the EU in 2006. Source: Carus *et al.* [2008].

Economics of hemp cultivation

The condition under which the traditional agricultural production takes place differs from the typical industrial production. To determine the quality or rating of the fibre many different factors need to be considered such as: cost of labour, machinery and harvesting, seed quantity and price, extent of tillage, phytosanitary measures, income volume and market prices, weather risk, competitive risk from supply and demand.

Cultivation

The actions of the hemp fibre plant cultivation can be divided into three sections: (i) basic tillage (ploughing or cultivator), (ii) seedbed and order (towing or drill string) and (iii) care and fertilisation (inorganic/organic fertiliser according to soil conditions and needs of the crop). To promote hemp plant growth the soil tillage

must be loose. Hemp is sowed in the end of April to early May. Depending on the weather, location and variety the plant is ready for harvest after 120 days. The seed rate varies, for technical use of fibre about 30-40kg of hemp seed is required per hectare. Hemp plant grows very fast and has thick vegetation, there is no pressure from grass, therefore phytosanitary measures are not required. Hemp cultivation requires high nitrogen soil to grow which can be achieved by nitrogen rich fertiliser.

Harvest
The harvest of hemp can be divided into sections: (I) growth interruption, (ii) retting and (iii) presses and premises. In general, 11 tons/ha of waste straw yield is produced due to unfavourable weather conditions and poor location. However, with practical experience the straw yield can be reduced to 6-8 tons/ha. Additional value of the harvest can be increased by using the seeds, selling the seeds can add upto 300-350 €/ha. However, additional costs associated with processing are 100-120 €/ha. Furthermore, the risk of poor weather increases because the plants must be harvested after the seeds have matured, i.e. upto 2-3 weeks more.

Economy
The reform of the Common Agricultural Policy (CAP) means farmers receive compensation regardless of the crop they cultivate. In addition to the direct payments received by farmers special payments exist called a processing aid for being the only farmer to produce hemp. Here, the farmers receive on average €90/ton for hemp.

Price situation of natural fibres in Europe

Flax and hemp fibres can be used in many technical applications by themselves or as substitute for other natural fibres. Therefore, their prices are not independent. The demand for flax fibres from the textile industry is the most important factor influencing the natural fibre prices. In the past, fashion waves have lead to significant price increases in flax and short flax fibres. This is because in times of fashion peak more short flax fibres are used for clothing textile.

In addition the quantity and quality of the harvest as well as the demand of

automotive and insulation industries play a major role in influencing the price of natural fibres. Furthermore, the production of exotic natural fibres such as jute and kenaf also play an important role.

Figure 8 shows the average price of flax and hemp fibres for technical applications in Germany since 2003. The decrease in price for flax from 2003 to 2007 was due to increased pressure from jute production. From early 2007 flax prices began to rise due to shortage of arable land (over-production in previous years and low margins in competition corn for energy) and lower crop yields (bad weather). The price of hemp is fairly stable due to the fact that significant price discounts to the insulation industry has stopped and also the automotive sector for non-woven has been fully utilised. The price of natural fibres differ despite the partial interchangeability of bast fibres such as flax, hemp, jute, kenaf. Apart from the actual fibre properties other factors which affect the price are parameters such as supply security and strategies of traders.

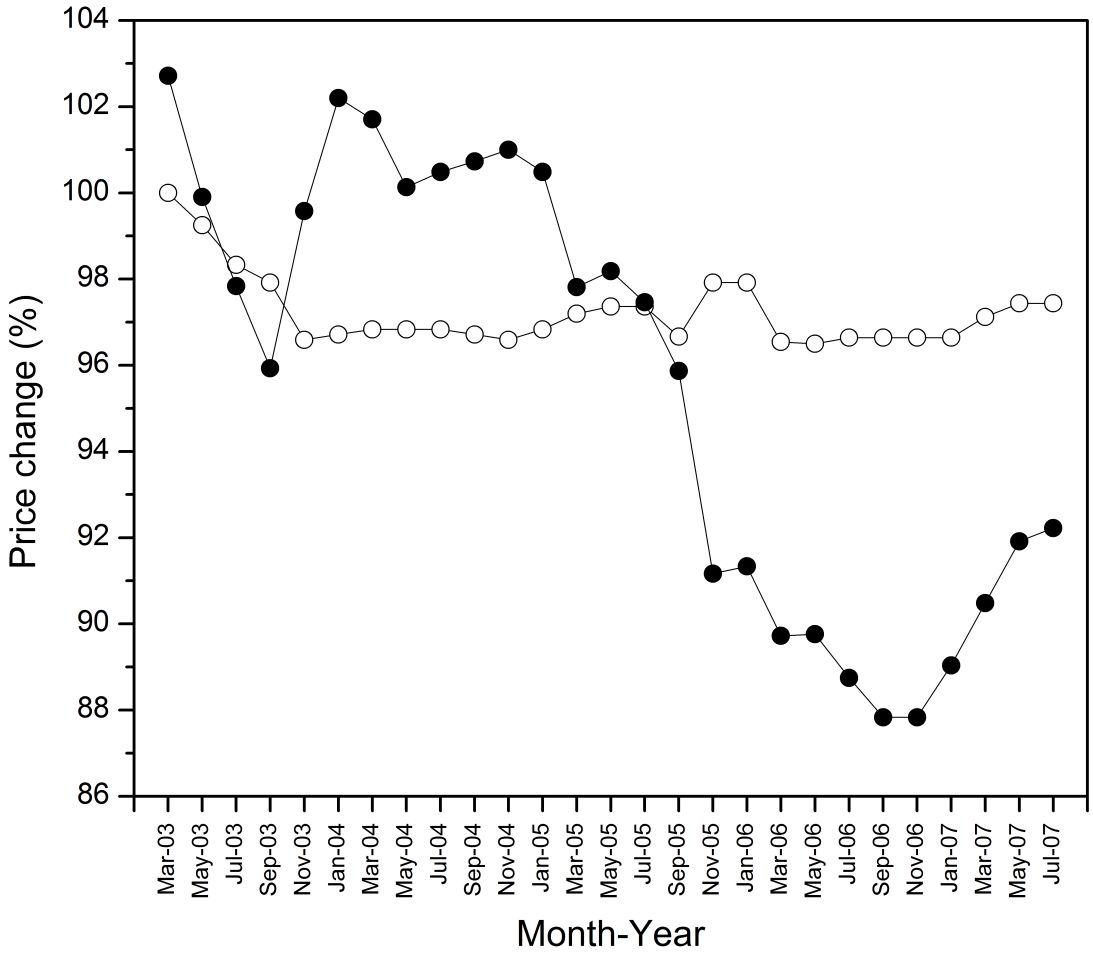

Figure 8: Index for the average price of (○) hemp and (●) flax fibres for technical applications in Germany since 2003. Price is normalised to that hemp in March 2003 = 100% (hemp fibre = 500€/ton in March 2003). Source: Carus *et al.* [2008].

The Figure 9 shows the typical price ranges for some common natural fibres at the beginning of 2007. Coconut (coir) fibres are relatively inexpensive because they do not compete with other natural fibres in the field of composites application (except for high-quality car seats).

In recent years the world prices for jute and sisal have significantly increased, meaning that flax and hemp short fibres produced in Europe are currently competitive - at least for the current economic conditions. The financial aid given to the EU farmers is soon expiring, currently all crop producers of flax and hemp

short fibres receive 0.09 €/kg. At present with the processing aid the fibre prices are between 0.50-0.60 €/kg while without the aid they will be around 0.60-0.70 €/kg, which is the upper end of the current price scale, and thus higher than prices of jute. Should the world prices on the top level stabilize or even rise further, the fibres produced in Europe without the processing aid can still be competitive.

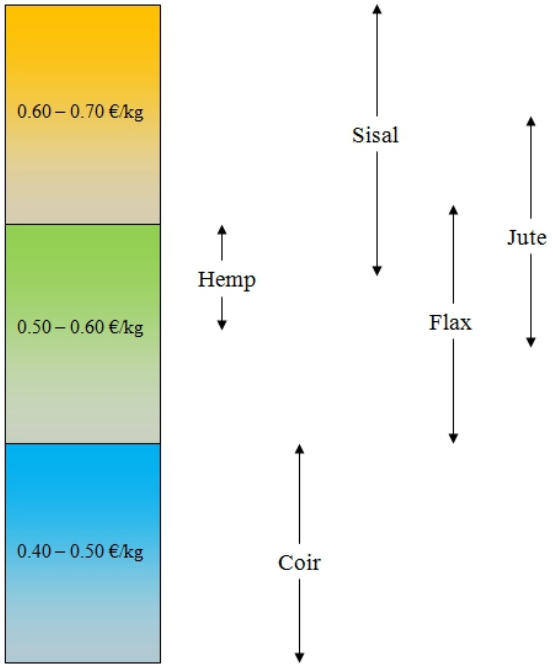

Figure 9: Price layers of technical short natural fibres, summer 2007 (suitable quality for automotive applications).

Market shares

Production methods for NFCs

Figure 10 shows the proportion of different production methods for natural fibre reinforced composites in the German automobile industry. Press moulding processes based on non-woven mats are by far the most commonly used manufacturing methods to produce natural fibre composites with a share of 95%. However it has slightly decreased in recent years where before it was over 99%. Natural fibre moulded composites use both thermosetting and thermoplastic as the matrix

system and are generally preferred when simple 3D shapes are required.

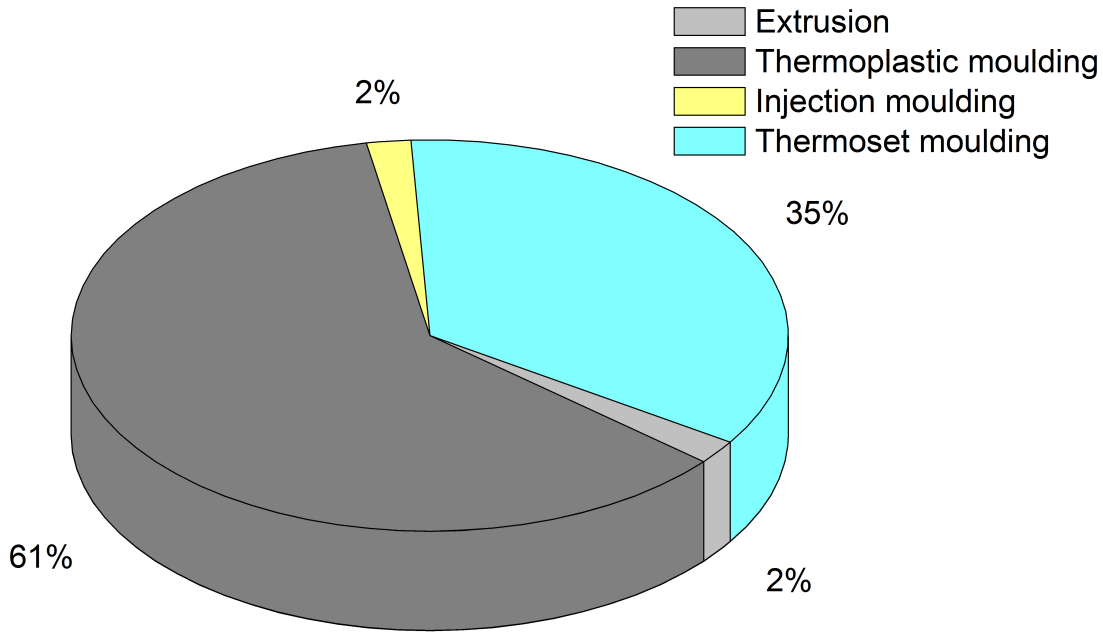

Figure 10: Share of different production methods for natural fibre composites in the German automotive industry (excluding wood and cotton compounds). The extrusion and injection moulding value are for purely thermoplastic process. Source: Carus *et al.* [2008].

For the first time new processes to produce natural fibre composites such as extrusion and injection moulding are also becoming visible. Although their market share is surprisingly small at the moment these processes are likely to make considerable gains in the next few years while the moulding processes have reached a maximum level. Natural fibre extruded composites offer better mechanical properties then press moulded composites. However extrusion processes require higher processing pressures and therefore investment costs are higher than press moulding processes. The advantage that injection moulded composites offer over moulding and extrusion processes is that complex or precision components can be produced in large quantity in a short time span. Injection processes are likely to be used in high-quality interior components such as mass-produced upholstery where heavy growth is expected.

It is believed that natural fibre moulding processes have exceeded their mar-

ket share and are now in decline. Although, this cannot be confirmed it could be said that the compression moulding market has stagnated. The reason for this assumed decline can be explained due to a shift within the suppliers, where the production volume has declined for many small and medium sized suppliers whereas for few large suppliers the volume has actually increased. So if you asked the suppliers you would inevitably get the qualitative impression that moulding processes has relatively declined, even though quantitatively it has actually stayed constant.

Natural fibre content

Figure 11 shows the natural fibre content in different matrix type of composite materials in the German automobile industry in 2005. Thermoset wood fibre composites often contain nearly 85 vol.% fibre, while natural fibres (without wood and cotton) when combined with thermoset matrixes have a fibre content on average 55 vol.% fibre. In the past, the fibre content of natural fibre reinforced thermoplastic composites have been in the range of 30-40 vol.% however recently they have increased and in 2005 the average fibre content was 46 vol.%. For all types of matrix the average natural fibre volume is about 51.5 vol.%.

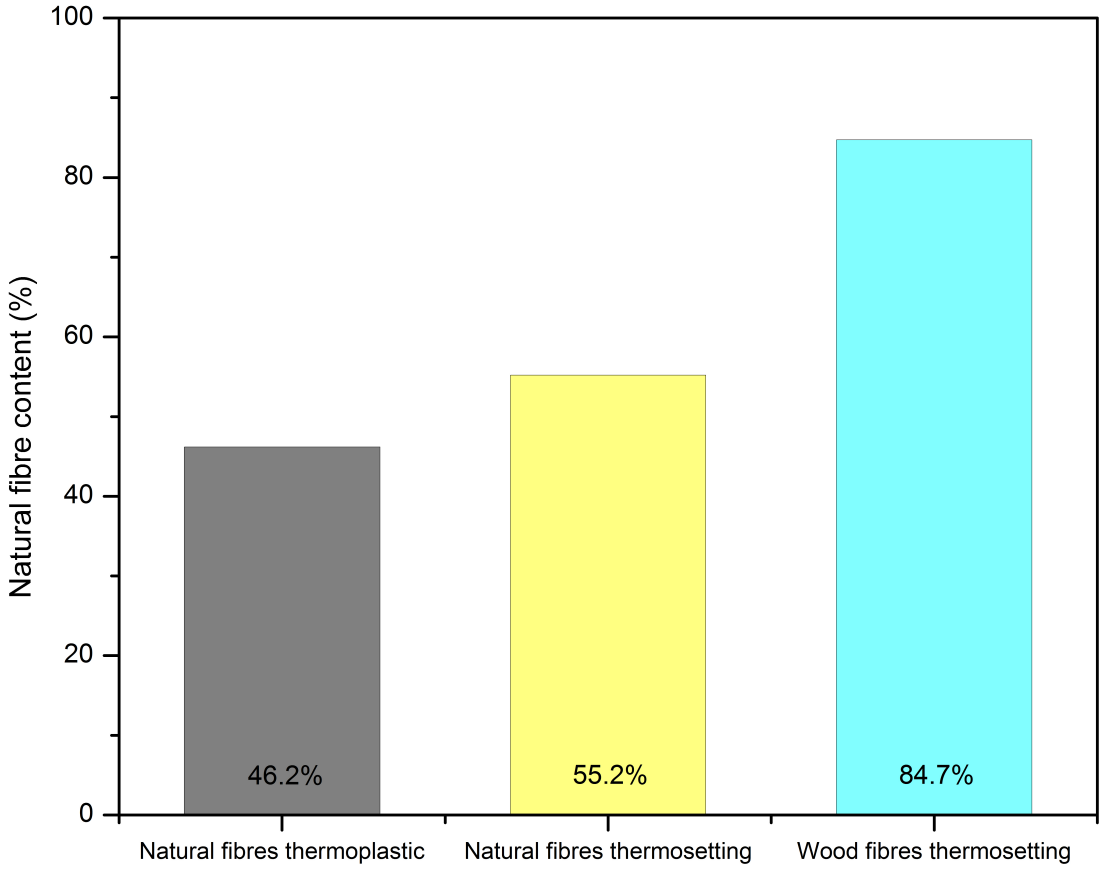

Figure 11: Natural fibre content in different matrix type of composites materials in the German automobile industry for 2005. Source: Carus *et al.* [2008].

Use of natural fibres in the automotive industry

Figure 12 shows the quantity of natural fibres used in the German automobile industry (excluding wood and cotton) and also the contribution of thermosetting and thermoplastic matrix. From 1999 to 2002 there was a significant increase in the amount of natural fibres used in the automobile industry; however after 2003 the usage has not increased greatly. From 1999 to 2003 the proportion of thermoplastic composites has also increased significantly and since then stayed constant.

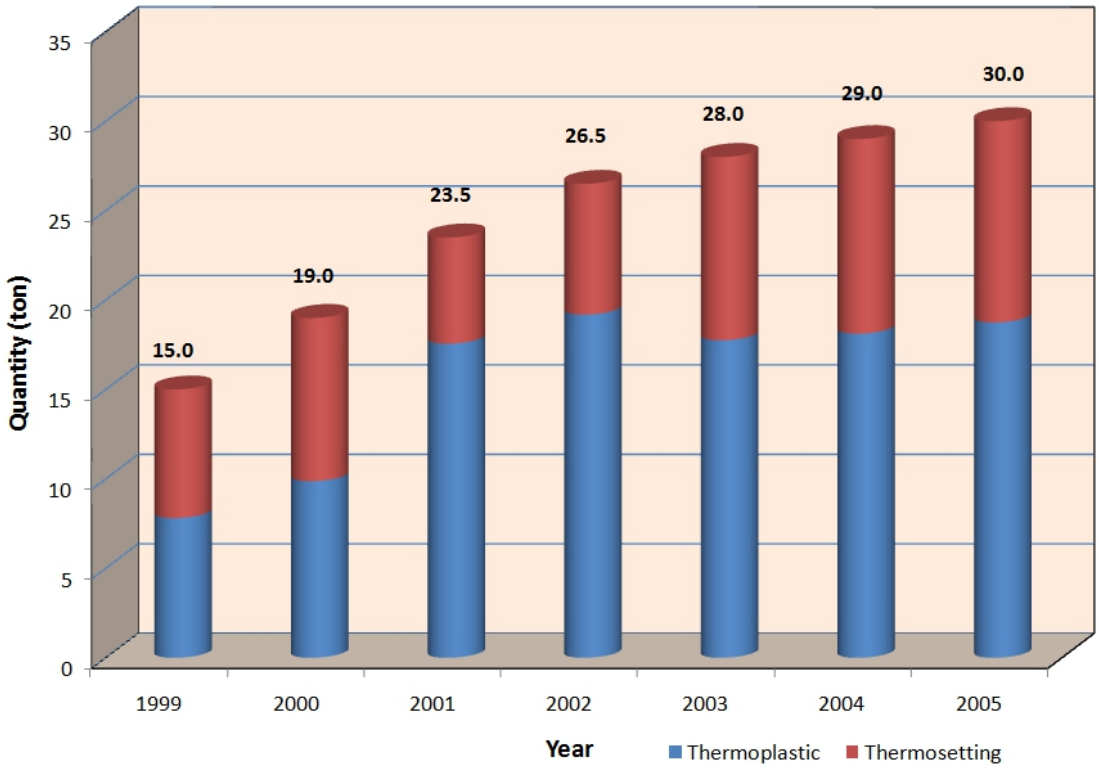

Figure 12: Natural fibres used in the German automobile industry (excluding wood and cotton) and also the contribution of thermosetting and thermoplastic matrix. Source: Carus *et al.* [2008].

Reinforcement forms

Non-woven vs. textile

In the last two decades most of the natural fibre reinforced composites and its developments were based on non-woven mats mainly due to their low processing cost. Many studies focus on non-woven mats as reinforcement for various types of matrix materials [Garkhail *et al.*, 2000; George *et al.*, 1999; Heijenrath & Peijs, 1996]. Random non-woven mats usually show good drape (the ability to adapt to complex geometries) and wet-out characteristics and are easy to process, but they demonstrate only limited mechanical properties due to short fibre lengths, and high resin content. Therefore, they are seldom used for high performance applications. Also there are large variations in properties of natural fibre non-

woven mats reinforced composites due to non-uniform distribution of natural fibres in the composites, therefore making it difficult to describe the composite properties accurately.

In recent years, new developments in textile technologies such as weaving, knitting and braiding have resulted in the formation of textile composites based on natural fibres that have superior mechanical properties [Goutianos & Peijs, 2003]. Normal natural fibre textile yarns have often high angle twist while the key for natural fibre yarns for composites is a low angle twist as this will lead to better impreggnation and higher strength (no off-axis). Woven fabrics are attractive as reinforcements since they provide excellent integrity and conformability for advanced structural applications. The driving force for the increased use of woven fabrics compared to their non-woven counterparts are excellent drapeability, reduced manufacturing costs and increased mechanical properties due in part to the increased fibre aspect ratio and orientation. The interconnectivity between adjacent fibres in the textile reinforcement provides additional interfacial strength to supplement the relatively weak fibre-resin interface. The non-delamination characteristics of three-dimensional braided composites under ballistic impact also makes them possess considerable potential in ballistic protection applications [Wambua *et al.*, 2003a]. Formation of different textile preforms based on natural fibres is an important stage in composite technology. Also, possible textile combinations based on hybrid yarns of natural fibre and thermoplastic fibres such as PP and PLA has lead to biobased ("Biotex") alternatives to PP/glass (Twintex).

Nanofibres

So far the majority of the research on natural fibre composites has been focused on fibres at the micro level. However, research in nanocomposite materials is growing fast and a significant effort is being focused on the ability to obtain control of nanoscale structures via innovative synthetic approaches [Berglund & Peijs, 2010; Eichhorn *et al.*, 2010]. Potential nanofibres offer better composite mechanical properties due to their higher strength. For natural fibres which are mainly made of a complex network of three polymers namely cellulose, hemicellulose and lignin; the cellulosic nanofibres can be separted from raw natural fibres by new techniques including chemical and physical treatments [Alemdar & Sain, 2008; Bhatnagar

& Sain, 2005; Wang & Sain, 2007; Wang *et al.*, 2009]. The cellulose nanofibres consist of monocrystalline cellulose domains with the microfibril axis parallel to the cellulose chains. The properties of nanocomposite materials depend not only on the properties of their individual components but also on their morphology and interfacial characteristcs. This rapidly expanding field is generating many new materials with novel properties.

Dufresne and co-workers [Dufresne *et al.*, 1996, 1997; Helbert *et al.*, 1996; Ruiz *et al.*, 2000] have carried out extensive work on separation, characterisation and processing of cellulose microfibrils and have analysed the properties of these nanocomposites. Hajji *et al.* [1996] have measured the tensile behaviour of nanocomposites under the influence of different processing conditions and filler content. The future of cellulose nanocomposites will mainly be focused on finding cheaper and better ways of obtaining nanoscale cellulose fibres which will therefore improve the mechanical performance of the overall composites.

The natural fibre composite company - a case study

The preceding chapters have focused on the development and environmental aspect of natural fibre composites. However, if a natural fibre composite was to be produced and marketed by a company, what are the factors that might contribute to the company's success and failure? The answer to the stated question can be analysed using Porter's Five-Forces Model.

Porter's five forces analysis is a framework for the industry analysis and business strategy which determines the competitive intensity and therefore attractiveness of a market. Attractiveness in this context refers to the overall industry profitability. An "unattractive" industry is one where the combination of forces acts to drive down overall profitability. A very unattractive industry would be one approaching "pure competition".

Figure 13 shows a graphical representation of Porter's Five Forces. Porter's five forces include three forces from 'horizontal' competition: threat of substitute products, the threat of established rivals, and the threat of new entrant; and two

forces from 'vertical' competition: the bargaining power of suppliers, bargaining power of customers.

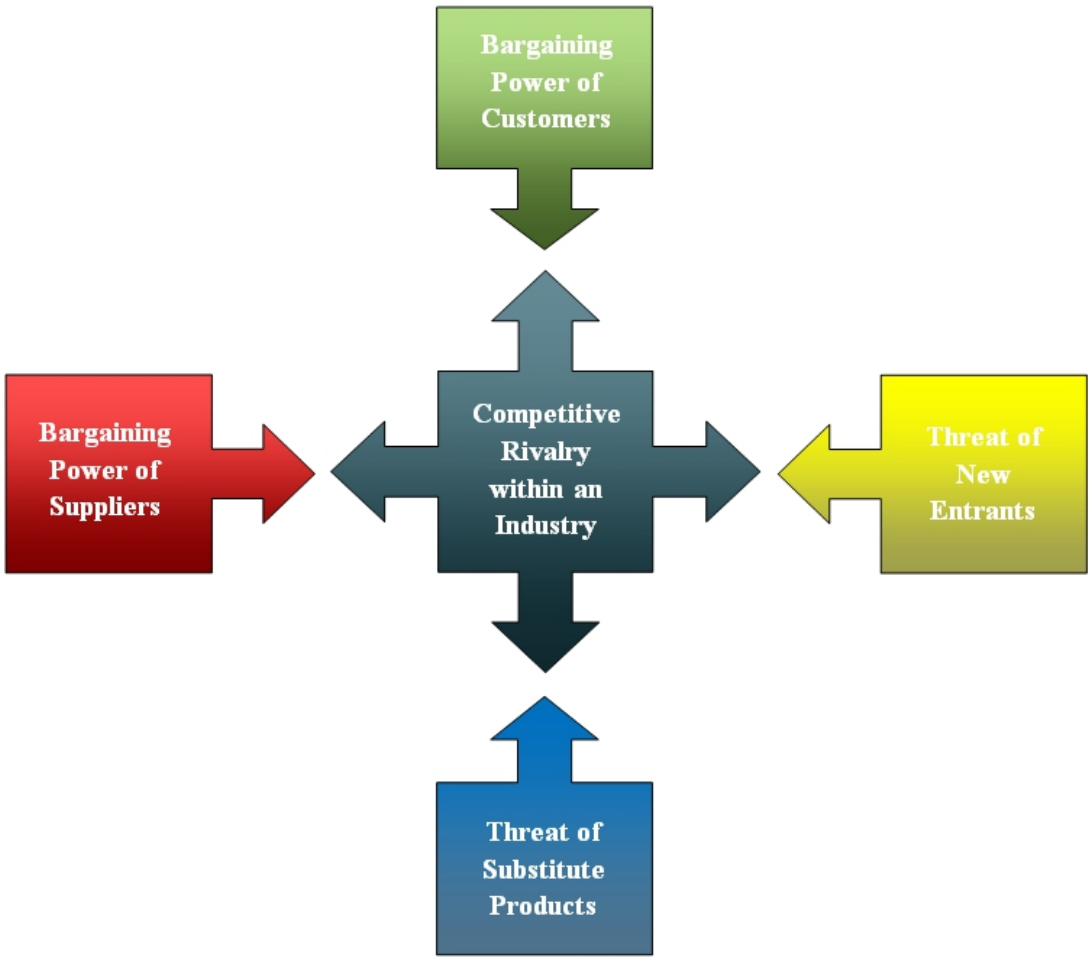

Figure 13: A graphical representation of Porter's Five Forces.

According to Porter, the five forces model should be used at the industry level in a market where similar or closely related products and/or services are sold to buyers. Firms that compete in a single industry should develop, at a minimum, one five forces analysis for its industry.

The threat of new entrants

Since the natural fibre composite producing companies have been able to find a

very distinctive niche in the industry, the entrance barriers are relatively high. The small number of companies has been able to grow over a long period of time, and have developed from within Research and Development departments. By relying on past experience, companies' officials know to a large extent what the target customer wants. As these existing companies pretty much dominate the natural fibre composite market, it will be very difficult for such a new organization to develop brand recognition/identification, and product differentiation. Relative brand strength is very low as consumers pay more attention to the direct contact with the producer than to the presence of the collective brand. These small groups of companies have focused on market diversification for years and the companies' cover a wide array of products and services. The opportunities to differentiate the product and services are very diverse, other fibre; matrix and processing techniques can be applied to produce a number of new composites. In addition, extremely large amounts of capital investment are required for new entrants into the industry. The capital requirements are extremely high due to machine and tool requirements. Lastly, the government policy towards industry appears to be very favourable with subsidies to farmers producing crops for the industry. Access to distribution channels could be an entry barrier; the natural fibre composite industry is relatively small and is governed for a major part by a small number of companies. It will not be easy to enter into this world as a new player. However, the new technical applications are aimed at a very different market such as upholstery, building and construction materials rather than the saturated automobile industry. Since natural fibre reinforced composites with good mechanical properties are not easy to produce there exists a learning curve within the industry which gives the existing competitors an advantage and provides a barrier of entry for new players.

The intensity of rivalry within the industry

Competition is always a threat to a company. Even though that the entrance barriers are relatively high in the niche industry in which the companies are operating in, the intensity of rivalry among existing competitors is probably quite strong. The number of competitors is high and increasing as new players are expected to enter this market from China and India. However, the current competitors seem

to be keeping a watchful eye on each other in order to retain the balance in the industry. The market for wood fibre composites (WPCs) in Europe is expected to increase from virtually nothing at the moment to somewhere in the region of €500 million to €1 billion over the next five years. In volume terms, this equates to up to 1.3 million tonnes of WPC material [Research-report, 2003]. It has even been suggested that the European market for WPCs will eventually exceed that in the USA in the longer term (10 years from now). The industry over-capacity depends largely on the demand from the automotive sector; however raw materials can be stored for years when demand is low or until economic times have improved. Probability of entry/exit of a major firm can be expected in terms of a change of owners of the existing firms, than in a possible establishment of a new or divestiture of an existing major player. Therefore, the attractiveness of industry can be described as average, in this connection - entry of a major firm cannot be expected (decreasing the attractiveness), neither an exit of a major firm (increasing the attractiveness). Potential of innovation is very high as it is a relatively new product, and the companies are focused on finding new ways to stay ahead of rivals with new processing techniques and fibre-matrix formulations. The structures of these industries are attractive thanks to the potential growth of profitability, which is expected in future. From the viewpoint of smaller producers (and potential new entrants), the structure of industries is not attractive, which is determined by their bargaining power towards the next part of the processing chain. Cost allocation per value added is fairly high due to high cost of unnecessary aspects of support activity such as tool and machine maintenance also the high volume of off-cuts produced from final components. Advertising battles are not a current phenomenon, though are liable to play a major part in the future. The economies of scale will be initially low due to the high start-up costs; however over time they will increase as it will cost much less to run injection or extrusion machines and presses when large volumes of the components need to be produced.

The threat of substitute products

The pressure from substitute products in the natural fibre composite industry is very strong and will continue to grow and may develop considerable potency in the future due to the rapid grow of the industry in China and India. The main

threat comes from substitute products such as wood plastic, cotton reinforced composites and other more exotic natural fibre composites. The threat from traditional composite that are reinforced with glass or carbon fibre is low due to the increased awareness of environmental effect particularly by Western governments. The main threat in terms of relative price performance of substitutes comes from China as it is capable of producing composites at one tenth the cost of European countries. It also has access to cheap raw materials as it is one of the biggest producers of natural fibres. Switching costs are often in favour of the buyer due to the large cost reduction and the ability of producing the composite in large volume in a short time span by companies in China. The perceived level of product differentiation is relatively low particularly in the automotive industry as it does not seem to make much difference which natural fibre is applied for a specific technical application.

The bargaining power of customers

At the moment the bargaining power of the customers is relatively high due to the availability of existing substitute products. The buyer concentration ratio is low as there are many companies within the industry offering different types of natural fibre composite for various applications. The industry is structured by three players; the composite producing companies, middle-men the distributors of the products and the customer who buy the final product. The degree of dependency upon the distributors is high as without them it will be difficult to sell direct to the customers. The bargaining power of the distributors is relatively high as the switching cost to another company is low. The distributors buy in large volumes increasing their bargaining power considerably. It is difficult to backward integrate in this industry as the producing companies are heavily dependent on the distributors. One advantage that companies have is the uniqueness of their products compared to other companies which will decrease the bargaining power of the customer slightly.

The bargaining power of suppliers

The bargaining power of suppliers is not very strong; the suppliers of natural fibres are farmers who often grow these fibres under contract making the composite

company concentration higher compared to the supplier concentration. The European Union often gives subsidies to grow natural fibres. The supplier switching cost is relatively low and often the companies switch suppliers to obtain desired quality, as the quality of natural fibres change every year. The presence of many different types of natural fibres as substitute considerably lowers the bargaining power of the suppliers. The possibility of forward integration by the suppliers is low due to the relatively high R&D and start-up cost that are involved in developing a natural fibre composite product.

Summary of Porter's model

In the present economic climate it a difficult time for a new company to enter the natural fibre composite industry as the initial investment cost are high and access to distribution channels are limited. Also competition within the industry is relatively high and expected to increase as new companies open up in China and India. There is significant competition from substitute products like wood plastic and cotton reinforced composites which will reduce the profit. The bargaining power of the customers is relatively high due to the availability of existing substitute products, however, one advantage that companies have is the uniqueness of their products within the industry. Finally, the bargaining power of the suppliers is low. Maybe when the economic climate is more stable it might be a better time for companies to enter the industry and be successful.

References

Abrate, S. (1998). *Impact on composite structures*. Cambridge University Press, Cambridge, UK. 79

Adedelmouleh, M., Boufi, S., Belgacem, M.N. & Dufresne, A. (2007). Short natural-fibre reinforced polyethylene and natural rubber composites: Effects of silane coupling agents and fibre loading. *Composite Science and Technology*, **67**, 1627–1639. 13

Adler, E. (1977). Lignin chemistry past, present and future. *Wood Science and Technology*, **11**, 169–218. xii, 26

Aggag, G. & Takahashi, K. (1996). Study of oscillation signals in instrumented Charpy impact testing. *Polymer Engineering and Science*, **36**, 2260–2266. 83

Ahmad, S.H., Rasid, R., Bonnia, N.N., Zainol, I., Mamun, A.A., Bledzki, A.K. & Beg, M.D.H. (2011). Polyester-kenaf composites: Effects of alkali fiber treatment and toughening of matrix using liquid natural rubber. *Journal of composite materials*, **45**, 203–217. 129

Ahmed, K.S., Vijayarangan, S. & Kumar, A. (2007). Low velocity impact damage characterization of woven jute glass fabric reinforced isothalic polyester hybrid composites. *Journal of Reinforced Plastics and Composites*, **26**, 959–976. 102, 114

Akimoto, H., Toda, M., Miyashita, J., Shonaike, G.O., Murakami, A., Hogg, P. & Ahmadnia, A. (2000). Impact performance of macrocomposite

laminates-1. Evaluation of energy absorbed in non-penetration impact test. *Journal of Reinforced Plastics and Composites*, **19**, 1363–1378. 80

Alemdar, A. & Sain, M. (2008). Isolation and characterization of nanofibers from agricultural residues - wheat straw and soy hulls. *Bioresource Technology*, **99**, 1664 – 1671. 211

Ali, M. (2012). Review: Natural fibres as construction materials. *Journal of Civil Engineering and Construction Technology*, **3**, 80 – 89. 186

Alix, S., Lebrun, L., Morvan, C. & Marais, S. (2011). Study of water behaviour of chemically treated flax fibres-based composites: A way to approach the hydric interface. *Composites Science and Technology*, **71**, 893–899. 54

Alvarez, V.A., Ruscekaite, R.A. & Vazquez, A. (2003). Mechanical properties and water absorption behavior of composites made from a biodegradable matrix and alkaline-treated sisal fibers. *Journal of Composite Materials*, **37**, 1575–1588. 128

Alvarez, V.A., Vazquez, A. & Bernal, C. (2005). Fracture behavior of sisal fiber-reinforced starch-based composites. *Polymer Composites*, **26**, 316–323. 128

Antich, P., Vazquez, A., Mondragon, I. & Bernal, C. (2006). Mechanical behavior of high impact polystyrene reinforced with short sisal fibers. *Composites Part A: Applied Science and Manufacturing*, **37**, 139 – 150. 85

Arbelaiz, A., Fernandez, B., Cantero, G., Llano-Ponte, R., Valea, A. & Mondragon, I. (2005a). Mechanical properties of flax fibre/polypropylene composites. influence of fibre/matrix modification and glass fibre hybridization. *Composites Part A: Applied Science and Manufacturing*, **36**, 1637–1644. 16

Arbelaiz, A., Fernandez, B., Cantero, G., Llano-Ponte, R., Valea, A. & Mondragon, I. (2005b). Mechanical properties of flax fibre/polypropylene composites. influence of fibre/matrix modification and glass

fibre hybridization. *Composites Part A: Applied Science and Manufacturing*, **36**, 1637–1644. 53

Ardente, F., Beccali, M., Cellura, M. & Mistretta, M. (2008). Building energy performance: A lca case study of kenaf-fibres insulation board. *Energy and Buildings*, **40**, 1 – 10. 146

Argento, A., Kim, W., Lee, E.C., Harris, A.M. & Mielewski, D.F. (2011). Rate dependencies and energy absorption characteristics of nanoreinforced, biofiber, and microcellular polymer composites. *Polymer Composites*, **32**, 1423–1429. 129

ASTM-D5045 (1999). Standard test methods for plane-strain fracture toughness and strain energy release rate of plastic materials. 131

Aziz, S.H., Ansell, M.P., Clarke, S.J. & Panteny, S.R. (2005). Modified polyester resins for natural fibre composites. *Composite Science and Technology*, **65**, 525–535. 13, 55

Baley, C. (2002). Analysis of the flax fibres tensile behaviour and analysis of the tensile stiffness increase. *Composites: Part A - Applied Science and Manufacturing*, **33**, 939–948. 31, 32

Baley, C., Busnel, F., Grohens, Y. & Sire, O. (2006). Influence of chemical treatments on surface properties and adhesion of flax fibre-polyester resin. *Composites Part A: Applied Science and Manufacturing*, **37**, 1626 – 1637. 65

Beckermann, G. & Pickering, K. (2008). Engineering and evaluation of hemp fibre reinforced polypropylene composites: Fibre treatment and matrix modification. *Composites Part A: Applied Science and Manufacturing*, **39**, 979 – 988. 186

Berglund, L.A. & Peijs, T. (2010). Cellulose biocomposites-From bulk moldings to nanostructured systems. *MRS Bulletin*, **35**, 1. 53, 78, 145, 211

Bezeredi, A., Voros, G. & Pukanszky, B. (1997). Mechanical damping in instrumented impact testing. *Journal of Materials Science*, **32**, 6601–6608. 83

Bhatnagar, A. & Sain, M. (2005). Processing of cellulose nanofiber-reinforced composites. *Journal of Reinforced Plastics and Composites*, **24**, 1259–1268. 211

Bibo, G.A. & Hogg, P.J. (1996). The role of reinforcement architecture on impact damage mechanisms and post-impact compression behaviour. *Journal of Materials Science*, **31**, 1115–1137. 88, 102

Bibo, G.A. & Hogg, P.J. (1998). Influence of reinforcement architecture on damage mechanisms and residual strength of glass-fibre/epoxy composite systems. *Composites Science and Technology*, **58**, 803 – 813. 88

Bjerre, A., Schmidt, A. & Risø, F. (1997). *Development of Chemical and Biological Processes for Production of Bioethanol: Optimization of the Wet Oxidation Process and Characterization of Products*. Risø-R, Risø National Laboratory. 25

Bledzki, A.K. & Gassan, J. (1999). Composites reinforced with cellulose based fibres. *Progress Polymer Science*, **24**, 221–274. 25, 30

Bledzki, A.K., Sperber, V.E. & Faruk, O. (2002). Natural and wood fibre reinforcment in polymer. *Rapra Review Reports*, **13**. 14, 16

Bledzki, A.K., Fink, H.P. & Specht, K. (2004). Unidirectional hemp and flax ep and pp composites: Influence of defined fiber treatments. *Journal of Applied Polymer Science*, **95**, 2150–2156. 13

Bodros, E. & Baley, C. (2008). Study of the tensile properties of stinging nettle fibres (urtica dioica). *Materials Letters*, **62**, 2143 – 2145. 186

Bos, H. (2004). *The potential of flax fibres as reinforcement for composite materials*. Ph.D. thesis, Eindhoven University of Technology, Eindhoven. xiii, xiv, 37, 43, 44, 65, 66, 146

Bos, H.L. & Donald, A.M. (1999). In situ ESEM study of the deformation of elementary flax fibres. *Journal of Materials Science*, **34**, 3029–3034. 32

Bos, H.L., van den Oever, M.J.A. & Peters, O.C.J.J. (2002). Tensile and compressive properties of flax fibres for natural fibre reinforced composites. *Journal of Materials Science*, **37**, 1683–1692. 31, 32

Bos, H.L., Mussig, J. & van den Oever, M.J.A. (2006). Mechanical properties of short-flax-fibre reinforced compounds. *Composites Part A: Applied Science and Manufacturing*, **37**, 1591–1604. 13, 61

Callister, W.D.J. (2003). *Materials Science and Engineering: An Introduction*. John Wiley and sons Inc., New York. 1

Cantwell, W. & Morton, J. (1991). The impact resistance of composite materials – a review. *Composites*, **22**, 347 – 362. 79

Cantwell, W., Curtis, P. & Morton, J. (1983). Post-impact fatigue performance of carbon fibre laminates with non-woven and mixed-woven layers. *Composites*, **14**, 301–305. 102

Caprino, G. & Lopresto, V. (2000). Factors affecting the penetration energy of glass fibre reinforced plastic subjected to a concentrated transverse load. In *Proc. ECCM-9, 9th European Conference on Composite Materials*, Brighton, UK. 88

Caprino, G. & Lopresto, V. (2001). On the penetration energy for fibre-reinforced plastics under low-velocity impact conditions. *Composites Science and Technology*, **61**, 65 – 73. 87

Caprino, G., Spataro, G. & Luongo, S.D. (2004). Low-velocity impact behaviour of fibreglass-aluminium laminates. *Composites Part A: Applied Science and Manufacturing*, **35**, 605 – 616. 87

Caprino, G., Lopresto, V. & Iaccarino, P. (2007). A simple mechanistic model to predict the macroscopic response of fibreglass-aluminium laminates under low-velocity impact. *Composites Part A: Applied Science and Manufacturing*, **38**, 290 – 300. 87

Carus, M., Vogt, D. & Breuer, T. (2008). *Study on the market and competition - situation for natural fibers and natural fibre materials (Germany and EU)*. Nova-Institute, Germany. 197, 198, 202, 205, 207, 209, 210

Chaturvedi, S.K. & Sierakowski, R.L. (1985). Effects of impactor size on impact damage-growth and residual properties in an smc-r50 composite. *Journal of Composite Materials*, **19**, 100–113. 79

Chen, H., Miao, M. & Ding, X. (2011). Chemical treatments of bamboo to modify its moisture absorption and adhesion to vinyl ester resin in humid environment. *Journal of Composite Materials*, **45**, 1533–1542. 54

Corbiere-Nicollier, T., Laban, B.G., Lundquist, L., Leterrier, Y., Manson, J.A.E. & Jolliet, O. (2001). Life cycle assessment of biofibres replacing glass fibres as reinforcement in plastics. *Resources,Conservation and Recycling*, **33**, 267 – 287. 146

Cox, H.L. (1952). The elasticity and strength of paper and other fibrous materials. *British Journal of Applied Physics*, **3**, 72. 60

Cui, H.P., Wen, D.W. & Cui, H.T. (2009). An integrated method for predicting damage and residual tensile strength of composite laminates under low velocity impact. *Computers Structures*, **87**, 456–466. 102

Davies, G.C. & Bruce, D.M. (1998). Effect of environmental relative humidity and damage on the tensile properties of flax and nettle fibers. *Textile Research Journal*, **68**, 623–629. 31

Davoodi, M.M., Sapuan, S.M., Ahmad, D., Aidy, A., Khalina, A. & Jonoobi, M. (2012). Effect of polybutylene terephthalate (pbt) on impact property improvement of hybrid kenaf/glass epoxy composite. *Materials letters*, **67**, 5–7. 81

de Bruijn, J.C.M. (2000). Natural fibre mat thermoplastic products from a processor's point of view. *Applied Composite Materials*, **7**, 415–420. 11, 12

de Weyenberg, I.V., Ivens, J., Coster, A.D., Kino, B., Baetens, E. & Verpoest, I. (2003). Influence of processing and chemical treatment of flax fibres on their composites. *Composites Science and Technology*, **63**, 1241–1246. 54, 55

DeRosa, I.M., Santulli, C., Sarasini, F. & Valente, M. (2009a). Effect of loading-unloading cycles on impact-damaged jute/glass hybrid laminates. *Polymer Composites*, **30**, 1879–1887. 103

DeRosa, I.M., Santulli, C., Sarasini, F. & Valente, M. (2009b). Post-impact damage characterization of hybrid configurations of jute/glass polyester laminates using acoustic emission and ir thermography. *Composites Science and Technology*, **69**, 1142–1150. 103

Devi, L.U., Bhagawan, S.S. & Thomas, S. (1997). Mechanical properties of pineapple leaf fiber-reinforced polyester composites. *Journal of Applied Polymer Science*, **64**, 1739–1748. 55

Dhakal, H., Zhang, Z., Richardson, M. & Errajhi, O. (2007a). The low velocity impact response of non-woven hemp fibre reinforced unsaturated polyester composites. *Composite Structures*, **81**, 559 – 567. 86

Dhakal, H.N., Zhang, Z.Y., Richardson, M.O.W. & Errajhi, O.A.Z. (2007b). The low velocity impact response of non-woven hemp fibre reinforced unsaturated polyester composites. *Composites Structures*, **81**, 559–567. 13

Doan, T.T.L., Gao, S.L. & Mader, E. (2006). Jute/polypropylene composites I. Effect of matrix modification. *Composites Science and Technology*, **66**, 952 – 963. 53, 54

Dufresne, A., Cavaille, J.Y. & Helbert, W. (1996). New nanocomposite materials: Microcrystalline starch reinforced thermoplastic. *Macromolecules*, **29**, 7624–7626. 212

Dufresne, A., Cavaille, J.Y. & Helbert, W. (1997). Thermoplastic nanocomposites filled with wheat straw cellulose whiskers. part ii: Effect of processing and modeling. *Polymer Composites*, **18**, 198–210. 212

Eichhorn, S. & Young, R. (2004). Composite micromechanics of hemp fibres and epoxy resin microdroplets. *Composites Science and Technology*, **64**, 767 – 772. 186

Eichhorn, S., Dufresne, A., Aranguren, M., Marcovich, N., Capadona, J., Rowan, S., Weder, C., Thielemans, W., Roman, M., Renneckar, S., Gindl, W., Veigel, S., Keckes, J., Yano, H., Abe, K., Nogi, M., Nakagaito, A., Mangalam, A., Simonsen, J., Benight, A., Bismarck, A., Berglund, L. & Peijs, T. (2010). Review: current international research into cellulose nanofibres and nanocomposites. *Journal of Materials Science*, **45**, 1–33. 211

Facca, A.G., Kortschot, M.T. & Yan, N. (2007). Predicting the tensile strength of natural fibre reinforced thermoplastics. *Composite Science and Technology*, **67**, 2454–2466. 13

Franco, P.J.H. & Gonzalez, A.V. (2004). Mechanical properties of continuous natural fibre-reinforced polymer composites. *Composites Part A: Applied Science and Manufacturing*, **35**, 339–345. 53, 54, 55

Fu, S.Y. & Lauke, B. (1996). Effects of fiber length and fiber orientation distributions on the tensile strength of short-fiber-reinforced polymers. *Composites Science and Technology*, **56**, 1179 – 1190. 61

Gamstedt, E.K., Sandell, R., Berthold, F., Pettersson, T. & Nordgren, N. (2011). Characterization of interfacial stress transfer ability of particulate cellulose composite materials. *Mechanics of materials*, **43**, 693–704. 129

Ganan, P., Garbizu, S., Llano-Ponte, R. & Mondragon, I. (2005). Surface modification of sisal fibers: Effects on the mechanical and thermal properties of their epoxy composites. *Polymer Composites*, **26**, 121–127. 74

Garkhail, S. (2001). *Composites based on natural fibres and thermoplastic matrices*. Ph.D. thesis, Department of Materials, Queen Mary College University of London, London, UK. xix, xx, 27, 29, 145, 182

Garkhail, S.K., Heijenrath, R.W.H. & Peijs, T. (2000). Mechanical properties of natural-fibre-mat-reinforced thermoplstics based on flax fibres and polypropylene. *Applied Composite Materials*, **7**, 351–372. 13, 60, 61, 65, 81, 210

Gassan, J., Mildner, I. & Bledzki, A.K. (1999). Influence of fiber structure modification on the mechanical properties of flax fiber-epoxy composites. *Mechanics of Composite Materials*, **35**, 435–440. 55

Geers, M., Peijs, T., Brekelmans, W. & de Borst, R. (1996). Experimental monitoring of strain localization and failure behaviour of composite materials. *Composites Science and Technology*, **56**, 1283–1290. 128

George, J., Weyenberg, I.V.D., Ivens, J. & Verpoest, J. (1999). Mechanical properties of flax fibre reinforced epoxy composites. In *2nd International Wood and Natural Fibre Composites Symposium*, Kassel, Germany. 13, 50, 210

George, J., Klompen, E. & Peijs, T. (2001). Thermal degradation of green and upgraded flax fibres. *Advanced Composites Letters*, **10**, 81–88. 11, 35, 52

Georgopoulos, S.T., Tarantili, P.A., Avgerinos, E., Andreopoulos, A.G. & Koukios, E.G. (2006). Thermoplastic polymer reinforced with fibrous agricultural residues. *Composite Science and Technology*, **90**, 303–312. 13

Goedkoop, M. & Spriensma, R. (2000). The eco-indicator 99 a damage oriented method for life cycle impact assessment methodology report. *Health San Francisco*, 132. 145, 159

Goriparthi, B.K., Suman, K.N.S. & Nalluri, M.R. (2012). Processing and characterization of jute fiber reinforced hybrid biocomposites based on polylactide/polycaprolactone blends. *Polymer composites*, **33**, 237–244. 81

Goutianos, S. & Peijs, T. (2003). The optimisation of flax fibre yarns for the development of high-performance natural fibre composites. *Advanced Composites Letters*, **12**, 237–241. 52, 55, 56, 211

Hajji, P., Cavaille, J.Y., Favier, V., Gauthier, C. & Vigier, G. (1996). Tensile behavior of nanocomposites from latex and cellulose whiskers. *Polymer Composites*, **17**, 612–619. 212

Hapuarachchi, T.D., Ren, G., Fan, M., Hogg, P.J. & Peijs, T. (2007). Fire retardancy of natural fibre reinforced sheet moulding compound. *Applied Composite Materials*, **14**, 251–264. 53

Hassan, A., Salema, A.A., Ani, F.N. & Bakar, A.A. (2010). A review on oil palm empty fruit bunch fiber-reinforced polymer composite materials. *Polymer Composites*, **31**, 2079–2101. 11

Heijenrath, R. & Peijs, T. (1996). Natural-fibre-mat-reinforced thermoplastic composites based on flax fibres and polypropylene. *Advanced Composite Letters*, **5**, 81–85. 56, 210

Helbert, W., Cavaille, J.Y. & Dufresne, A. (1996). Thermoplastic nanocomposites filled with wheat straw cellulose whiskers. part i: Processing and mechanical behavior. *Polymer Composites*, **17**, 604–611. 212

Hepworth, D.G., Bruce, D.M., Vincent, J.F.V. & Jeronimidis, G. (2000). The manufacture and mechanical testing of thermosetting natural fibre composites. *Journal of Materials Science*, **35**, 293–298. 13, 55

Hill, C. & Hughes, M. (2010). Natural fibre reinforced composites opportunities and challenges. *Journal of Biobased Materials and Bioenergy*, **4**, 148–158. 16

Hollaway, L. (1994). *Handbook of Polymer Composites for Engineers*. British Plastics Federation, Woodhead Publishing, Cambridge. 3

Hornsby, P.R., Hinrichsen, E. & Tarverdi, K. (1997). Preparation and properties of polypropylene composites reinforced with wheat and flax straw fibres. Part I fibre characterisation. *Journal of Materials Science*, **32**, 443–449. 31, 32, 81

Hu, W., Ton-That, M.T., Denault, J. & Belanger, C. (2011). Characterization of polypropylene composites reinforced with flax fibers treated by mechanical and alkali methods. *Science and Engineering of Composite Materials*, **18**, 79–85. 54

Hughes, M. (2012). Defects in natural fibres: their origin, characteristics and implications for natural fibre-reinforced composites. *Journal of Materials Science*, **47**, 599–609. 29

Hughes, M., Hill, C.A.S. & Hague, J.R.B. (2002). The fracture toughness of bast fibre reinforced polyester composites part 1evaluation and analysis. *Journal of Materials Science*, **37**, 4669–4676. 128, 135

Hull, D. & Clyne, T.W. (1981). *An Introduction to Composite Materials*. Cambridge University Press, Cambridge. 1

ISO14044 (2006). Environmental management – life cycle assessment – requirements and guidelines. xviii, 147

ISO/TR14047 (2003). Environmental management – life cycle impact assessment – examples of application of iso 14042. 145

Jandas, P.J., Mohanty, S., Nayak, S.K. & Srivastava, H. (2011). Effect of surface treatments of banana fiber on mechanical, thermal, and biodegradability properties of pla/banana fiber biocomposites. *Polymer Composites*, **32**, 1689–1700. 54

Joffe, R., Wallstrom, L. & Berglund, L.A. (2001). Natural fiber composites based on flax - Matrix effects. In *International Scientific Colloquium, Modelling for Saving Resources*, Riga, Latvia. 128

Joffe, R., Andersons, J. & Wallstrom, L. (2003). Strength and adhesion characteristics of elementary flax fibres with different surface treatments. *Composites: Part A - Applied Science and Manufacturing*, **34**, 603–612. 31

John, M.J. & Thomas, S. (2008). Biofibres and biocomposites. *Carbohydrate Polymers*, **71**, 343 – 364. 11

Joseph, K., Mattoso, L.H.C., Toledo, R.D., Thomas, S., de Carvalho, L.H., Pothen, L., Kala, S. & James, B. (2000). Natural fiber reinforced thermoplastic composites. In E. Frollini, A. Leao & L.H.C. Mattoso, eds., *Natural Polymers and Agrofibers Based Composites*, 159–202, San Carlos, Brazil. 11, 53, 54

Joseph, S., Sreekala, M.S., Oommen, Z., Koshy, P. & Thomas, S. (2002). A comparison of the mechanical properties of phenol formaldehyde composites reinforced with banana fibres and glass fibres. *Composites Science and Technology*, **62**, 1857 – 1868. 81

Joshi, S., Drzal, L., Mohanty, A. & Arora, S. (2004). Are natural fiber composites environmentally superior to glass fiber reinforced composites? *Composites Part A: Applied Science and Manufacturing*, **35**, 371 – 376. 146

Kalia, S., Kaith, B. & Kaur, I. (2009). Pretreatments of natural fibers and their application as reinforcing material in polymer compositesa review. *Polymer Engineering & Science*, **49**, 1253–1272. 53

Kamath, M.G., Dahiya, A. & Hegde, R.R. (2004). Needle punched nonwoven. @ONLINE http://www.engr.utk.edu/mse/Textiles. xiii, 45, 46, 48

Karaduman, Y. & Onal, L. (2011). Water absorption behavior of carpet waste jute-reinforced polymer composites. *Jounral of composite materials*, **45**, 1559–1571. 81

Keener, T.J., Stuart, R.K. & Brown, T.K. (2004). Maleated coupling agents for natural fibre composites. *Composites Part A: Applied Science and Manufacturing*, **35**, 357 – 362. 81

Kelly, A. & Tyson, W.R. (1965a). Fibre-strengthened materials in high-strength materials. In V.F. Zackay, ed., *Proceedings 2nd Berkeley International Materials Conference*, John Wiley and sons Inc., New York. 60

Kelly, A. & Tyson, W.R. (1965b). Tensile properties of fibre reinforced metals: Copper/Tungsten and Copper/Molybdenum. *Journal of the Mechanics and Physics of Solids*, **13**, 329–350. 60

Khalili, S.M.R., Farsani, R.E. & Rafiezadeh, S. (2011). An experimental study on the behavior of pp/epdm/jute composites in impact, tensile and bending loadings. *Journal of reinforced plastics and composites*, **30**, 1341–1347. 81

Khetan, R.P. & Chang, D.C. (1983). Surface damage of sheet molding compound panels subject to a point impact loading. *Journal of Composite Materials*, **17**, 182–194. 79

Kim, B.J., Yao, F., Han, G. & Wu, Q. (2012). Performance of bamboo plastic composites with hybrid bamboo and precipitated calcium carbonate fillers. *Polymer composites*, **33**, 68–78. 81

Kobayashi, T. (2004). *Strength and toughness of materials*. Springer, Tokyo, Japan. 122

Krenchel, H. (1964). *Fibre Reinforced*. Akademisk Forlag, Copenhagen. 60

Ku, H., Wang, H., Pattarachaiyakoop, N. & Trada, M. (2011). A review on the tensile properties of natural fiber reinforced polymer composites. *Composites Part B: Engineering*, **42**, 856 – 873. 186

Kumar, V. & Kumar, R. (2012). Improved mechanical and thermal properties of bamboo-epoxy nanocomposites. *Polymer composites*, **33**, 362–370. 81

Kushwaha, P.K. & Kumar, R. (2010). Effect of silanes on mechanical properties of bamboo fiber-epoxy composites. *Journal of Reinfroced Plastics and Composites*, **29**, 718–724. 54

Lai, W.L. & Mariatti, M. (2008). The properties of woven betel palm (areca catechu) reinforced polyester composites. *Journal of Reinforced Plastics and Composites*, **27**, 925–935. 54

Lal, K.M. (1983). Residual strength assessment of low velocity impact damage of graphite-epoxy laminates. *Journal of Reinforced Plastics and Composites*, **2**, 226–238. 102

Li, Y., Mai, Y.W. & Ye, L. (2005). Effects of fibre surface treatment on fracture-mechanical properties of sisal-fibre composites. *Composite Interfaces*, **12**, 141–163. xx, 29, 128

Li, Y., Pickering, K. & Farrell, R. (2009). Determination of interfacial shear strength of white rot fungi treated hemp fibre reinforced polypropylene. *Composites Science and Technology*, **69**, 1165 – 1171. 186

Li, Z., Wang, X. & Wang, L. (2006). Properties of hemp fibre reinforced concrete composites. *Composites Part A: Applied Science and Manufacturing*, **37**, 497 – 505. 186

Lilholt, H. & Lawther, J.M. (2000). Natural organic fibres. *In Comprehensive Composite Materials*, **6**, 303–325. xx, 22, 24

Liu, D. & Malvern, L.E. (1987). Matrix cracking in impacted glass/epoxy plates. *Journal of Composite Materials*, **21**, 594–609. 79

Liu, D., Lee, C.Y. & Lu, X. (1993). Repairability of impact-induced damage in smc composites. *Journal of Composite Materials*, **27**, 1257–1271. 80

Liu, Q. & Hughes, M. (2008). The fracture behaviour and toughness of woven flax fibre reinforced epoxy composites. *Composites Part A: Applied Science and Manufacturing*, **39**, 1644 – 1652. 128

Liu, X. & Dai, G. (2008). Impregnation of thermoplastic resin in jute fibre mat. *Frontiers of Chemical Engineering in China*, **2**, 145–149. 13

Lu, J. & Wool, R.P. (2001). New bio-based thermosetting resins from soybean oil for smc. *Abstract of Papers of the American Chemical Society*, **221**, 196. 180

Lu, X., Zhang, M.Q., Rong, M.Z., Shi, G., Yang, G.C. & Zeng, H.M. (1999). Natural vegetable fibre/plasticized natural vegetable fibre - a candidate for low cost and fully biodegradable composite. *Advanced Composites Letters*, **8**, 231–236. xii, 24

Luo, S. & Netravali, A.N. (1999). Interfacial and mechanical properties of environment-friendly green composites made from pineapple fibers and poly(hydroxybutyrate-co-valerate) resin. *Journal of Materials Science*, **34**, 3709–3719. 56

Mackenzie, J.K. (1950). The elastic constants of a solid containing spherical holes. *Proceedings of the Physical Society. Section B*, **63**, 2. 61, 88

Madhukar, M.S. & Drzal, L.T. (1991). Fiber-matrix adhesion and its effect on composite mechanical properties: II. Longitudinal (0)$and Transverse$(90) tensile and flexure behavior of graphite/epoxy composites. *Journal of Composite Materials*, **25**, 958–991. 53

Madsen, B. & Lilholt, H. (2003). Physical and mechanical properties of unidirectional plant fibre composites–an evaluation of the influence of porosity. *Composites Science and Technology*, **63**, 1265 – 1272. 60

Mantia, F.L. & Morreale, M. (2011). Green composites: A brief review. *Composites Part A: Applied Science and Manufacturing*, **42**, 579 – 588. 11

Masoodi, R., El-Hajjar, R.F., Pillai, K.M. & Sabo, R. (2012). Mechanical characterization of cellulose nanofiber and bio-based epoxy composite. *Materials & design*, **36**, 570–576. 129

Mehta, G., Mohanty, A.K., Misra, M. & Drzal, L.T. (2004). Effect of novel sizing on the mechanical and morphological characteristics of natural fiber reinforced unsaturated polyester resin based bio-composites. *Journal of Materials Science*, **39**, 2961–2964. 50

Mehta, G., Drzal, L.T., Mohanty, A.K. & Misra, M. (2006). Effect of fiber surface treatment on the properties of biocomposites from nonwoven industrial hemp fiber mats and unsaturated polyester resin. *Journal of Applied Polymor Science*, **99**, 1055–1068. 50

Miao, M. & Finn, N. (2008). Conversion of natural fibres into structural composites. *Journal of Textile Engineering*, **54**, 165–177. 146

Mieck, K.P., Reussmann, T. & Nechwatal, A. (2003). About the characterization of the mechanical properties of natural fibres. *Materialwissenschaft und Werkstofftechnik*, **34**, 285–289. 30

Mishra, S., Misra, M., Tripathy, S.S., Nayak, S.K. & Mohanty, A.K. (2002). The influence of chemical surface modification on the performance of sisal-polyester biocomposites. *Polymer composites*, **23**, 164–170. 53, 54

Mishra, S., Mohanty, A.K., Drzal, L.T., Misra, M., Parija, S., Nayak, S.K. & Tripathy, S.S. (2003). Studies on mechanical performance of biofibre/glass reinforced polyester hybrid composites. *Composites Science and Technology*, **63**, 1377 – 1385. 81

Mohanty, A.K., Misra, M. & Hinrichsen, G. (2000). Biofibers, biodegradable polymers and biocomposites: An overview. *Macromolecular Materials and Engineering*, **276-277**, 1–24. xx, 23

Motuku, M., Janowski, G.M., Vaidya, U.K., Hosur, M.V., Mahfuz, H. & Jeelani, S. (2000). Damage evolution in low velocity impacted unreinforced vinyl ester 411-350 and 411-c50 resin systems. *Polymer Composites*, **21**, 878–899. xv, 83

Mukherjee, P.S. & Satyanarayana, K.G. (1986). An empirical evaluation of structur-property relationship in natural fibres and their fracture behaviour. *Journal of Materials Science*, **21**, 4162–4168. 30

Mukherjee, T. & Kao, N. (2011). Pla based biopolymer reinforced with natural fibre: A review. *Journal of Polymers and the Environment*, **19**, 714–725. 11

Murkherjee, A., Ganguly, P.K. & Sur, D. (1993). Structural mechanics of jute. The effects of hemicellulose or lignin removal. *Journal of the Textile Institute*, **84**, 348–353. 53, 54, 141

Mwaikambo, L.Y. & Ansell, M.P. (2003). Hemp fibre reinforced cashew nut shell liquid composites. *Composites Science and Technology*, **63**, 1297–1305. 180

Mwaikambo, L.Y., Tucker, N. & Clark, A.J. (2007). Mechanical properties of hemp-fibre-reinforced euphorbia composites. *Macromolecular Materials and Engineering*, **292**, 993–1000. 50

Oksman, K. (2000). Mechanical properties of natural fibre mat reinforced thermoplastic. *Applied Composite Materials*, **7**, 403–414. 53, 78, 81

Oksman, K., Skrifvars, M. & Selin, J.F. (2003). Natural fibres as reinforcement in polylactic acid (PLA) composites. *Composites Science and Technology*, **63**, 1317 – 1324. 81

Okubo, K., Fujii, T. & Yamashita, N. (2005). Improvement of interfacial adhesion in bamboo polymer composite enhanced with micro-fibrillated cellulose. *JSME International Journal Series A Solid Mechanics and Material Engineering*, **48**, 199–204. 128

Pakarinen, A. (2012). *Evaluation of fresh and preserved herbaceous field crops for biogas and ethanol production*. Ph.D. thesis, Department of Agricultural Sciences, University of Helsinki, Finland. xiii, 36

Pandey, J.K., Ahn, S.H., Lee, C.S., Mohanty, A.K. & Misra, M. (2010). Recent advances in the application of natural fiber based composites. *Macromolecular Materials and Engineering*, **295**, 975–989. 16

Panthapulakkal, S. & Sain, M. (2007). Agro-residue reinforced high-density polyethylene composites: Fibre characterisation and analysis of composite properties. *Composites Part A: Applied Science and Manufacturing*, **38**, 1445–1454. 13

Patel, H.K., Ren, G., Fan, M., Hogg, P.J. & Peijs, T. (2010). Hemp fibre as alternative to glass fibre in sheet moulding compounds Part 1 influence of fibre content and surface treatment on mechanical properties. *Plastics, Rubber and Composites*, **39**. 88, 97, 135, 140

Pavithran, C., Mukherjee, P.S., Brahmakumar, M. & Damodaran, A.D. (1987). Impact properties of natural fibre composites. *Journal of Materials Science Letters*, **6**, 882–884. 27

Peijs, A., Venderbosch, R. & Lemstra, P. (1990). Hybrid composites based on polyethylene and carbon fibres part 3: Impact resistant structural composites through damage management. *Composites*, **21**, 522 – 530. 92, 102

Peijs, A.A.J.M. & Venderbosch, R.W. (1991). Hybrid composites based on polyethylene and carbon fibres part IV influence of hybrid design on impact strength. *Journal of Materials Science Letters*, **10**, 1122–1124. 80, 87

Peijs, A.A.J.M., Venderbosch, R.W. & de Kok, J.M.M. (1993). Hybridization as a concept for damage management in advanced composites. In *Proceedings of the International Conference on Advanced Composite Materials*, 755–762, Wollongong, Australia. 102

Peijs, T. (2000). Natural fiber based composites. *Materials Technology*, **15**, 281–285. 11, 53, 145

Peijs, T., Smets, E. & Govaert, L. (1994). Strain rate and temperature effects on energy absorption of polyethylene fibres and composites. *Applied Composites Materials*, **1**, 34 – 54. 87

Peijs, T., Garkhail, S., Hejenrath, R., den Oever, M.V. & Bos, H. (1998). Thermoplastic composites based on flax fibres and polypropylene: Influence of fibre length and fibre volume fraction on mechanical properties. *Macromol Symposium*, **127**, 193–203. 16, 53, 61

Pervaiz, M. & Sain, M.M. (2003). Sheet-molded polyolefin natural fiber composites for automotive applications. *Macromolecular Materials and Engineering*, **288**, 553–557. 50

Phuong, N.T., Sollogoub, C. & Guinault, A. (2010). Relationship between fiber chemical treatment and properties of recycled pp/bamboo fiber composites. *Journal of Reinforced Plastics and Composites*, **29**, 3244–3256. 54, 81

Pickering, K. (2008). *Properties and Performance of Natural-Fibre Composites*. Woodhead Publishing, Cambridge. 49

Placet, V., Trivaudey, F., Cisse, O., Gucheret-Retel, V. & Boubakar, M.L. (2012). Diameter dependence of the apparent tensile modulus of hemp fibres: A morphological, structural or ultrastructural effect? *Composites Part A: Applied Science and Manufacturing*, **43**, 275 – 287. 186

Prasad, S.V., Pavithran, C. & Rohatgi, P.K. (1983). Alkali treatment of coir fibres for coir-polyester composites. *Journal of Materials Science*, **18**, 1443–1454. 50

Prichard, J.C. & Hogg, P.J. (1990). The role of impact damage in post-impact compression testing. *Composites*, **21**, 503–511. 102

Puettmann, M. & Wilson, J. (2005). Life-cycle analysis of wood products: Cradle-to-gate lci of residential wood building materials? *Wood and Fiber Science*, **37**, 18 – 29. 146

Qin, C., Soykeabkaew, N., Xiuyuan, N. & Peijs, T. (2008). The effect of fibre volume fraction and mercerization on the properties of all-cellulose composites. *Carbohydrate Polymers*, **71**, 458 – 467. 53, 54, 56

Rebitzer, G., Ekvall, T., Frischknecht, R., Hunkeler, D., Norris, G., Rydberg, T., Schmidt, W., S. Suh, B.W. & Pennington, D. (2004). Life cycle assessment: Part 1: Framework, goal and scope definition, inventory analysis, and applications. *Environment International*, **30**, 701 – 720. xviii, 144

Research-report (2003). *Wood plastic composites study - Technology and UK market opportunities*. Optimat Ltd and MERL Ltd: The Waste and Resources Action Programme, Banbury, UK. 215

Revellino, M., Saggese, L. & Gaiero, E. (2000). *Comprehensive Composite Materials*, vol. 2, chap. Compression moulding of SMCs, 763–805. Elsevier. 52

Rijswijk, K.V., Brouwer, W.D. & Beukers, A. (2003). Application of natural fibre composites in the develpment of rural societies. Tech. rep., Report for Food and Agriculture Organization of the United Nations. 12

Rokbi, M., Osmani, H., Imad, A. & Benseddiq, N. (2011). Effect of chemical treatment on flexure properties of natural fiber-reinforced polyester composite. In M. Guagliano & L. Vergani, eds., *11th International Conference on the Mechanical Behavior of Materials (ICM11)*, vol. 10 of *Procedia Engineering*. 54

Romhany, G., Czigany, T. & Karger-Kocsis, J. (2006). Determination of j-r curves of thermoplastic starch composites containing crossed quasi-unidirectional flax fiber reinforcement. *Composites Science and Technology*, **66**, 3179 – 3187. 128

Rosa, I.M., Santulli, C. & Sarasini, F. (2009). Acoustic emission for monitoring the mechanical behaviour of natural fibre composites: a literature review. *Composites part A*, **40**, 1456–1469. 86

Rouison, D., Couturier, M., Sain, M., MacMillan, B. & Balcom, B. (2005). Water absorption of hemp fiber/unsaturated polyester composites. *Polymer Composites*, **26**, 509–525. 53

Rout, J., Misra, M., Tripathy, S.S., Nayak, S.K. & Mohanty, A.K. (2001). The influence of fibre treatment on the performance of coir-polyester composites. *Composites Science and Technology*, **61**, 1303 – 1310. 81

Ruiz, M.M., Cavaille, J.Y., Dufresne, A., Gerard, J.F. & Graillat, C. (2000). Processing and characterization of new thermoset nanocomposites based on cellulose whiskers. *Composite Interfaces*, **7**, 117–131. 212

Sahraoui, S. & Lataillade, J.L. (1990). Dynamic effects during instrumented impact testing. *Engineering Fracture Mechanics*, **36**, 1013 – 1019. 83

Sanadi, A.R., Prasad, S.V. & Rohatgi, P.K. (1986). Sunhemp fibre-reinforced polyester. *Journal of Materials Science*, **21**, 4299–4304. 81

Santulli, C. (2001). Post-impact damage characterisation on natural fibre reinforced composites using acoustic emission. *NDT and E International*, **34**, 531–536. 85, 103

Santulli, C. (2006). Post-impact flexural tests on jute/polyester laminates monitored by acoustic emission. *Journal of Materials Science*, **41**, 1255–1259. 103

Santulli, C., Janssen, M. & Jeronimidis, G. (2005). Partial replacement of e-glass fibers with flax fibers in composites and effect on falling weight impact performance. *Journal of Materials Science*, **40**, 3581–3585. 85

Satyanarayana, K.G., Sukumaran, K., Kulkarni, A.G., Pillai, S.G.K. & Rohatgi, P.K. (1986). Fabrication and properties of natural fibre-reinforced polyester composites. *Composites*, **17**, 329–333. 13

Sawpan, M.A., Pickering, K.L. & Fernyhough, A. (2009). Characterisation of hemp fibre reinforced poly(lactic acid) composites. *International Journal of Materials and Product Technology*, **36**, 199–204. 128

Sawpan, M.A., Pickering, K.L. & Fernyhough, A. (2011). Effect of fibre treatments on interfacial shear strength of hemp fibre reinforced polylactide and unsaturated polyester composites. *Composites Part A-Applied Science and Manufacturing*, **42**, 1189–1196. 54

Schmehl, M., Mussig, J., Schonfeld, U. & Buttlar, H.B.V. (2008). Life cycle assessment on a bus body component based on hemp fiber and ptp. *Journal of Polymers and the Environment*, **16**, 51–60. 146

Schrauwen, B. & Peijs, T. (2002). Influence of matrix ductility and fibre architecture on the repeated impact response of glass-fibre-reinforced laminated composites. *Applied Composite Materials*, **9**, 331–352. 87, 88, 92, 102

Shen, L. & Patel, M. (2008). Life cycle assessment of polysaccharide materials: A review. *Journal of Polymers and the Environment*, **16**, 154–167. 146

Siau, J.F. (1995). *Wood: Influence of moisture on physical properties*. Ph.D. thesis, Department of Wood Science & Forest Products, Virginia Polytechnic Institute & State University, USA. 24, 27

Silva, R., Spinelli, D., Filho, W.B., Neto, S.C., Chierice, G. & Tarpani, J. (2006). Fracture toughness of natural fibers/castor oil polyurethane composites. *Composites Science and Technology*, **66**, 1328 – 1335. 128, 141

Singleton, A.C.N., Baillie, C.A., Beaumont, P.W.R. & Peijs, T. (2003). On the mechanical properties, deformation and fracture of a natural fibre/recycled polymer composite. *Composites Part B: Engineering*, **34**, 519–526. 11, 35, 50, 53, 81

Sjoblom, P.O., Hartness, J.T. & Cordell, T.M. (1988). On low-velocity impact testing of composite materials. *Journal of Composite Materials*, **22**, 30–52. 79

Soykeabkaew, N., Arimoto, N., Nishino, T. & Peijs, T. (2008). All-cellulose composites by surface selective dissolution of aligned ligno-cellulosic fibres. *Composites Science and Technology*, **68**, 2201 – 2207. 56

Sreekala, M.S., Kumaran, M.G. & Thomas, S. (1997). Oil palm fibers: Morphology, chemical composition, surface modification, and mechanical properties. *Journal of Applied Polymer Science*, **66**, 821–835. 62

Sreekala, M.S., Kumaran, M.G., Joseph, S., Jacob, M. & Thomas, S. (2000). Oil palm fibre reinforced phenol formaldehyde composites: Influence of fibre surface modifications on the mechanical performance. *Applied Composite Materials*, **7**, 295–329. xiii, 53, 54, 56, 81

Sreekumar, P.A., Agoudjil, B., Boudenne, A., Unnikrishnan, G., Ibos, L., Fois, M. & Thomas, S. (2012). Transport properties of polyester composite reinforced with treated sisal fibers. *Journal of Reinforced Plastics and Composites*, **31**, 117–127. 54

Stamboulis, A., Baillie, C.A., Garkhail, S.K., Melick, H.G.H.V. & Peijs, T. (2000). Environmental durability of flax fibres and their composites based on polypropylene matrix. *Applied Composite Materials*, **7**, 273–294. 35, 52, 53

Stamboulis, A., Baillie, C.A. & Peijs, T. (2001). Effects of environmental conditions on mechanical and physical properties of flax fibers. *Composites Part A: Applied Science and Manufacturing*, **32**, 1105–1115. 53

Summerscales, J., Dissanayake, N.P., Virk, A.S. & Hall, W. (2010a). A review of bast fibres and their composites. part 1 fibres as reinforcements. *Composites Part A: Applied Science and Manufacturing*, **41**, 1329 – 1335. 11

Summerscales, J., Dissanayake, N.P., Virk, A.S. & Hall, W. (2010b). A review of bast fibres and their composites. part 2 composites. *Composites Part A: Applied Science and Manufacturing*, **41**, 1336 – 1344. 11

Summerscales, J., Hall, W. & Virk, A. (2011). A fibre diameter distribution factor (FDDF) for natural fibre composites. *Journal of Materials Science*, **46**, 5876–5880. 30

Suradi, S.S., Yunus, R.M. & Beg, M.D.H. (2011). Oil palm bio-fiber-reinforced polypropylene composites: effects of alkali fiber treatment and coupling agents. *Journal of Composite Materials*, **45**, 1853–1861. 54

Symington, M.C., Banks, W., West, O.D. & Pethrick, R. (2009). Tensile testing of cellulose based natural fibers for structural composite applications. *Journal of Composite Materials*, **43**, 1083–1108. 186

Tan, T., Santos, S.F., Savastano, H., Jr. & Soboyejo, W.O. (2012). Fracture and resistance-curve behavior in hybrid natural fiber and polypropylene fiber reinforced composites. *Journal of materials science*, **47**, 2864–2874. 129

Thamae, T., Marien, R., Chong, L., Wu, C. & Baillie, C. (2008). Developing and characterizing new materials based on waste plastic and agro-fibre. *Journal of Materials Science*, **43**, 4057–4068. 146

Thanomsilp, C. (2001). *Toughening Composites for Liquid Composite Moulding*. Ph.D. thesis, Department of Materials Science, Queen Mary University of London. 124

Thanomsilp, C. & Hogg, P.J. (2003). Penetration impact resistance of hybrid composites based on commingled yarn fabrics. *Composites Science and Technology*, **63**, 467 – 482. 85

Thanoslip, C., Cauchi-Savona, S., Peijs, T. & Posyachinda, S. (2007). Use of rice husk powder as a substitute for $CaCO_3$ in thermoset-based molding compounds. *Journal of Biobased Materials and Bioenergy*, **1**, 87–93. 70, 180

Thiruchitrambalam, M., Athijayamani, A., Sathiyamurthy, S. & Thaheer, A.S.A. (2010). A review on the natural fiber-reinforced polymer composites for the development of roselle fiber-reinforced polyester composite. *Journal of Natural Fibers*, **7**, 307–323. 11

Thomason, J.L. & Groenewoud, W.M. (1996). The influence of fibre length and concentration on the properties of glass fibre reinforced polypropylene: 2. thermal properties. *Composites Part A: Applied Science and Manufacturing*, **27**, 555 – 565. 60

Thomason, J.L., Vlug, M.A., Schipper, G. & Krikor, H.G.L.T. (1996). Influence of fibre length and concentration on the properties of glass fibre-reinforced polypropylene: Part 3. strength and strain at failure. *Composites Part A: Applied Science and Manufacturing*, **27**, 1075 – 1084. 60

Thygesen, A., Madsen, F.T., Lilholth, H., Felby, C. & Thomsen, A.B. (2002). Change in chemical composition, degree of crystallisation and polymerisation of cellulose in hemp fibres caused by pre-treatment. In *Sustainable natural and polymeric composites - science and technology*, 23, 315–323, Proceedings of the Riso International Symposium on Materials Science. 24

Towo, A.N. & Ansell, M.P. (2008). Fatigue evaluation and dynamic mechanical thermal analysis of sisal fibre-thermosetting resin composites. *Composite Science and Technology*, **64**, 925–932. 13

van den Heuvel, P.W.J., van der Bruggen, Y.J.W. & Peijs, T. (1996). Failure phenomena in multi-fibre model composites: Part 1. an experimental investigation into the influence of fibre spacing and fibre–matrix adhesion. *Composites Part A: Applied Science and Manufacturing*, **27**, 855–859. 53

van den Oever, M.J.A., Bos, H.L. & Kemenade, M.J.J.M.V. (2000). Influence of the physical structure of flax fibres on the mechanical properties of flax fibre reinforced polypropylene composites. *Applied Composite Materials*, **7**, 387–402. xii, 31, 35

van der Werf, H.M. & Turunen, L. (2008). The environmental impacts of the production of hemp and flax textile yarn. *Industrial Crops and Products*, **27**, 1 – 10. 155

Venderbosch, R.W., Peijs, T., Meijer, H.E.H. & Lemstra, P.L. (1996). Fibre-reinforced composites with tailored interphases using ppe/epoxy blends as a matrix system. *Composites Part A: Applied Science and Manufacturing*, **27**, 895 – 905. 53

Vidal, R., Martinez, P. & Garrain, D. (2009). Life cycle assessment of composite materials made of recycled thermoplastics combined with rice husks and cotton linters. *The International Journal of Life Cycle Assessment*, **14**, 73–82. 146

Virk, A.S., Hall, W. & Summerscales, J. (2010). Failure strain as the key design criterion for fracture of natural fibre composites. *Composites Science and Technology*, **70**, 995 – 999. 28

Vissers, C. (2000). *Alternative Composites for the Automotive Industry: Can Glass Mat Reinforced Thermoplastics be Replaced by Natural Mat Reinforced Thermoplastics Or Perhaps by All-polypropylene Composites?*. Stan Ackermans Institute, Center for Technical Design, Eindhoven University of Technology, Eindhoven, The Netherlands. xx, 153

Wambua, P., Ivens, J. & Verpoest, I. (2003a). Natural fibres: can they replace glass in fibre reinforced plastics? *Composite Science and Technology*, **63**, 1259–1264. 16, 211

Wambua, P., Ivens, J. & Verpoest, I. (2003b). Natural fibres: can they replace glass in fibre reinforced plastics? *Composites Science and Technology*, **63**, 1259–1264. 53, 81

Wang, B. & Sain, M. (2007). Isolation of nanofibers from soybean source and their reinforcing capability on synthetic polymers. *Composites Science and Technology*, **67**, 2521 – 2527. 212

Wang, H., Huang, L. & Lu, Y. (2009). Preparation and characterization of micro- and nano-fibrils from jute. *Fibers and Polymers*, **10**, 442–445. 212

Wang, S.X., Wu, L.Z. & Ma, L. (2010). Low-velocity impact and residual tensile strength analysis to carbon fiber composite laminates. *Materials & Design*, **31**, 118 – 125. 102

Wibowo, A.C., Mohanty, A.K., Misra, M. & Drzal, L.T. (2004). Hemp fiber reinforced cellulosic plastic bio-composites: Thermo-mechanical and morphological characterization. *Industrial and Engineering Chemistry Research*, **43**, 4883–4888. 56

Wong, D.W., Lin, L., McGrail, P.T., Peijs, T. & Hogg, P.J. (2010). Improved fracture toughness of carbon fibre/epoxy composite laminates using dissolvable thermoplastic fibres. *Composites Part A: Applied Science and Manufacturing*, **41**, 759 – 767. 102

Wong, S., Shanks, R.A. & Hodzic, A. (2004). Mechanical behavior and fracture toughness of poly(l-lactic acid)-natural fiber composites modified with hyperbranched polymers. *Macromolecular Materials and Engineering*, **289**, 447–456. 128, 133

Wotzel, K., Wirth, R. & Flake, R. (1999). Life cycle studies on hemp fibre reinforced composites and abs for automotive parts. *Angew Makromol Chem*, **272**, 121–127. 146

Wu, C.S. (2009). Renewable resource-based composites of recycled natural fibers and maleated polylactide bioplastic: Characterization and biodegradability. *Polymer Degradation and Stability*, **94**, 1076 – 1084. 11

Xie, Y., Hill, C.A.S., Xiao, Z., Militz, H. & Mai, C. (2010). Silane coupling agents used for natural fiber/polymer composites: A review. *Composites Part A-Applied Science and Manufacturing*, **41**, 806–819. 55

Xu, X., Jayaraman, K., Morin, C. & Pecqueux, N. (2008). Life cycle assessment of wood-fibre-reinforced polypropylene composites. *Journal of Materials Processing Technology*, **198**, 168 – 177. 146

Yuanjian, T. & Isaac, D.H. (2007). Impact and fatigue behaviour of hemp fibre composites. *Composites Science and Technology*, **67**, 3300–3307. 103

Yusliza, Y., Zuraida, A. & Sopyan, I. (2008). Fracture behavior of natural fiber reinforced biopolymer matrix composite. In A. Lau, J. Lu, V. Varadan, F. Chang, J. Tu & P. Lam, eds., *Multi-functional materials and structures, pts 1 and 2*, vol. 47-50 of *Advanced Materials Research*, 1189–1192. 129

Zafeiropoulos, N.E., Williams, D.R., Baillie, C.A. & Matthews, F.L. (2002). Engineering and characterisation of the interface in flax fibre/polypropylene composite materials. Part I. Development and investigation of surface treatments. *Composites Part A: Applied Science and Manufacturing*, **33**, 1083 – 1093. 62

Zah, R., Hischier, R., Leao, A. & Braun, I. (2007). Curaua fibers in the automobile industry - a sustainability assessment. *Journal of Cleaner Production*, **15**, 1032 – 1040. 146

Zampaloni, M., Pourboghrat, F., Yankovich, S.A., Rodgers, B.N., Moore, J., Drzal, L.T., Mohanty, A.K. & Misra, M. (2007). Kenaf natural fibre reinforced polypropylene composites: A discussion on manufacturing problems and solutions. *Composites Part A: Applied Science and Manufacturing*, **38**, 1569–1580. 13

Zarate, C.N., Aranguren, M.I. & Reboredo, M.M. (2003). Influence of fiber volume fraction and aspect ratio in resol-sisal composites. *Journal of Applied Polymer Science*, **89**, 2714–2722. 50

Zhang, Z. & Richardson, M. (2007). Low velocity impact induced damage evaluation and its effect on the residual flexural properties of pultruded grp composites. *Composite Structures*, **81**, 195 – 201. 104, 114

Zhu, T. (2004). *Life cycle assessment in designing greener semiconductor*. Master's thesis, MSc thesis. Department of Chemical and Environmental Engineering, University of Arizona, USA. xviii, 149

Zini, E. & Scandola, M. (2011). Green composites: An overview. *Polymer Composites*, **32**, 1905–1915. 11